UNIVERSITY OF BIRMINGHAM

PREPARATION, MODIFICATION AND CHARACTERISATION OF SELECTIVE ZEOLITE BASED CATALYSTS FOR PETROCHEMICAL APPLICATIONS

BY

SAEED HAJIMIRZAEE

A thesis submitted to

The University of Birmingham for the degree of

DOCTOR OF PHILOSOPHY

School of Chemical Engineering

College of Engineering and Physical Sciences

The University of Birmingham

April 2015

UNIVERSITY OF
BIRMINGHAM

University of Birmingham Research Archive

e-theses repository

Abstract

Use of zeolite based catalyst for important petrochemical reactions such as alkylation, dehydration and hydrogenation was investigated. Specific reactions studied for these processes included dialkylation of naphthalene over HY zeolite supported on alumina, dehydration of methanol over ZSM-5 zeolite dispersed in alumina matrix and hydrogenation of naphthalene over Ni/HY and Co/ZSM-5 zeolite.

For each reaction, the catalysts were characterised by XRF for elemental analysis, XRD for phase analysis and crystal size measurements, nitrogen adsorption–desorption to measure BET surface are, pore size and pore volume of the samples, and Temperature Programmed Desorption (TPD) of t-Butylamine to analysis the acid sites strength and its distribution. Reducibility analysis was carried out for catalysts used for hydrogenation of naphthalene using TPR. TGA of used catalysts were used to measure the amount of coke deposited on the catalyst surface after reaction.

The dialkylation of naphthalene with isopropanol to produce 2,6-diisopropylnaphthalene (2,6-DIPN) was carried out over HY zeolite. The effect of reaction conditions on the alkylation of naphthalene using isopropanol over HY zeolite was carried out by undertaking a series of reactions at the temperature range of 160 ℃-280 ℃, pressure 1-50 bar, isopropanol/naphthalene molar ratio 1-6, WHSV 9.4- 28.3 h^{-1} for a time on stream of 6 hours. To increase the selectivity to 2,6-DIPN, modification of HY zeolite was carried using transition metals, such as Fe^{3+}, Ni^{2+}, Co^{2+} and Cu^{2+} by means of wet impregnation method.

The results showed that HY zeolite modified by Fe^{3+} has improved selectivity to 2,6-DIP by increasing the 2,6/2,7-DIPN ratio from 2.8 to 6.6 under optimum reaction conditions: 50 bar, 220 ℃, isopropanol/naphthalene = 4 mole ratio, WHSV = 18.8 h^{-1} after 6 hours time on stream. The modification upon the zeolite changed the naphthalene conversion from 77% for parent HY zeolite to 73%, 76%, 88% and 96% for zeolite modified with Fe(III), Co(II), Ni(II) and

Cu(II), respectively. The experimental results indicate that the selectivity to 2,6-DIPN is in the order of Fe–HY > Ni–HY > Cu–HY > Co–HY > HY. Modification of zeolite increased the 2,6-/2,7-DIPN from 2.8 for parent HY zeolite to 6.7 for Fe–HY, 4.6 for Co–HY, 5.9 for Ni–HY and 5.0 for Cu–HY catalyst sample.

Dehydration of methanol to light olefins was studied using ZSM-5 zeolite in alumina matrix support catalyst. The effects of reaction conditions such as temperature, pressure, space velocity and feed composition as well as the effect of zeolite/support ratio on the conversion of methanol to light olefins ($C_2^=$-$C_4^=$) were studied. Use of γ-alumina as support improved the catalyst selectivity to propene and light olefins. Zeolite/alumina catalyst with 25% wt. ZSM-5 dispersed in a matrix containing 75 % alumina led to highest selectivity to propene and light olefins but highest amount of coke was observed on this catalyst in comparison with other samples. The effect of zeolite impregnation using phosphorus, Cs, Ca and Fe on the conversion of methanol and selectivity to light olefins was studied. Modification in all cases increased the shape selectivity to light olefins. ZSM-5 zeolite ion exchanged by Cs led to highest selectivity to light olefins and particularly propene by changing the acid sites distribution.

Hydrogenation of naphthalene to decalin and tetralin over two zeolite based catalyst Co/ZSM-5, Ni/HY were studied and results were compared with a synthesised Co/Silica catalyst and a commercial NiMo/Alumina catalyst. Ni/HY catalyst exhibited higher activity, longer life time and better selectivity to tetralin compared to Co/ZSM-5. After 6 h TOS, the activity of Ni/HY in conversion of naphthalene was still stable while the commercial NiMo/alumina catalyst showed some deactivation. Co/Silica catalyst showed high conversion during the first hour of the reaction, however, it decreased significantly after that time as a result of coke deposition. TGA analysis of used catalyst samples revealed a larger coke deposit on Ni/HY catalyst after 6 h TOS reaction than the other catalysts, which is probably due to stronger acid sites of the zeolite leading to undesirable side reactions and production of coke precursor materials.

Dedicated

To my wife for her continuous courage, trustworthy love and absolute loyalty

To my father for his priceless words of wisdom and unconditional support

To my mother for her valuable moral support and endless sacrifice

Acknowledgment

This Thesis would not have been possible to write without the help and guidance of several individuals who shared or contributed their knowledge in the preparation and completion of this research. It is a pleasure to express my gratitude to them all in my modest acknowledgment.

I would like to give special thanks to my supervisor, **Professor Joe Wood**, for his patience, advice and guidance from the beginning of this research as well as giving me motivation, enthusiasm, and immense knowledge.

I gratefully acknowledge my co-supervisor, **Dr. Gary Leeke** for his valuable advice, supervision and crucial contribution to this thesis.

Many thanks go in particular to **Dr. Reza M. Behbahani** for his valuable advice, guidance and financial support for part of this research.

I would also like to thank my family for supporting me spiritually through my entire life and in particular for their support and encouragement during my PhD tenure.

Finally, I would like to thank everybody who contributed or helped me to the successful completion of this research.

Table of Contents

List of Figures

List of Tables

Nomenclature

AlPO	Alumina-phosphates
BEA	Beta zeolite
CHA	Chabazite zeolite
CMC	Carboxy methyl cellulose
Conv.	Conversion (mol%)
DAN	Di-alkylated-naphthalene
Decalin	Decahydronaphthalene
DIPN	Di-isopropyl-naphthalene
DME	Dimethyl ether
DTBN	Di-tibutyl-naphthalene
DTG	1st derivative TGA curve
EXAFS	Extended X-ray absorption fine structure
FAU	Faujasite
FCC	Fluid Catalytic Cracking
FID	Flame ionisation detector
HM	H-Mordenite
HPLC	High performance liquid chromatography
IPA	Isopropyl alcohol
IZA	International Zeolite Association
LHSV	Liquid hour space velocity
LTA	Linde type A zeolite
MFI	Mobile five zeolite
MOR	Mordenite
MTA	Metric tons annually
MTBE	Methyl t-butyl ether
MTO	Methanol to olefins
MTP	Methanol to propylene
PBN	Poly butylene naphthalene
PEN	Polyethylene naphthalene
PIPN	Poly-isopropyl-naphthalene

RGA	Refinery Gas Analyser
RV	Relief valve
SAPO	silica-alumina-phosphates
SCF	Supercritical Fluid
SEM	Scanning electron microscopy
t-BA	tert-Butylamine
TCD	Thermal conductivity detector
TEM	Transmission electron microscopy
Tetralin	Tetrahydronaphthalene
TGA	Thermogravimetric analysis
TOS	Time on stream (h)
TPD	Temperature programmed desorption
TPR	Temperature programmed reduction
TrMB	Tri methyl benzene
USY	Ultra stable Y zeolite
WHSV	Weigh hourly space velocity
XRD	X-ray powder diffraction
XRF	X-ray fluorescence

Symbols

C_i	Concentration (mmol.l^{-1})
d	Zeolite pore diameter (Å)
E_a	Activation energy (kcal.mol^{-1})
k_i	reaction rate constants
M^{m+}	Extra framework cation
P	Pressure (bar)
S_i	Selectivity (%)
T (in TO$_4$)	Tetrahedral metals in zeolite structure
W_{150}	Weight of the sample at 150 ºC in TGA
W_{800}	Weight of the sample at 800 ºC in TGA
X	Conversion (mol%)

Chapter 1: INTRODUCTOIN

1.1 Background and motivation

The increasing costs of petrochemicals, energy and raw material demands, are forcing changes in the chemical industry with regard to energy efficiency and waste reduction. Moreover, by emerging the concepts of sustainable development and principles of green chemistry (Anastas and Eghbali, 2010), companies have to design chemical products and processes with fewer or no hazardous substances, more efficient technologies, plus a cleaner and healthier environment. In fact, as far as chemistry is concerned, catalysis is the key to sustainability (Rothenberg, 2008).

The simplified definition of a catalyst is a substance that facilitates a reaction by opening a different, faster reaction pathway without being consumed in the process. As the catalyst is not consumed during the reaction, many consecutive cycles can be carried out on each active site, so only a small amount of catalyst is required relative to the substrate (Rothenberg, 2008). The subject of catalysis is divided into three categories: homogeneous-, heterogeneous-, and bio-catalysis. Heterogeneous catalysts are solid particles or powders such as zeolites, supported metal oxides, acidic ion-exchange resins with several advantages compared to other catalysts. From the green chemistry point of view, heterogeneous catalysts can present significant advantages to develop a catalytic processes with lower generation of by-products or harmful unwanted materials. Separation of catalysts from the reactants and products can be carried out more easily in case of heterogeneous catalysts. Moreover, regeneration and recovery of catalyst, especially where expensive noble metals or chiral ligands are involved, is a significant advantage of heterogeneous catalysts (Sherrington et al., 2001) .

Zeolites are excellent solid acid heterogeneous catalysts with unique structural characteristics which are used widely in petroleum refining, synfuels production, and petrochemical production. They have been used for important chemical reactions such as aromatisation, alkylation, dehydration, disproportionation, hydroalkylation, hydrocracking, hydrogenation, etc., (Pramatha and Prabir, 2003). Zeolites are microporous crystalline aluminosilicate solids made of silicon, aluminium and oxygen atoms that form a framework with cavities and channels inside where a wide variety of cations, water and/or other small molecules may reside. By the end of February 2007, 176 unique zeolite framework types had been approved and assigned a 3-letter code by the Structure Commission of the IZA (IZA-SC) in the sixth edition of the Atlas of Zeolite Framework Types (Baerlocher et al., 2007). Both synthetic and natural zeolites have been used commercially due to their unique properties for application in adsorption, ion-exchange, molecular sieve, and catalysis processes. Post-synthesis treatment and modification of zeolites is often used to have a zeolite with desirable framework composition and essential catalytic characteristics (Čejka et al., 2010). Many comprehensive review papers have been published explaining important aspects of zeolite modification methods such as ion-exchange, dealumination, metal incorporation, reinsertion of heteroatoms into zeolite framework and treatment with acids and other components. (Weitkamp and Puppe, 1999, Szostak, 2001).

1.2 Objectives of this thesis

Zeolites as catalyst have shown promising results for application in petrochemical industries. These porous materials provide a suitable confined space for the establishment of shape selective reactions due to their unique pore structure. However, modification of zeolite to improve the catalyst selectivity to desired product by changing the pore size or acid sites strength and distribution is still challenging. The purpose of this study was to find a relation

between physicochemical properties of zeolite after modification versus its catalytic behaviour in terms of reactants conversion, selectivity to desired product(s) and amount of coking after reaction. Moreover, typical reaction parameters (e.g. temperature, pressure, space velocity, reactant composition, etc.) were varied in order to investigate their influence on the reaction mechanism. Three important petrochemical reactions were chosen:

1. Dialkylation of naphthalene to 2,6-diisopropylnaphthalene.

2. Dehydration of methanol to light olefins (ethene and propene).

3. Hydrogenation of naphthalene to tetralin, cis- and trans-decalin.

For the first reaction, the effects of reaction conditions such as temperature, pressure, weight hourly space velocity (WHSV) and isopropanol/naphthalene molar ratio on conversion of naphthalene and product selectivity over HY zeolite as catalyst were studied. Then, the effects of HY zeolite modification using different transition metals (e.g. Fe, Co, Ni and Cu) on the alkylation of naphthalene with isopropanol were investigated.

For the second reaction, the effect of reaction conditions such as temperature, pressure, feed composition and WHSV on the conversion of methanol and product distribution over pure ZSM-5 zeolite were studied and discussed in detail. Subsequently, the effect of using different ratios of alumina (as support) to zeolite was studied. The conversion to light olefins over these catalysts was studied with respect to their characteristics such as acidity, pore volume and BET surface area. Finally, product distribution over ZSM-5 zeolites modified by iron, calcium, caesium, and phosphorous were studied in order to investigate the best promoter.

For the third reaction, hydrogenation of naphthalene over three prepared catalysts (Ni/HY, Co/ZSM-5 and Co/Silica) was carried out under optimal reaction conditions as determined by a previous research group member (Hassan, 2011) and results were compared with commercial NiMo catalyst.

Catalyst properties such as the crystal size, surface area and pore geometry of different samples were reported. In each case, fresh and selected used catalysts were characterised using the range of techniques described below:

- Temperature Programmed Desorption (TPD) of t-Butylamine was used to analyse and determine the number and strength of active acid sites of the zeolite catalysts.

- X-ray diffraction (XRD) was used to approximate crystal size of the samples, strain or stress in the material, the approximate extent of heteroatom substitution, crystallinity, or the presence of stacking disorder.

- X-ray fluorescence (XRF) was used to determine the elemental composition of samples after modification.

- Nitrogen adsorption-desorption isotherms at 77 K, was used to measure the surface area, pore volume, and pore size distribution of the catalyst samples.

- Thermogravimetric analysis (TGA) of used catalysts was used to determine the amount of coke deposited on the catalysts.

1.3 Thesis layout

An introduction and background information about the present work is provided in Chapter 1. A literature review is presented in Chapter 2, which covers basic concepts of heterogeneous catalysis, zeolites and their application in petrochemical industries as catalyst. Chapter 2 also covers a literature survey about the reactions studied: dialkylation of naphthalene, hydrogenation of naphthalene and dehydration of methanol to light olefins. Chapter 3 is the compilation of details of the chemicals used, experimental setup, operating procedures followed by analytical equipment methods and calibrations employed in this study. Chapter 4 reports the experimental results for dialkylation of naphthalene by isopropanol over HY zeolite followed

by discussion about effect of reaction conditions and catalysts modification on conversion and product selectivity. Dehydration of methanol to light olefins over ZSM-5 zeolite including a discussion about effect of using support and zeolite modification on the product selectivity is reported in Chapter 5. Chapter 6 contains the experimental results and discussion for hydrogenation of naphthalene over Nickel/Cobalt zeolite based catalyst. This is followed by the final Chapter, 7, where the conclusion and future work recommendations for this study are given. Appendices contain GC calibration curves, GC and GC-MS analysis of feed and product compounds, BET calculations, crystal size calculations from XRD, acid sites calculation and papers published from this research.

1.4   Publications and Conferences

Publications resulting from this thesis are listed below, and copies are provided in Appendix G:

- S. Hajimirzaee, G. Leeke, J. Wood, "Modified Zeolite Catalyst for Selective Dialkylation of Naphthalene", Chemical Engineering Journal, Volume 207–208, 2012, 329-341

- S. Hajimirzaee, M. Ainte, B. Soltani, R. Behbahani, G. Leeke, J. Wood , "Dehydration of Methanol to Light Olefins upon Zeolite/Alumina Catalysts: Effect of Reaction Conditions, Catalyst Support and Zeolite Modification", Chemical Engineering Research and Design, In press, 93, 2015, 541-553

Conferences:

- S. Hajimirzaee , "Modified Zeolite Catalyst for Selective Dialkylation of Naphthalene", 22nd International Symposium on Chemical Reaction Engineering (ISCRE 22), 2-5 September 2012, Maastricht, Netherlands

Chapter 2: LITERATURE SURVEY

2.1   Introduction

2.1.1   Catalysis and green chemistry

Chemistry plays a vital role in shaping the quality of our modern life. The chemicals industry and other related industries provide us with a vast variety of essential products. However, these chemical industries are often viewed to be polluting and causing significant environmental damage. The disaster of Bhopal in Madhya Pradesh County, India on December 3, 1984 has become a notorious day (UCIL, 1984). In the midnight, a cloud of poisonous gas leaked from a pesticide factory owned by Union Carbide India Limited (UCIL) containing 15 metric tons of methyl isocyanate (MIC). The gas leak caused death of 4,000 local residents immediately and health problems for 50,000 to possibly 500,000 people. Five years later, in February 1989, the Supreme Court of India directed a final settlement of all Bhopal litigation in the amount of $470 million. Although, the Government of India, Union Carbide Corporation (UCC) and UCIL accepted the Court's direction, it was condemned by the victims. For many years after this tragedy, the delay in delivering the compensation led to further death of suffered victims. More than 20,000 people still live in the area close that factory and are exposed to toxic chemicals through groundwater and soil contamination. New generation continues to get sick from cancer or birth defects due to impact of that disaster.

An explosion of a dioxin reactor in Meda, Italy (1976), a cyanide spill in Baia Mare, Romania (2000) and explosion of an ammonium nitrate plant in Port Neal, Iowa, USA (1994) are some further examples of these man-made disasters (McKinney et al., 2007). But chemists and engineers who design these processes have never set out to harm the environment or human health. These accidents in most cases have occurred through a lack of knowledge for example,

operator error, poor plant management, lack of procedures such as permit to work, etc. The challenge for the chemical industry in the twenty first century is to continue to provide the materials we need but in an economically viable manner, without the harmful environmental side effects. When looking at Green Chemistry from an industrial perspective, it is important to reduce the raw material use, capital investment, costs of waste treatment and disposal, derivatives, energy consumption, toxicity, etc. (Lancaster, 2002). Catalysts in this case can reduce the energy requirement of a process by increasing the rate of reaction through lowering the activation energy. They can be used in small amounts to carry out a single reaction, recycled many times with a lower amount of waste generated compared to stoichiometric reactions and therefore catalysis can be considered to be "green". Catalysts have been successfully used in the chemical industry for more than 100 years. Synthesis of important chemicals such as sulphuric acid, ammonia, nitric acid and hydrogenation are some examples of catalytic processes. Recent developments include homogeneous transition metal complexes, zeolites and highly selective metallic catalysts. However, to use a catalyst for industrial processes, a catalyst with high activity and selectivity as well as improved stability is required (Hagen, 2006).

2.1.2 Heterogeneous catalysis

Heterogeneous catalysis is crucial to chemical technology. Chemical bonds are broken and new chemical bonds are formed repeatedly during the catalytic process without significant change of the catalyst. In the absence of the catalysts, this chemical transformation would either not occur or would take place at very slow rate, thus designing of new catalysts with high efficiency requires an in-depth understanding from the catalyst in the reactor down to the atomic scale.

Van Santen (1991) categorises the research in catalysis to three levels:

1) The macroscopic level which is including the test of catalyst in reactors. Information regarding catalyst activity per unit volume, mechanical strength, mass and heat transfer as well as information regarding catalyst shape (e.g. extrudates, spheres, or loose powders) can be provided in this level.

2) The mesoscopic level provide information regarding kinetic studies, activity per unit surface area, and the relationship between the composition and structure of a catalyst versus its catalytic behaviour (much of the characterisation studies belong to this category).

3) The microscopic level comprises fundamental studies such as the details of adsorption on surfaces, reaction mechanisms, theoretical modelling, and surface science.

A heterogeneous catalytic reaction involves three main steps: 1) adsorption of reactant(s) from a fluid phase (gas or liquid) onto a solid surface, 2) surface reaction of adsorbed species, and 3) desorption of product(s) into the fluid phase (Davis and Davis, 2003). For instance, the following physical and chemical steps occur during a catalytic reaction on a porous catalyst in gas phase. Figure 2.1 illustrates these steps.

1) Diffusion of the reactant(s) from the bulk gas phase to the catalyst surface.

2) Diffusion of reactant(s) into the pores.

3) Adsorption of the reactant(s) on the surface of the pores.

4) Chemical reaction on the catalyst surface.

5) Desorption of the product(s) from the catalyst surface.

6) Diffusion of the product(s) out of the pores.

7) Diffusion of the product(s) into the bulk gas phase.
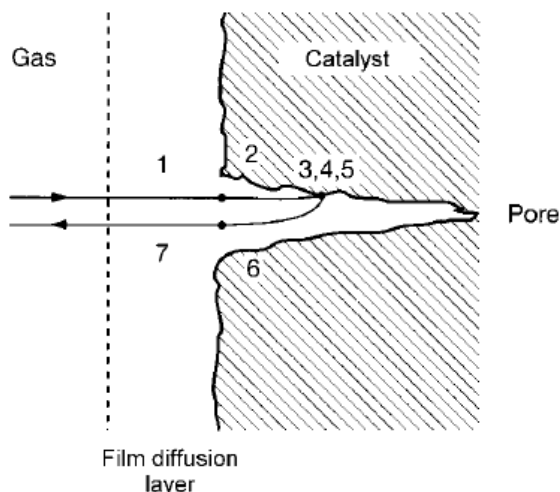
Figure 2.1. The physical and chemical steps of a heterogeneously catalysed gas-phase reaction (Hagen, 2006).

Since the surface of a metal or metal oxide powder (as active catalyst) is extremely small compared to the bulk surface area and may not accessible by the reactants, a valuable catalytic material such a transition metal is sometimes dispersed onto a porous support with high surface area. The shape and size of the heterogeneous solid catalysts must be carefully determined and adjusted according to the end use (e.g. pressure drop, voidage, active material, reactor, etc.). Common types in the order of decreasing in pressure drop are spheres > pellets > extrudates > rings > stars or lobes. Figure 2.2 shows some samples of the heterogeneous solid catalysts with different shapes and structures for applications in petrochemical industries, refineries, production of fertilisers and emission control in stationary and automobile engines. The shape and size of the catalyst particles can significantly influence the catalytic activity, mechanical resistance to crushing and abrasion, pressure drop and fabrication costs (Campanati et al., 2003). Although some catalysts are made of single component, most of them composed of three distinguishable substances: 1) active component, 2) support, 3) promoter. The active component is responsible for catalysing the main chemical reaction. Proper selection of the active component is the first step in catalyst design.

More than 70% of catalytic reactions such as reforming, hydrocracking, coal liquefaction, oxidation and hydrogenation use some form of metallic components (Richardson, 1989). Alkali and alkaline earth metals in salt form are used as electropositive promoters to increase catalyst activity and selectivity in many reactions as they revert to ionic states easily under catalytic conditions.

Figure 2.2. Commercial heterogeneous solid catalysts with different shape and structure for refineries and petrochemical applications (Süd-Chemie, 2014).

Rare earth metals have widely used in automotive catalytic converters, petroleum industries and refineries. The activation of H_2 and C-H bonds with transition metals complexes has been discovered more than three decades ago. Rare earth metals are highly active for insertion of unsaturated C-C multiple bonds (Roesky and Cui, 2010). Rare earth oxides, also are used for basic catalysis in hydrogenation of olefins, dehydration of alcohols, condensation of ketones and double bond migration of olefins (Hattori, 1995). Table 2.1 lists the different types of solid state catalytic materials.

Table 2.1. Different types of solid state catalytic materials (Richardson, 1989).

Type	State	Examples
Metals	Dispersed	Low: (Pt, Ru)/ Al_2O_3
		High: Ni/ Al_2O_3, Co/Diatomite
	Porous	Raney Ni, Co, Fe- Al_2O_3-K_2O
	Bulk	Pt, Ag gauze
Multi metallic clusters, alloys	Dispersed	(Pt-Re, Ni-Cu, Pt-Au)/ Al_2O_3
Metal oxides	Single	Al_2O_3, Cr_2O_3, Co_3O_4, ZrO_2 , Mn_2O_3
	Dual (co-gels)	SiO_2-Al_2O_3 , TiO_2-Al_2O_3
	Complex	$CuCr_2O_4$, $CuAl_2O_4$, $ZnCr_2O_4$, $BaTiO_3$
	Dispersed	NiO/ Al_2O_3 , MoO_3/ Al_2O_3
	Cemented	NiO-$CaAl_2O_4$
Sulphides	Dispersed	MoS_2/Al_2O_3 , WS_2/Al_2O_3, CoMoS
Acids	Dual (co-gels)	SiO_2-Al_2O_3
	Crystalline	Zeolites
	Natural Clays	Montmorillonite, Kaolinite
	Promoted acids	SbF, HF, supported halides
Bases	Dispersed	CaO, MgO, K_2O, Na_2O
Other compounds	Chlorides	$TiCl_3$, $AlCl_3$
	Carbides	Ni_3C, WC
	Nitrides	Fe_2N
	Borides	Ni_3B
	Silicides	TiSi
	Phosphides	NiP
Other forms	Molten salts	$ZnCl_2$, Na_2CO_3

2.2   **Zeolites**

2.2.1   **Natural zeolites**

In 1756, Swedish mineralogist Axel Fredrik Cronstedt discovered naturally occurring zeolite. Since then, about 40 types of natural zeolites have been discovered in which most of them have low Si/Al ratio. This is due to the absence of organic structure–directing agents which is necessary for formation of siliceous zeolites. Sometimes natural zeolites are found as large single crystals in nature, however it is very difficult to make such large crystals in the laboratory. Zeolites with high porosity such as Faujasite (FAU), whose laboratory synthesised examples are zeolites X/Y, are scarce in nature (Auerbach et al., 2003). Two natural zeolites used extensively in industry are Mordenite (MOR) and Clinoptilolite (HEU). These materials have been used for agronomy, horticulture and soil remediation to improve the soil chemical and physical properties, treatment of effluents containing radioactive contaminants or other heavy metals, or as molecular sieve to trap or separate gases in agriculture (e.g. ammonia) (Guthrie, 1997). Natural zeolites can be used as a catalyst but their catalytic activity is limited by their impurities and low surface areas (IZA, 2001). Figure 2.3 shows Clinoptilolite and Mordenite, two naturally occurring zeolites.

Figure 2.3. Left: Clinoptilolite-Na from Andalusia, Spain (Rewitzer, 2009), Right: Mordenite from San Juan, Argentina (irocks.com, 2008).

2.2.2   **Zeolites structure**

Zeolites are microporous crystalline aluminosilicates with pore sizes ranging from 3 to 7Å. About 176 framework structures have been listed in the most recent Atlas of Zeolite Framework Types (Baerlocher et al., 2007). The most important characteristic properties of these solid materials are well-defined structure, high surface area, selective sorption of small molecules (molecular sieves) and ion exchange. Zeolite are composed of TO_4 tetrahedra (T = Si, Al) which are interlinked through oxygen atoms to have a 3D network. The zeolite composition can follow this formula:

M^{m+}	$Si_{1-n}Al_nO_2$	nH_2O
Extra framework cation	Framework	Sorbed phase

The extra framework cations can be ion-exchanged with other cations (e.g. alkali metals, alkaline earth metals and transition metals). Depending on the synthesis conditions, the amount of Al within the framework can vary from Si/Al≈1 to ∞. Moreover, post-synthesis modifications of zeolite can insert Al or Si into the framework. Increasing the Si/Al ratio of the framework can improve the hydrophobicity as well as the hydrothermal stability (Pramatha and Prabir, 2003). Zeolite frameworks contain cages of spherical or other shapes which are interconnected by channels. The diameter of the channels is determined by the number of *T* atoms surrounding the opening of the channels as *n*-member rings. Large pore zeolites are constructed of 12-member rings (*d*>7Å), medium pore zeolites contain 10-member rings (5Å<*d*<6Å) and small-pore zeolites contain 6- or 8-member rings (diameter d: 2.8Å<*d*<4Å) (Deutschmann et al., 2000). Figure 2.4 illustrates different zeolite frameworks and some examples of synthesised zeolites with same framework structure but different composition.

(a)

(b)

(c)
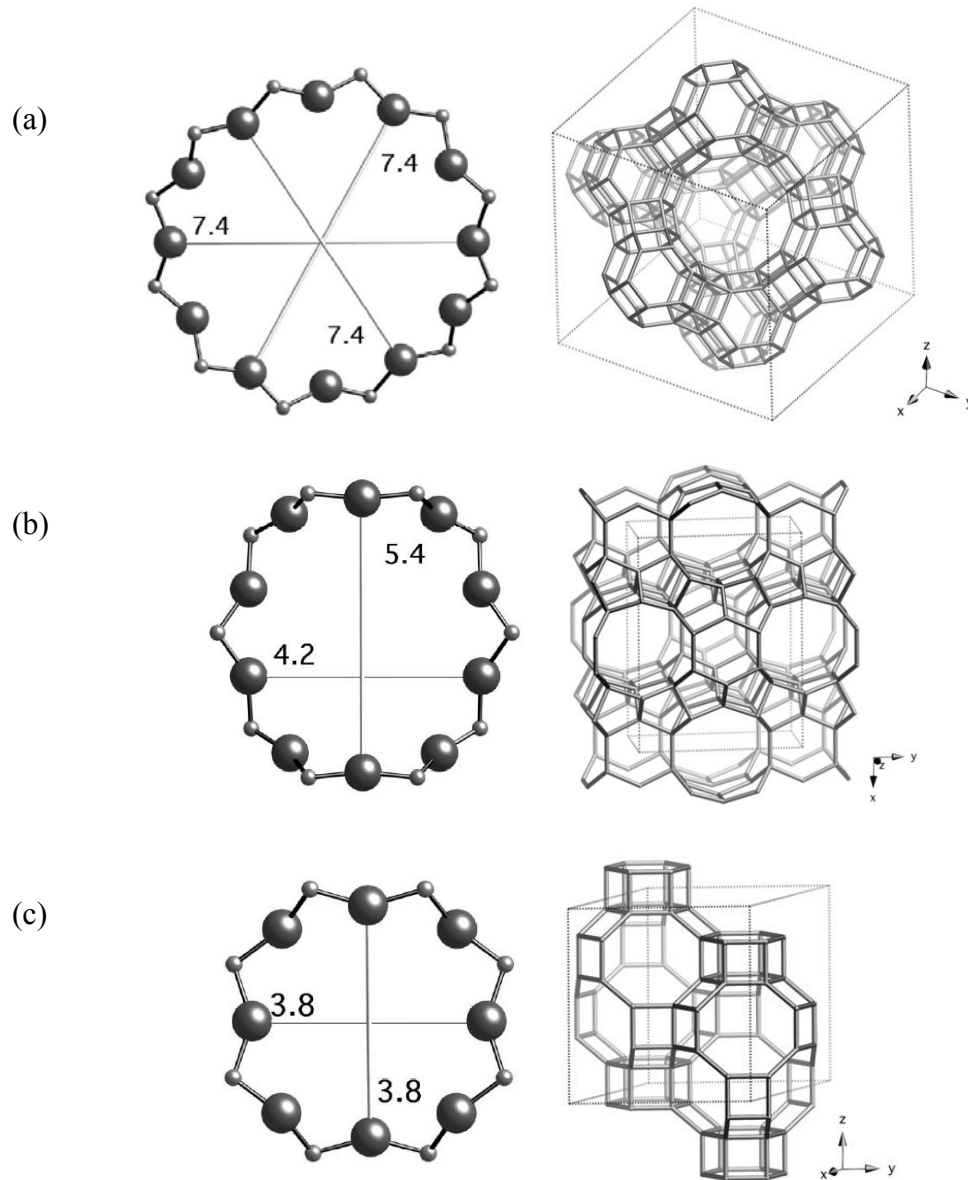
Figure 2.4. Different framework of zeolites (a) Faujasite type 12-ring, examples: Linde X, Linde Y, SAPO-37, ZSM-20, (b) Ferrierite type 10-ring, examples: NU-23, ZSM-35 (c) Chabazite type 8-ring, examples: AlPO-34, Linde D, SAPO-34 (Baerlocher et al., 2007).

The Structure Commission of the International Zeolite Association (IZA-SC) identifies each framework type with a three-letter code. Table 2.2 lists some of the important zeolites with three-letter codes based on Si/Al ratio or phosphate content.

Table 2.2. Nomenclature and specifications of important zeolites (Pramatha and Prabir, 2003).

Low Silica $\frac{Si}{Al} \leq 2$		Intermediate Silica $2 < \frac{Si}{Al} \leq 5$		High Silica $5 < \frac{Si}{Al}$		Other elements	
IUPAC name	Example	IUPAC name	Example	IUPAC name	Example	IUPAC name	Example
ANA	Analcime	BHP	Linde Q	BEA	Zeolite β	AEI	AlPO4-18
BIK	Bikitaite	FAU	NaY	FER	Ferrierite	AEL	AlPO4-11
CAN	Cancrinite	FER	Ferrierite	MEL	ZSM-11	AFN	AlPO4-14
EDI	Edingtonite	LTL	Linde L	MFI	ZSM-5	AFR	SAPO-40
FAU	NaX	MAZ	Mazzite	MFS	ZSM-57	AFX	SAPO-56
FRA	Franzinite	MEI	ZSM-18	MSO	MCM-61	CAN	Tiptopite
LTA	Linde A	MER	Merlinoite	MTF	MCM-35	CHA	SAPO-47
PHI	Phillipsite	MOR	Mordenite	MTT	ZSM-23	FAU	SAPO-37
SOD	Sodalite	OFF	Offretite	MWW	MCM-22	OSI	UiO-6
THO	Thomsonite	STI	Stilbite	ZSM	ZSM-48	SAV	Mg-STA-7

2.2.2.1 **Low-silica zeolites**

Low-Silica zeolites or aluminium-rich zeolites are nearly saturated in aluminium with a molar ratio of Si/Al≈1 with maximum possible aluminium content in the tetrahedral framework (e.g. zeolite A and X) and as a result they contain the maximum number of cation exchange sites. This characteristic gives them a strong hydrophilic surface selectivity (Kulprathipanja, 2010). Their pore volumes are the highest among other known zeolites and give them a distinct economic advantage in bulk separation and purifications where high capacity is required (Flanigen, 1984).

2.2.2.2 Intermediate-silica zeolites

Intermediate-Silica zeolites were invented for the first time by scientists at Union Carbide Laboratories in the early 1950's with improved thermal, hydrothermal, and acid stability. They found significant commercial market as both an adsorbent and hydrocarbon conversion catalyst when they were introduced for the first time. The surface of these zeolites is still heterogeneous and exhibits high selectivity for water and other polar molecules (Flanigen, 1984). The intermediate zeolites with 2<Si/Al<5 consist of the natural zeolites such as mordenite, erionite, clinoptilolite, Chabazite and the synthetic zeolites such as omega, mordenite, Y, and L. These materials still have hydrophilic property in this Si/Al range (Kulprathipanja, 2010).

2.2.2.3 High-silica zeolites

High-silica zeolites with Si/Al > 5 or higher are more hydrophobic and organophilic in nature, with more diluted numbers of strong Brønsted acidic sites and also higher thermal and hydrothermal stability (Szostak, 2001). High silica zeolites can be obtained directly during the synthesis procedure by addition of organic component to aluminosilicate and silicate gels or by post-synthesis or modification such as hydrothermal steaming, use of aqueous $(NH_4)_2SiF_6$, $SiCl_4$ or F_2 gases (Flanigen, 1984). Removal of framework aluminium by dealumination results in better catalytic properties and enhanced thermal stability (Pramatha and Prabir, 2003)

2.2.2.4 Other elements

Many elements now have been incorporated into zeolite framework. Substitution of P in zeolite framework by Si leads to silica-alumina-phosphates (SAPOs), with cation-exchange abilities. Aluminophosphates (AlPOs) have alternating AlO_2^- and PO_2^+ units. The framework is neutral, organophilic, and non-acidic. Incorporation of elements such as Si, Mg, Fe, Ti, Co, Zn, Mn,

Ga, Ge, Be, Li, As, and B into the tetrahedral sites of AlPOs gives a vast number of element-substituted molecular sieves (MeAPO, MeAPSO, SAPO) which are important heterogeneous catalysts (Pramatha and Prabir, 2003).

2.2.3   **Application of zeolites**

Zeolites have a wide use in industries such as detergents, gas separation, desiccants and catalysts. Natural zeolites are mainly used in bulk mineral applications due to their lower cost. Figure 2.5 shows the application of zeolites in different industries. In 2008, a total of 1.27×10^6t was estimated to be consumed in those applications. The second largest use of zeolites is as catalysts (17%) which accounts for more than 55% of the market on a cash basis owing to the greater expense of zeolites used as catalysts compared with other uses. More than 95% of the total zeolite catalyst consumption is zeolite Y which is used for Fluid Catalytic Cracking (FCC) process. Smaller volumes are used for petrochemical synthesis or in hydrocracking process. In 2008 it was estimated that the catalyst consumption has been around 0.3×10^6 t (Davis and Inoguchi, 2009). Zeolites are used as adsorbents for drying and purification of petrochemical streams (e.g., ethylene, propylene) and natural gas, bulk separations of chemicals (e.g. normal paraffins or xylenes) and in air separation industries to produce oxygen by pressure swing adsorption (PSA) or vacuum pressure swing adsorption (VPSA). In 2008, about 0.18×10^6 t (10%) of zeolite was used as adsorbent. Zeolites are also used in transformation of photochemical organics, sensor industries, removal of odour, filler in paper, conversion of solar energy, plastic additives, soil conditioner and fertiliser, pozzolanic cement and concrete, lightweight aggregate, and dietary supplement in animal nutrition (Flanigen, 1980).
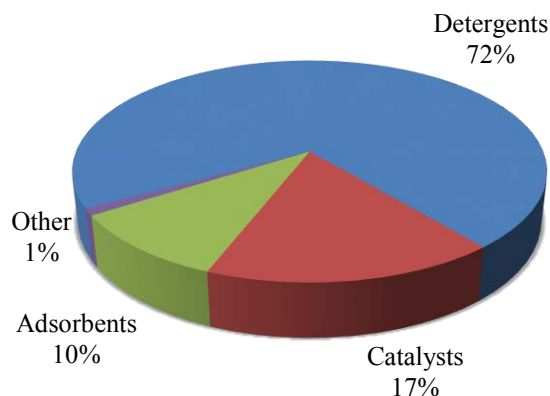
Figure 2.5. Application of zeolites in different industries in 2008 (Davis and Inoguchi, 2009).

In 2008, it was estimated that the world production of natural zeolites is about 3.0×10^6 t. The biggest consumers of natural zeolites are China and Cuba to mainly enhance the cement strength. The price of zeolites significantly depends on the application. For example, in United States, the price of natural zeolite for bulk applications is about 0.04-0.25 USD/kg and 1.5-3.5 USD/kg for industrial adsorbent applications. The typical price of zeolite for catalyst applications varies from 3-4 USD/kg for FCC to about 20 USD/kg for specialty catalysts. This price is 5-9 USD/kg for adsorbents and about 2 USD/kg for detergents. (Davis and Inoguchi, 2009).

2.2.4   Zeolites as catalyst

Table 2.3 lists the main applications of zeolites as catalyst. The catalysis over zeolites can be categorised to three different classes: 1) Inorganic reactions, 2) Organic reactions, and 3) Hydrocarbon conversion. Zeolites as catalysts have many unique properties such as acidity, shape-selectivity, high surface area and structural stability which will be discussed further in the following sections.

Table 2.3. Application of zeolites as catalyst (Pramatha and Prabir, 2003).

Inorganic reactions	Organic reactions	Hydrocarbon conversion
H_2S oxidation	Aromatisation (C4 hydrocarbons)	Alkylation
NO reduction of NH_3	Alkylation (naphthalene, benzene ethylbenzene, aniline, biphenyl, polyaromatics, etc.)	Cracking
CO oxidation, reduction		Dehydration
Decomposition of H_2O		Fischer-Tropsch synthesis
	Aromatics (hydrogenation, oxidation, nitration, disproportionation, hydroalkylation, hydroxylation, oxyhalogenation, etc.)	Friedel-Crafts alkylation
		Hydrocracking
		Hydrogenation , Dehydrogenation
		Hydrodealkylation
		Isomerisation
	Chiral (enantioselective) hydrogenation	Methanol to gasoline
		Methanation
	Cyclohexane (oxidation, isomerisation, aromatisation, ring opening)	Shape-selective reforming

2.2.4.1 Acidity and basicity

A basic definition is that a Lewis acid is an electron pair acceptor and a Lewis base is a species with an available (reactive) pair of electrons or an electron donor. Brønsted argued that all acid-base reactions involve the transfer of a proton (H^+ ion). According to this theory, an acid is a "proton donor" and a base is a "proton acceptor". Therefore, in solid surfaces, the Brønsted acid site is able to transfer a proton from the solid to the absorbed molecule while the Lewis acid sites are able to accept electron pair from the adsorbed molecule.

The acidic nature of zeolites is due to the metal cations or hydroxyl protons on their extra-framework. In aluminosilicate-type zeolites, the 4^+ charges on framework silicon atoms at tetrahedral positions (T position) and the 2^- charges on the coordinating oxygen atoms lead to neutral SiO_4 tetrahedra. Substitution of silicon atoms in the framework by aluminium atoms can change the corresponding tetrahedra charges from neutral to 1^-. These negative framework

charges are balanced by extra-framework metal cations or hydroxyl protons forming weak Lewis acids site or strong Brønsted acid sites, respectively, responsible for the catalytic activity of the zeolite materials (Hunger, 2010).

The first type of hydroxyl protons on zeolites are those located on oxygen bridges connecting silicon and aluminium atoms of the framework. These hydroxyl groups are commonly donated structural or bridging OH groups or Si-OH-Al (Figure 2.6.a). The second important type of hydroxyl groups in zeolites are the silanol groups or Si-OH, also called terminal OH groups, which are located on the external surface of crystal particles (Figure 2.6.b). Dealumination of the zeolite framework by calcination, hydrothermal treatment, or treatment with strong acids, is the most important reason for the formation of these silanol groups. Depending on the treatment conditions, silicon migration, formation of silanol groups, formation of hydroxyl groups at extra-framework aluminium may occur (Figure 2.6.c). Sometimes, dealumination of the zeolite framework is accompanied by the formation of Lewis acid sites at extra-framework aluminium species and framework defects (Figure 2.6.d). If these Lewis acid sites are located in the area close to bridging OH groups, super-acidic Brønsted sites are formed (Hunger, 2010).
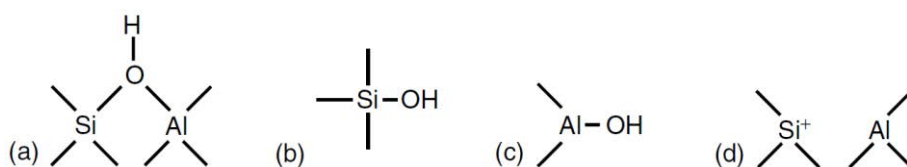
Figure 2.6. Different types of hydroxyl group and acid sites in zeolites (Hunger, 2010).

Although, acidic zeolites as solid catalysts have a wide range of application in chemical industries, less attention has been paid in the literature to use these microporous and mesoporous materials as a basic catalyst. These solid catalysts with basic properties have a considerable potential for a number of important industrially processes (e.g. Claus reaction). The nature of basic sites in zeolites is less well-defined than that of acid sites. This is probably

due to the fact that the basic framework oxygen atoms or alkali metal cations on the zeolite framework act as weak Lewis acid sites as well. The basicity of zeolites can be enhanced by changing the electronegative charge of the framework or by introduction of a basic component to their structure. Alkali-exchange of zeolites in aqueous solution or by solid-state ion exchange leads to materials which possess basic framework oxygen atoms of relatively low base strength (Hunger, 2010).

Different techniques such as IR Spectroscopy, Alkane Cracking, UV-Visible Spectroscopy, Temperature-Programmed Desorption of Amines, Microcalorimetry and Solid-state NMR Spectroscopy have been used to quantify the Brønsted and Lewis sites in a solid acid system, however, most of these techniques cannot easily discriminate between Lewis and Brønsted sites. In other words, no single characterisation can provide all the information unambiguously, so a combination of two or more techniques is required (Farneth and Gorte, 1995).

2.2.4.2 Shape selectivity

Shape selective catalysis is based on the difference between the dimensions of reactants, products, or intermediate molecules and size of the pores. Only molecules with dimensions less than a critical size can enter the pores and react on the internal catalytic sites. Moreover, in the final product, only molecules that can leave the pores appear. Thus, shape selective catalysis can be used to improve the yield of desired products and/or to prevent production of undesired products (Csicsery, 1986).

Three types of shape selectivity can be distinguished depending on whether pore size limits the entrance of the reactant's molecules, removal of the produced molecule from the pores, or the formation of certain transition states.

These three variants, which can however, overlap are:

- Reactant selectivity

- Product selectivity

- Restricted transition state selectivity

Reactant selectivity means that starting material molecules that are larger than the pore size cannot enter the pores, in other words, only starting materials with a certain size and shape can penetrate into the zeolite pores (Figure 2.7.a). The term "molecular sieve" applies to this class of zeolites. Table 2.4 compares the kinetic molecular diameters of some reagents with the pore opening of some zeolites. These data are useful to choose a suitable zeolite for a particular starting material. However, it should be noted that the kinetic diameter is only a rough estimate of the molecular size since molecules are not rigid objects (Chen et al., 1989).

Table 2.4. Pore sizes of zeolites and molecule diameters.

Zeolite	Pore size (Å)	Molecule	Kinetic diameter (Å)
KA	3.0	He	2.5
SAPO-34	3.8	NH_3	2.6
NaA	4.1	H_2O	2.8
CaA	5.0	N_2, SO_2	3.6
Erionite	3.8×5.2	Propane	4.3
ZSM-5	5.1×5.5 5.3×5.6	n-Hexane	4.9
Beta	5.6	Isobutane	5.0
CaX	6.9	Benzene	5.3
Mordenite	6.7-7.0	p-Xylene	5.7
NaX	7.4	CCL_4	5.9
AlPO-5	7.3	Cyclohexane	6.2
VPI-5	12.7	o-,m-Xylene	6.3

Dehydration of butanol over CaA zeolite is an example of reactant selectivity in zeolites. The straight-chain alcohol is dehydrated much faster than iso-butanol which has a larger molecular diameter (Hagen, 2006).

Product selectivity in zeolite occurs when the size of the molecule formed inside the pores is too large to diffuse out of the pores. Methylation of toluene and the disproportionation of toluene over ZSM-5 are the well-known examples of product selectivity in the zeolites. In both cases all three isomers o-, m-, and p-xylene are formed inside the pores and although the thermodynamic equilibrium corresponds to p-xylene fraction (as desired product) is only 24%, it can be obtained with selectivity of more than 90 %. This is due to the fact that p-xylene has smaller dimensions with a diffusion rate of 10^4 faster than other two isomers. In other words, although all the isomers are produced relatively rapidly in the zeolite cavity, the diffusion of p-xylene out of the cavity is much faster (Hagen, 2006).
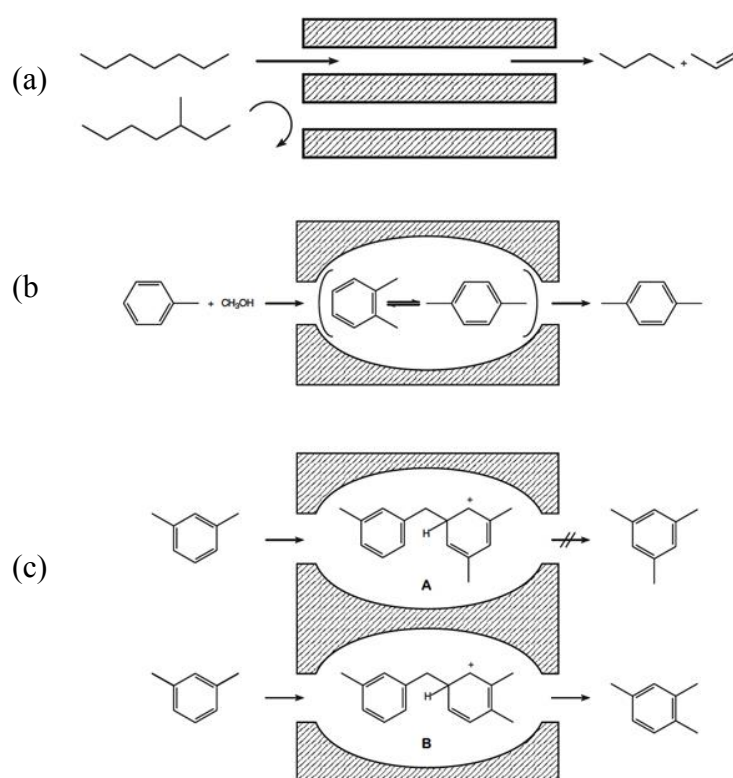
Figure 2.7. Shape selectivity of zeolites with examples of reactions: a) Reactant selectivity: cleavage of hydrocarbons, b) Product selectivity: methylation of toluene, c) Restricted transition state selectivity: disproportionation of m-xylene (Hagen, 2006).

Restricted transition state selectivity depends on the available space in the cavities or pores of the zeolite. In this case, the chemical reaction pathway is altered because certain reactions are prevented due to the required space for corresponding transition state. Only those intermediates that have a geometrical fit to the zeolite cavities can be formed during catalysis and reactions that require smaller transition states can be proceed with no hindrance.

In practice, it is often difficult to distinguish between product selectivity and restricted transition state selectivity. Alkylation of benzene with ethylene over ZSM-5 zeolite to produce ethylbenzene is an example of restricted transition state selectivity. By suppression of other side reactions it is possible to achieve high ethylbenzene selectivity (Csicsery, 1986).

2.2.5 Modification of zeolites

The structure and framework composition of zeolites can be tailored and utilised for specific applications. There are two routes to achieve this goal: (1) direct synthesis and (2) post-synthetic treatment and modification.

The direct synthesis is the main route of the synthesis of zeolites. Many parameters such as composition of synthesis mixture, synthesis temperature, and time, solution pH, aging and seeding, directing agent or template have influence on the zeolite structure. However, in most cases, the direct synthesis route does not lead to the formation of zeolites with desirable properties for the final applications.

In addition to the direct synthesis method, post synthetic treatment such as ion exchange, preparation of metal-supported zeolites, dealumination, reinsertion of heteroatoms (e.g. B, Ga, Ge, or Al) into zeolite framework, and other modification methods provides a more practical route to modify the zeolites to acquire desirable framework compositions and other properties (Chen and Zones, 2010). For example, for catalytic cracking process over HY zeolite, strong

acid activity and high thermal and hydrothermal stability is required. It is well known that the higher the SiO_2/Al_2O_3 ratio, the more stable the zeolite structure. Unfortunately, few zeolites can be prepared with the desired SiO_2/Al_2O_3 ratio through direct synthesis and this ratio is limited to a maximum value around six. Dealumination, in this case is a useful way to increase the SiO_2/Al_2O_3 ratio. Three dealumination methods have been used to produce the desired properties:

1) Hydrothermal treatment (e.g. steaming).

2) Chemical treatment (e.g. reaction with EDTA, $(NH_4)_2SiF_6$, $SiCl_4$, F_2 gas).

3) Combination of hydrothermal and chemical treatment (e.g. treatment with HCl, HNO_3, NaOH, KF).

The Si/Al ratio plays a significant role, since the catalytic activity of a zeolite depends on the number of acidic OH groups on the aluminium in the framework, and it is directly related to the formation of carbonium or carbenium ions inside the zeolite. Dealumination can improve the porous structure and enhance some important zeolite properties (e.g. zeolite acidity, catalytic activity, thermal and hydrothermal stability, resistance to aging and coking). However, severe dealumination can decrease the zeolite crystallinity. Dealumination might be expected to reduce the catalytic activity of zeolites; however, if the effect of increase in the acid strength surpasses the effect of the decrease in the acidic centres, dealumination can sometimes result in enhancement of catalytic activity. The enhancement of the acid strength of OH groups is caused by their interaction with aluminium species dislodged from the framework and left in the cavities (Kozo Tanabe and Hideshi, 1989).

The aluminosilicate structure of the zeolites is ionic and contain Si_4^+, Al_3^+ and O_2^- ions. Replacing some of the Si_4^+ ions by Al_3^+ ions in the SiO_4 tetrahedra of zeolite framework is led to generation of an excess negative charge. In this case, a compensating source of positive

charge (cations) must be added to neutralise the framework charge. These non-framework cations play an important role in determining the catalytic properties of the zeolite. An aqueous salt solution may be used to incorporate the cations from the salt into the zeolite.

Solid-state reactions between zeolites and compounds of cations, which are desired to enter the porous structure of the zeolite, is another method of preparation. Advantages over conventional ion-exchange in liquid phase are:

1) Prevention of handling large volume of salt solutions

2) Less generation of waste salt solution

3) Introducing metal cations into narrow pore cavities where the ion-exchange in aqueous solutions is not efficient

In this method, first, an intimate mixture of the two components (e.g. zeolite and compound with cation) is prepared. The mixture is subsequently heated in an inert gas stream or high vacuum to release volatile products such as hydrogen halides, ammonia, water, etc. Typically reaction temperature of 250-350°C and reaction time of a few hours are required (Karge, 1997).

2.3   Alkylation process

2.3.1   Introduction

Alkylation is the process where an alkyl group is introduced into a molecule. The alkyl group may be transferred as an alkyl carbocation, a free radical, a carbanion or a carbene (or their equivalents). According to nucleophilic or electrophilic character of alkylating agents, they can be categorised to two different groups.

Nucleophilic alkylating agents deliver negatively charged group to the hydrocarbons (carbanion). They can also displace halide substituents on a carbon atom and alkylate alkyl and aryl halides, in the presence of catalysts. Examples of this group are organometallic compounds e.g. organocopper, organomagnesium, and organosodium (Mehrotra, 2007).

Electrophilic alkylating agents deliver a positively charged alkyl group to the hydrocarbons. The use of alkyl halides with a Lewis acid catalyst to alkylate aromatic substrates in Friedel-Crafts reactions is an example for this group. Alkyl halides can also react directly with amines alcohols, carboxylic acids and thiols. It should be noted that the soluble electrophilic alkylating agents are often very toxic, due to their ability to alkylate DNA and should be handled with proper care. These alkylating agents have been also used as anti-cancer drugs in the form of antineoplastic agents, and as chemical weapons such as mustard gas (Scott, 1970).

2.3.2   Friedel-Crafts alkylation

The Friedel–Crafts reactions for the first time developed by Charles Friedel and James Crafts in 1877 to attach an alkyl halide with an aromatic compound in the presence of Lewis acid which results in replacement of hydrogen by an alkyl substituent. The Friedel-Crafts reaction (FC) is a well-known method to introduce alkyl substituents on an aromatic ring by generation

of a carbocation or related electrophilic species. These electrophiles can be generated via a reaction between an alkyl halide and a Lewis acid. The most common Friedel-Crafts Lewis acid catalysts are $AlCl_3$, $SbCl_5$, $BeCl_2$, $TiCl_4$, $SnCl_4$, and BF_3. Furthermore, strong Brønsted-acids including sulphuric acid, hydrofluoric acid or super acids such as HF, SbF_5, HSO_3F and SbF_5 have also been shown to accelerate the FC transformation (Carey and Sundberg, 2007). One of the major setback of the Friedel–Crafts alkylation reaction for synthesis of organic compounds is that it requires stoichiometric or super stoichiometric amounts of a Lewis acid or Brønsted acid and toxic alkyl halides which eventually leads to production of huge amounts of salt by-products. Therefore, using only catalytic amounts of a metal or acid catalyst in FC reaction would be highly desirable to have a more environmentally and economically benign process. Moreover, replacement of the alkyl chlorides by other alkylating agents with less toxicity, such as alcohols, would be a major improvement as water would be the only side product (Rueping and Nachtsheim, 2010). Other limitations of the Friedel-Crafts alkylation by Lewis or Brønsted acids in liquid phase are:

- Rearrangement of the alkyl group by forming a more stable carbocation.

- Introduction of more than one alkyl group in the molecule ring.

- The steps in the Friedel-Crafts alkylation are reversible and rearrangements may occur.

The use of zeolites as recyclable, environment friendly acidic catalysts whose pore structure is able to induce unique selectivity effects has been reported both in patent (Hardacre et al., 2004, Hendriksen et al., 2001) and literature (Reddy et al., 1993, Marczewski et al., 1989).

2.3.3   **Alkylation of naphthalene**

2.3.3.1 **Introduction**

Alkylated naphthalene derivatives are important products to the chemical industry. For example, 2-methylnaphthalene is an intermediate for the synthesis of vitamins A (Kamalakar et al., 2000), K1 and K3 (Gläser and Weitkamp, 2003) or 2,6-dialkylated naphthalene can be oxidised to 2,6-naphthalenedicarboxylic acid serves as a building block for liquid-crystalline polymers such as polyethylene naphthalene (PEN), poly butylene naphthalene (PBN) or liquid crystalline polymers (Collin, 1991). Figure 2.8 shows some of the applications of polyalkylated naphthalene products in different industries.

Figure 2.8. Poly-alkylated naphthalene applications in food and drinks packaging industry, as films in flexible circuitry and optical displays/touch screens and as fibres for tyre cord and high performance sailcloth.

2.3.3.2 **Di-alkylated-naphthalene**

Di-alkylated-naphthalene (DAN) mixtures such as di-(isopropyl)-naphthalene (DIPN) or di-(t-butyl-naphthalene (DTBN) are mostly prepared from naphthalene or mono-isopropyl-naphthalene through alkylation or trans-alkylation. Depending on the reaction conditions used (e.g., catalyst type, temperature, pressure, contact time, feed molar ratio, etc.) isomers with

different proportions are present in the mixture. Generally, DIPN product mixture obtained under mild reaction conditions and at short contact time are rich in α,α-isomers whereas β, β-isomers are more obtained under severe conditions and at longer reaction times. Theoretically, 10 substitutional isomers are possible: 1,2-, 1,3-, 1,4-, 1,5-, 1,6-, 1,7-, 1,8-, 2,3-, 2,6- and 2,7-DIPN, however 1,2-, 1,8- and 2,3-DIPN cannot be detected in the mixture (Brzozowski et al., 2001).
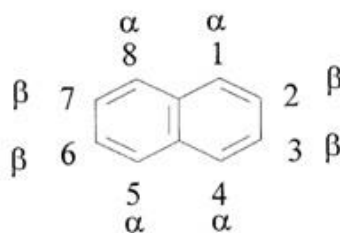
Figure 2.9. Different possible substitution positions of naphthalene for alkyl groups.

Due to the higher electron density, the α-isomers in the naphthalene nucleus are more reactive than the β-isomers. In other words, the α-substitution is kinetically more preferred, whereas the β-substitution is thermodynamically more preferred (Friedman and Nelson, 1969).

2.3.3.3   **Effect of alkylating agent**

Different alkylating agents, such as methanol (Bai et al., 2009), ethanol (Kamalakar et al., 2000), isopropyl alcohol (Song and Kirby, 1994), propene (Kim et al., 1995), isopropyl bromide (Moreau et al., 1992b), tert-butyl alcohol (Kamalakar et al., 2002), cyclohexyl bromide (Moreau et al., 1992a), and cyclohexene (Moreau et al., 1993), have been evaluated in this type of reaction over various zeolite catalysts. Choosing a proper alkylating agent for the alkylation of naphthalene depends on different parameters such as the final desired product, desired selectivity and ease of separation of final product. Table 2.5 lists the most important products and their applications from alkylation of naphthalene with different alkylation agents.

Table 2.5. Application and name of some naphthalene alkylated products.

Reactants	Products	Application	Reference
Naphthalene + Methanol	2-methylnaphthalene	an intermediate in the synthesis of the vitamins K1 and K3	(Collin, 1991)
Naphthalene + Methanol	2,6-dimethylnaphthalene	2,6-Naphthalenedicarboxylic acid (NDCA) to produce polyester resins	(Collin, 1991)
Naphthalene + Methanol	2,6-dimethylnaphthalene	2,6-dihydroxynaphthalene (DHN)	(Collin, 1991)
Naphthalene + Ethanol	2,6-diethylnaphthalene	Polyethylene Naphthalene dicarboxylate (PEN)	(Kirk and Othmer, 1981)
Naphthalene + t-Butanol	2,6-dibutylnaphthalene	Polybutylene Naphthalene (PBN)	(Papageorgiou and Karayannidis, 2001)
Naphthalene + Isopropanol	2,6-diisopropylnaphthalene	Advanced polymer material with high thermal and mechanical stability	(Kirk and Othmer, 1981)
Naphthalene + Propylene	Diisopropylnaphthalene mixture	High quality solvent for copying material	(Brzozowski and Vinu, 2009)

Wang et al. (2003) states that the isopropyl group is more sterically hindered than the methyl group, implying higher possibility of 2,6-DIPN selectivity. They add that 2,6-DIPN is more easily oxidised into the naphthalene-2,6-dicarboxylic acid and has more atomic economy in the oxidation process as compared with 2,6-di-t-butylnaphthalene or 2,6-dicyclohexylnaphthalene. However, Armengol et al. (1997), Smith and Roberts (2000) and Kamalakar (2002) focus on t-butyl alcohol because of it being a much bulkier substituent than isopropyl or cyclohexyl from which it was expected high β,β-selectivity would result, especially high 2,6-selectivity. On the other hand, Moreau et al. (2000) point out that 2,6-DTBN could be isolated from the reaction mixture by recrystallisation. They calculated the heat of formation for both DIPN and DTBN and stated that the selectivity of 2,6-DTBN is higher than 2,6-DIPN due to lower heat of formation of 2,6-DTBN and therefore this component is more stable. Wang et al. (2008) has made a computational analysis in molecular dimensions of 2,6-DAN and 2,7-DAN and

concluded that the big difference between the dimensions of DTBN isomers can lead to a higher 2,6/2,7 ratio on shape selective alkylation of naphthalene. Table 2.6 shows the different properties of 2,6 and 2,7 dialkylated naphthalene isomers.

Table 2.6. Effect of the alkyl group on the dimensions of β,β-isomers (Wang et al., 2008).

	Isopropyl-		tert-Butyl-	
	2,6-	2,7-	2,6-	2,7-
Critical diameter (Å)	7.21	7.26	7.1	7.5
Molecular length (Å)	13.14	13.14	11.7	11.1
Molecular thickness (Å)	6.52	6.52	4.3	4.3
Heat of formation (Kcal/mol)	3.44	3.44	3.04	3.06

Kamalakar et al. (2002) has provided two reasons for choosing t-butanol as the alkylating agent. Firstly, the t-butyl group encounters more hindrance when compared to ethyl and isopropyl groups in the 2,6-positions of naphthalene, which can help to obtain 2,6-DTBN naphthalene selectively by avoiding formation of polyalkylated naphthalenes. Secondly, the t-butyl alcohol forms a stable cation which facilitates the alkylation reaction.

2.3.3.4 Zeolite as catalyst for dialkylation of naphthalene

Zeolite has been used for alkylation of many aromatics such as aniline, benzene, biphenyl, ethylbenzene, naphthalene, polyaromatics, etc. Different zeolite catalysts, such as HY, Hβ, HZSM-5, Mordenite, SAPO-5 and MCM-41 have been studied for the alkylation of naphthalene and proved to be the most promising solid acidic catalysts with high selectivity to 2,6-DAN production (Chu and Chen, 1995, Kamalakar et al., 1999, Sugi et al., 2008). For example, high shape selectivity was observed over H-Mordenite, but it suffers from low activity owing to its narrow pores (Katayama et al., 1991). It is therefore challenging to achieve both high naphthalene conversion and high 2,6-DAN selectivity by modification of zeolite to change

its acidity, porosity and stability. The main goals of choosing a proper zeolite catalyst and/or modification of that zeolite are to obtain:

- High conversion of naphthalene to DAN products.

- High selectivity of 2,6-DAN than other isomers.

- Longer catalyst life time.

Acidity and pore size of the zeolites are the most important parameters which have been studied carefully by researchers. Although, other parameters (e.g., BET surface area, pore volume, crystal size, etc.) are important, but there is no clear discussion of these effects on the catalyst activity and selectivity in the literature.

2.3.3.4.1 **Acidity effect**

Acidity is an important factor for the alkylation of aromatic compounds. Many researchers pointed out that in the alkylation of naphthalene, an optimum number of acidic centres are required (Kamalakar et al., 1999, Wang et al., 2008). Kamalakar et al. (2002) stated that medium or weak Brønsted acidic centres are required for selective formation of 2,6- DAN and later they showed that a large amount of unwanted products such as tri- and poly-alkylated naphthalene are produced due to the strong acidic centres present in the zeolite. Wang et al. (2008) reported similar observation. They stated that 2,6-/2,7-DTBN ratio was more sensitive to the change of strong acid sites, and the moderate numbers of strong acid sites might associate with comparatively higher selectivity for 2,6-DTBN, in other words, the key factor for higher selectivity is not the total number of acid sites, but the number of moderate acid sites and distribution of internal channel surface of catalytic sites (strong acid sites). There are many different ways to increase or decrease the acidity of zeolite catalyst to achieve optimum acidity strength. Modification of zeolite by introducing some guest species into the zeolite channels,

changing the Si/Al ratio and dealumination by means of steaming can change the acidity distribution of zeolite.

2.3.3.4.2 Modification by ion-exchange

Introduction of guest elements as cations (e.g. alkali, alkaline earth, transition metals and rare earth elements) inside the zeolite structure can decrease its total surface area but increases the number of acidic centres. Transition metals such as zinc, cadmium, or gallium ions create new Lewis acid sites in the zeolite framework. In contrast, insertion of inert alkali or alkaline earth metals such as sodium, potassium, calcium or magnesium can decrease the total acidity of zeolite by neutralising the Brønsted acidic centres and enhancing the basic properties of lattice oxygen (Corma, 2003). Moreover, impregnation of zeolite with cations of variable valence such as Cu^+, Co^{2+}, Fe^{2+}, Mo^{6+}, or V^{5+} enhances the activity of zeolites in redox reactions. In addition the charged species in the zeolite usually produce a relatively strong electrostatic field that, in principle, can polarise molecules restrained in the microporous matrix resulting in their activation (Pidko, 2008). Kamalakar et al. (1999, 2000) have investigated the effect of rare earth modified HY and HMCM-41 zeolite for the alkylation of naphthalene. They modified the zeolites by lanthanum, cerium and potassium and observed the following trend for the conversion of naphthalene: LaKY **>** HMCM-41 **~** LaY > CeMCM-41 > LaMCM-41 but zeolite modification decreased the selectivity to 2,6-DIPN in all cases. They reported that the trend in the ammonia TPD is similar to the trend in the catalyst activity. The effects of ion exchanged zeolite with alkali, alkaline earth, transition metals and rare earth cations on many different Friedel-Crafts reactions have been studied but there are a lack of data on performance of these catalysts for selectivity and activity of zeolites for alkylation of naphthalene.

2.3.3.4.3 **Modification by changing Si/Al ratio**

Practically, changing the Si/Al ratio is possible by extracting Si or Al element from the zeolite structure. Wang et al. (2008) studied different methods to change the Si/Al ratio on a commercial HY zeolite. They used solutions such as HCl, Oxalic acid ($H_2C_2O_4$), NaOH and steaming for the modification of zeolite. Table 2.7 summarises the results of this study.

Table 2.7. HY zeolite modification by chemical and hydrothermal treatment (Wang et al., 2008).

Zeolite name	Treatment medium	Modified zeolite name	Si/Al ratio	Acidity (mmol of NH_3 adsorbed/g)
Commercial HY	------	------	5.20	0.59
Commercial HY	HCl	HY-H	7.04	0.59
Commercial HY	Oxalic acid ($H_2C_2O_4$)	OY	8.66	0.3
OY	Water vapour (at 650 °C)	OSY	17.76	0.36
OSY	NaOH	OSY-B	11.85	0.10
OSY-B	Water vapour (at 650 °C)	OSY-BS	12.19	0.13
OSY-BS	HCl	OSY-BS-H	18.83	0.29

It is clear from Table 2.7 that dealumination by acid and hydrothermal treatment led to an increase in Si/Al ratio and therefore increasing in total acidity while using NaOH decreased this ratio by dissolving the silicon placed on the surface of zeolite. Moreover, NaOH can reinsert the extra framework aluminium into the FAU framework. Song and Kirby (1994) reported that the removal of Al from H-Mordenite zeolite structure affects the channel structure by increasing the mesopore volume and thus increasing the diffusivity of reactant and product molecules to and from active sites. Therefore, dealumination of H-Mordenite generally leads to a decrease in the number of acidic sites, an increase in the acid strength, and increased diffusivity. Steam treatment or hydrothermal treatment of zeolites as a tool for dealumination has been reported comprehensively in literature (Barthomeuf, 1987, Song and Kirby, 1994, Kim et al., 1995).

2.3.3.4.4 **Pore Size effect**

Chu and Chen (1995) studied the effect of pore structure on the activity and selectivity of the zeolite in the alkylation of naphthalene. They observed that at same reaction conditions, the activity trend of zeolites were as follows: USY > H-Beta > H-Mordenite > H-ZSM-5, while the selectivity trend to 2,6-DIPN was H-mordenite > H-Beta > USY > H-ZSM-5. They concluded that the USY zeolite gives the highest activity and stability, although its selectivity to 2,6-DIPN is less than other zeolites. Moreover, H-ZSM-5 zeolite is not active due to narrow pore channels. Kamalakar et al. (2002) discussed the relation between product molecule size and zeolite pore size. They calculated the critical molecule diameters of products from t-butylation of naphthalene using CERIUS software as shown in Table 2.8:

Table 2.8. Critical molecular diameters (Å) of different DTBN isomers (Kamalakar et al., 2002).

Product	Along X-axis	Along Y-axis	Along Z-axis
2,6-DTBN	13.424	7.132	6.727
2,7-DTBN	13.458	8.041	6.726
1,5-DTBN	10.125	10.007	6.727
1,8-DTBN	10.124	8.671	6.313
2-DTBN	11.487	7.019	3.727
1-DTBN	10.124	8.671	6.313

Critical molecular diameters of the expected products were calculated using shadow indices of the CERIUS2 software. They state that among all the isomers of DTBN, 2,6-DTBN is more linear than other isomers and is less hindered and can diffuse more easily through the pore mouth of large pore zeolites. The molecular diameters calculated from the simulation studies also support the experimental results. It is observed that modified HY zeolite yielded 2,6-DTBN/2,7-DTBN up to 1–1.9. The 2,6-DTBN selectivity is more predominant than 2,7-DTBN, which is mainly due to the more linear nature of the 2,6-DTBN when compared to the 2,7-DTBN.

2.3.3.5 **Effect of Temperature**

Most researchers are in agreement that by increasing the temperature, the conversion of naphthalene is increased, in accordance with the Arrhenius effect. Wang et al. (2003) report that in alkylation of naphthalene by isopropanol, conversion increases rapidly with temperature up to 230 °C, beyond which the increase is slow. Increasing the temperature up to 230°C decreases IPN production while more DIPN and PIPN are produced but in higher temperature, this trend becomes slow. They indicate that the maximum 2,6-/2,6- DIPN ratio is at 250 °C. Marathe et al. (2002) reported that the conversion of naphthalene in the alkylation of naphthalene by t-butanol, which forms a more stable carbocation, is not rapid beyond 180 °C. Liu et al. (1997) state that at higher temperatures secondary reactions, such as dealkylation, disproportionation or transalkylation of DTBN can take place and in some cases, polybutene compounds such as dimers and trimers of t-butyl group are observed. They report that the various reactions which occur in the reaction system of naphthalene alkylation with t-butanol by increasing the temperature have the following order (Scheme 2.1):

Monoalkylation > Dialkylation > isomerisation of DTBN > Transalkylation ~ disproportionation ~ dealkylation

→ Temperature increasing
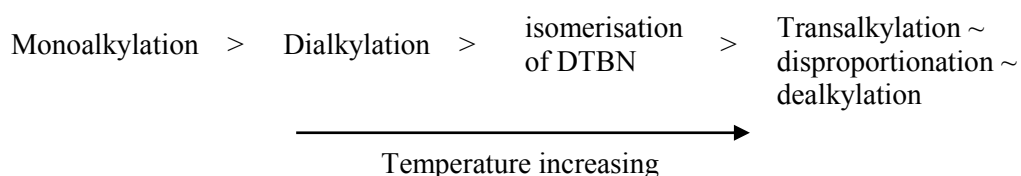
Scheme 2.1 Effect of increasing the temperature on the order of various reactions in alkylation of naphthalene.

The reaction pathway for t-butylation of naphthalene proposed by Liu et al. (1997) is shown on Scheme 2.2. The main reactions in this system are alkylation, dealkylation and oligomerisation of t-butyl groups.
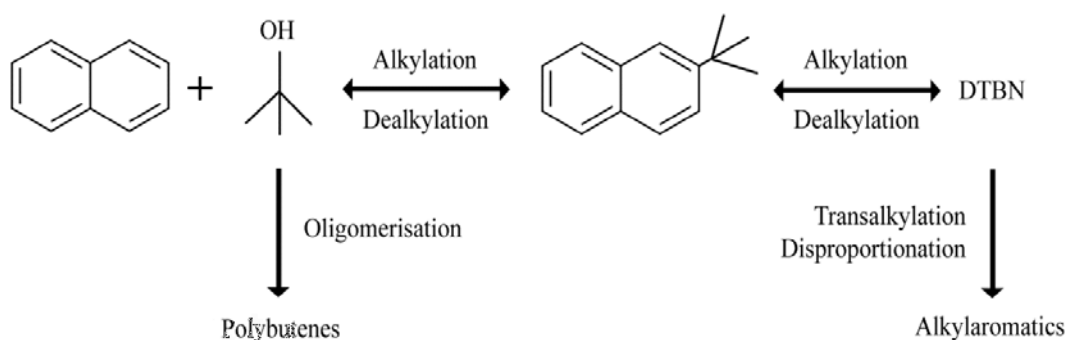
Scheme 2.2 Possible reactions of naphthalene alkylation by t-butanol at different temperatures (Liu et al., 1997).

2.3.3.6 Effect of Pressure

Wang et al. (2003) studied the effect of pressure on the isopropylation of naphthalene over USY and H-Mordenite zeolite. They observed that at pressures higher than 10 bar, USY exhibits high and stable activity with a conversion of around 90% while at atmospheric pressure, a little deactivation appears, with a conversion of 85% after 6 h TOS. In contrast, for H-Mordenite zeolite both catalytic activity and stability decrease with the decrease of reaction pressure. Marathe et al. (2002) used CO_2 as solvent for naphthalene dialkylation under pressure over rare earth metal modified HY zeolite (RE-HY). They increased the pressure of reaction by increasing the amount of CO_2 charged into the reactor. Table 2.9 lists the effect of pressure on the conversion and product selectivity for this reaction.

Table 2.9. Influence of pressure on the butylation of naphthalene over RE-HY catalyst (temperature: 433 K, alcohol/naphthalene: 2 mol, TOS: 3 h, catalyst: 2 g) (Marathe et al., 2002).

P (bar)	Conversion (%)	Product distribution (%)			Selectivity ratios	
		MTBN	DTBN	Others	MTBN (β/α)	DTBN (2,6-/2,7-)
Self-generated (no CO_2)	42.0	67.8	31.9	0.3	46.3	4.6
70	46.3	66.2	33.4	0.4	36.9	5.5
92	45.0	74.5	25.5	--	42.2	5.5

The same authors observed that by increasing the pressure from self-generated pressure to 70 bar, conversion of naphthalene, DTBN selectivity and 2,6-/2,7- molar ratio were increased but by further increasing from 70 to 92 bar, both naphthalene conversion and DTBN selectivity decreased. Glaser and Weitkamp (2003) studied the effect of supercritical CO_2 on alkylation of naphthalene. They used high excess of CO_2 and diluted reactants (less than 8.5%), so they could be able to change the properties of the reaction mixture. They increased the pressure from 200 to 400 bar and observed increasing naphthalene conversion and catalyst life time. The higher catalyst activity at 400 bar is attributed to an increased solubility of higher molecular weight, polyaromatic coke precursors at increased density of the reaction medium. However, the higher conversion of naphthalene reached at this pressure could be a result of an increased reaction rate due to increased reactant concentrations. Finally, they conclude that the increased density of the supercritical reaction phase can be utilised to reduce or even avoid catalyst deactivation that might occur rapidly in the gas phase.

2.3.3.7 Effect of weight hourly space velocity (WHSV)

Many researchers have reported that by increasing the weight hourly space velocity in the alkylation of naphthalene in a fixed bed reactor, naphthalene conversion is decreased. This reduction is mainly due to lower residence time for the reaction to occur. Krithiga et al. (2005) studied the effect of WHSV on isopropylation of naphthalene over AL-MCM-48 zeolite. They observed that by increasing the WHSV from 4.5 to 8.75 h^{-1}, the selectivity to IPN was increased while less DIPN and PIPN were produced. They explained that since the alkylation reaction is consecutive, when WHSV is high only a small part of IPN has enough reaction time to be further alkylated into DIPN and PIPN. Hence, to obtain good conversion and selectivity of DIPN, low WHSV is reasonable. Anand et al. (2003) studied the effect of WHSV on

isopropylation of naphthalene over HY zeolite. They observed that by increasing the WHSV from 3.3 to 9.6 h^{-1}, more IPN and DIPN were produced while selectivity to PIPN was decreased. They stated that in the isopropylation of naphthalene over HY zeolite, there is no external mass transfer limitation. Moreover, the IPN or DIPN selectivity does not strongly depend to the naphthalene conversion. Wang et al. (2003) investigated the effect of WHSV on alkylation of naphthalene in a broaden range. They changed the WHSV from 2 to 27 h^{-1}. They observed that both 2-/1-IPN and 2,6-/2,7-DIPN ratios decreased with the increasing the WHSV. They indicated that the high WHSV allows first the formation of thermodynamically favourable 1-IPN, while the low WHSV facilitates the rearrangement of 1-IPN into 2-IPN. Finally, they recommended a WHSV of 5 to 6 h^{-1}.

2.3.3.8 Effect of mole ratio of reactants

The molar ratio of reactants (alcohol/naphthalene) has been found to strongly influence the activity and selectivity of zeolite in the alkylation of naphthalene. Wang et al. (2003) showed that by increasing the isopropyl alcohol (IPA) in the reactant mixture, the conversion and PIPN selectivity rapidly increase, while, IPN and β,β-selectivity and 2-/1-IPN ratio decrease (Table 2.10).

Table 2.10. Effect of reactant ratio on the catalytic performance of USY zeolite in the isopropylation of naphthalene (temperature = 250 ºC, pressure = 3.0 MPa, WHSV = 5.3 h^{-1}, TOS = 6 h) (Wang et al., 2003).

Naphthalene/ IPA/decalin	Conv. (mol%)	Selectivity (mol%)			2-/1- IPN	2,6-/2,7- DIPN	β,β- Selectivity (mol%)
		IPN	DIPN	PIPN			
1:1:10	66.7	44.6	40.4	15.1	2.95	1.31	70.3
1:2:10	93.5	22.6	43.4	34.0	1.48	1.46	58.0
1:4:10	100	5.7	29.9	64.4	1.26	0.93	33.5

The same authors explained that due to the consecutive alkylation of IPN by isopropyl alcohol into DIPN and then into PIPN, at high IPA/naphthalene ratio, conversion of naphthalene and

selectivity for PIPN is increased. At the same time, the initially produced α-IPN, which is more thermodynamically preferred than β-IPN, tends to be further alkylated into α,β- and/or α,α-DIPN isomers with excess alkylating reagent in the reaction mixture before there is enough time to be transferred into β-IPN through isomerisation. Kamalakar et al. (2002) studied the effect of reactant molar ratio in the alkylation of naphthalene by t-butanol over Ce-HY zeolite. They increased the t-butanol/naphthalene molar ratio in the feed from 5 to 9 and observed low conversion of naphthalene at higher t-butanol content. They explained that this is due to the formation of undesired polymerised compounds and polybutylenes, which poison the catalyst.

2.3.3.9 Effect of different solvents

Different organic solvents such as benzene, trans-decalin, tetralin, hexane, cyclohexane and 1,3,5 tri-methyl-Benzene (TrMB) have been used for alkylation of naphthalene over zeolite and it was found that cyclohexane is the more beneficial solvent for this reaction (Smith and Roberts, 2000). Song and Kirby (1994) compared the effect of using decalin and TrMB as solvent on the alkylation of naphthalene by isopropanol over H-Mordenite zeolite. They observed that replacing decalin with TrMB as solvent increased the naphthalene conversion and selectivity to 2-IPN, but decreased the selectivity to 2,6-DIPN. Mingjin et al. (2003) investigated the effect of three different solvents for alkylation of naphthalene by isopropanol over modified Cu-H-Beta zeolite. They observed that cyclohexane and TrMB exhibit higher conversion and higher β,β-selectivity. They related this trend to the polarisability of the solvents and added that non-polar solvents are more beneficial for naphthalene alkylation. They also explained that in the narrow pore channels of zeolite, the solvent with a smaller diameter is more favourable for the formation and diffusion of the linear molecules, such as 2-IPN and 2,6-DIPN.

2.4   Dehydration process

2.4.1   Introduction

Dehydration synthesis is an elimination chemical reaction that involves the loss of a water molecule from the reacting molecule. A Brønsted acid catalyst can protonate the hydroxyl group (–OH) to $-OH_2^+$ to help the hydroxyl group to have a better leaving group. Dehydration of alcohols to ethers or alkenes, conversion of carboxylic acids to acid anhydrides and conversion of amides to nitriles are the famous examples of this reaction. There are two primary requirements for dehydration reaction to occur: 1) to have a reactant with a hydroxyl group and 2) to have another reactant with a hydrogen atom. In addition, the hydroxyl group and hydrogen atom should be able to cleave during the reaction (Carey and Sundberg, 2007).

2.4.2   Applications, catalysts and operating conditions of dehydration process

One of the main applications of dehydration synthesis is to produce alkenes or ethers. At high temperatures and in the presence of a strong acid, such as sulphuric or phosphoric acid, dehydration of alcohols to alkenes is carried out. The required range of reaction temperature depends on the substitution of the hydroxy-containing carbon and it as follow:

Primary alcohols: 170-180°C

Secondary alcohols: 100-140 °C

Tertiary alcohols: 25-80°C

If the reaction is not sufficiently heated, the alcohols do not dehydrate to form alkenes, but react with one another to form ethers. Dehydration of primary alcohols proceeds via an E2 mechanism since the primary carbocation is highly unfavourable but dehydration of secondary

and tertiary alcohols usually occurs via an E1 mechanism which proceeds via a carbocation intermediate that can often undergo rearrangement.
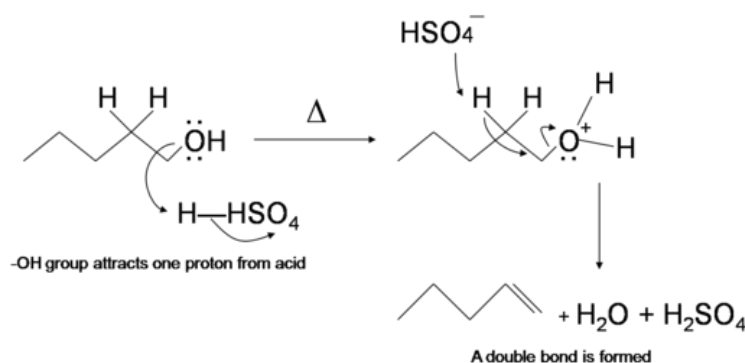
Scheme 2.3 Dehydration of primary alcohol through the E2 mechanism (Vollhardt and Schore, 2007).

Scheme 2.3 illustrates the mechanism for dehydration of primary alcohol by the E2 route using sulphuric acid as catalyst. Oxygen donates two electrons to a proton from H_2SO_4 to form an alkyloxonium ion. Then the nucleophile HSO_4^- attacks closest hydrogen and the alkyloxonium ion leaves in a concerted process to make a double bond. Scheme 2.4 and 2.5 illustrate the mechanism for dehydration of secondary and tertiary alcohols, respectively, through E1 mechanism using sulphuric acid as catalyst. Similarly to the previous reaction, secondary and tertiary hydroxyl group protonate to form alkyloxonium ions. However, in this case the ion leaves first to form a carbocation as the reaction intermediate. Then, the nucleophile HSO_4^- removes hydrogen from the carbon next to the carbocation to form a double bond. According to Zaitsev's rule, the most stable alkene is the major product in an elimination reaction (McMurry, 2011).
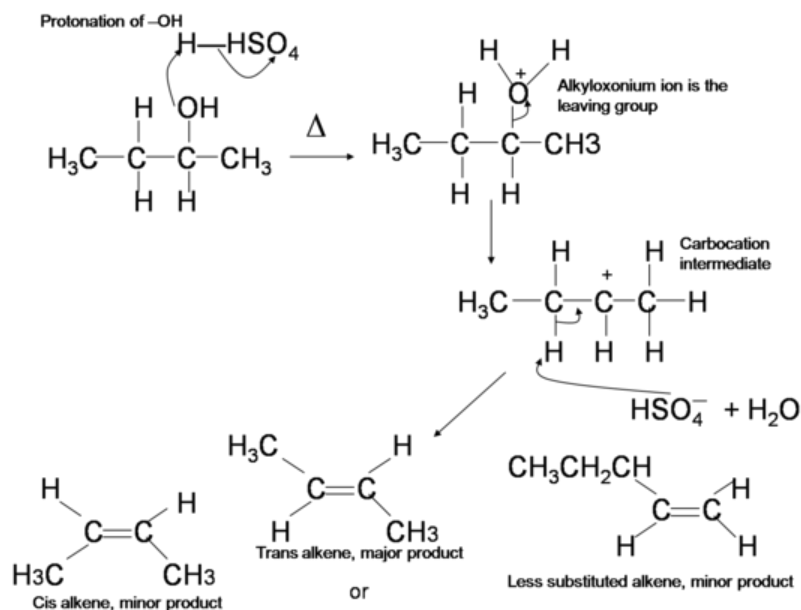
Scheme 2.4 Dehydration of secondary alcohol through the E1 mechanism (Vollhardt and Schore, 2007).

Alcohols are amphoteric (amphiprotic) means they can act as a weak base or as a weak acid. The lone pair of electrons on the oxygen atom makes the hydroxyl group a weak base. Oxygen can donate two electrons to an electron-deficient proton. Thus, in the presence of a strong acid, R–OH acts as a base and protonates into the very acidic alkyloxonium ion (+OH$_2$).
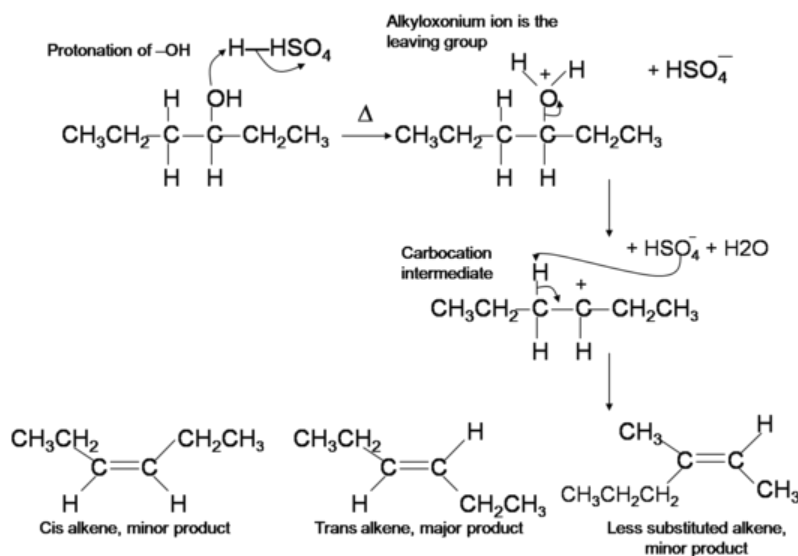
Scheme 2.5 Dehydration of tertiary alcohol through the E1 mechanism (Vollhardt and Schore, 2007).

This basic characteristic of alcohol is essential for the dehydration reaction with an acid to form alkenes. Dehydration of alcohols mainly depends on the type of alcohol, concentration of acid and temperature. Since tertiary alcohols are most reactive, they can react under milder conditions (e.g., less concentrated acid, lower temperatures).

Both homogeneous and heterogeneous catalysts have been used widely for dehydration of alcohols. Strong homogeneous acids such as H_2SO_4, $KHSO_4$ or H_3PO_4, are found to be effective for dehydration, but in many cases formation of rearranged products occurs and ethers are obtained as side products. Other common dehydrating agents that are extensively applied are: P_2O_5, I_2, $ZnCl_2$, DMSO, $KHSO_4$, KOH, anhydrous $CuSO_4$, and phthalic anhydride (Smith, 2013). Boron trifluoride diethyl complex ($BF_3.OEt_2$) in CH_2Cl_2 can dehydrate tertiary alcohols under mild conditions (25ºC, 2 h). It has been shown that tertiary and secondary alcohols can react under mild conditions with triphenylbismuth dibromide and iodine under an inert atmosphere to give the corresponding alkenes in good yields (Dorta et al., 1994).

High surface nitrides of Mo, W, Zr and Hf elements as catalyst have been shown to be very active for dehydration of alcohols with high resistance against water, but with no selectivity to alkene isomers (Lee et al., 1992). Carbide form of titanium and vanadium for selective dehydration of alcohols to alkenes have been studied by Guenard et al. (2002). Certain metal oxides (e.g. Cr_2O_3, TiO_2 and WO_3) show characteristic selectivity in dehydration of alcohols.

Solid acid catalysts such as zeolites, silica, silica-alumina and sulphated- zirconia have been studied extensively for dehydration of alcohols (Berteau et al., 1991, Figueras et al., 1971, Chang and Silvestri, 1977, Froment et al., 1992). Berteau et al. (1991) have studied dehydration of 1-butanol on silica rich and alumina rich silica-alumina catalyst. They showed that high content of alumina in the catalyst only presents medium and weak Lewis acid sites, coupled with a strong basicity which dehydrates 1-butanol to 1-butene and dibutylether while high

content of silica presents both Brønsted (mainly) and Lewis acid sites. In this case, 1-butanol is dehydrated to 1-butene which immediately isomerises to cis- and trans-2-butenes.

Pure zirconia (ZrO_2), sulphated zirconia, zirconia based binary and ternary oxides were prepared and applied to the dehydration of alcohols (Hsu et al., 2009, Nitta et al., 1984). Modification of zirconia with sulphuric acid can increase its surface area and acid sites, though the pore volume, the pore diameter, and the particle size are reduced. It has been reported that zirconia treated with H_2SO_4 exhibits super-acidic character with both Brønsted and Lewis acid sites and they can improve the activity and selectivity in conversion of alcohols to alkenes (Nitta et al., 1984). Zeolites with different pore structures have been used for dehydration of alcohols. Park and Seo (2009) have investigated the catalytic activity and deactivation behaviour of zeolites with CHA, LTA, MFI, BEA, MOR and FAU topology in conversion of methanol to olefins. They observed that the product composition over the zeolites in the dehydration of methanol is strongly related to their pore structure and acidity where CHA, LTA and MOR zeolites showed high selectivity for lower olefins, MFI, FAU and BEA zeolites showed high selectivity for alkyl aromatics. They have reported that the deactivation rates of the zeolites in the reaction increased in the following order: CHA ≈ MFI << BEA < FAU < LTA < MOR. The dehydration of alcohols to light olefins over acidic zeolites will be discussed in more details in the following section.

2.4.3   Dehydration of alcohols to light olefins

2.4.3.1 Introduction

Rapid depletion of oil resources due to the excessive use of fossil fuels as our major source of energy is one of the most important problems of the next century. With current high consumption rate of fossil fuels, it has been estimated that the known oil reservoirs to be depleted within about 40 years, and the known natural gas reserves to be depleted within about 70 years. Although the discovery of new oil and natural gas reservoirs may postpone the complete depletion of these fossil fuels, significant fuel shortage problems are expected in the coming century. Rapid depletion of oil resources will cause a serious problem for the synthesis of many petrochemical products we use in our everyday life, since about 57% of oil is consumed only for transportation purposes. Another problem with this high rate of oil consumption is an increase to CO_2 emission rates from about 295 ppm to 380 ppm during the last century which increased the Earth's surface temperature by about 0.6 °C. CO_2 recycling through synthesis of methanol is a challenging solution for the problems of oil depletion and increased atmospheric CO_2 (Dogu and Varisli, 2007). In this regard, methanol can play an important role as this component is one of the simplest organic molecules that can be used as building block for many products such as formaldehyde, acetic acid, methyl methacrylate (MMA), methyl t-butyl ether (MTBE), dimethyl ether (DME), gasoline, etc. Methanol can be economically converted to ethylene and propylene, two largest volume petrochemical feed stocks.

2.4.3.2 Light olefins

Light olefins such as ethylene, propylene, and butylenes, are basic building blocks for many petrochemicals such as polypropylene, cumene, acrylonitrile, oxo-alcohols, propylene oxide, isopropanol, etc. Olefins are also useful for production of clean fuels such as alkylates which

have high octanes or can be used as octane-enhancers such as ethers. Figure 2.10 shows the different routes for production of light olefins. Most of light olefins today are being produced through the steam cracking of either natural gas or light hydrocarbon liquids. The refinery Fluid Catalytic Cracking (FCC) unit has been also a source of propylene, typically as a by-product of gasoline production. In recent years, FCC units have been built or modified to make propylene as the main product (UOP, 2011). Since the propylene market is growing faster than ethylene, and also many of the new steam crackers being built utilise ethane as a feedstock with no production of propylene, propylene supply from ethylene expansion is not expected to meet demand. Although some refineries will move toward higher severity operations to increase propylene production through FCC process, operations are driven by fuel demands and new FCC units will not fill the market demand either.
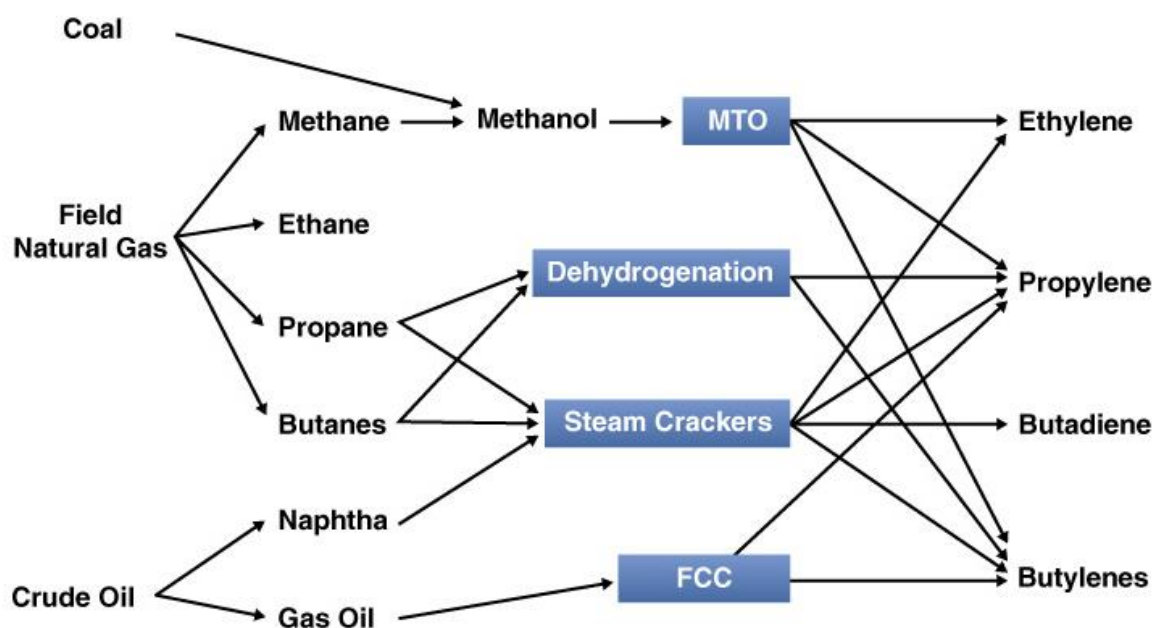
Figure 2.10. Different routes for production of light olefins (UOP, 2011).

Table 2.11 lists the sources for production of ethylene and propylene. World production of these two components currently is around 100MTA ethylene and 60MTA propylene and the annual growth in demand is equal to around 4% for ethylene and 6% for propylene which can create an imbalance in future supplies. Therefore, utilising methanol as an alternative raw material to satisfy the rising demand for light olefins, while at the same time avoiding the potential imbalance caused by the present distribution of the sources of production, offers significant opportunities (Andersen, 2004).

Table 2.11. Current production sources for ethylene and propylene (CMAI, 2002).

Production Source	Ethylene	Propylene
Ethane	28%	-
Propane, Butane (LPG)	10%	69%
Naphtha, Gas oil	60%	
Catalytic cracking	-	29%
Other	2%	2%

Recently, two technologies for producing olefins from methanol have been commercialised. UOP/Hydro MTO technology, developed by UOP and Norsk Hydro, and Lurgi MTP (Methanol to Propylene), developed by Lurgi and Statoil. The UOP/Hydro MTO technology (Figure 2.11) is based on SAPO-34 zeolite in a fixed bed reactor at pressures from 1 to 3 bar and at temperatures varying from 350 to 500°C, depending on the desired ethylene/propylene ratio. The methanol as feed is diluted with water to limit undesired reactions such as oligomerisation and coking. The process yield of ethylene and propylene are of around 80 and 90 mol% in the fraction of C_4 olefins.
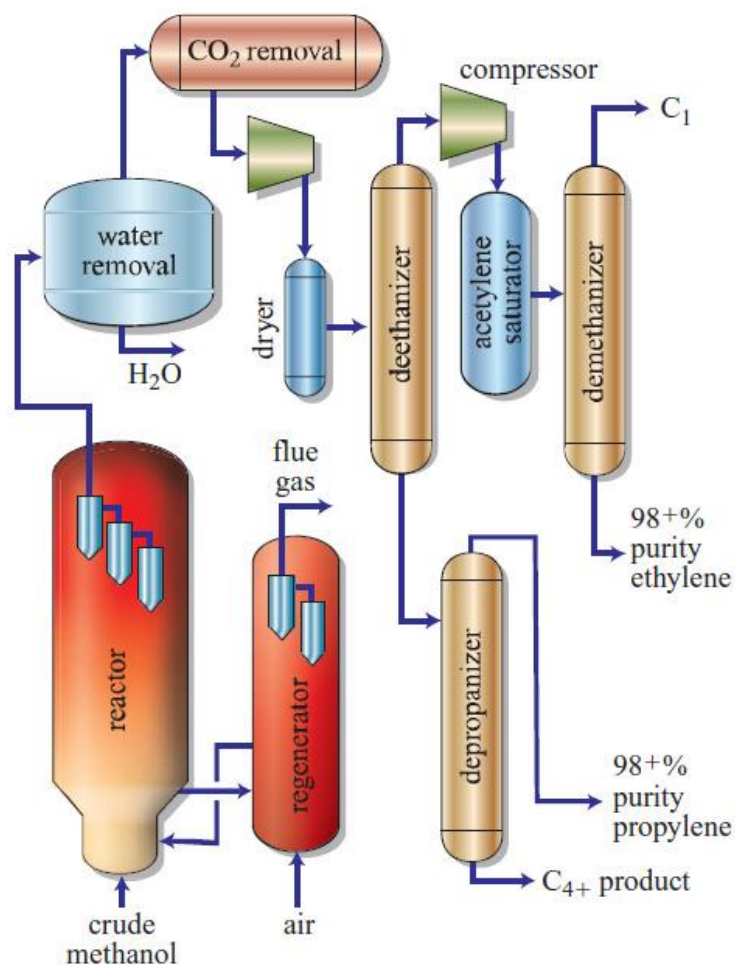
Figure 2.11. Process flow diagram of UOP/Hydro MTO technology (UOP, 2011).

The Lurgi MTP technology (Figure 2.12) uses a zeolite ZSM-5-based catalyst in six fixed bed reactor in series at pressures from 0.1 to 1 bar and at temperatures between 400 and 500°C. The feed is a mixture of water, dimethyl ether and methanol combined with a recycle stream containing C_4 to C_6 hydrocarbon. The propylene yield is around 70% while significant amount of by-products such as gasoline and LPG are produced (Andersen, 2004).
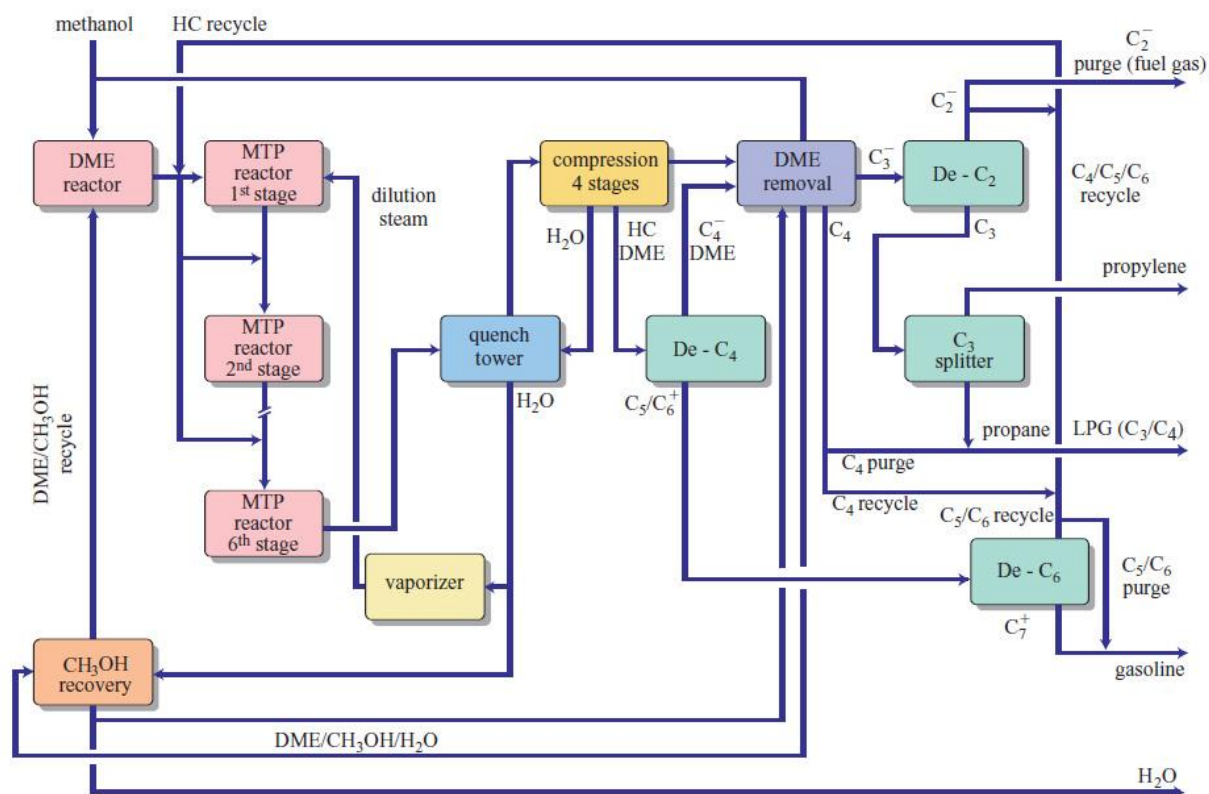
Figure 2.12. Process flow diagram of Lurgi MTP technology (Meyers, 2004).

The olefin selectivity in the MTO process using zeolite catalysts with small and medium pore size and to a lesser extent, on large-pore zeolites have been studied carefully in literature. The effects of acidity, pore size, pore structure and crystal size of the zeolite as well as effect of operation reaction conditions upon product selectivity has been investigated. These investigations will be explained in the following section.

2.4.3.3   Zeolite as catalyst for production of light olefins

Extensive research has been devoted to improve the process efficiency and selectivity to light olefins. High selectivity to ethylene was achieved over Ni-SAPO-34 catalyst (Inui and Kang, 1997) while better selectivity to propene was observed over high silica ZSM-5 zeolite modified by phosphoric acid (Liu et al., 2009) or zirconium oxide (Zhao et al., 2006).

In a review by Stocker (1999) more than twenty mechanisms have been proposed for this reaction, however there is now a general agreement about the so-called ''hydrocarbon pool'' mechanism which was initially proposed by Dahl and Kolboe (1993). Figure 2.13 shows their early proposed mechanism. Based on this mechanism, the formation of olefins occurs through continuous addition of methyl groups to the pool and reaction with methanol following by splitting off the alkenes.
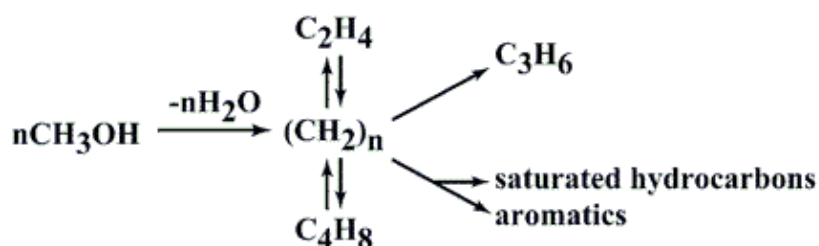
Figure 2.13. Kolboe's phenomenological hydrocarbon pool mechanism for MTO catalysis. (Haw et al., 2003)

Wang et al., (2006) investigated the MTO mechanism using in-situ solid-state NMR spectroscopy. They observed that at reaction temperature of 275-400ºC and under steady-state conditions, the MTO process is dominated by the hydrocarbon pool mechanism. In this case methanol is added to the reactive organic species such as polymethylbenzenes, large olefins, cyclic carbenium ions and probably methylbenzenium cations. Light olefins are formed through elimination of alkyl chains from these organic centres. However, at reaction temperatures lower than 275ºC, the conversion of methanol on acidic zeolites is dominated by the dehydration of methanol to dimethyl ether (DME) either through a direct or indirect route. In the direct route, two methanol molecules adsorb simultaneously and react with each other on one Brønsted acid site to form one DME and one water molecule (Bandiera and Naccache, 1991). Following the indirect route, methanol molecules adsorbed on bridging OH groups are converted first to

methoxy groups, which subsequently react with another methanol molecule to form DME (Ono and Mori, 1981, Forester and Howe, 1987).

During the conversion of methanol to light olefins, zeolite catalysts suffer from rapid deactivation due to the deposition of carbonaceous residues in the catalyst pores which block the reactants from accessing the active acid sites (Bibby et al., 1992). Although ZSM-5 zeolite shows much higher resistance to coke formation compared to SAPO-34 or other zeolites for MTO reaction, structural factors of zeolite that can affect coke deposition and catalyst deactivation should be investigated to further decrease coking and thus improve the cost effectiveness of the process. In the MTO reaction, besides the production of the desired light olefins, undesired polyolefins, aromatic compounds and carbon deposits are also formed which may lead to catalyst deactivation (Mores et al., 2011).

2.4.3.3.1 **Acidity effect**

It is well understood that low numbers of Brønsted acid sites leads to higher selectivity to light olefins in conversion of methanol to hydrocarbons (Gayubo et al., 1996, Chang et al., 1984, Dehertog and Froment, 1991). Benito et al., (1996) observed that an increase in Si/Al in the ZSM-5 zeolite framework leads to a pronounced decrease in total acidity of the zeolite and consequently in acidic site density. Chang et al., (1984) studied the effect of acidity on product selectivity in conversion of methanol to hydrocarbon, by changing the SiO_2/Al_2O_3 ratio from 35 to 1670 in ZSM-5 zeolite. They observed that by increasing this ratio, the selectivity to C_2-C_5 olefins is increased. There is in an interesting fact about SAPO-34, in which, by increasing the Si/Al ratio, concentration of Brønsted acid sites are increased while in other zeolite materials including ZSM-5, the Brønsted acidity is decreased as the atomic ratio of Si/Al is increased. It

can be explained by the assumption that a SAPO crystal is obtained by silicon substitution into a hypothetical alumina-phosphate framework (Froment et al., 1992).

2.4.3.3.2 **Pore size effect**

Froment and his co-workers (Dehertog and Froment, 1991, Froment et al., 1992, Marchi and Froment, 1991), have extensively studied the effect of varying pore size zeolites on the conversion of methanol to light alkenes. They reported that zeolites with small pore opening of about 0.45 nm (e.g. chabazite, erionite, zeolite T, ZSM-34, SAPO-34, and SAPO-44) show very good shape-selectivity in the MTO process. Their unique property is that all of them only let molecules with straight chain structure (e.g. linear paraffins, linear olefins and primary alcohols) pass through the pores while bulkier molecules such as branched isomers and aromatics cannot penetrate to the pores. An interesting fact is that SAPO molecular sieves show mild acidity, while chabazite and erionite are strong acids in the protonic form. This characteristic of SAPOs molecular sieves makes them an excellent choice for conversion of methanol to light olefins (Liang et al., 1990).

Medium pore zeolites are crystalline molecular sieves consisting of linked silica- and alumina-tetrahedra forming 10-membered oxygen ring channels with pore size of 0.5 to 0.6 nm (Chen et al., 1994b). In this group, ZSM-5 and its isostructural analogs such as ZSM-11 and ZSM-48 have been studied for the conversion of methanol to olefins (Bleken et al., 2011) but soon it was recognised that the shape selectivity properties of ZSM-5 is superior to other medium pore zeolites (Derouane et al., 1981).

Large-pore zeolite such as Mordenite (Marchi and Froment, 1993), X and Y zeolite, SAPO-5, MeAPO-5, and MAPO-5 has also been used as catalysts for methanol conversion into olefins.

Although, Mordenite is a highly active catalyst for the conversion of methanol to hydrocarbons but from one side it has high selectivity to heavy compounds (e.g. C_5^+ aliphatics and aromatics) and from the other side, it becomes deactivated rapidly (Marchi and Froment, 1993).

2.4.3.3.3 **Modification of zeolite**

Many efforts have been made to increase the shape selectivity of zeolite by modifying its acid sites distribution using phosphoric acid (Liu et al., 2009), oxalic acid (Lücke et al., 1999), transition metals (Dubois et al., 2003), alkali metals (Mei et al., 2008) or alkaline earth metals (Goto et al., 2010). Al-Jarallah et al., (1997) modified a high silica MFI zeolite using impregnation with metal nitrates of Ag, Ca, Cd, Cu, Ga, In, La and Sr to study their effects on the activity and selectivity of the catalyst for conversion of methanol to lower alkenes (Figure 2.14). They observed that introducing La and Ag to the zeolite framework led to better selectivity to the alkenes while other metals like Ca, Sr, Cd, Ga and In improve other catalytic activities such as cracking by producing more CO, CO_2, H_2 and O_2 confirming the cracking of methanol over the modified zeolite. They explained that barium and lanthanum with atomic radii of 2.78 Å and 2.74 Å have modified the pores by reduction of the pore volume and re-distribution of the pore sizes in a way that improve the shape selectivity of the catalyst towards the lower alkenes.
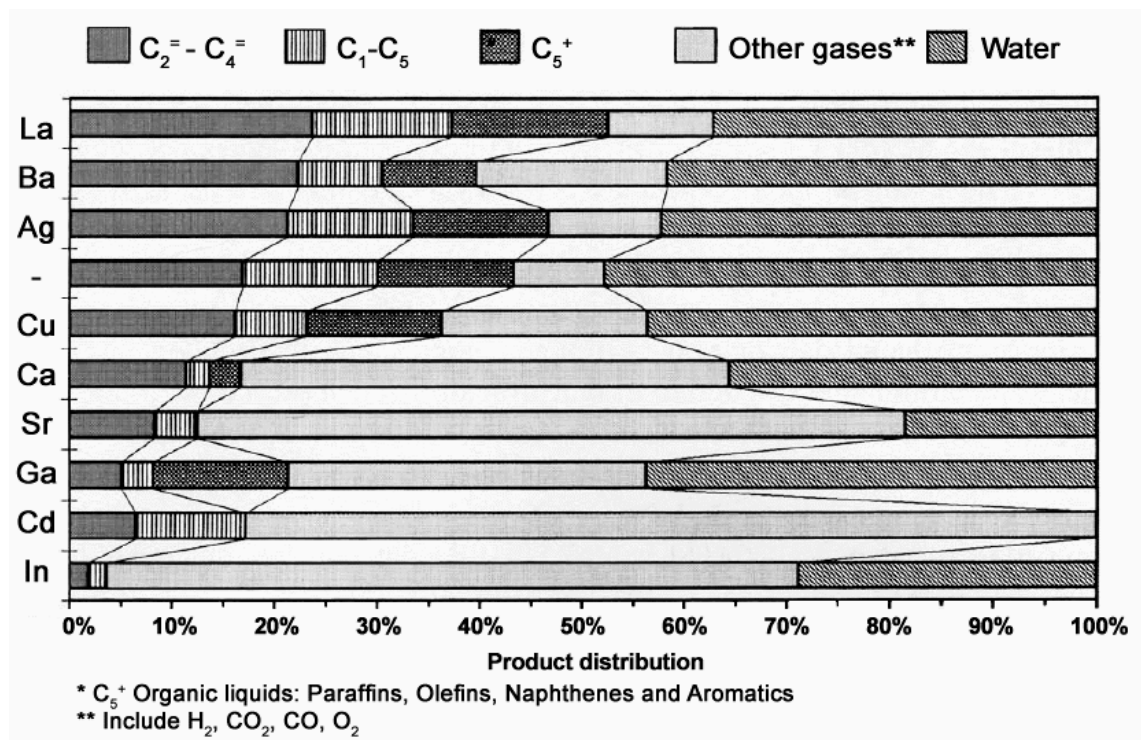
Figure 2.14. Product distribution for various modifications of MFI zeolite at T=400°C, WHSV=4 h^{-1} and MeOH/N$_2$ =2.8 wt./wt. (Al-Jarallah et al., 1997).

Sano et al., (1992) have reported that using zeolites containing alkaline earth metals can improve the catalyst life time, significantly. They believe that these metals (Mg, Ca, Sr, Ba) can suppress the coking and dealumination of the zeolite by changing the strong acid sites of zeolite to weak one. Later, they have shown that the alkaline earth metals can interact with the steam generated during the dehydration reaction and migrate from weak acid sites to the outer surface of zeolite crystals, resulting in the regeneration of strong acid sites again and therefore promoting the coke deposition. It has been reported in the literature that iron from transition metals (Inaba et al., 2007), calcium from alkaline earth metals (Zhang et al., 2010) and caesium from alkali metals, as well as treatment with phosphoric acid, have shown significant improvement in selectivity to propene in the MTP process.

2.4.3.4 **Effect of temperature**

The effect of temperature on the conversion and selectivity of methanol to hydrocarbons over ZSM-5 zeolite has been studied carefully in the literature and some kinetic models have been proposed (Chang et al., 1984, Dehertog and Froment, 1991, Aguayo et al., 2002, Travalloni et al., 2008). Chang et al., (1977) studied the effect of temperature on catalytic activity of ZSM-5 for conversion of methanol to hydrocarbons over a range of 260-540 ℃ (Figure 2.15). They observed that at 260 ℃ the main reaction is dehydration of methanol to DME with some unreacted methanol while the conversion of methanol to DME approaches to completion between 340 ℃ to 375 ℃ with formation of significant amount of aromatics.
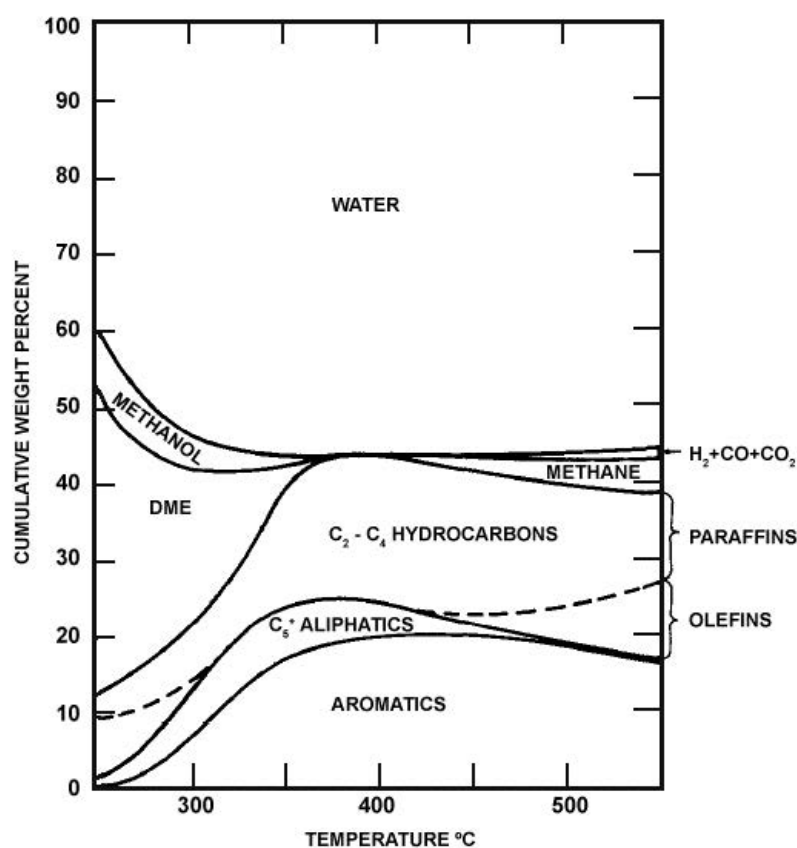
Figure 2.15. Effect of temperature on the yield of hydrocarbons during the dehydration of methanol over ZSM-5 zeolite. Reaction conditions: LHSV=0.6-0.7 h⁻¹, Pressure= 1 atm (Chang and Silvestri, 1977).

With further increase in temperature, light olefins and methane start to increase as a result of secondary cracking reactions. At temperatures higher than 500 ºC, the decomposition of methanol to H_2 and CO occurs. Chang et al., (1984) studied the methanol conversion on ZSM-5 at reaction temperature from 400 ºC to 500 ºC using a simple kinetic model:

$$A \xrightarrow{k_1} B \xrightarrow{k_2} C$$
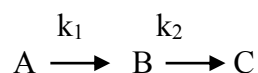
where A are oxygenates (as CH_2), B the olefins and C are aromatics and paraffins. They reported the apparent activation energy for formation of olefins of 19.3 kcal/mol. However, based on the collected data, a little or no temperature dependency of aromatisation was observed, confirming strong pore diffusion control in the catalyst. Chen and Reagan (1979) discovered the autocatalytic nature of this reaction and proposed the below scheme:

$$A \xrightarrow{k_1} B$$

$$A + B \xrightarrow{k_2} B$$

$$B \xrightarrow{k_3} C$$
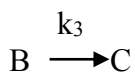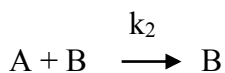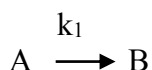
where A represent oxygenates, B olefins and C aromatics and paraffins. This autocatalytic step makes the selectivity to C_3^+ olefins greater than values calculated from thermodynamics (Froment et al., 1992). Travalloni et al., (2008) studied the effect of temperature on different solid acid catalysts including SAPO-34, Mordenite, Beta and ZSM-5 zeolite (Figure 2.16). Among the studied catalysts, SAPO-34 provided the higher initial selectivity during the first 1 hour) to C_2 and C_3 compounds at high temperature (e.g. 450 ºC or 500 ºC). This indicates that SAPO-34 has a great potential for production of light olefins if this regeneration of catalyst is carried out in parallel with the reaction. ZSM-5, Mordenite and Beta zeolites showed high activities at temperatures higher than 300 ºC. The highest selectivity to C_2 and C_3 compounds

were provided by ZSM-5 at high temperatures and by Mordenite at lower temperatures, before an extensive deactivation of its strong acid sites occurred. Most of the researchers are in the same agreement that high temperature is required to achieve high olefin selectivity in the conversion of methanol to light olefins over ZSM-5 zeolite.
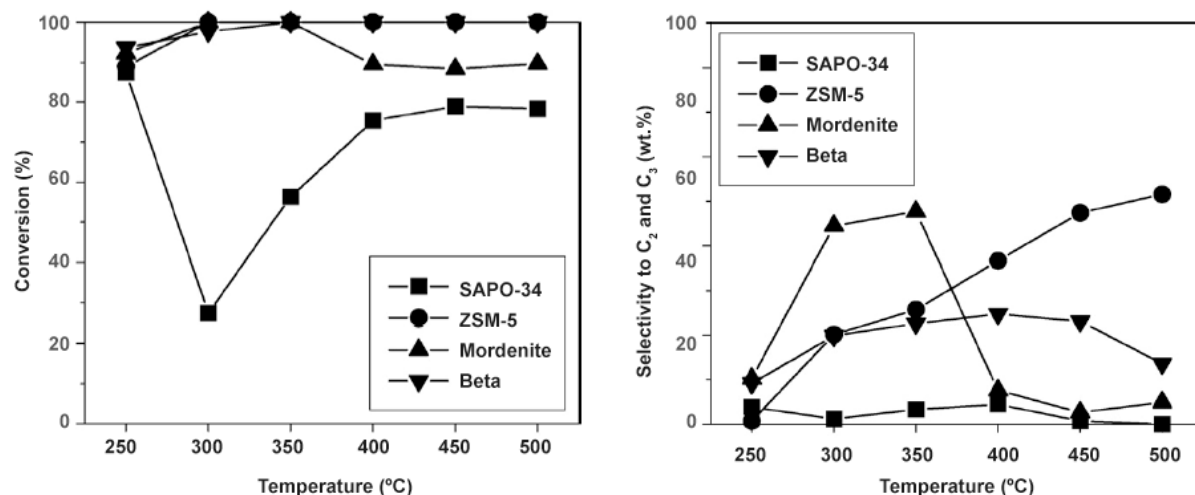
Figure 2.16. Effect of temperature on methanol conversion and selectivity to C_2 and C_3 compounds, pressure= 1 atm, catalyst weight= 0.1 g, WHSV=0.94 h^{-1} , TOS= 5.5 h (Travalloni et al., 2008).

2.4.3.5 **Effect of pressure**

In the conversion of methanol to hydrocarbons over zeolites, it has been shown that the partial pressure of methanol has a very strong influence on the selectivity to olefins. Decreasing the pressure tends to suppress the formation of aromatics and heavy hydrocarbons in favour of forming the olefins (Froment et al., 1992). Chang et al., (1979) studied the effect of pressure on the conversion of methanol to hydrocarbons over ZSM-5 zeolite by varying the methanol partial pressure to 0.04, 1 and 50 atm at constant temperature and over a wide range of space velocity. They observed that by raising the methanol partial pressure to 50 atm the formation of poly-methyl-benzenes is increased. Wu et al. (2013) studied the effect of methanol partial pressure on catalytic activity and selectivity of ZSM-5 zeolite. They changed the methanol partial

pressure from 5 kPa to 50 kPa at 460 ºC at varying space time by co-feeding N_2 as inert gas. They observed that methanol conversion was decreased notably with decreasing methanol partial pressure at the same space time but selectivity to $C_3^=$ and $C_4^=$ was increased and selectivity to $C_2^=$ remained unchanged. Caesar and Morrison (1978) found that decreasing the methanol partial pressure by dilution with water is led to a significant increase in ethylene selectivity.

2.4.3.6 **Effect of weight hourly space velocity (WHSV)**

Studies on the effect of space velocity on the conversion of methanol or DME to hydrocarbon distribution clearly indicate that light olefins are intermediates. At low space times the main hydrocarbons are olefins, but the yields are very low due to the low conversion. The yield of light olefins increases with space time and reaches a maximum, indicative of their intermediate character (Froment et al., 1992). An important characteristic of the methanol conversion to hydrocarbon over ZSM-5 zeolite is that a further increase in space time, after a complete conversion (e.g. >99%) results in a continuing change in hydrocarbon distribution (Stocker, 1999). At very low space times the conversion of methanol or DME to hydrocarbons is very slow, but in a narrow range of space times the conversion increased rapidly. This observation was interpreted by Chen and Ragan (1979) as an indication of the autocatalytic nature of this reaction but Espinoza (1986) proved that this jump is related to the required concentration of the intermediate DME. He used DME as co-feed and the jump in conversion was not observed.

2.5 Hydrogenation process

2.5.1 Introduction

Hydrogenation is a process to reduce or saturate an organic compound by addition of hydrogen atoms to a molecule. As the non-catalytic hydrogenation takes place only at very high temperatures, catalysts are required to make this reaction feasible. Most hydrogenation processes use gaseous hydrogen (H_2), but some use alternative sources of hydrogen such as isopropanol or formic acid. These processes are called transfer hydrogenations. Four components are involved in the hydrogenation process: 1) the unsaturated compound, 2) the hydrogen or other hydrogen sources, 3) a catalyst and 4) sometimes a solvent. Depending on the unsaturated compound and the activity of the catalyst, the reduction reaction is carried out at different temperatures and pressures. The most common catalysts for hydrogenation reactions are the metals nickel, platinum, and palladium and their oxides (Hagen, 2006). For high-pressure hydrogenations, copper chromite and supported nickel are extensively used (Ertl et al., 2008). The hydrogenation usually favours syn-addition of hydrogen from the less hindered face of the double bond. In this mode of hydrogenation both hydrogen atoms are added to the same face of the π bond (Carey and Sundberg, 2007). Catalytic hydrogenation is a very important synthetic route as most functional groups can be made to undergo reduction. Molecules containing multiple functional groups can usually be reduced selectively to the desired product. Catalytic hydrogenations can be carried out in liquid or gas phase using either a batch or continuous reactor. Choose of suitable reactor depends on various factors such as the choice of catalyst, the reaction conditions (e.g. temperature, hydrogen pressure, residence time, etc.), yield, heat formation, mass-transport phenomena, solvent and economic reasons. However, most of continuous processes usually are carried out in fixed-bed or fluidised-bed reactors.
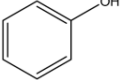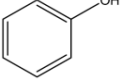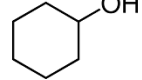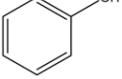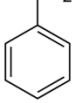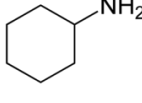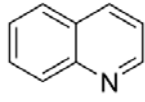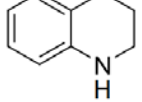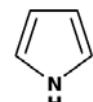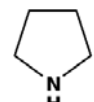
2.5.2   Applications, catalysts and operating conditions of hydrogenation process

Hydrogenation processes have wide application in petrochemical, oil upgrading, fine chemicals, food and pharmaceutical industries. In the petrochemical industry, for example, many of the compounds cannot be used directly as they contain double or multiple bonds and need to be converted to saturated compounds before use. In the fine chemical and pharmaceutical industries, the hydrogenation reaction is often used to produce the end product. In the food industries, hydrogenation is used to saturate the unsaturated fatty acids in vegetable oils to convert them into solid fats (e.g. margarine).

Table 2.12 lists the most important examples of hydrogenation of substituted benzene. The activity of catalysts for the hydrogenation of aromatic rings are in the order of Rh > Ru > Pt > Ni > Pd (Johnson-Matthey). The rate of the hydrogenation of the aromatic ring depends on the nature of the ring and presence of any substituent on the ring, however presence of amine or hydroxyl groups generally has little effect on the reaction.

For example, partial hydrogenation of benzene to cyclohexene can be carried out at 25–200 °C and 10–70 bar over heterogeneous Ru catalyst. Phenols can be converted directly to cyclohexanones under mild conditions using Pd catalysts, however, basic alkali or alkaline earth metals are used as promoter to improve the selectivity (Johnson-Matthey, 2009). Liquid phase reactions are typically run with reaction temperatures and pressures between 50-180°C under 5-15 bar of H_2 pressure. Heterocyclic compounds such as pyridines, quinolines, isoquinolines, pyrroles, indoles, acridines and carbazoles can be hydrogenated over Pd, Pt, Rh and Ru catalysts using acidic solvents such as acetic acid and aqueous HCl to facilitate hydrogenation process (Johnson-Matthey, 2009).

Table 2.12. Examples of aromatic ring hydrogenation and process operating conditions (Johnson-Matthey).

Unsaturated substrate	Product(s)	Catalyst	Temperature range (°C)	Pressure range (bar)	Solvent
		Rh/Ru/Pt/Ni/Pd over C or Alumina	50-150	3-50	None
		Rh/Ru/Pt/Ni/Pd over C	150-200	10-70	None/Water
		Ni/Rh over Alumina	100-150	1-50	None/low polarity solvent
		Ni/Rh over C	5-150	1-50	Acidic solvent
	+ H₂O	Ni/Rh over Alumina	100-150	3-50	Acidic
		Rh/Ru/Pt over C	50-150	3-10	Low polarity solvent
		Rh/Ru/Pt over C	30-150	3-50	None or alcohol
		Rh/Ru/Pt over C or Alumina	30-150	3-50	Alcohols + dilute acid, acetic acids

2.5.3 Hydrogenation of naphthalene

2.5.3.1 Introduction

Hydrogenation by heterogeneous catalysts is an important industrial process. In petrochemical processes, hydrogenation is used to saturate aromatics or for ring opening to produce high cetane diesel fuel (Corma et al., 1997). Hydrogenation of naphthalene as a model compound of aromatic hydrocarbons in diesel fuel has been used widely (Schmitz et al., 1996, Keane and Patterson, 1999, Pawelec et al., 2002, Ito et al., 2002, Rautanen et al., 2002, Kirumakki et al.,

2006). Naphthalene can be hydrogenated to cis- and trans-decahydronaphthalene (cis- and trans-decalin) via partial hydrogenation of its intermediate, tetrahydronaphthalene (tetralin). For high quality diesel fuel, decalins (saturated hydrocarbons) are more favourable products than tetralin (Ito et al., 2002).

Another application of naphthalene hydrogenation in industry is production of tetralin, a very useful high boiling point solvent which has been widely used in paint, coatings, inks, pharmaceuticals and paper industries. Tetralin is conventionally synthesised in a complicated Bergman cyclisation reaction but it can simply be produced through the hydrogenation of naphthalene in the presence of noble metals or transition metal catalysts (Cheng et al., 2009).

Recently, cyclic saturated hydrocarbons (e.g. decalin, bicyclohexyl, methylcyclohexane, etc.) have been used as a promising new mobile hydrogen storage media for proton exchange membrane fuel cells with higher stability and lower cost (Hiyoshi et al., 2006). For hydrogen production from decalin, cis-isomer is more preferable, since dehydrogenation rate of cis-decalin is faster than that of trans-decalin. Also, cis-decalin can be used to produce sebacic acid that can be used in the manufacture of Nylon 6, 10, plasticisers and softeners (Weissermel and Arpe, 2003).

Noble metals (e.g. platinum) usually show high selectivity to tetralin because naphthalene can strongly interact with metals surface and prevents the hydrogenation of tetralin (Ito et al., 2002). However, due to the high price of noble metals, transition metals are sometimes preferred, although the selectivity to tetralin is low.

In hydrogenation of naphthalene, tetralin appears both as a primary product and as an intermediate. Naphthalene is first hydrogenated to tetralin, and tetralin is further hydrogenated to cis- and trans-decalin through octa-hydro-naphthalene. Lylykangas et al. (2002) found the cis/trans ratio to be about 1:1 in hydrogenation of naphthalene, and varied from 0.8:1 to 1.6:1

in hydrogenation of tetralin, owing to more severe deactivation in the latter case. It has been reported that the selectivity to decalin formation is more related to the level of deactivation rather than reaction conditions (e.g. temperature, pressure, or initial concentration of aromatics) (Lylykangas et al., 2002). Rautanen et al. (2002) have proposed a detailed mechanism for the formation of tetralin and decalin from naphthalene. Figure 2.17 and Figure 2.18 illustrates the mechanism for hydrogenation of naphthalene to tetralin and from tetralin to cis-decalin and trans-decalin, respectively.
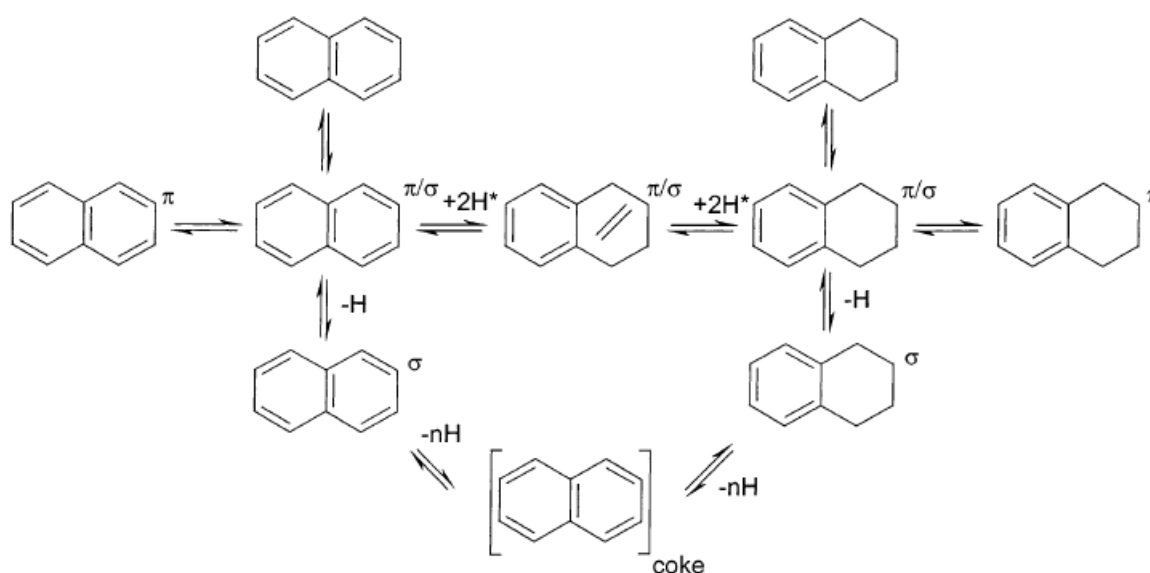
Figure 2.17. Reaction mechanism for the hydrogenation of naphthalene to tetralin (Rautanen et al., 2002).

In general, two types of reaction mechanism have been proposed for the hydrogenation of aromatic rings. In one model, the hydrogenation of aromatic compounds is carried out through consecutive addition of adsorbed hydrogen atoms while in the other model, a complex is formed during the first hydrogenation step which contains the adsorbed aromatic compound and hydrogen, together with catalyst sites. In the second hydrogenation step, isomerisation to a corresponding cyclohexene and further to a fully hydrogenated product occurs. Rautanen et al., (2002) asserted that the reaction mechanism in the hydrogenation of naphthalene is through

formation of both π/σ and π-bonds, but the dominant adsorption form and reaction route depend on the active material on the catalyst, catalyst support, and the reaction conditions. Naphthalene is hydrogenated to tetralin mainly through π/σ-adsorption by forming dihydronaphthalene as an intermediate. Tetralin forms a surface complex with hydrogen and active sites. The surface complex of tetralin is then isomerised to $\Delta^{9,10}$-octalin, which is further hydrogenated to cis-decalin or isomerised to $\Delta^{1,9}$-octalin.
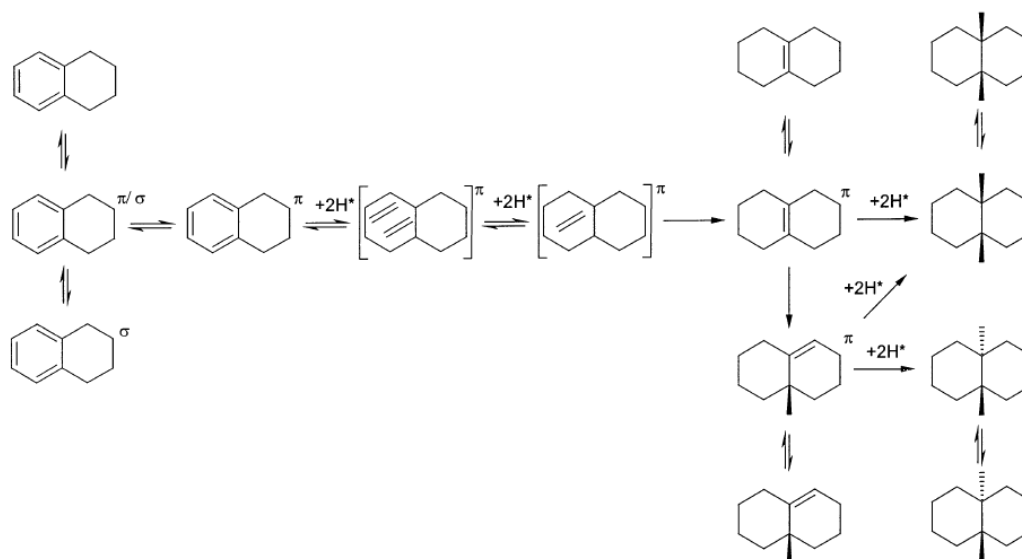
Figure 2.18. Reaction mechanism for the hydrogenation of tetralin to cis-decalin and trans-decalin (Rautanen et al., 2002).

2.5.3.2 Transition metals supported catalysts

Although, it is well established that the noble metal catalysts (such as Pd-Pt/Alumina) have excellent hydrogenation properties at moderate pressures, these catalysts are expensive and are susceptible to fast deactivation by sulphur (Kirumakki et al., 2006). Therefore, designing a highly active catalyst that can work under milder reaction conditions with less expensive metals is required. Ni-based catalysts are good alternatives to noble metal catalysts for hydrogenation processes due to their low cost and acceptable resistance to sulphur poisoning (Pena et al.,

1996). Hydrogenation of naphthalene over supported Ni catalysts has been studied extensively (Barrio et al., 2003, Rautanen et al., 2002, Kirumakki et al., 2006).

Kirumakki et al. (2006), synthesised a series of $NiO–SiO_2–Al_2O_3$ catalysts by sol–gel method to better understand the metal–support interactions and nature of active species in the reaction. They state that the major product formed on hydrogenation of naphthalene was tetralin while only a small amount of decalin was produced. They also proved that low yield of decalin in this reaction is not because naphthalene is adsorbed on the catalyst more strongly but because of weak adsorption of tetralin on the active sites.

2.5.3.3 Zeolite supported catalyst

Many efforts have been made to use zeolite supported catalyst for hydrogenation of naphthalene and it is believed that use of zeolite as support can enhance the activity, selectivity and tolerance to impurities and poisoning material such as sulphur (Song and Schmitz, 1997). Zeolite-supported Pt and Pd catalysts were used by Schmitz et al., (1996) in shape selective hydrogenation of naphthalene. They used H-Mordenite (HM) and HY zeolites as support with different SiO_2/Al_2O_3 ratios and observed that the cis/trans ratio in the product is not a simple function of zeolite pore structure and other factors such as the concentration of acid sites on the zeolite support, and the choice of the noble metal (Pt or Pd) is important. They observed high selectivity of 80% to cis-decalin over Pt/HY and 93% selectivity to trans-decalin over Pd/HM-21 at 200°C and reported that selectivity to trans-decalin is increased by increasing the weak acid sites fraction on the zeolite. Deep reduction of aromatics in distillate fuels can be achieved by hydrogenation of these compounds over noble metal or transitional metal catalysts. Although, noble metal catalysts are active for the hydrogenation of aromatics, even at temperature less than 200°C, they are not normally used for hydrotreating reactions due to higher cost and rapid poisoning of these metals by sulphur containing compounds.

Noble metal catalysts are very sensitive to even very small amounts of sulphur, but recent studies have shown that some noble metal catalysts when supported on zeolite exhibit higher sulphur tolerance (Song and Schmitz, 1997). Du et al. (2010) incorporated different molecular sieves (e.g. ZSM-5, Beta, USY and SAPO-11) with Pd-Pt supported alumina for the hydrogenation of naphthalene in hexane. They reported that in the hydrogenation of naphthalene to decalin, the catalyst Pd–Pt supported on Al_2O_3/SAPO-11 have a better activity compared to other catalysts due to improved metal dispersion, optimum acidity and larger pores. Sachtler and Stakheev (1992) stated that the characteristic of the metal particles in zeolite supported metals are mainly determined by the interaction of the metals with the support. They believe that the zeolite matrix not only imposes steric constraints for reacting molecules (shape-selective catalysis) and provides acid sites (bifunctional catalysis) but it also affects the electronic properties of the metal. They have claimed that the electron-deficient metal particles which are formed in a metal/zeolite bifunctional catalyst have a better resistance to sulphur poisoning.

However, the main problem of the using zeolite as support in conversion of bulky molecules is mesoporosity which will result in diffusion limitation. In order to overcome the diffusion limitation of zeolite in bulky molecular involved reaction, mesoporous zeolites (such as HY and β zeolite) have been successfully used. It has been proved that mesoporous zeolite can overcome the mass transfer limitation and exhibit excellent catalytic properties for the conversion of bulky molecules (He et al., 2013).

2.6 **Conclusion**

In this chapter, a review of three important petrochemical reactions including dialkylation of naphthalene, dehydration of methanol and hydrogenation of naphthalene was given. The effects of reaction conditions such as temperature, pressure, WHSV, solvent and feed composition for the first two reactions were studied. The effects of catalyst modification, pore size and acid sites distribution upon the catalyst selectivity were investigated. For the third reaction, the effect of using different types of transition metals as well as type of zeolite as support was reviewed. These reviews will be used for comparison of the experimental results in terms of catalyst activity and selectivity with literature results.

Chapter 3 EXPERIMENTAL AND ANALYTICAL METHODS

In this chapter, the materials and apparatus as well as methods for characterisation of gas and liquid products for three different reactions (alkylation, dehydration and hydrogenation) will be described. In addition, the catalyst characterisation methods and instruments which have been used will be presented and explained. Chemical, gases and zeolite which have been used in this research is explained in section 3.1. Section 3.2 gives details about methods for catalyst sample preparation or modification. The apparatus, operating procedure and analytical methods for GC-FID are described in section 3.3. The methods for characterisation of catalyst samples are described in section 3.4

3.1 Chemicals, Gases and catalysts

Table 3.1 lists the specification of gases used in this research. All gases were supplied by BOC Industrial Gases. All the chemicals, solvents and catalysts which were used for this research are listed in Table 3.2. All the chemicals were used as purchased without further purification.

Table 3.1. Specification of gases used in this research.

Gas	Application
Air (Zero grade)	GC flame gas
Argon (Zero grade N5.0)	TPD carrier gas and loop gas
Carbon monoxide (Research grade N3.7)	Loop gas for CO pulse chemisorption
Carbon dioxide (CP grade N4.5)	Used as SCF in alkylation of naphthalene
Helium (Zero grade N4.6)	GC carrier gas
Hydrogen (Zero grade N4.5)	For hydrogenation reaction and GC flame gas
Nitrogen (Grade N6.0)	GC make-up gas
Nitrogen (Zero grade N4.8)	To purge the rig before and after the reaction
Calibration gas*	GC calibration

* The composition of calibration gas is listed in Appendix A

Table 3.2 Name and specifications of chemicals and catalysts used in this research.

Material	Supplier	Specifications
Acetic acid	Sigma-Aldrich	99.7%
Boehmite	Condea Chemie GmbH	Pseudoboehmite, Pural SB®1
Caesium nitrate	Sigma-Aldrich	99%
Calcium nitrate.4H_2O	Sigma-Aldrich	99%
Carboxy-methyl cellulose	Sigma-Aldrich	M.W. 90 kg.mol^{-1}
Cobalt (II) acetate	Sigma-Aldrich	Analytical grade
Cobalt (II) nitrate	Sigma-Aldrich	Analytical grade
Copper (II) nitrate	Fischer-Scientific	Analytical grade
Cyclohexane	Fischer-Scientific	99.6%
Diisopropylnaphthalene	Fischer-Scientific	1.055–1.06 g.ml^{-1} (mixed isomers)
Ethanol	Fischer-Scientific	HPLC grade
HY zeolite	Zeolyst International	CBV 720, SiO_2/Al_2O_3 = 30
Iron nitrate.9H_2O	Honeywell Riedel-de Haen	99%
Isopropyl alcohol (IPA)	Alfa-Aesar	99.6%
Methanol	Fischer-Scientific	99.99
Naphthalene	Sigma-Aldrich	99.7%
Nickel (II) nitrate	Fischer-Scientific	Analytical grade
NiMo/Alumina	Albemarle	APC-2E
Orthophosphoric acid	Fischer-Scientific	85 wt.% in water
Silica Q-10	Fuji Silysia Chemical Ltd	75-150 μm, Surface are=260 m^2.g^{-1}
ZSM-5 catalyst	Zeolyst International	CBV 8014, SiO_2/Al_2O_3 = 80

3.2   Catalysts preparation

For the purpose of this research, different zeolite based catalysts were prepared:

- In alkylation of naphthalene, for first set of experiments, pure HY zeolite with no modification over alumina as support was used and for the next set of experiments, modified HY zeolite supported on alumina was used.

- In hydrogenation of naphthalene two different zeolite based catalysts, Co/ZSM-5 and Ni/HY zeolite were prepared and tested. Furthermore, Co/Silica, a non-zeolite based catalysts was prepared and tested and results were compared to a commercial NiMo/Alumina catalysts.

- ZSM-5 zeolite was used both in powder form and supported form for dehydration of methanol.

3.2.1   Preparation and modification of HY/Alumina catalyst

In order to test the zeolite in a fixed bed reactor, the zeolite powder was converted into pellets. A sample of HY zeolite (80 g) was sieved to 210 μm and added to boehmite (aluminium oxide hydroxide), carboxy-methyl cellulose (CMC), acetic acid, and distilled water in the ratios of 30/10/3.7/100 in weight, respectively. The mixture was kneaded to make a paste, and extruded into rods with 3 mm diameter and 5 mm length using Instron 4467 Universal Testing Machine with 30 kN uniaxial loading. The catalyst pellets were then dried at room temperature for 24 hours. The dried pellets were then converted to proton form by calcining at 500 ºC for 5 h at the rate of 10 ºC.min^{-1} in the presence of air. Boehmite was used as a support, carboxy-methyl cellulose as a temporary binder and acetic acid was used as peptising agent to improve the plasticity of the compounded batch for better extrusion characteristics (Addiego et al., 2005, Campanati et al., 2003). Figure 3.1 shows HY zeolite over alumina pellets.

Figure 3.1. HY zeolite over alumina pellets.

Modification of zeolite was carried out by the wet impregnation method. In a 100 ml beaker, an appropriate amount of metal nitrate (6.0 g $Fe(NO_3)_3$-$9H_2O$, 4.4 g $Ni(NO_3)_2$-$6H_2O$, 4.4 g $Co(NO_3)_2$-$6H_2O$ and 3.6 g $Cu(NO_3)_2$-$3H_2O$) was dissolved in 30 ml distilled water and stirred thoroughly. Subsequently, powdered HY zeolite was sieved to 210 µm, added to the solution and stirred with a magnetic stirrer for 1 h under heating at 60 ºC. The ion exchanged zeolite was recovered by filtration and repeatedly washed with distilled water and dried at 70 ºC in a vacuum oven overnight. The ion-exchanged zeolite was ground, meshed (210 µm) and calcined by same method. Catalyst pellets were prepared by the same procedure for manufacturing parent HY zeolite above.

3.2.2 Preparation and modification of ZSM-5/Alumina catalyst

The ammonium form of ZSM-5 zeolite was converted to hydrogen form by calcining the sample in flowing air at 500 ºC for 5 h with a heating rate of 10 ºC.min^{-1}. To make catalyst pellets with different ZSM-5 to γ-alumina ratio, a desired amount of ZSM-5 and boehmite were mixed to make the required amounts of supported ZSM-5 (25, 50, 75 and 85% wt. ZSM-5) with the corresponding finished catalysts named ZSM-5(25), ZSM-5(50), ZSM-5(75) and ZSM-5(85), respectively. Then 10 ml of distilled water and 0.1 g of nitric acid were added to make it into a

paste. The paste was extruded into rods with 3 mm diameter and 5mm in length using an Instron 4467 Universal Testing Machine with 30 kN uniaxial loading. The samples were dried in an oven at 80 ºC for 1 hour and calcined at 500 ºC with heating rate of 10 ºC.min^{-1} for 5 h. The commercial ZSM-5 zeolite named ZSM-5(100) was used as reference in powder form with no support.

Modification of zeolite was carried out by the wet impregnation method using phosphoric acid and nitrates of Cs, Ca and Fe. For each sample, the desired amount of ion-exchanging component (2.4 g orthophosphoric acid, 1.5 g CsNO$_3$, 7.7 g Ca(NO$_3$)$_2$.4H$_2$O, 11.9 g Fe(NO$_3$)$_3$.9H$_2$O) was dissolved in 25 ml of solvent (ethanol or distilled water), separately. Subsequently, 10 g of ZSM-5 powder, sieved to 100 μm, was added to the solution and stirred using a magnetic stirrer at room temperature for 2 hours. The treated zeolite was filtered and washed with ethanol (or distilled water) and dried in an oven at 80 ºC for 1 hour followed by calcination at 500 ºC for 5 hours. All the samples were crushed and sieved to 100 μm (140 mesh) particles for the catalytic test in the reactor.

3.2.3   Preparation of Co/ZSM-5, Ni/HY, Co/Silica and NiMo/Alumina catalysts

To prepare Co/ZSM-5 catalyst, a sample of ZSM-5 zeolite and boehmite in the ratio of 1:2 (weight basis) was mixed together and sieved to 100 μm. In a 100 ml beaker, 25 g cobalt (II) nitrate was dissolved in 20 ml ethanol and stirred in a magnetic stirrer until a uniform solution was obtained. The mixed powder was then added to the solution and stirred for 1 hour at 60 ºC. The ion-exchanged sample was then recovered by filtration, washed with ethanol and dried at 70 ºC in a vacuum oven overnight. Then, the dried sample was ground, meshed (210 μm) and calcined at 500 ºC with heating rate of 10 ºC.min^{-1} for 5 hours. Subsequently, 12 g of

impregnated zeolite-alumina, 7 g distilled water containing 0.35 g (5%wt) nitric acid was mixed together until a uniform paste was produced then extruded to 3mm diameter pellets.

To prepare Ni/HY catalyst, HY zeolite and boehmite in the ratio of 1:2 (weight basis) was mixed together and sieved to 100 μm. Subsequently, 25 g $Ni(NO_3)_2.6H_2O$ in 20 ml ethanol was added to the dry powder in a beaker and stirred by magnetic stirrer for 1 hour at 60 ºC until a uniform solution was obtained. The catalyst sample was then recovered by filtration, washed with ethanol and dried at 70 ºC in a vacuum oven. The dried sample then was ground, meshed and calcined at 500 ºC with heating rate of 10 ºC.min^{-1} for 5 hours. To make Ni/HY catalyst in pellet form, 18 g of powder sample and 18g distilled water containing 0.9 g (5%wt) acetic acid was mixed and extruded to 3mm diameter pellets.

To prepare Co/Silica catalyst, 4 g cobalt (II) acetate was dissolved in 20 ml ethanol and stirred using a magnetic stirrer for 4 hours at 60 ºC. Subsequently, 20 g silica was added to the mixture and stirred for 2 h. The mixture was then filtered, dried and calcined with same method.

NiMo/Alumina commercial catalyst from Azko Chemical Division containing molybdenum oxide as active component and nickel oxide as promoter in cylindrical shaped pellets was used in hydrogenation of naphthalene. The catalyst was reduced with hydrogen at 500 °C flow rate of 10 ml.min^{-1} for 2 hours before starting up the reaction. Figure 3.2 shows the four different catalysts used in hydrogenation of naphthalene.

Figure 3.2. Co/ZSM-5 (a), Ni/HY (b), Co/Silica (c) and NiMo/Alumina (d) catalyst pellets.

3.3   Apparatus and procedure

3.3.1   Catalytic rig

All the experiments were carried out in a fixed bed reactor (i.d. 15 mm, length 550 mm) made of 3/4" OD 316SS tube, held inside a single zone furnace. The feed, either gas or liquid, is preheated before entering the reactor by two traced heating lines which are controlled by two thermocouples (T1 and T2). The temperature of catalyst bed is measured using a Type K thermocouple (T3) inside the reactor with an accuracy of ± 2 ℃. A back pressure regulator (V6) is fitted after the reactor to ensure that the process operates within the desired pressure with an accuracy of ± 1 bar. The pressure of separator is adjusted by another back pressure regulator (V8). Two pressure gauges (P1 and P2) are installed before and after the reactor to monitor the reaction pressure as well pressure drop. To protect the reactor from over-pressure, a relief valve set at 270 bar (RV1) has been installed on top of the reactor. A HPLC pump (Kontron 320, Speck Analytical) with flow rate range of 0.01-9.99 ml.min^{-1} is used to pump the liquid feed to the reactor. A supercritical CO_2 pump (PU-1580-CO_2, Jasco) is used to pump CO_2 in supercritical phase as a reactant medium to the reactor. A mass flow controller (Brooks Smart Mass Flow, Model 5850S) is used to control the H_2 flow rate to the reactor. A one way valve is fitted before needle valves (V1, V2 and V3) to make sure there is no backflow in the lines.

Glass beads were used above and under the catalyst bed to secure the catalyst pellets inside the reactor and also to ensure a well distributed inlet gas/vapour stream. Glass wool is used to separate the layers of glass beads and catalyst for easier separation of the catalysts from glass beads after reaction for further characterisation of catalyst. The details of experimental procedure for each studied reaction are described in the following sections. Figure 3.3 and Figure 3.4 show the schematic diagram and the experimental rig used in this study.
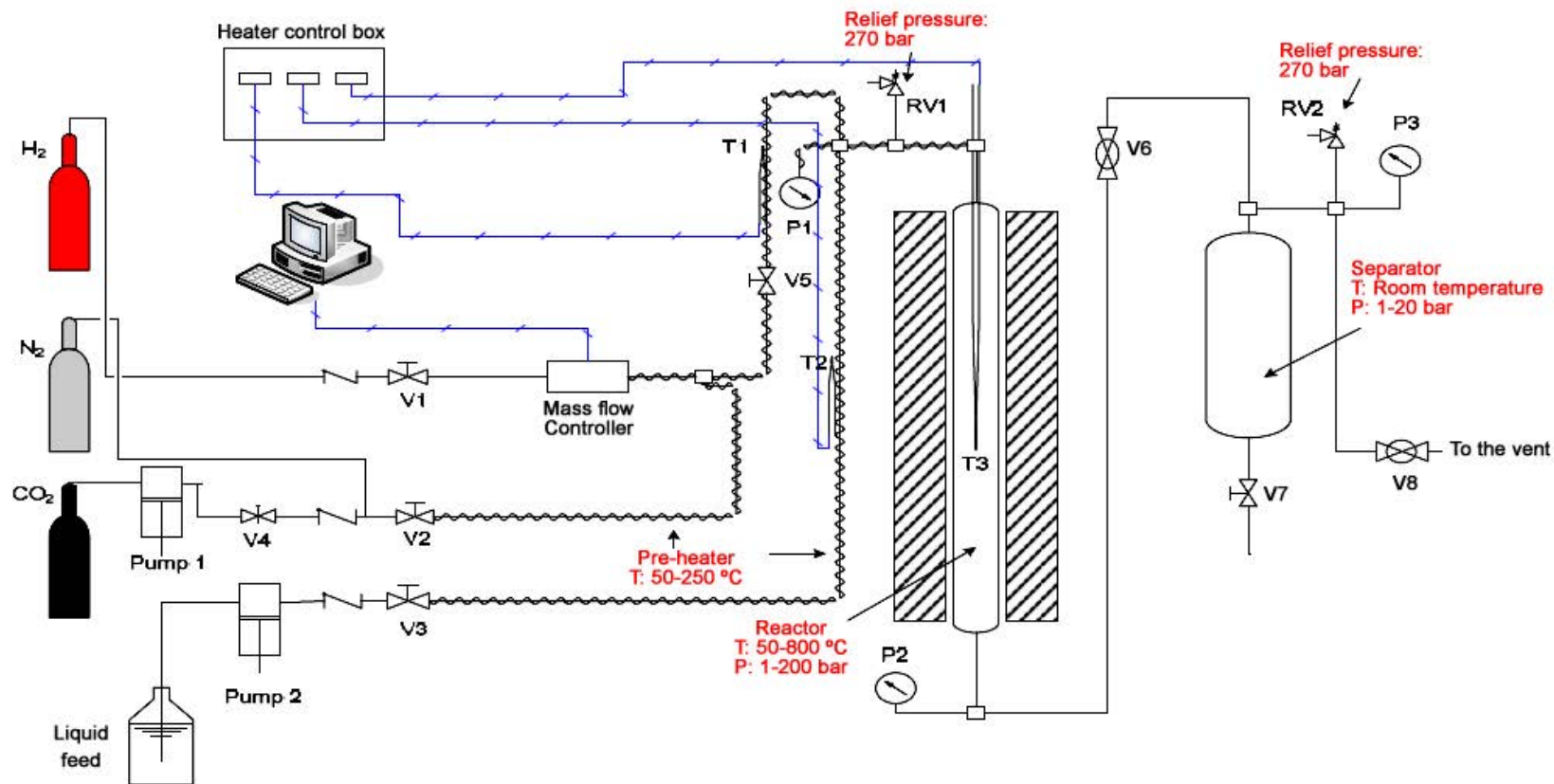
Figure 3.3. Schematic diagram of the apparatus with fixed bed reactor.

Pump 1	Pump 2	V1, V2, V3, V4, V5, V7	V6, V8	RV1, RV2	T1, T2, T3	P1, P2, P3	Mass flow controller	separator
Sc CO_2 pump (PU-1580-CO_2, Jasco)	HPLC pump (Kontron 320, Speck Analytical)	Needle Valve	Back pressure regulator (Tescom, 26-1700 series)	Pressure relief valve	Thermocouples (Type K, 1/8")	Pressure gauge	Model 5850S, Brooks Smart Mass Flow	304L SS DOT-Compliant Cylinder

Figure 3.4. The experimental rig.

3.3.1.1 **Alkylation of naphthalene**

After loading the catalyst in the reactor tube, the system was purged with nitrogen, the main heater was switched on and the temperature set to the operating values then the pump was switched on. For reactions above atmospheric pressure, the system was pressurised with nitrogen before switching on the pump.

Initially, a blank run was carried out using pellets manufactured from alumina without zeolite at typical reaction conditions (temperature: 220 °C, pressure: 50 bar, WHSV: 18.8 h^{-1}, IPA/naphthalene: 4, TOS 1 h) to make sure that no reaction occurred over alumina. Also to make sure that the solvent has no effect on the reaction or undergo cracking under typical

reaction conditions, cyclohexane was pumped to the reactor packed with HY zeolite pellets. After following the usual experimental procedure and analysis, no product was observed in that case. For a typical run using HY zeolite, 1.28 g (10 mmol) naphthalene, 2.40 g (40 mmol) isopropanol and 100 ml (926 mmol) cyclohexane as solvent were mixed together and pumped into the reactor from the top at constant flow rate of 0.8 ml.min^{-1}. The liquid products were collected from the gas–liquid separator. The range of reaction conditions in the fixed bed reactor were as follows: temperature 160–280 ºC, pressure 1–50 bar, Weight Hourly Space Velocity (WHSV) 9.4–28.3 h^{-1}, isopropanol/naphthalene molar ratio of 1–6 and Time on Stream (TOS) 6 h. A summary of all experimental run conditions over HY zeolite for dialkylation of naphthalene are listed in Table 4.1 in Chapter 4.

Conversion of naphthalene and selectivity of isomers at a certain time on stream were calculated as follows:

$$X_{naphthalene} = \frac{C^0_{naphthalene} - C_{naphthalene}}{C^0_{naphthalene}}$$

$$S_i = \frac{C_i}{\sum C_i}$$

where C_i is the molar concentration of different product compounds such as iso-, di-, and tri-propyl naphthalene.

3.3.1.2 Dehydration of methanol

A blank run was carried out at typical reaction conditions with lowest tested residence time to make sure no non-catalytic methanol decomposition occurs in the reactor. For a typical run, the feed containing 50 wt.% methanol in distilled water was introduced to the top of reactor using HPLC pump at constant volume flow rate of 1.25 ml.min^{-1} filled with ZSM-5 zeolite. The gas

and liquid products were collected from the gas-liquid separator after cooling from the reaction temperature to 20 °C. The gas samples were withdrawn from the system using Wheaton® glass serum bottles and analysed off-line. The following reaction conditions were investigated in the fixed bed reactor: temperature 340-460 °C, pressure 1-20 bar, WHSV 7-53 h^{-1}, feed composition of methanol 25-75 wt.% in water and Time on Stream (TOS) 4 h.

3.3.1.3 Hydrogenation of naphthalene

A similar procedure was used for hydrogenation of naphthalene. H_2 was used to pressurise the system during the hydrogenation reactions. The flow rate of H_2 during pressurisation was set to 10 ml.min^{-1} and once the reactor reached the desired pressure, the flow rate was adjusted to the set point being studied. Once the temperature and pressure reached the required values and were stable, the liquid feed pump was turned on. In a typical run a mixture of naphthalene and cyclohexane (50/50 wt./wt.) was pumped to the top of the reactor at constant flow rate of 0.5 ml.min^{-1} filled with catalyst sample (Co/ZSM-5, Ni/HY, Co/Silica or NiMo/Alumina). A liquid sample product of 2 ml was collected every 30 minutes for the first 2 hours and then once every hour for the remaining time on stream. All the experiments were carried out under optimal reaction conditions (temperature 300 °C, pressure 60 bar) which were determined by a previous research group member (Hassan, 2011). Conversion of naphthalene, selectivity and yield of isomers at a certain time on stream was calculated as follows:

$$X_{naphthalene} = \frac{C^0_{naphthalene} - C_{naphthalene}}{C^0_{naphthalene}}$$

$$S_i = \frac{C_i}{\sum C_i}$$

$$Y_i = S_i \cdot X_{naphthalene}$$

3.3.2   Analytical methods

3.3.2.1 Alkylation of Naphthalene

The liquid product of alkylation of naphthalene was collected from the gas–liquid separator and components were identified using a GC (Trace GC Ultra Gas Chromatograph) equipped with an FID detector and TR5-ms capillary column (15 m x 0.25 mm, 0.25 µm film thickness). The following conditions were used for GC method:

The column oven temperature program started with initial temperature of 100 ºC for 2 min, increased to 200 ºC at a heating rate of 4 ºC.min^{-1} and maintained for 2 min. Injection volume of 0.1 µl, split ratio of 80, injection temperature and detector temperature of 250 ºC were used, helium was used as carrier gas with 1 ml.min^{-1} flow. Further analysis was performed by GC–MS (GCT Premier) to provide verification of the GC results and to obtain the masses related to each peak. The GC-MS instrument was equipped with a DB5 column (30 m x 0.25 mm, 0.25 µm film thickness) with following conditions: temperature ramp of 60–280 ºC at a rate of 5 ºC.min^{-1} , held for 5 min, inlet temperature 250 ºC, 1 µl injection volume, split ratio 100 and using helium as carrier gas.

Brzozowski (2004) reported that using non-polar GC columns is more likely to cause analytical errors in GC analysis of diisopropylnaphthalene (DIPN) isomeric mixtures and therefore, intermediate or polar columns are preferred. However in this work, the GC method was verified by injecting commercial DIPN isomer mixture to confirm that all the possible DIPNs can be isolated and identified (Figure A.1, Appendix B). The peak integration was carried out using the Thermo-Qual browser and the areas for peak integration were carefully picked off manually so as to ensure that the peaks were reliably separated and the area to the baseline was included in the integration. Figure A.2 (Appendix B) shows the GC–MS trace, which shows slightly improved separation and sharper peaks compared with the GC trace. The tri-isopropyl

naphthalenes occur at retention times between 26.17 and 27.46 min, showing 8 major peaks corresponding to different isomers and substitutions around the aromatic rings. The tetra-isopropyl-naphthalenes occur between 28.82 and 31.9 min and display five major isomer peaks. Peaks above 32.5 min retention time are due to heavier poly-alkylated compounds. Bouvier et al., (2010) demonstrated the potential of two dimensional (GC x GC) analysis and polar GC columns for more accurate determination of the products of the dialkylation of naphthalene reaction over H-Mordenite.

3.3.2.2 Dehydration of Methanol

The gas and liquid products were collected from the gas–liquid separator after cooling from the reaction temperature to 20 ºC. The gas samples were withdrawn from the system using Wheaton® glass serum bottles and analysed off-line by using an Agilent 7890A GC equipped with HayeSepQ 80/100 (0.5m), HayeSepQ 80/100 (6ft), Molsieve5A 60/80 (6ft), HayeSepQ 80/100 (3ft), Molsieve 5A 60/80 (8ft), DB-1 (2m x 0.32mm x 5μm), HP-AL/S (25m x0.32mm x 8μm) and 3 detectors including an FID and two TCD detectors. FID connected to DB-1 and HP-AL/S columns were used for hydrocarbon detection with the following conditions: helium as carrier gas flowing at 3.3 ml.min^{-1} in constant flow mode (12.7 psi at 60 ºC), split ratio 1:60, with a 25 μl loop. One TCD connected to HayeSepQ 80/100 (0.5m), HayeSepQ 80/100 (6ft) and Molsieve 5A 60/80 (6ft) was used to detect permanent gases with following conditions: helium as carrier gas flowing at 25 ml.min^{-1} in constant flow mode (36 psi at 60 ºC), with a 500 μl loop. Another TCD connected to HayeSepQ 80/100 (3ft) and Molsieve 5A 60/80 (8ft) was used to detect hydrogen with following conditions: nitrogen as carrier gas flowing at 24 ml.min^{-1} in constant flow mode (26 psi at 60 ºC), with a 500 μl loop. The column oven temperature program was as follows: hold at 60 ºC for 5 min, ramp to 200ºC at 5 K.min^{-1} then hold for

15min. Liquid products were identified and analysed by using a Trace GC Ultra Gas Chromatograph equipped with a FID detector and HP-5 column (30m x0.32mm x 0.25μm). The analytical conditions were as follows: Column oven temperature program had an initial temperature of 40 ℃ for 2 min, heating up to 240 ℃ at a rate of 10 ℃.min^{-1}, injection temperature and detector temperature of 250 ℃, carrier flow rate (N_2) of 2 ml.min^{-1}, split ratio of 50 and injection volume of 0.1 μl. Further analysis was performed by GC–MS to provide verification of the GC results.

3.3.2.3 Hydrogenation of Naphthalene

To analyse the liquid products of naphthalene hydrogenation, Trace GC Ultra Gas Chromatograph equipped with a FID detector and DB-1 capillary column (60 m × 0.25 mm × 0.25 μm) with following conditions were used: The temperature of oven was maintained at 40℃ for 2 minutes and then raised to 250 ℃ at a heating rate of 5 ℃.min^{-1} and held for 5 min. An injection volume of 0.1 μl, split ratio of 100, injection temperature and detector temperature of 250 ℃ were used, helium with flow rate of 1 ml.min^{-1} was used as carrier gas. The concentrations of naphthalene and the products were assumed to be proportional to their peak areas.

3.4   Catalyst characterisation techniques

Several characterisation techniques were used to analyse fresh and used catalysts. Acidity measurement was carried out using Temperature Programmed Desorption (TPD) of t-Butylamine. Nitrogen adsorption-desorption at 77 K was used to measure the specific surface area, pore size distribution and pore volume for fresh and coked catalysts. XRD was used to analyse the structure of zeolite crystals before and after impregnation. Thermo-gravimetric analysis (TGA) of spent catalysts was used to determine the amount of coke deposited on the catalyst after reaction. This section summarises the instrument and details of the method used in each characterisation technique.

3.4.1   Acidity measurement by Temperature Programmed Desorption (TPD)

Various techniques have been successfully applied to study the nature, concentration, total strength and strength distribution of the active sites present in the zeolites. Most of these methods are based on the adsorption of gas-phase probe molecules, which are chosen on the basis of their reactivity and molecular size. Conventional methods, such as temperature-programmed desorption (TPD) and adsorption calorimetry of adsorbed probe molecules give information regarding the strength and distribution of the active sites. Spectroscopic methods such as infrared and NMR spectroscopy have also been used to study the nature of the acid sites on zeolites e.g. the relative amounts of Lewis and Brønsted acid sites (Dondur et al., 2005).

TPD is one of the most widely used and versatile techniques to characterise the acid sites of zeolites. Determining the quantity and strength of these acid sites is crucial to understand and predict the performance of zeolites as catalyst. There are three types of molecular probes commonly used for characterising acid sites using TPD: ammonia, non-reactive vapours, and reactive vapours. TPD of ammonia is a very common method for characterisation of site

densities in solid acids due to the simplicity of the technique; however it often overestimates the quantity of acid sites. Its small molecular size allows ammonia to penetrate into all pores of the solid where larger molecules commonly found in cracking and hydrocracking reactions only have access to large micropores and mesopores. It should be noted that ammonia is a very basic molecule which is capable of titrating weak acid sites which may not contribute to the activity of the catalyst. Moreover, the strongly polar adsorbed ammonia is capable of adsorbing additional ammonia from the gas phase. Therefore, this technique has been argued to be not useful as it cannot distinguish between Lewis and Brønsted acid sites and sometime it over estimates the acid density of solid acids (Gorte, 1999).

The most commonly used reactive probes are the alkyl amines including ethylamine, n-propylamine, isopropylamine and t-Butylamine. These amines are reactive and decompose to alkene and ammonia over Brønsted acid sites at high temperatures, thus, this technique is particularly can be used to measure the Brønsted acid site concentrations. This method is based on the formation of alkylammonium ions (from adsorbed alkyl amines that are protonated by Brønsted sites) that decompose to ammonia and olefins in a well-defined temperature range via a reaction similar to the Hofmann-elimination reaction (Kresnawahjuesa et al., 2002). As long as the alkyl group can give up a hydrogen atom to olefin and the amine is small enough to access the Brønsted sites, the measured acid sites density is independent of the particular used amine (Parrillo et al., 1990). The only information which is required to measure the strong Brønsted acid sites is the amount of alkyl amine decomposed to ammonia and olefin using an online GC-MS (Kresnawahjuesa et al., 2002). It should be noted that the decomposition temperature depends on both zeolite type and nature of alkyl group. For instance, this temperature is in the range of 275-300 ºC for decomposition of t-Butylamine over HZSM-5 (Si/Al=35) zeolite (Pál-Borbély, 2007).

The measurement procedure was started by removing the moisture followed by flowing a steady stream of analysis gas (carrier gas with a base compound) through the sample. Programmed desorption begins by raising the temperature linearly with time while a steady stream of inert carrier gas flows through the sample. At a certain temperature, the heat overcomes the activation energy; therefore, the bond between the adsorbate and adsorbent will break and the adsorbed species desorb. Depending on the type and strength of the acid site, they usually desorb the acid sites at different temperatures. These desorbed molecules enter the stream of inert carrier gas and are swept to the detector (e.g. TCD detector or mass spectrometer), which measures the gas concentrations. The volume of desorbed species, combined with the stoichiometry factor and the temperature at which pre-adsorbed species desorb, yields the number and strength of active sites.

In this work, the acidity of both the modified and parent catalysts was measured using TPD of t-Butylamine (t-BA) using a Micromeritics AutoChem II 2920 machine. 100 mg of the catalyst sample was placed inside the U-shaped sample tube and exposed to helium at 120 ℃ for 1h to remove the moisture, then the temperature of the sample was decreased to 40 ℃. Subsequently, pulses of t-Butylamine were injected from a loop (0.5 cm^3) into the sample until it became saturated. Once again, the sample was exposed to helium and its temperature was increased to 120 ℃, where it was kept constant for 1 hour. This was done to ensure that the physisorbed t-Butylamine was completely removed from the sample. A TPD profile was then obtained from 120 ℃ to 500 ℃ by heating the sample at a rate of 10 ℃.min^{-1}. The amount of t-Butylamine desorbed during the process was quantified with a TCD detector. The areas under the peaks were integrated using Autochem II 2920 software to determine the amount of t-Butylamine desorbed during TPD. Figure 3.5 shows the TPD method used for characterisation of zeolite sample. More details regarding calibration curves to measure the acid sites from the area of

peaks during TPD as well as an example regarding decomposition of isopropylamine to propylene and ammonia during TPD analysis of ZSM-5 zeolite are given in Appendix C.
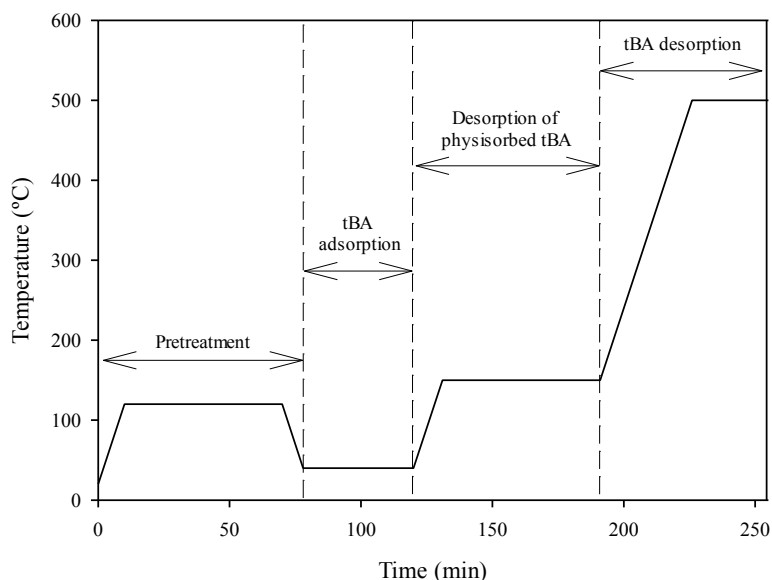
Figure 3.5. TPD method for characterisation of catalyst samples.

3.4.2   **Reducibility analysis by Temperature Programmed Reduction (TPR)**

Temperature-Programmed Reduction (TPR) can be used to measure the number of reducible species in the catalyst. It can also reveal the temperature at which the reduction occurs. An important aspect of TPR analyses is that the sample needs to have a reducible metal in its structure. The TPR analysis is performed by flowing a reducing gas (typically hydrogen in an inert carrier gas such as nitrogen or argon) through the sample, usually at room temperature. While the reducing gas is flowing through the sample, temperature is increased linearly with time and the amount of hydrogen consumed by adsorption/reaction is monitored and recorded. Changes in the concentration of the gas mixture are determined by a detector (e.g. TCD detector). This information yields the hydrogen uptake volume. TPR analysis was carried out using Micromeritics AutoChem 2920 machine. 100 mg of the catalyst sample was placed inside

the U-shaped sample tube and exposed to helium at 120 ºC for 1h to remove the moisture, then the temperature of the sample was decreased to 40 ºC. Subsequently, 5% hydrogen in argon with the flow rate of 10 ml.min^{-1} was fed to the sample. Temperature was increased to 800 ºC with ramp rate of 5 ºC.min^{-1} and was held for 30 min and the changes in the composition of effluent gas were recorded by a TCD detector.

3.4.3   Surface area and pore analysis by N$_2$ adsorption/desorption at 77 K

The specific surface areas and pore diameters were measured using adsorption-desorption of nitrogen at 77 K using a Micromeritics ASAP 2010 instrument. This instrument can perform analysis including single point and multipoint BET surface area, Langmuir surface area, micro pore volume and area, adsorption and desorption isotherms, mesopore volume and total pore volume. The BET Surface Area analysis is used to evaluate the total surface area of the catalyst before and after reaction. Pore-plugging phenomena which might occur due to coking can also be studied. After outgassing the sample, a mixture of nitrogen and helium (typically 5 to 30% nitrogen) flows over the sample which is immersed in a liquid nitrogen bath. Both the adsorption and desorption of the nitrogen are recorded. The amount of nitrogen desorbed and the sample weight are used to calculate total specific surface area. The total pore volume of the catalyst samples (both fresh and used) can be determined using N$_2$ adsorption/desorption near the saturation pressure of the adsorbate (P/P$_o$=0.995). As an example, BET surface area of HY zeolite was calculated using t-plot method. The slope and intercept of the plot were used to calculate the surface area. Calculations are presented in Appendix D.

3.4.4   Crystallography by X-Ray Diffraction (XRD)

X-ray powder diffraction (XRD) patterns of both fresh and modified zeolite were recorded on an Equinox 3000 diffractometer with CuKα_1 radiation source (λ = 1.5406 Å) in order to determine crystallite dimensions, relative crystallinity and structure destruction after modification. The detector was Curved Position Sensitive and the scan type was unlocked coupled. The XRD pattern was recorded in the range of 2θ=10-90º with step size of 0.02 and speed of 1 deg.min^{-1}.

3.4.5   Elemental analysis by XRF

X-ray fluorescence (XRF) is a powerful quantitative and qualitative analytical tool for elemental analysis of materials. There are two main approaches to the use of XRF spectrometry for elemental analysis: wavelength dispersive (WDXRF) and energy dispersive XRF spectrometry (EDXRF). WDXRF is known for its unrivalled accuracy, precision and reliability; however the instrument is more sensitive and requires more expensive equipment (Suarez-Fernandez et al., 2001). WDXRF instruments use an X-ray tube source to directly excite the sample. Elemental analysis of catalysts was carried out by Bruker S8 Tiger WDXRF spectrometer. The sample is first dried and ground to a fine consistency of 400 mesh then mixed with equal amount of wax to make a uniform homogeneous powder. The mixed powder was then placed in a die set and pressed by a hydraulic press to 2 tons. The pellet was then removed from the die cast and optically analysed to make sure it does not contain any cracks and has a smooth finish.

3.4.6   **Thermogravimetric analysis (TGA)**

The total amount of coked material on the catalyst after reaction was analysed by a NETZSCH TG 209 thermo-gravimetric analyser. Typically, 20 mg of the sample was placed in an alumina crucible and heated in a flow of air (20 ml.min^{-1}) from room temperature to 150 ºC at a heating rate of 10 K.min^{-1} and then held for 30 min to remove all the moisture, subsequently, the temperature was increased further to 800 ºC using the same heating rate and it was kept constant for 1 h. The change in weight of sample corresponds to the amount of coke on the catalyst which can be quantified to compare the performance of each catalyst.

The weight percentage of coke content was calculated as follows:

$$coke\% = \frac{W_{150} - W_{800}}{W_{800}} * 100$$

Where W_{150} is the weight of the sample at 150 ºC and W_{800} is the weight of the sample at 800ºC. All samples were repeated three times and the percentage error calculated. The sample was then cooled to room temperature at a rate of 10 °C.min^{-1} (Figure 3.6). The weight loss between 150°C and 800°C was attributed to coke.
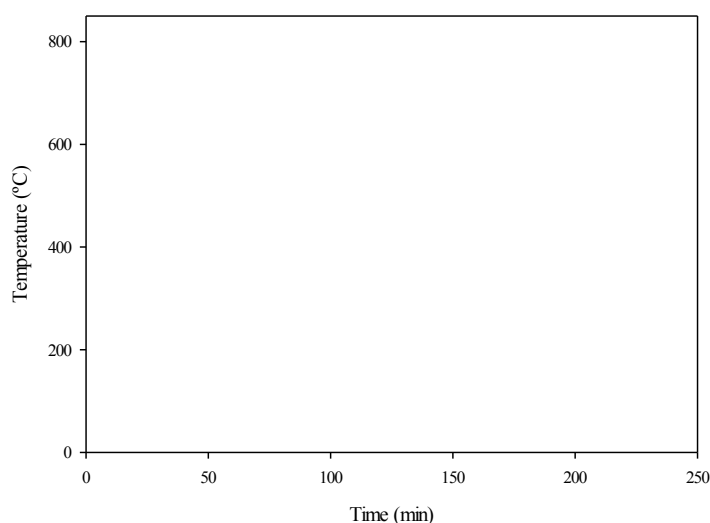
Figure 3.6. TGA temperature profile for analysis of coked zeolite.

Chapter 4 DIALKYLATION OF NAPHTHALENE BY ISOPROPANOL OVER HY ZEOLITE

As it was concluded from literature review in Chapter 2, zeolites such as H-mordenite (HM), H-beta (Hβ), HY, HZSM-5 and MCM-22 have been found to be preferred catalysts for the synthesis of 2,6-dialkylnaphthalene or 2,6-DAN. These porous materials applied as catalysts provide a suitable confined space for the establishment of shape selective reactions due to their unique pore structure. However, modification of zeolite to improve the catalyst selectivity to desired product by changing the pore size or acid sites distribution is still challenging.

The effect of reaction conditions such as temperature, pressure, space velocity, reactant composition on the catalyst activity and selectivity of zeolite in this process have been studied but further understanding is still required to analyse the effect of operating conditions on phase behaviour and their effect on reaction mechanism.

In section 4.1 of this chapter, the influences of changes in the process parameters (e.g. temperature, pressure, residence time and feed composition) upon the reaction are studied and optimum reaction conditions are found from experimental data. The observations on conversion and product distribution are explained in context of the phase behaviour of the system at different reaction conditions. Aspen Hysys 7.1 is used to calculate the process phase envelope. To investigate how the coking can change the reaction pathway, naphthalene conversion and product distribution at different reaction conditions and different TOS were studied. Flash calculations by Aspen Hysys were used to study possible condensation of reactants or products during the reaction over zeolite pores to become coke precursors.

In section 4.2, the effect of HY zeolite modification using transition metals (e.g. Fe, Co, Ni and Cu) to change the acid sites density and distribution and its influences on the catalyst activity and selectivity to desired products is reported.

Section 4.3 provides more information about characterisation of the catalysts. The results from this section are used to confirm the discussion for observations reported in previous sections. This chapter is based on the paper: Saeed Hajimirzaee, Gary A. Leeke and Joseph Wood 2012. Modified zeolite catalyst for selective dialkylation of naphthalene. Chemical Engineering Journal, 207–208, 329-341 (Hajimirzaee et al., 2012). A copy of this paper can be found in Appendix G.1.

4.1 Di-isopropylation of naphthalene

The effect of reaction conditions on the isopropylation of naphthalene over HY zeolite was investigated by undertaking a series of reactions at temperature range from 160 ºC to 280 ºC, pressure from 1 bar to 50 bar, isopropanol/naphthalene molar ratio from 1 to 6, WHSV from 9.4 to 28.3 h^{-1} for a time on stream of 6 h. Table 4.1 lists a summary of all reaction conditions studied in isopropylation of naphthalene over HY zeolite.

Table 4.1. Summary of reaction conditions in isopropylation of naphthalene over HY zeolite.

Experiment	T (ºC)	P (bar)	Feed flow rate (ml.min^{-1})	Isopropanol/ Naphthalene	Phase
1	140	1	0.8	4	Gas
2	160	1	0.8	4	Gas
3	180	1	0.8	4	Gas
4	200	1	0.8	4	Gas
5	220	1	0.8	4	Gas
6	240	1	0.8	4	Gas
7	260	1	0.8	4	Gas
8	280	1	0.8	4	Gas
9	220	1	0.8	4	Gas
10	220	15	0.8	4	Gas
11	220	35	0.8	4	Liquid
12	220	50	0.8	4	Liquid
13	280	1	0.8	4	Gas
14	280	15	0.8	4	Gas
15	280	35	0.8	4	Gas
16	280	50	0.8	4	Super critical
17	220	1	0.4	4	Gas
18	220	1	0.6	4	Gas
19	220	1	0.8	4	Gas
20	220	1	1.0	4	Gas
21	220	1	1.2	4	Gas
22	220	1	0.8	1	Gas
23	220	1	0.8	2	Gas
24	220	1	0.8	4	Gas
25	220	1	0.8	6	Gas

4.1.1 Effect of Temperature

The effect of temperature on the reaction was investigated from 160 to 280 ºC in increments of 20 ºC. The main components in the product were categorised as isopropyl-naphthalene (IPN),

di-isopropyl-naphthalene (DIPN) and other alkylated naphthalene isomers (e.g. tri- or tetra-isopropyl-naphthalene) which are included as poly-isopropyl-naphthalene (PIPN), as detected by GC analysis. Figure 4.1 displays the schematic diagram of possible reactions in the alkylation of naphthalene by isopropanol, with different routes on this diagram being favoured at different temperatures.
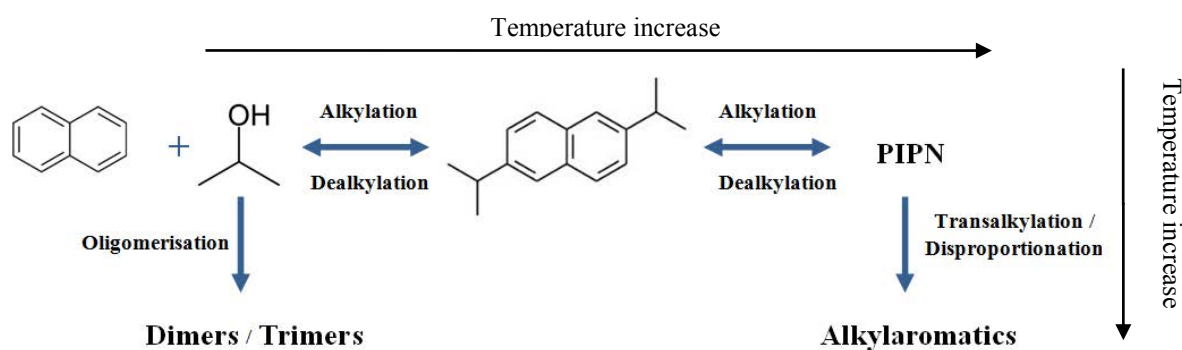
Figure 4.1. Schematic diagram of possible reactions in the alkylation of naphthalene by isopropanol (Liu et al., 1997).

Liu et al., (1997) studied the alkylation of naphthalene with t-butanol over HY and H-Beta zeolites. They observed that at higher temperatures secondary reactions such as dealkylation, disproportionation or transalkylation of di-alkylated naphthalene takes place. Alcohol can also be converted to its dimers and trimers. They conclude that the reaction sequences at different temperatures are in the following order:

Monoalkylation > Dialkylation > isomerisation of DIPN > Transalkylation ~ disproportionation ~ dealkylation

temperature increasing
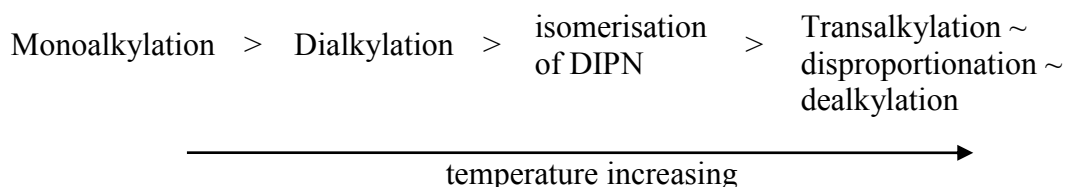
Figure 4.2 shows the naphthalene conversion as a function of time at different temperatures. At the beginning of the reaction, naphthalene conversion is ≥95 % at all temperatures except 140ºC (lowest temperature) and 280ºC (highest temperature).
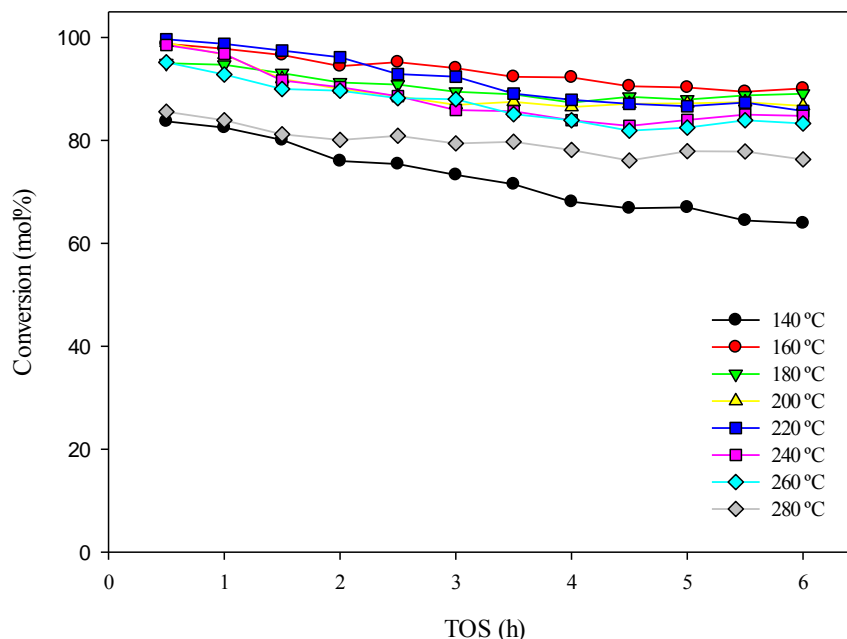
Figure 4.2. Naphthalene conversion over HY zeolite at different temperatures, pressure: 1 bar, IPA/naphthalene: 4, WHSV: 18.8 h^{-1}.

Naphthalene conversion at each temperature decreased gradually over time on stream which can be attributed to the deactivation and poisoning of active sites during the reaction. However, the rate of decrease in naphthalene conversion is more distinguished at the lowest temperature (140 ºC) which can be related to the phase change of the system during the reaction at this temperature. Figure 4.3 illustrates the phase envelope of fresh feed before reaction and mixture of reactants and products after 6 h reaction at different temperatures. The experimental points, or conditions investigated in the reaction are marked as black dots. The phase envelope at 180ºC is not shown in this figure as it was very similar to the phase envelope at temperatures of 160ºC and 200 ºC. As can be observed in Figure 4.3, during the reaction, the experimental conditions at 140 ºC and 160 ºC are in the two-phase region however, at the beginning of the reaction before products are formed these conditions are in the gas phase. This change in composition will change the phase diagram of the whole system which can cause the experimental point to lie within a different phase boundary. The experimental point at 140 ºC is shifted into the two-phase region after the reactor reaches a steady state of operation.
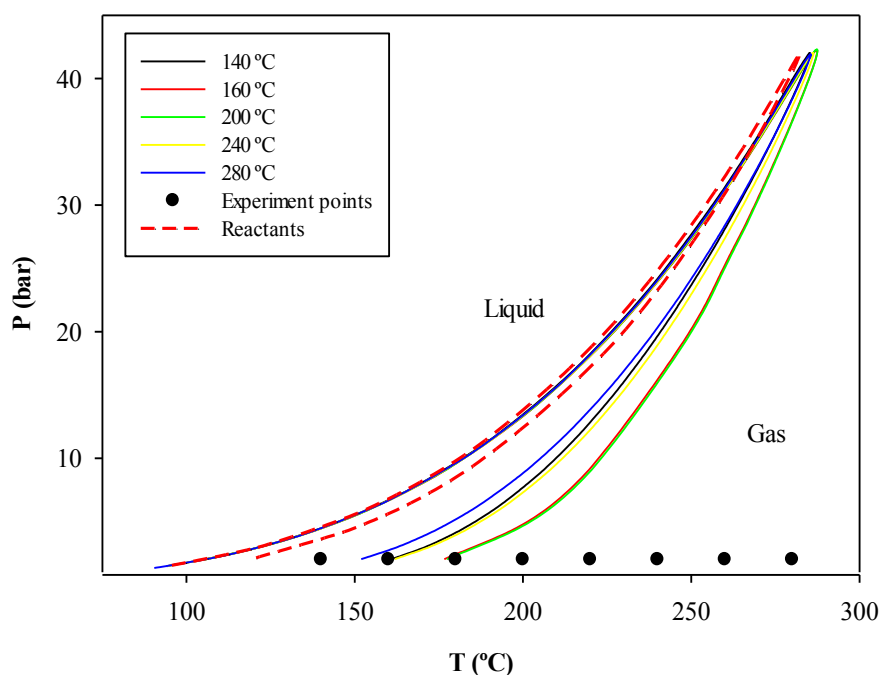
Figure 4.3. Phase envelop of fresh feed before reaction and mixture of reactants and products after 6 h reaction at different temperatures (IPA: 40 mmol, naphthalene: 10 mmol, cyclohexane: 100 ml).

This phase change from the gas to two-phase region can lead to condensation of heavier hydrocarbons on the surface of zeolite or entrance of pore channels. Condensation of heavy hydrocarbon within the catalyst pores can limit the diffusion of reactants for further reactions and additionally, it causes coking of the catalyst (Baiker, 1999). By increasing the temperature from 140 °C to 160 °C, naphthalene conversion rapidly increased to its highest value, however further increase in temperature suppressed the catalyst activity due to faster coking. The composition in terms of IPN, DIPN and PIPN during 6 h TOS reaction is almost constant at different temperatures, except at 160 °C (Figure 4.4-Figure 4.6). At this temperature, IPNs decreased noticeably while PIPN increased; however selectivity to DIPN remained almost constant. This change can be related to the phase change after almost 3 hours of the reaction from gas to liquid phase.
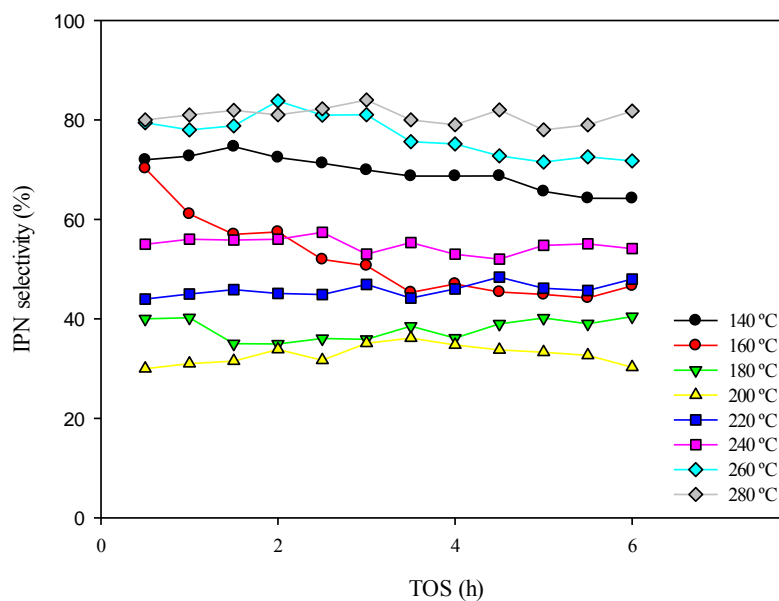
Figure 4.4. IPN selectivity at different temperatures, pressure: 1 bar, IPA/naphthalene: 4, WHSV: 18.8 h^{-1}.
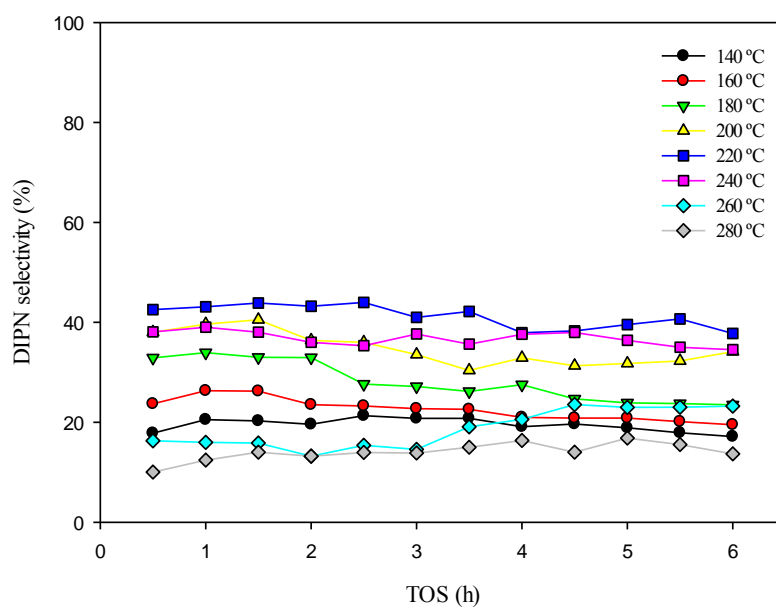
Figure 4.5. DIPN selectivity at different temperatures, pressure: 1 bar, IPA/naphthalene: 4, WHSV: 18.8 h^{-1}.

As it can be seen from Figure 4.3, all of the experimental points are located outside of the reactant phase envelope (red dashed line), however as soon as the reaction starts, this diagram shifts to the right side and as a result it takes almost 3 hours for the experimental point (at

97

160ºC) to fall within the two phase region. Low conversion and high selectivity to IPN at 140ºC can be related to the required activation energy to consecutively convert IPN to the higher alkylated molecule (e.g. DIPN and PIPN). In other words, although this temperature is enough to alkylate the naphthalene molecule in the first step to produce IPNs, it is not enough for further steps in the alkylation.
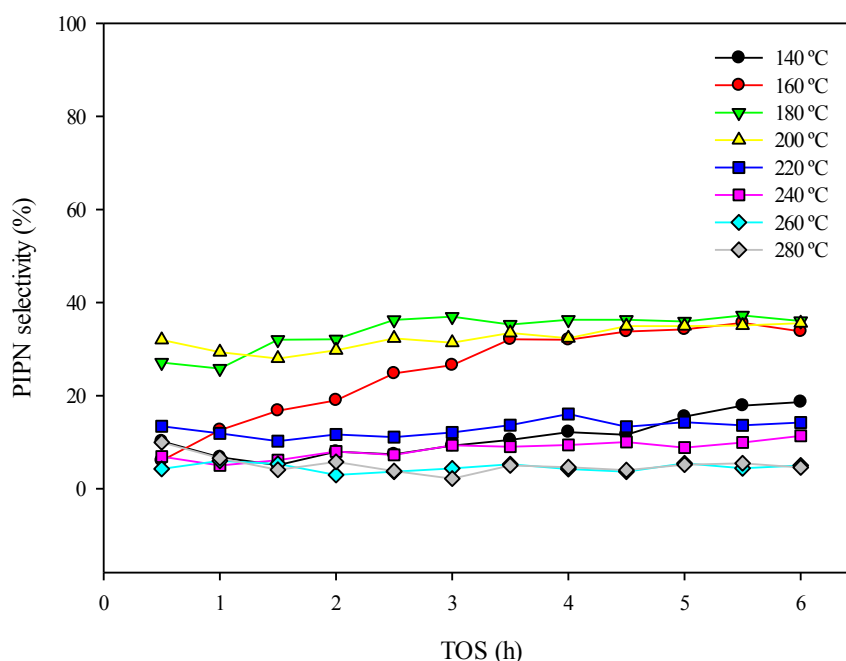
Figure 4.6. PIPN selectivity at different temperatures, pressure: 1 bar, IPA/naphthalene: 4, WHSV: 18.8 h^{-1}

Figure 4.7 illustrates the effect of reaction temperature on naphthalene conversion and product distribution over HY zeolite after 6h TOS. In this figure, naphthalene conversion, selectivity to different products (IPN, DIPN and PIPN) as well as 2,5-/2,7- DIPN ratio is displayed as a function of temperature after a constant reaction time (6 hours). The reason for choosing 6 h TOS for comparison is that at this time naphthalene conversion and product selectivity is more stable. Moreover, this time is enough to study or compare the coking on the catalyst sample at different conditions.
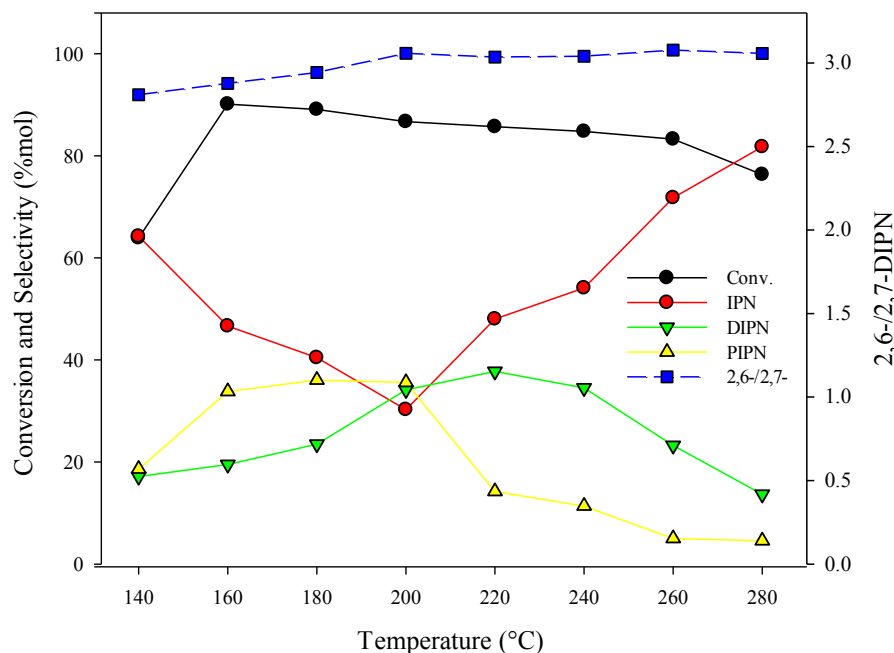
Figure 4.7. Effect of reaction temperature on naphthalene conversion and product distribution over HY zeolite, pressure: 1 bar, WHSV: 18.8 h^{-1}, isopropanol/naphthalene: molar ratio 4, TOS: 6 h.

Conversion of naphthalene sharply increased from 64% to 90% by increasing the temperature from 140 ℃ to 160 ℃. This can be attributed to the change in reaction phase from two-phase to gas phase. By progressively increasing the temperature from 160 ℃ to 280 ℃, conversion decreased from 90% to 76%. This implied the catalyst deactivation after 6 h occurs mainly at elevated temperatures. Selectivity to IPN decreased from 64% to 30% by increasing the temperature from 140 to 200 ℃, however this increased to 82% at 280 ℃. Such significant change in IPN selectivity is due to change in reaction pathway caused by secondary reactions (e.g. trans-alkylation and de-alkylation) of DIPN at elevated temperatures (Krithiga et al., 2005). Figure 4.7 shows that the selectivity to PIPNs was increased from 19% to 34% by increasing the temperature from 140 to 160 ℃, however it did not change significantly from 160 to 200 ℃. By further increasing the temperature from 200 to 280 ℃, PIPN selectivity decreased to 5%. The DIPN content increased from 17% at 140 ℃ to 38% at 220 ℃ and then

decreased to 14% at 280 ℃. This was attributed to the decomposition of PIPNs to DIPN and

IPN at higher temperature (e.g. 220 ℃), however at temperatures of more than 220 ℃, DIPN

also starts to decompose to IPN.

Figure 4.8 shows the schematic diagram of naphthalene alkylation by isopropanol proposed by

Colón et al. (1998). They suggested the following steps for mono-alkylation, dialkylation and

polyalkylation of naphthalene:

(1) First, the mono-alkylated ion is initially formed and absorbed on the surface but under this

form it cannot undergo attack by a positive isopropyl carbenium ion.

(2) Thereafter, it releases a proton giving mono-isopropyl-naphthalene and restores the acid site

on the surface.

(3) A new isopropyl carbenium ion can form from the reactant alcohol and attack mono-

isopropyl-naphthalene, leading to a di-isopropylated naphthalenium ion.

(4) Alternatively to step (3), mono-isopropyl-naphthalene could be attacked by an isopropyl

carbenium ion already present on the surface.
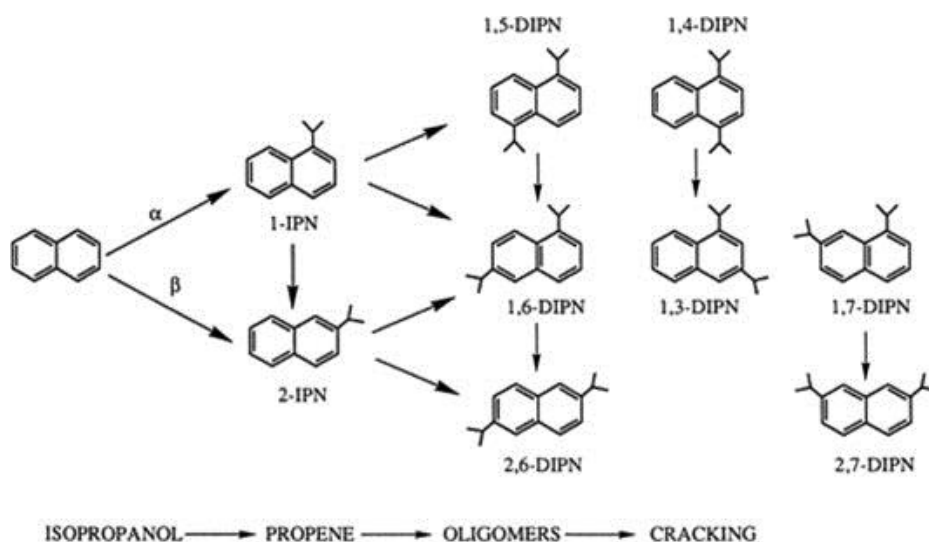
Figure 4.8. Schematic diagram of various steps in alkylation of naphthalene (Colón et al., 1998).

The higher electron density at the α-position of the naphthalene molecule should lead to 1-IPN (kinetic product). The more thermodynamically stable 2-IPN can, however, be formed through intra-molecular alkyl shift of the adsorbed 1-isopropylnaphthalenium ion. Further alkylation of both 1- and 2-IPN leads to the di-isopropyl-naphthalene isomers, tri-isopropyl-naphthalene, tetra-isopropyl-naphthalene and eventually poly-alkylated-naphthalene. Colón et al. (1998) stated that high density of the acid sites on the catalyst lead to a high concentration of isopropyl carbenium ions on the surface which favours mono-alkylation following by further alkylation through step (4). It also enhances the tendency of isopropanol towards oligomerisation and cracking.

The 2,6-/2,7DIPN ratio was increased from 2.8 to 3.1 with an increase in temperature from 140 to 200 ºC, and it remains almost constant at higher temperatures. Due to the higher energy barrier for 2,7-DIPN production (18 kcal/mol) compared to 2,6-DIPN (4 kcal/mol) (Horsley et al., 1994), it can be concluded that higher energy is required for the isomerisation of 2,7-DIPN to 2,6-DIPN, which was enhanced with temperature. Based on the conversion of naphthalene and selectivity to DIPN, 220 ºC was considered to be the optimum reaction temperature.

4.1.2   Effect of Pressure

The effect of pressure on alkylation of naphthalene was studied at 220 ºC and over the pressure range of 1 to 50 bar. Figure 4.9 shows the naphthalene conversion at 1, 15, 35 and 50 bar. The conversion is gradually decreased during 6 h TOS at 1 bar and 35 bar from approximately 98% to 86% and 88%, respectively. At 15 bar, the conversion declined during the first 2 hours to 94%, however, it jumped to 97% at 3h TOS and remained almost constant after that. This behaviour can be related to the phase change during the reaction at this pressure.
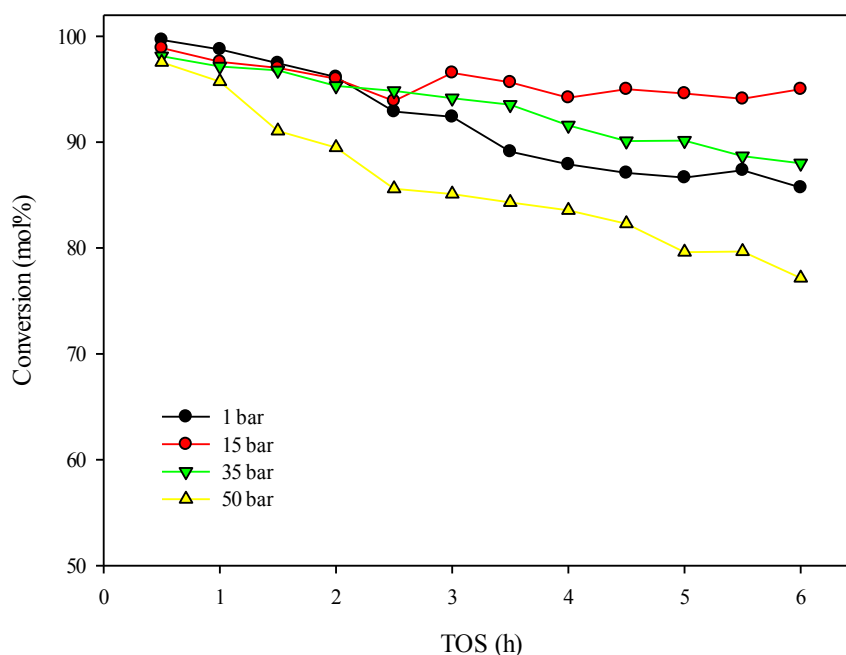
Figure 4.9. Naphthalene conversion over HY zeolite at different pressures, temperature: 220 ºC, IPA/naphthalene: 4, WHSV: 18.8 h^{-1}.

Figure 4.10 illustrates the phase diagram of the system for fresh feed before reaction and mixture of reactants and products after 6 hours at different pressures. The experimental points are highlighted as black dots. The points corresponding to a temperature of 220 ºC and pressure of 1 bar or 15 bar are in the gas phase before reaction, however, the point at 15 bar shifts to two-phase region during the reaction. The results suggest that this shift from gas phase to two-phase region occurs after 3 h TOS. The higher conversion after 3 hours is possibly due to the increase in solubility of heavy hydrocarbons and mass-transfer rate as it is believed that bulky precursors of carbonaceous deposits can be easily removed from the zeolite pores by a liquid product stream (Brzozowski et al., 2010). A sharper decrease in naphthalene conversion from 98% to 77% at 50 bar could be attributed to faster coking at higher pressure and in the liquid phase. Since the reaction takes place with no change in the number of moles and also it is in the liquid phase, thermodynamic equilibrium should not be influenced by pressure. However, increasing the pressure can enhance the rate of reaction through forcing hindered reactants into

the pores of the zeolite. Increasing the reaction rate at elevated pressures led to an increase in the production of PIPNs as result of a consecutive reaction. PIPNs could be a source of coking in this reaction due to their high molecular weight. Colon et al. (1998) showed that up to 80% of the coke formed after 1 hour on HY zeolite in the alkylation of naphthalene is mainly composed of poly-alkylated naphthalenes including pyrenic and indenopyrenic compounds. They explained that coke deposition on the zeolite can be initiated from different sources such as polyalkylation of naphthalene, transalkylation between polyalkylated compounds and naphthalene, isomerisation between the isopropylated products, oligomerisation and even reactions involving the solvent. However, depending on the diffusion rate of various products within the zeolite pores, different coke precursors may form.
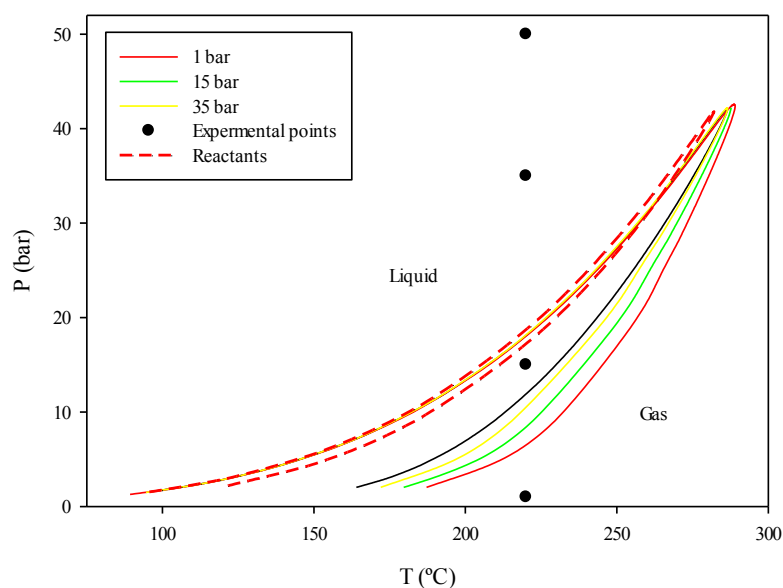
Figure 4.10. Phase diagram of the fresh feed (IPA/naphthalene=4), and mixture of reactants and products at different pressures, T=220 ºC, TOS=6 h.

Selectivity to IPN, DIPN and PIPN products are illustrated in Figure 4.11 to Figure 4.13 respectively. At 1 bar pressure, most of the products are in form of IPN and DIPN. Selectivity to IPN increased slightly from 44% to 48%, DIPN decreased from 43% to 38% and PIPN is

constant around 14%. This suggests that the conversion of IPN to DIPN is suppressed as a result of coking with increasing reaction time at this pressure. Low selectivity to PIPN at 1 bar implies a lower formation rate of this compound compared to IPN or DIPN.

At 15 bar pressure, the experimental point is located in the gas phase at the beginning of the reaction (Figure 4.10). Increasing pressure from 1 bar to 15 bar, led to an increase in selectivity to di-alkylated and poly-alkylated products over the first 3 hours of the reaction. During this time, IPN selectivity slightly increased from 36% to 39%, DIPN selectivity decreased from 37% to 34% and PIPN selectivity was almost constant at around 27%. After 3 hours TOS, a sharp drop in selectivity to IPN from 39% to 20% and DIPN from 34% to 24% was observed and at the same time a sharp rise in selectivity to PIPN from 27% to 55%, can be related to the phase change. Changing from gas phase to liquid phase in this case was thought to improve the solubility of heavier products and extract them from inside the pores and as a result move the reaction equilibrium to the right side (Figure 4.1). In turn this could have led to the observed increase in PIPN concentration in the product stream.

In terms of evaluating the effect of higher pressures upon the reaction, it should be noted that reaction at 35 bar and 50 bar pressure takes place in liquid phase. Selectivity to DIPN at 35 bar changed slightly from 29% to 26% between 0.5 and 6 hours reaction time and at 50 bar it gradually decreased from 37% to 28% over the same time range (Figure 4.12). At 50 bar, PIPN selectivity increased from 12% to 30% between 0.5 – 6 hours reaction time, however this change is from 37 to 40% at 35 bar. This suggests a higher formation rate of PIPN at higher pressure which results in faster formation of coke precursors that eventually lead to a decrease in naphthalene conversion. During the reaction, the internal surface of the zeolite pores becomes saturated with products, thus for adsorption and reaction, the reactant molecules have to compete with the products and it becomes more complicated in case of coke precursors with

higher molecular weight. As a result, the reaction at the outer surface of the zeolite crystals becomes more predominant, especially when the mass transfer properties depends to pressure and coke precursors can easily be dissolved from the catalyst surface. Although, the reaction inside the pores may still occur, it becomes very slow due to diffusion resistances by the irreversible adsorption of higher molecular weight products (e.g. poly-nuclear aromatics) on the active sites. These compounds build up inside the pores almost independently of the properties of the phase surrounding the catalyst particles (Gläser and Weitkamp, 2003).
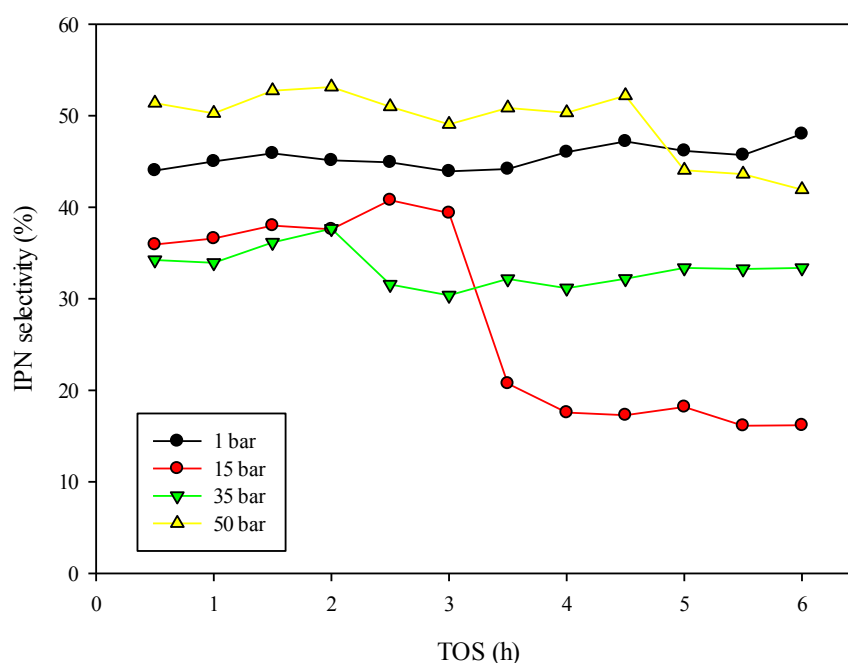
Figure 4.11. IPN selectivity at different pressures, temperature: 220 ºC, IPA/naphthalene: 4, WHSV: 18.8 h^{-1}.
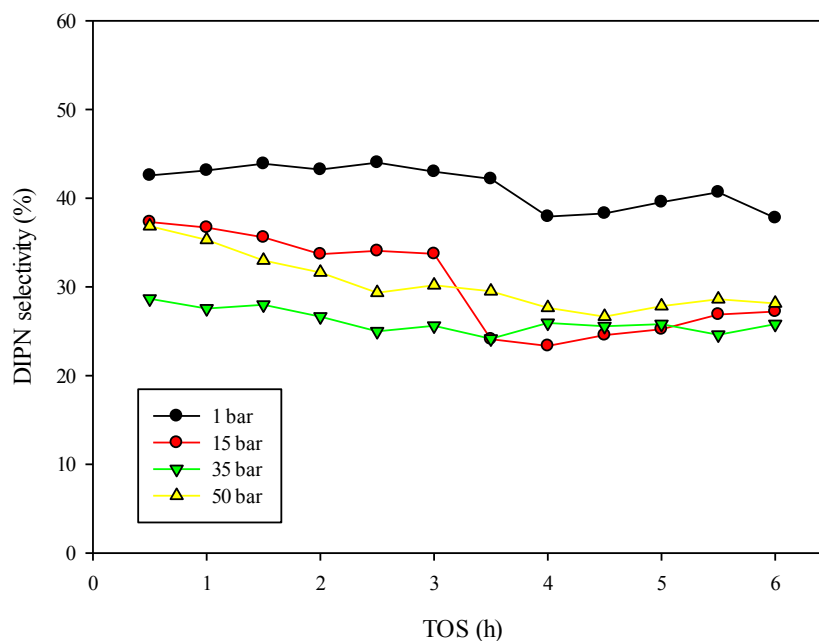
Figure 4.12. DIPN selectivity at different pressures, temperature: 220 ºC, IPA/naphthalene: 4, WHSV: 18.8 h^{-1}.
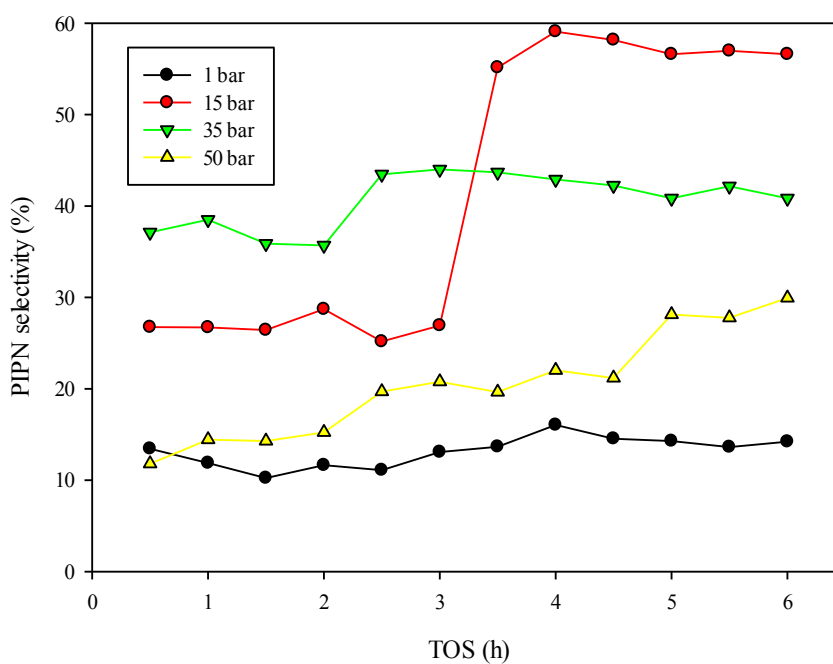
Figure 4.13. PIPN selectivity at different pressures, temperature: 220 ºC, IPA/naphthalene: 4, WHSV: 18.8 h^{-1}.

To better understand the effect of pressure on naphthalene conversion and product distribution, another series of reactions were carried out at higher temperature (280 ºC).

The effect of reaction pressure at 220 ºC and 280 ºC on naphthalene conversion and products distribution after 6 h TOS are illustrated in Figure 4.15 and Figure 4.16, respectively. As it can be seen from phase diagram of the system at 280 ºC (Figure 4.14), the experimental points at pressure of 1, 15 and 35 bar are in the gas phase, however, the reaction condition at 50 bar is in supercritical. As it was mentioned in Section 2.3.3.6 of Chapter 2, reaction in supercritical phase can reduce or even avoid catalyst deactivation that might occur rapidly in the gas phase or liquid phase, since supercritical fluids can potentially dissolve coke precursors more readily. At 280ºC, by increasing the pressure from 1 to 50 bar the conversion of naphthalene increased from 76% to 98%. When the pressure was increased from 1 to 35 bar, both DIPN increased from 14% to 35% and PIPN from 5% to 45%, respectively. IPN was decreased from 82% to 20%, but by further increasing the pressure from 35 to 50 bar, the trends changed. The selectivity to PIPN was decreased to 28% while DIPN and IPN selectivity were respectively increased to 46% and 25% at this pressure (50 bar). A significant contributing factor to the observed shifts in selectivity could be the change of the reaction conditions from subcritical to supercritical conditions.
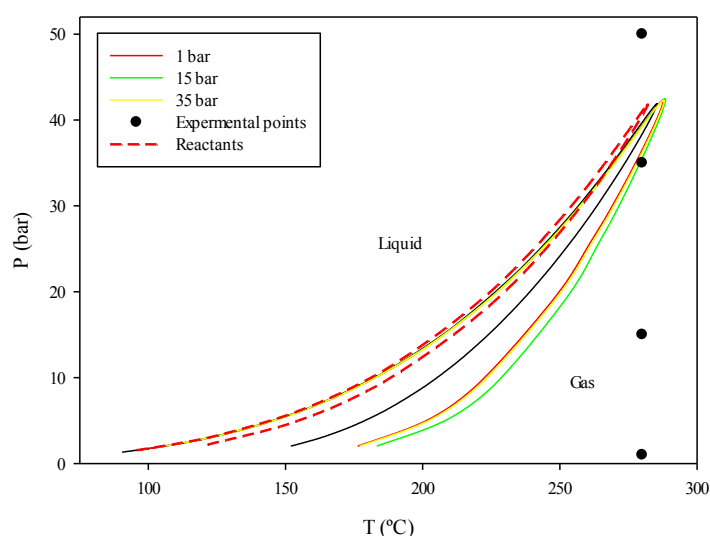
Figure 4.14. Phase diagram of the fresh feed (IPA/naphthalene=4), and mixture of reactants and products at different pressures, T=280 ºC, TOS=6 h.
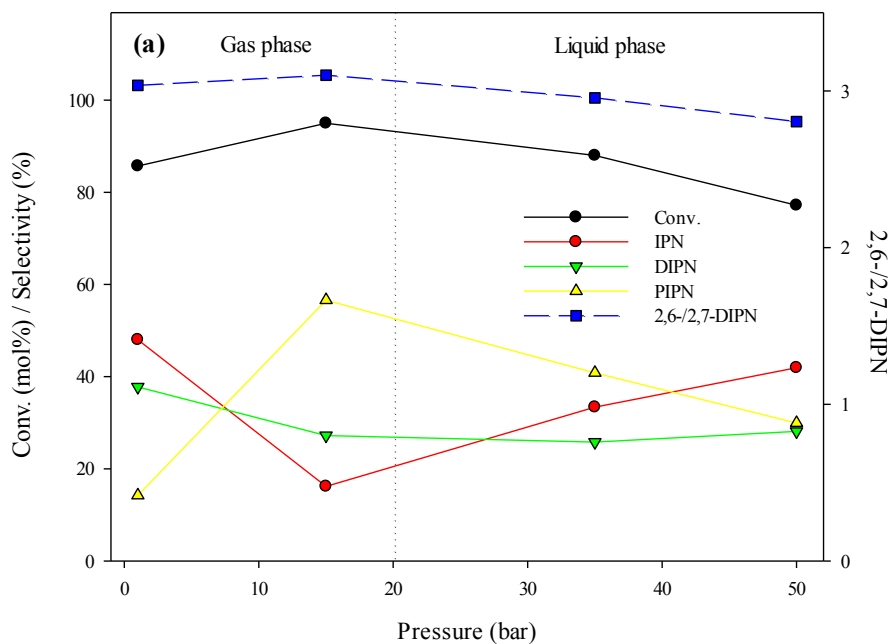
Figure 4.15. Effect of reaction pressure on naphthalene conversion and product distribution over HY zeolite, temperature: 220 °C, WHSV: 18.8 h^{-1}, IPA/naphthalene: 4, TOS: 6 h.
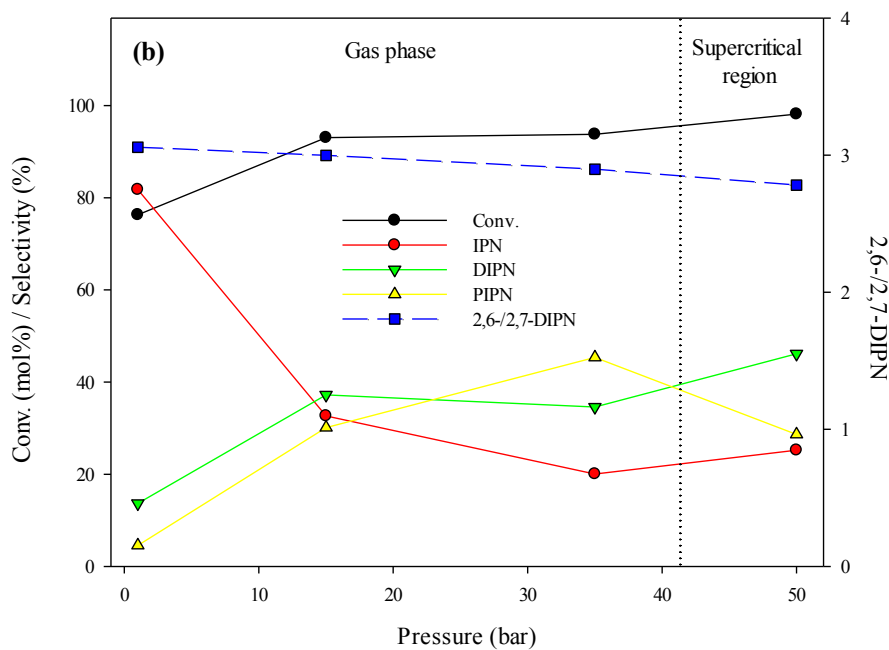

Figure 4.16. Effect of reaction pressure on naphthalene conversion and product distribution over HY zeolite, temperature: 280 °C, WHSV: 18.8 h^{-1}, IPA/naphthalene: 4, TOS: 6 h.

To explain this observation values of density and dynamic viscosity of fresh feed at 220 ℃ and 280 ℃ have been plotted on Figure 4.17a and 4.17b, respectively, as a function of pressure. The values were calculated by Aspen Hysys V7.1 (Peng–Robinson was chosen as equation of state). The density and viscosity dramatically increases during the phase change from gas to liquid (T=220 ℃, P=18 bar) and from gas to supercritical (T=280 ℃, P=42 bar). The increases in density and viscosity observed in 4.17a and b are consistent with the phase changes shown by the experimental points on the bubble and dew point diagram of Figure 4.10 and Figure 4.14. It was of interest to study conditions close to the critical point, where fine turn of behaviour can occur with modest changes in operating conditions, possibly leading to related changes in catalyst deactivation behaviour.

To study the effect of supercritical conditions on catalyst activity, two experiments conducted at conditions pertaining to two different phases were carried out for long duration catalyst test (e.g. 20 h). The first experiment was performed at 280℃ and 35 bar (gas phase) and the second experiment was performed at 280 ℃ and 50 bar (supercritical). Figures 4.18 and 4.19 show the naphthalene conversion and product distribution during 20 h TOS at 35 bar and 50 bar, respectively.
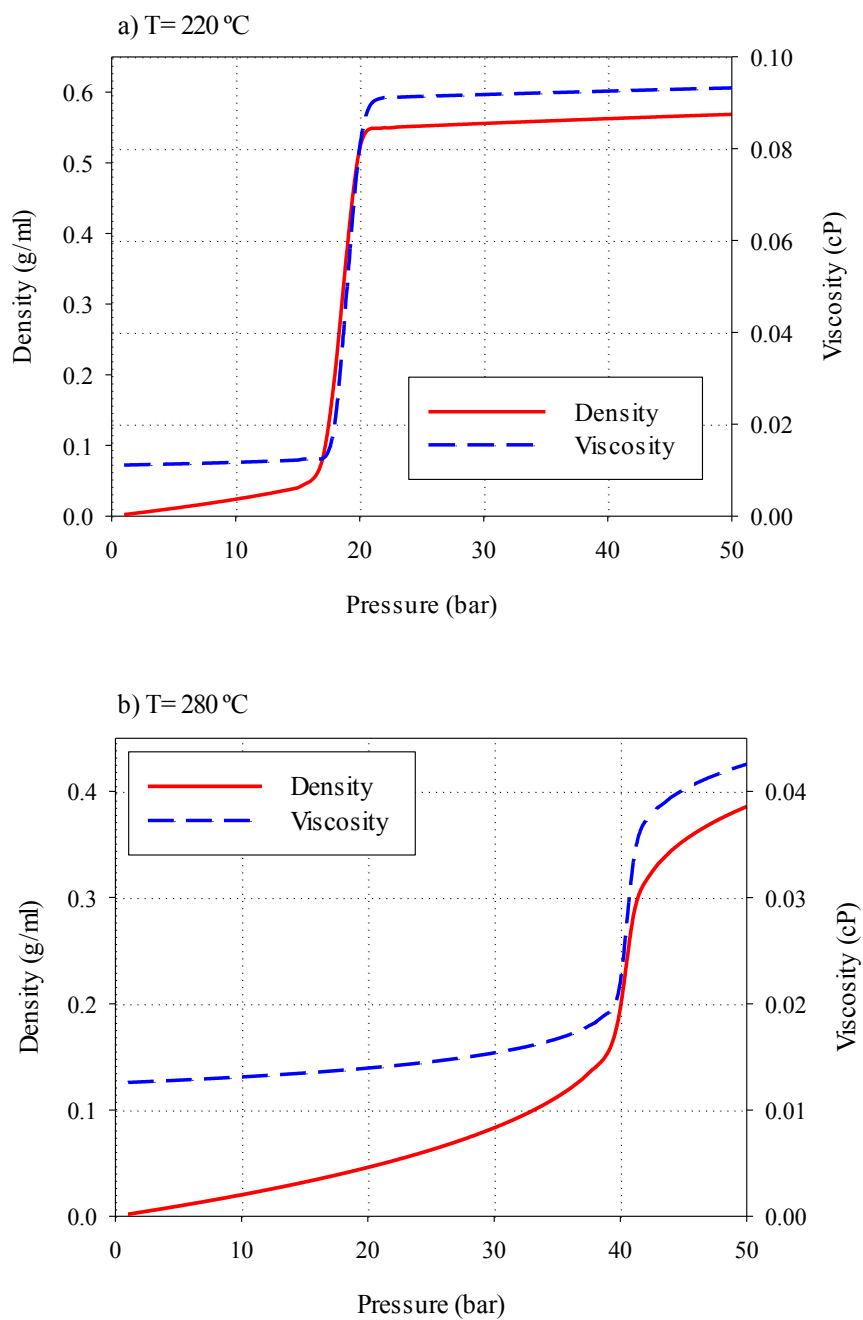
Figure 4.17. Mass density and dynamic viscosity of fresh feed, naphthalene: 10 mmol, isopropanol: 40 mmol, cyclohexane: 100 ml, a) temperature: 220 °C, b) temperature: 280 °C.
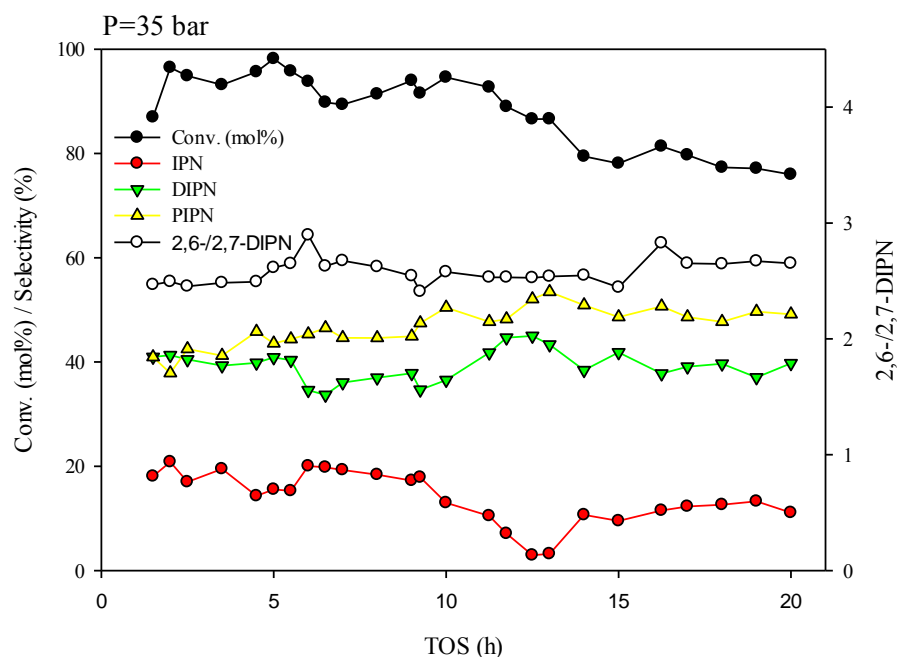
Figure 4.18. Naphthalene conversion and product distribution over HY zeolite at 280 °C, 35 bar, WHSV:18.8 h^{-1}, IPA/naphthalene: 4.
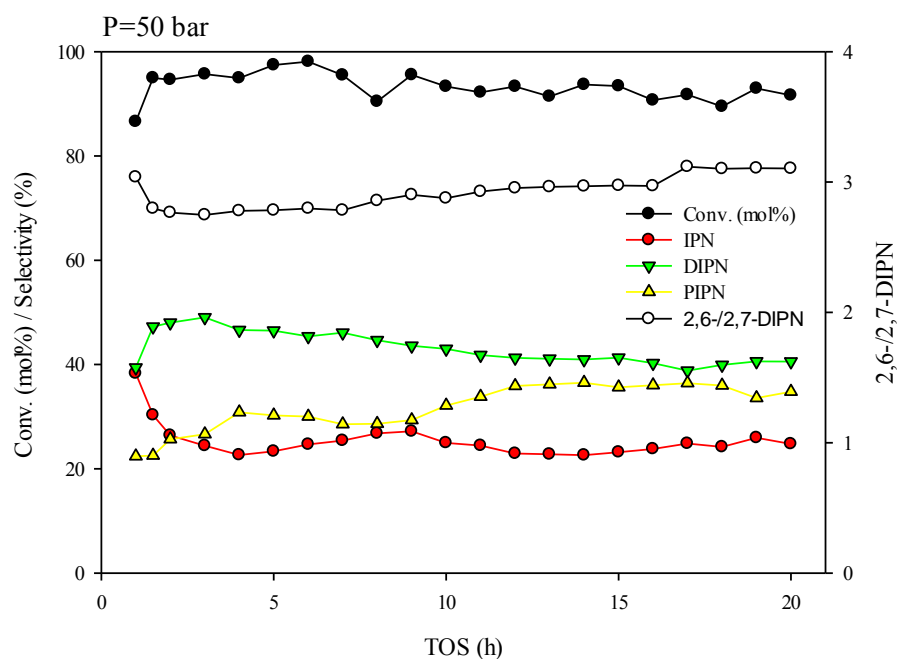
Figure 4.19. Naphthalene conversion and product distribution over HY zeolite at 280 °C, 50 bar, WHSV:18.8 h^{-1}, IPA/naphthalene: 4.

From the figures it can be concluded that changing the conditions from gas phase (35 bar) to supercritical (50 bar), decreased the production of PIPNs and led to higher selectivity to IPN

and DIPN. This could possibly be due to the higher diffusivity (compared with liquid phase) and solubility (compared with gas phase) exhibited in the supercritical region (Gläser and Weitkamp, 2003). Arunajatesan et al., (2003) have shown that in a catalysis reaction there is an optimal condition at which the reaction medium would possess liquid-like densities to solubilise (i.e., desorb) the coke precursors and gas-like transport properties to effectively transport the oligomeric species out of the catalyst pores. Figure 4.17.b shows that at 40 bar, a significant change of density and viscosity of fresh feed occurs due to the change of reaction conditions. Conversion at the pressure of 35 bar decreased from 99% to 76% after 20 h while at 50 bar the catalyst is still active after 20 h and conversion is maintained at more than 90%. It can be concluded that catalyst life time can be prolonged in supercritical conditions.

In the gas phase, the solubility of reaction products is much lower than that in the supercritical phase and before desorption of the product molecules from surface of the catalyst, isomerisation or further alkylation to heavier compounds occurs which eventually lead to coke deposition and catalyst deactivation.

In other words, in the supercritical region, it is easier for lighter components (IPN and DIPN) to diffuse from the zeolite channels instead of being trapped in the channels and converting to PIPN as a result of consecutive reactions.

4.1.3 **Effect of residence time**

The effect of weight hourly space velocity (WHSV) on the conversion and product distribution was investigated by varying the feed flow rate from 0.4 to 1.2 ml.min^{-1}. Table 4.2 lists the calculated WHSV values proportional to each flow rate. Conversion of naphthalene over HY zeolite at different WHSVs is displayed on Figure 4.20. Naphthalene conversion is almost constant during the first 3 hours at flow rates of 0.4, 0.6 and 0.8 ml.min^{-1}, however it is higher

at feed flow rate of 0.4 ml.min^{-1} possibly due to lower rate of deactivation. At higher flow rates, the initial conversion is lower due to shorter contact time.

Table 4.2. Range of studied feed flow rate.

Feed flow rate (ml.min^{-1})	0.4	0.6	0.8	1.0	1.2
WHSV (h^{-1})	9.4	14.1	18.8	23.5	28.3

At feed flow rate of 1.0 ml.min^{-1}, conversion started from 95% at the first sample taken at 0.5 h and decreased to 82% after 6 h, whilst at 1.2 ml.min^{-1}, initial naphthalene conversion at 0.5 h was as low as 88% and decreased to 79% after 6 h reaction time. Chu and Chen (1995) studied the effect of space velocity on alkylation of naphthalene by isopropanol over USY zeolite. They observed that at 1 bar and 200 ºC by increasing space velocity from 0.83 to 2.1 h^{-1}, conversion decreased from 95 to 70%. Similarly, Anand et al., (2003) studied effect of varying WHSV from 3.3 to 9.6 h^{-1} in isopropylation of naphthalene over HY zeolite and observed a noticeable drop in conversion from 93% to 86%.
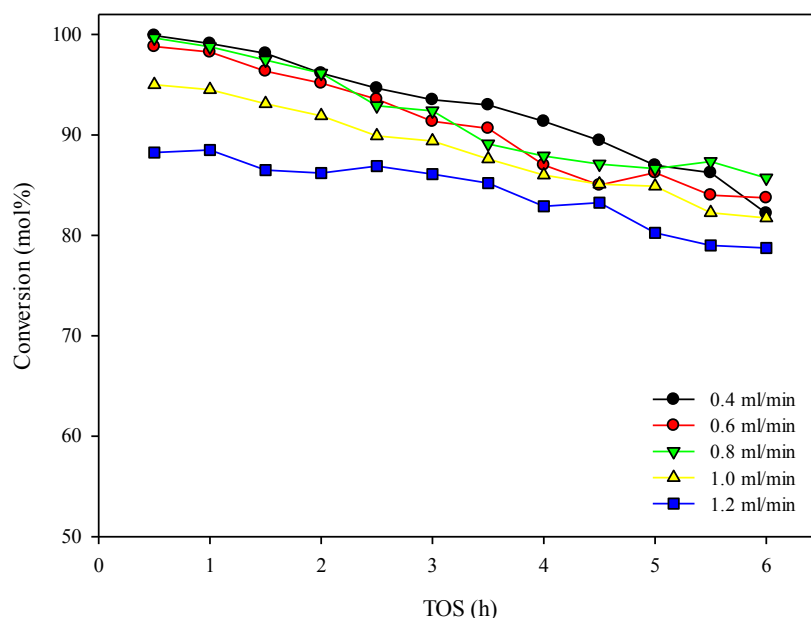
Figure 4.20. Effect of feed flow rate on naphthalene conversion. Temperature: 220 °C, pressure: 1 bar, IPA/naphthalene: 4.

The selectivities to IPN, DIPN and PIPN at different feed flow rates are presented in Figure 4.21 to Figure 4.23, respectively. The selectivity to IPNs are almost constant during 6h time on stream at flow rate range of 0.4 to 1.0 ml.min^{-1} (Figure 4.21). However, at highest flow rate (1.2 ml.min^{-1}), the trend to IPN selectivity is different and it decreased gradually from 54% to 41%.

An increase in feed flow rate did not affect DIPN selectivity trends significantly even at high flow rates (Figure 4.22). By increasing flow rate from 0.4 to 0.8 ml.min^{-1}, the average DIPN selectivity (during 6 h TOS) increased from almost 30% to 43% but by further increasing the flow rates, selectivity to DIPNs decreased to 35%. As the highest selectivity to DIPNs (as desired products) was obtained at 0.8 ml.min^{-1} (WHSV= 18.8 h^{-1}), it was selected as the optimum flow rate and used for subsequent experiments.
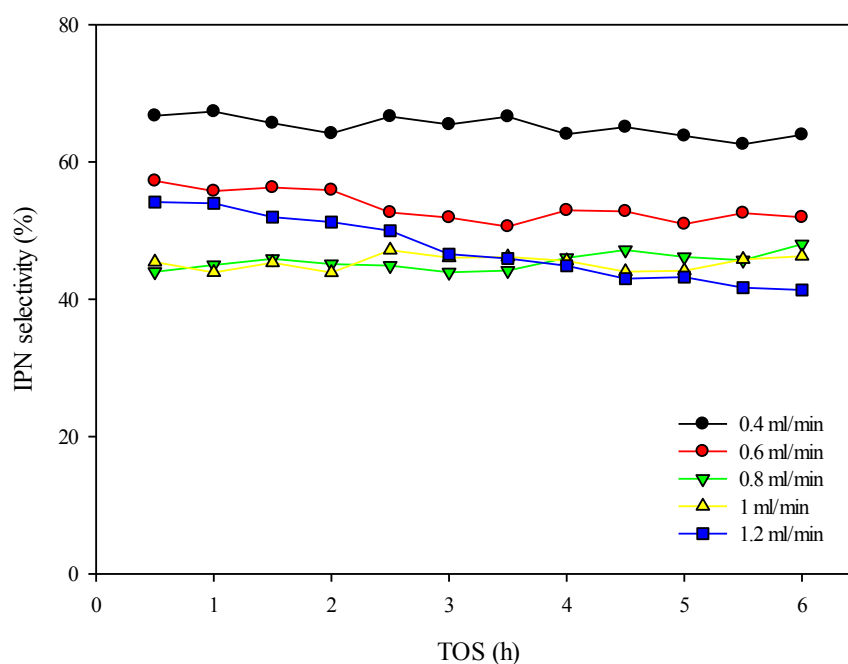
Figure 4.21. Effect of feed flow rate on selectivity to IPN. Temperature: 220 °C, pressure: 1 bar, IPA/naphthalene: 4.
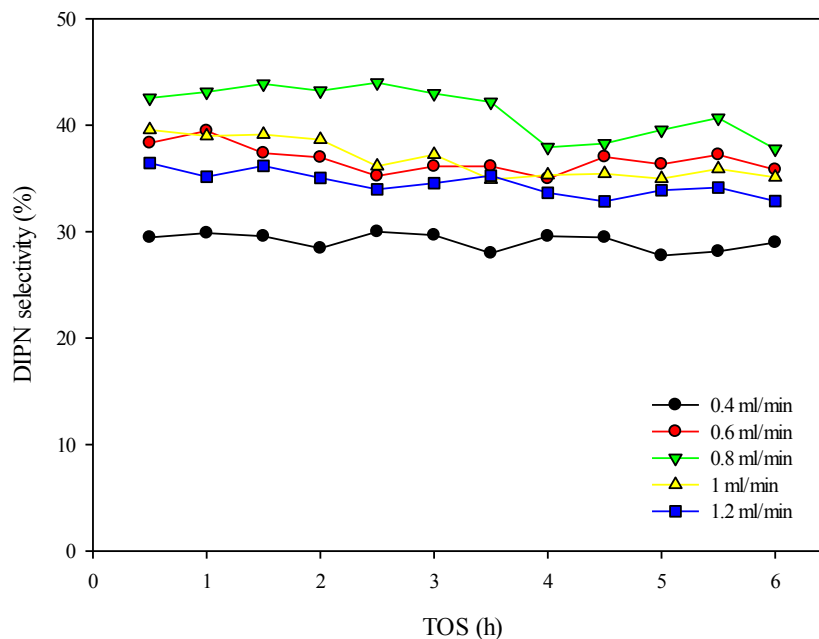
Figure 4.22. Effect of feed flow rate on selectivity to DIPN. Temperature: 220 °C, pressure: 1 bar, IPA/naphthalene: 4.
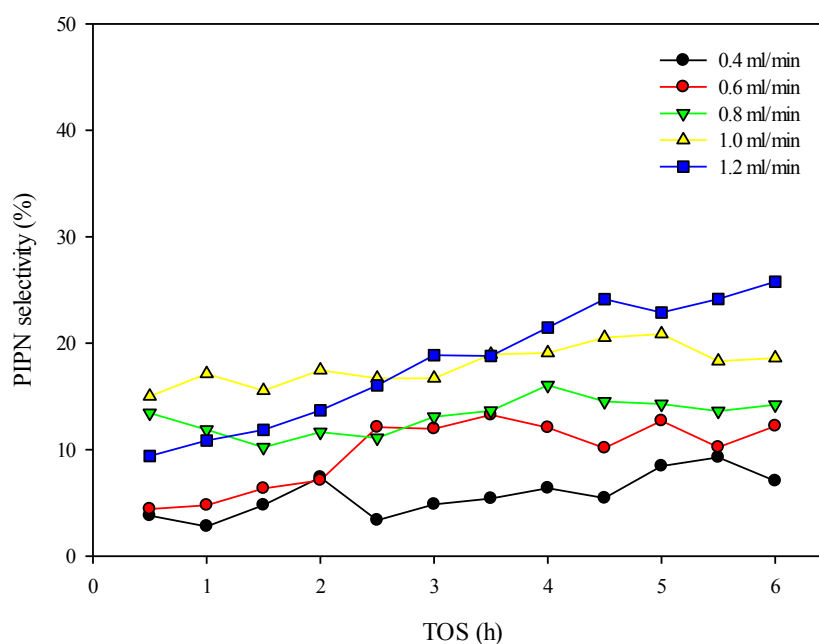
Figure 4.23. Effect of feed flow rate on selectivity to PIPN. Temperature: 220 °C, pressure: 1 bar, IPA/naphthalene: 4.

Selectivity to PIPNs increased by increasing the flow rate (Figure 4.23). While at 0.4 ml.min^{-1}, PIPN selectivity is as low as 5%, it jumps to approximately 20% at 1.0 ml.min^{-1}. At the highest flow rate (1.2 ml.min^{-1}) the trend of PIPN selectivity is different in contrast to lower flow rates.

During 6 h reaction time, it increased from 9% to 26%. Such a sharp increase in PIPN selectivity at this flow rate implies on a non-shape selective reaction on the outer surface of zeolite catalyst. It is thought that in this case there is not enough time for reactants to diffuse into the pore channels to produce a more selective product as it is assumed that the polyalkylation takes place on catalytic acid centres located on the zeolite external surface (Moreau et al., 1992b, Song et al., 1999). In other words, low conversion and high PIPN selectivity at higher WHSV can be attributed to strong internal diffusion limitations inside the mesopores of the zeolite at higher space velocities (or lower residence time).

4.1.4   Effect of alcohol to naphthalene ratio

The effect of molar ratio of reactants on the catalysts activity and selectivity in alkylation of naphthalene by isopropanol over HY zeolite was studied by changing the IPA/naphthalene molar ratio from 1 to 6, while the amount of solvent and other reaction conditions were kept constant. Figure 4.24 shows the effect of isopropanol/naphthalene molar ratio on the conversion. At IPA/naphthalene molar ratio of 1, naphthalene conversion decreased from 85% at 0.5 h to 77% at 6 h TOS. Conversion of naphthalene was improved by increasing the reactants ratio to 2. In this case, conversion started from 92% at 0.5 h and decreased to 80% after 6 h TOS.

Liu et al., (1997) observed that at an alcohol/naphthalene molar ratio of 1, conversion was slightly higher compared to an alcohol/naphthalene molar ratio of 2. They observed that at the lower ratio of reactants, selectivity to 2,7-DIPN is more favourable compared to 2,6-DIPN. They explain that in the absence of alcohol for further alkylation, isomerisation of di-alkylated naphthalene products (e.g. 2,7-DIPN) is more dominant.
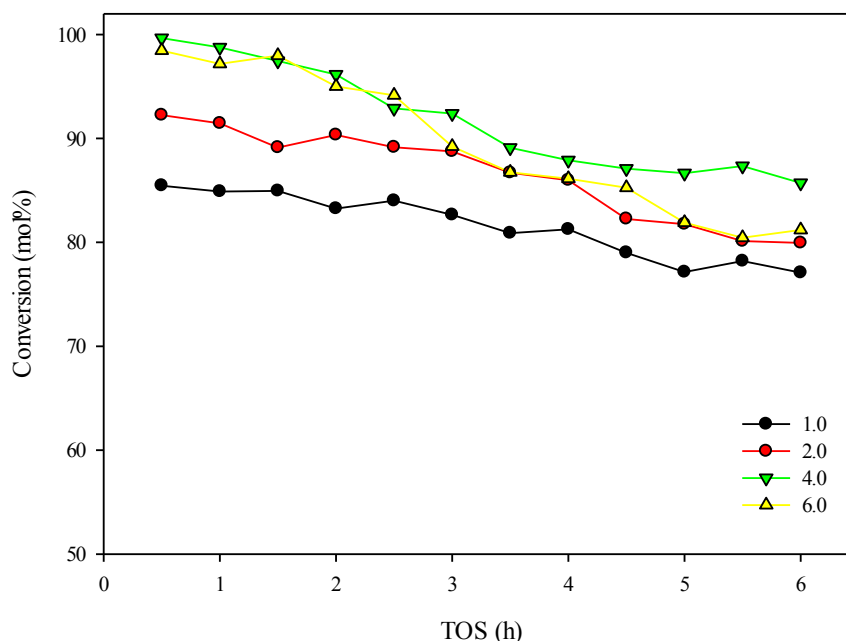
Figure 4.24. Effect of alcohol to naphthalene molar ratio on conversion, temperature: 220 °C, pressure: 1 bar, WHSV: 18.8 h^{-1}.

Marathe et al., (2002) studied the effect of reactants ratio in the alkylation of naphthalene by t-butanol over modified HY zeolite in a batch reactor. In contrast to the results of this research, they observed that by increasing the alcohol/naphthalene ratio to more than 2, conversion decreased while more mono- and di-alkylated naphthalenes were produced. They explained that this change is due to an increase in concentration of alcohol on the surface of the catalyst which may promote reactions between t-butanol molecules (such as dehydration, addition and cracking) to a greater extent than reactions between t-butanol and naphthalene. Moreover, the water formed in the reaction can act as a poison for the catalyst. This reaction is more likely to occur with t-butanol (tertiary alcohol) as this type of alcohol is more active compared to iso-propanol (secondary alcohol). The maximum naphthalene conversion which was reported by Marathe et al., (2002) using t-butanol as alkylating agent was 45% after 3 h TOS. Thus, using a secondary alcohol (e.g. isopropanol) as an alkylating agent is preferred for this reaction as the naphthalene conversion is not limited by the instability of the alkylating agent (e.g. t-butanol) at higher temperatures which can result in lower conversion of naphthalene. By increasing the

IPA/naphthalene molar ratio from 1 to 4, conversion was increased. Initial naphthalene conversions (0.5 h) at IPA/naphthalene ratios of 1, 2 and 4 were 85, 92 and 99%, respectively. These values decreased to 77, 80 and 86% respectively, after 6 h TOS. At the IPA/naphthalene ratio of 6, initial conversion (0.5 h) is similar to the value at a reactant ratio of 4, however it decreased to 81% after 6 h TOS. The rapid decrease in naphthalene conversion at molar ratio greater than 4 is possibly due to the faster deactivation of the catalyst by coking at relatively high space velocity.

The effects of IPA/naphthalene molar ratio on selectivity to IPN, DIPN and PIPN are illustrated in Figure 4.25 to Figure 4.27 respectively. Generally, the increase in the IPA/naphthalene molar ratio led to a decrease in IPN selectivity and an increase in DIPN and at higher ratios on PIPN selectivity. This can be explained by the consecutive alkylation of IPN by isopropanol to first DIPNs and then PIPNs. During 6 h TOS, the overall change in IPN, DIPN and PIPNs are constant except at high IPA/naphthalene ratio. In this case, PIPN decreased after 4.5 h and more IPN was produced. It can be explained as deactivation of strong acid sites at this point as it is believed that the strong acid sites are responsible for producing heavier alkylated naphthalene compounds (Yadav and Salgaonkar, 2005, Wang and Manos, 2007).

Although, existence of strong acid sites is required to enhance the naphthalene conversion, it was reported by Wang et al., (2008) that 2,6-/2,7-DAN ratio is very sensitive to the change of strong acid sites number, and the moderate numbers of strong acid sites may associate to higher selectivity to 2,6-DAN. More discussion will be provided in section 4.3.1 regarding acid site distribution and its effect on product distribution and selectivity.
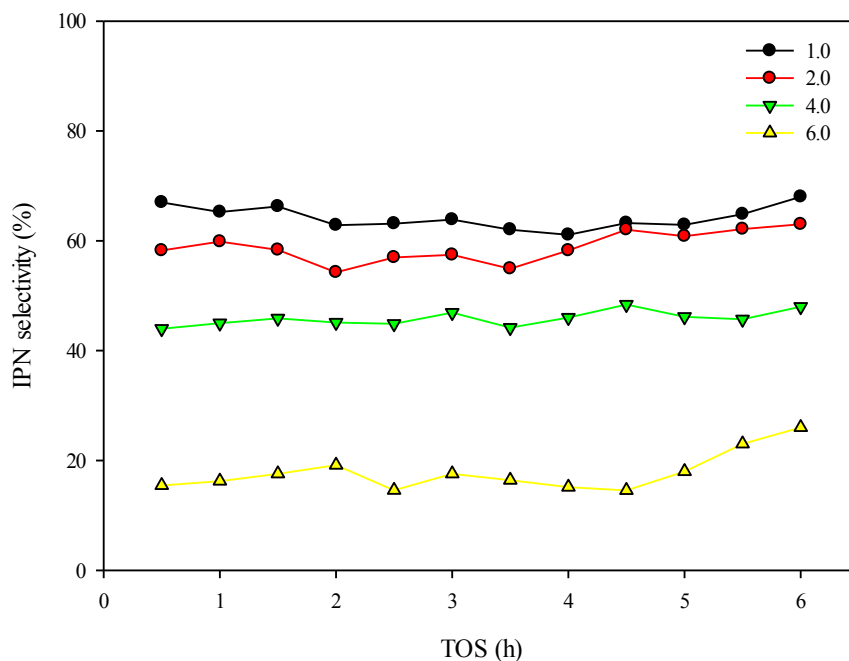
Figure 4.25. Effect of alcohol to naphthalene molar ratio on IPN selectivity, temperature: 220 °C, pressure: 1 bar, WHSV: 18.8 h^{-1}.

IPN selectivities at molar ratios of 1, 2 and 4 were about 64, 58 and 46%, respectively. DIPN selectivity was approximately 27, 32 and 44% at the same molar ratios. PIPN selectivity was in the range of 10-15% for these ratios, however by further increasing the IPA/naphthalene ratio to 6.0, IPN decreased to 15-25%, DIPN decreased to 42-32% while PIPNs tripled to 45-50%. A high ratio of IPA/naphthalene can facilitate the alkylation reaction by providing enough carbocation for the consecutive reaction and as a result higher selectivity to PIPN.
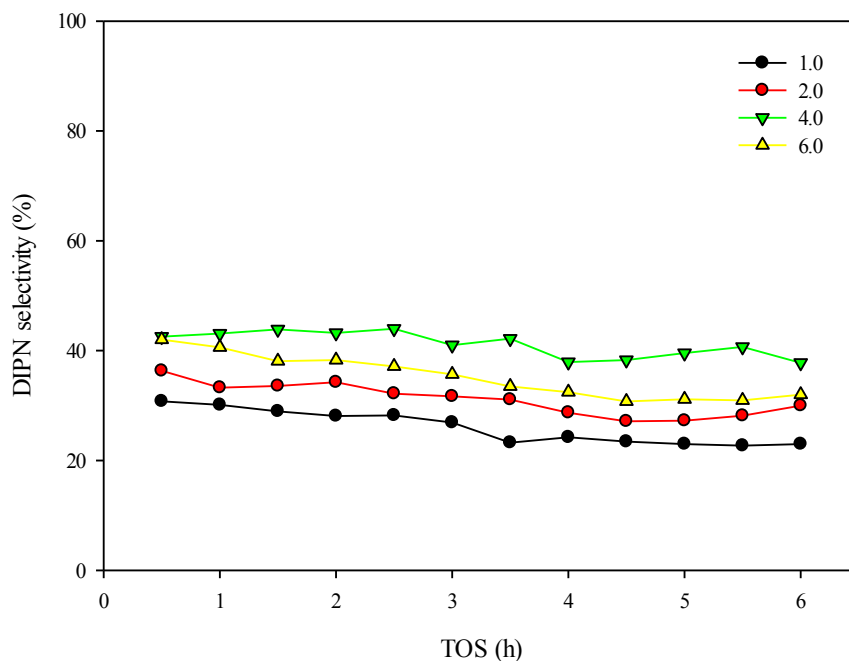
Figure 4.26. Effect of alcohol to naphthalene molar ratio on DIPN selectivity, temperature: 220 °C, pressure: 1 bar, WHSV: 18.8 h^{-1}.
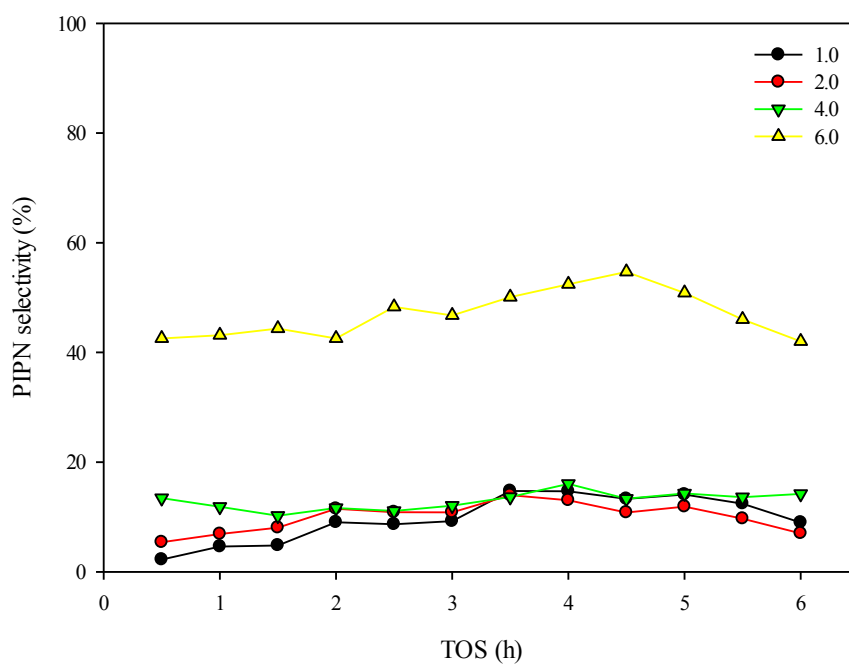
Figure 4.27. Effect of alcohol to naphthalene molar ratio on PIPN selectivity, temperature: 220 °C, pressure: 1 bar, WHSV: 18.8 h^{-1}.

4.2 Zeolite modification

Modification of the zeolite framework can be performed with the aim to change the acidic, basic or redox properties. A catalyst with both acidic and basic properties can be obtained by introducing metals to the zeolite framework through ion exchange or impregnation procedures. Such catalysts are suitable for use as zeolite-based catalysts for a continuously expanding number of commercial applications (Martinez and Corma, 2011).

Sometimes, post-synthesis modification of zeolite is used to change the catalyst activity and selectivity by changing the framework structure, pore size or acid site concentration and distribution. This can be achieved by different methods for example, changing the Si/Al ratio by dealumination or insertion of new atoms in the framework, hydrothermal treatments, treatment by strong acids (e.g. oxalic acid, acetic acid, etc.) or complexing agents (e.g. EDTA) and ion exchanging (Campanati et al., 2003).

In this research, the effects of HY zeolite modification using wet impregnation of metal salts of iron, cobalt, nickel and copper was studied at following reaction conditions: temperature: 220°C, pressure: 50 bar, WHSV: 18.8 h^{-1} and IPA/naphthalene: 4 molar ratio. Table 4.4 provides more information about the zeolite properties before and after modification. Detailed analysis and further discussion will be provided in Section 4.3 regarding the impact of modifications on the zeolite properties (e.g. pore size, pore volume, surface area, acidity and crystallinity). The results of reactions of naphthalene with isopropanol over various modified zeolite catalysts after 6 h time on stream are illustrated in Figure 4.28. The modification procedure carried out upon the zeolite changed the naphthalene conversion from 77% for parent HY zeolite to 73%, 76%, 88% and 96% for zeolite modified with Fe(III), Co(II), Ni(II) and Cu(II), respectively.
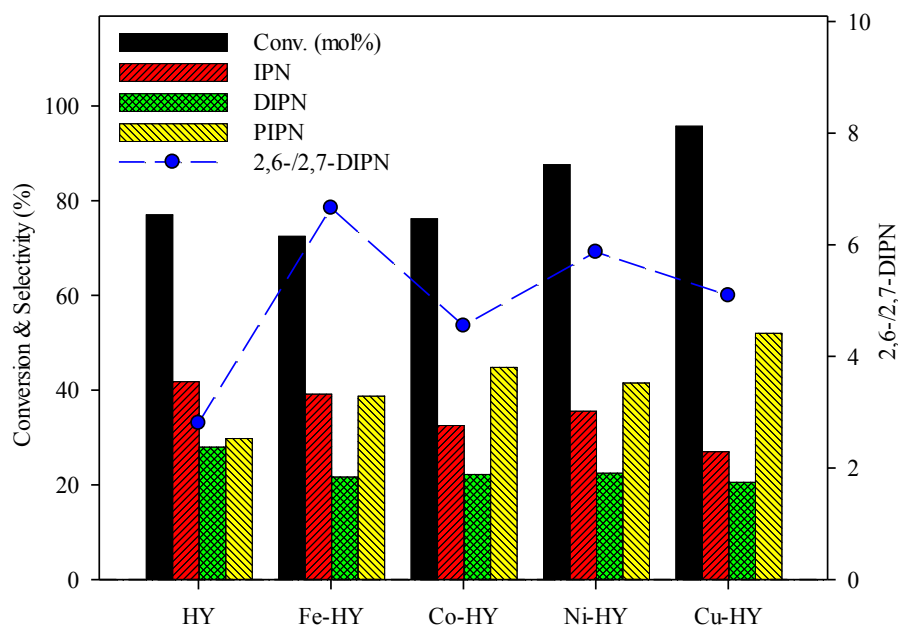
Figure 4.28. Product distribution and naphthalene conversion over different zeolite catalysts, temperature: 220 °C, pressure: 50 bar, WHSV: 18.8 h^{-1}, IPA/naphthalene: 4, TOS 6 h.

Modification of zeolite with metals decreased the selectivity to IPN from 42% for the parent zeolite to 39% with Fe(III), 32% Co(II), 35% Ni(II) and 27% Cu(II). DIPN selectivity decreased from 28% over HY zeolite to about 22% over modified samples.

Selectivity to PIPN, which are coke precursors increased from 30% for parent HY zeolite to 39% with Fe(III), 45% CO(II), 42% Ni(II) and 52% CU(II). Selectivity to 2,6-DIPN was effected remarkably after modification of zeolite. The 2,6-/2,7-DIPN ratio increased from 2.8 (parent HY zeolite) to 6.7 (Fe–HY), 4.6 (Co–HY), 5.9 (Ni–HY) and 5.0 (Cu–HY). Details regarding the distribution of acidic sites of modified and unmodified HY zeolite are provided in Section 4.3.1. Wang et al.(2008) have reported that the moderate or low numbers of strong acid sites are associated with higher selectivity for 2,6-DAN. The higher ratio of 2,6-/2,7-DIPN over Fe–HY zeolite can therefore be ascribed to lower strong acidic centres (25%). Meanwhile, higher selectivity to IPN over Co–HY and Ni–HY is due to a higher distribution of weak acid sites on these samples. Maheswari et al. (2003) have reported that only weak and medium acidic

sites are responsible for the initiation of mono-alkylation reactions. Naphthalene conversion and selectivity to IPN, DIPN and PIPN are illustrated in Figure 4.29 to 4.31, respectively.
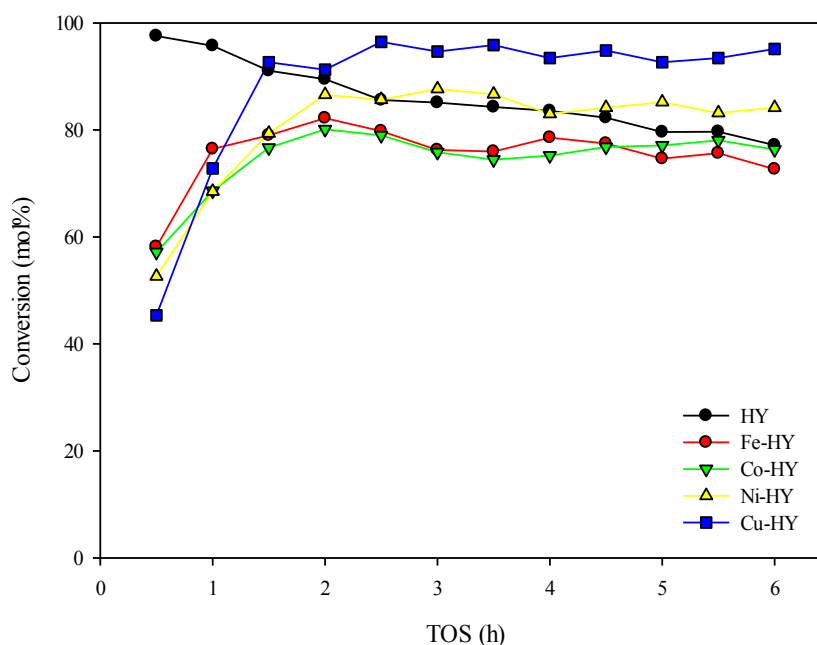
Figure 4.29. Effect of zeolite modification on naphthalene conversion, temperature: 220 °C, pressure: 50 bar, WHSV: 18.8 h^{-1},IPA/naphthalene: 4.

It can be seen from Figure 4.29 that modification increased the stability of HY zeolite against coking as the conversion trend is almost steady for modified zeolite while for the parent HY zeolite, conversion decreased gradually over the reaction time. The lower conversion of the modified catalysts during the first 1 hour could be attributed to the blockage of pores with impurities or excess metals which are washed away at the beginning of the reaction as such low conversion was not observed for zeolites without modification. Impurities in this case are inorganic material which exists in the pore channels or blocks the entrance of the pores after wet impregnation of zeolite followed by calcination. Although calcination decomposes excess material which has not been impregnated in the pores, not all of it is removed during the

calcination process. Increasing the zeolite resistance against coking is possible by modification

through changing the acidic centres which are responsible of producing coke precursors.
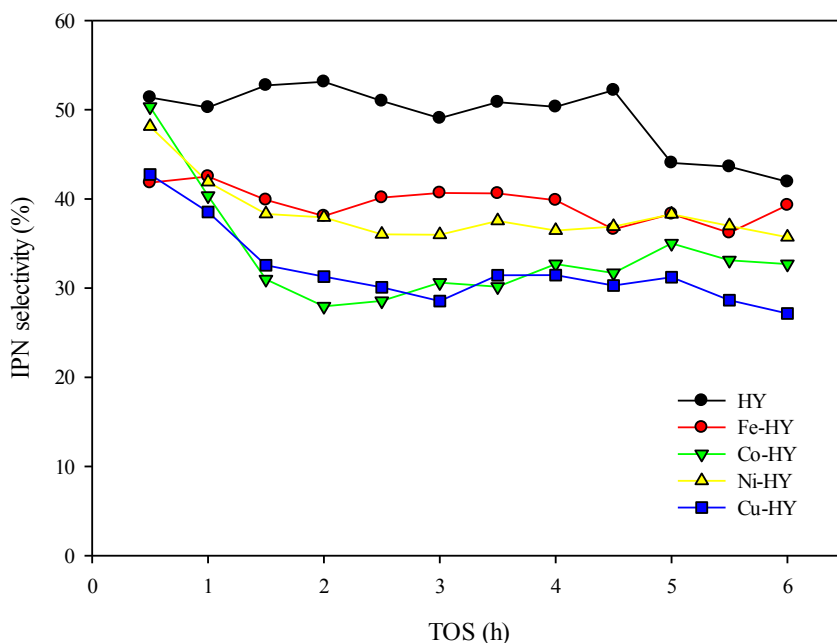
Figure 4.30. Effect of zeolite modification on IPN selectivity, temperature: 220 °C, pressure: 50 bar, WHSV: 18.8 h^{-1},IPA/naphthalene: 4.
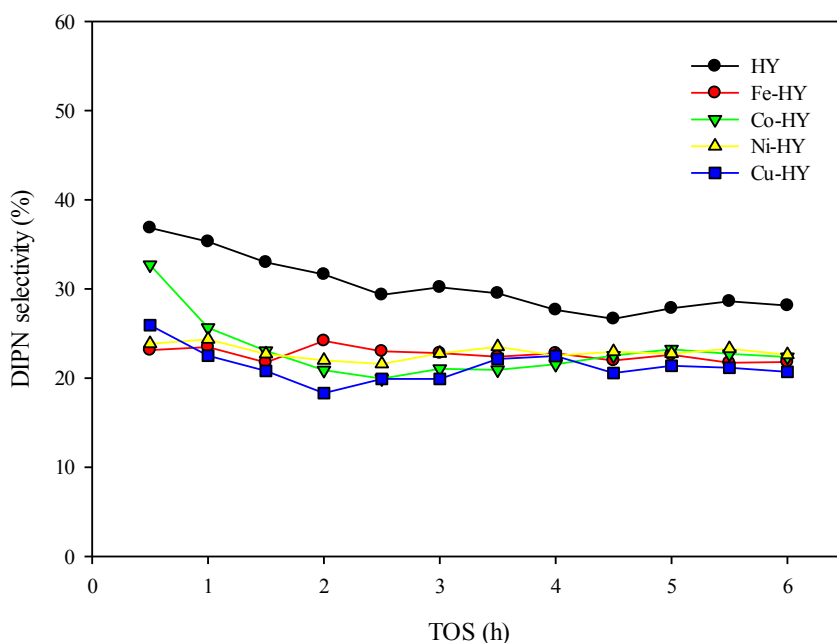
Figure 4.31. Effect of zeolite modification on DIPN selectivity, temperature: 220 °C, pressure: 50 bar, WHSV: 18.8 h^{-1},IPA/naphthalene: 4.
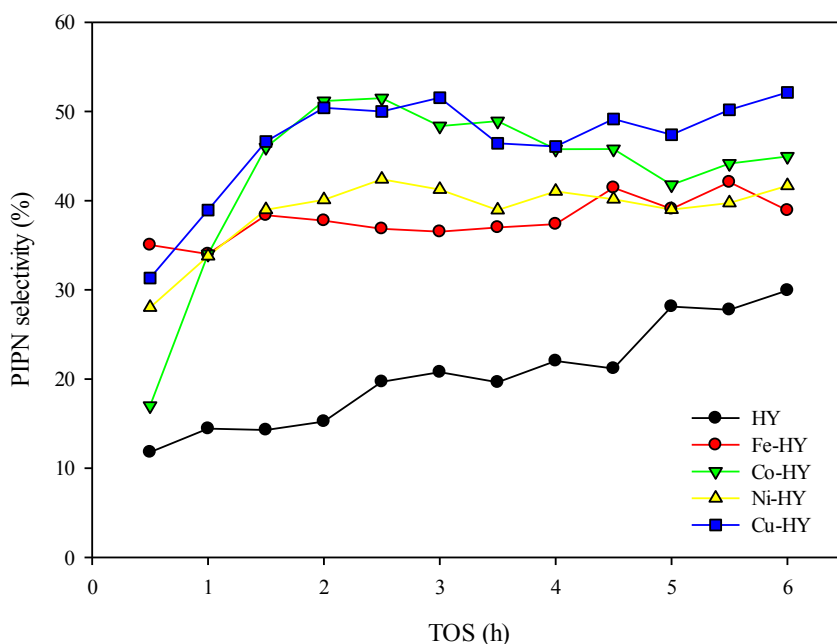
Figure 4.32. Effect of zeolite modification on PIPN selectivity, temperature: 220 °C, pressure: 50 bar, WHSV: 18.8 h^{-1}, IPA/naphthalene: 4.

Figure 4.30 to Figure 4.32 suggest that modification of zeolite by transition metals can improve the catalyst activity by increasing the naphthalene conversion and enhance the alkylation process by producing less IPN. However, the ease of the alkylation reaction due to presence of these metals led to high selectivity to PIPNs (as undesirable products) rather than DIPNs. Although, β-β selectivity improved significantly (e.g. by producing more 2,6-DIPN), non-shape selectivity is still observed after modification.

Sugi (2010) explains that shape-selective isopropylation of naphthalene occurs only by the exclusion of bulky isomers (e.g. PIPNs) in confined zeolite channels based on steric interaction at transition states for the products. Steric interaction due to the channels depends on the type of zeolite and in this case, channels of HY zeolite are too large to recognise the difference of the bulkiness of the transition states between DIPN isomers which led to non-shape selective production of PIPNs.

4.3   Characterisation of the catalysts

4.3.1   Acidity measurement by TPD

Acidity is an important factor for the alkylation of naphthalene and an optimum number of acidic centres are required for a selective catalyst (Kamalakar et al., 1999, Maheswari et al., 2003). Kamalakar et al. (2002) stated that medium or weak Brønsted acidic centres are required for selective formation of 2,6-DAN, however they showed that a large amount of unwanted products, such as tri- and poly-alkylated naphthalene are observed due to the strong acidic centres present in the zeolite. As it was described in Section 2.2.4.1 of this thesis, the extra-framework metal cations generate weak Lewis acids site, while strong Brønsted acid sites are created by hydroxyl protons located on oxygen bridges (Si-OH-Al), silanol groups (Si-OH) or extra-framework aluminium (Al-OH).

Wang et al. (2008) made a similar observation; they found that 2,6-/2,7-DAN ratio was highly sensitive to changes in the number of strong acid sites, and the moderate numbers of strong acid sites could be responsible for the comparatively higher selectivity for 2,6-DAN. In other words, the key factor for higher selectivity is not the total number of acid sites, but the number of moderate strength acid sites and the distribution of internal channel surface catalytic sites (strong acid sites). In this work total acidity and acid strength distribution were determined by Temperature Programmed Desorption (TPD) of t-Butylamine in the temperature range of 50–500 °C. The t-Butylamine is a suitable base for the TPD test as its high vapour pressure (boiling point=44.4°C) and its molecular structure do not have diffusional limitations in the microporous zeolite and so it gives a more accurate measurement than the adsorption of ammonia (Aguayo et al., 1994). It is well noted that strength of the acid sites can be related to the temperature that ammonia or alkyl-amines are desorbed from acidic centres (Karge et al., 1991, Arena et al., 1998) and from these temperatures can be categorised as weak, medium and strong acid sites.

Weak acid sites are due to surface hydroxyl groups, while trivalent aluminium in the framework structure is responsible for medium and strong Lewis acid sites. Desorption of t-Butylamine in various temperature regions is indicative of the acidic properties with different strengths. However, it should be noted that alkylammonium ions can get decomposed over strong Brønsted acid sites to ammonia and olefins at high temperatures via a reaction similar to the Hofmann-elimination reaction (Kresnawahjuesa et al., 2002). As it was described in Section 3.4.1, the quantity of the alkyl amine decomposed in the high temperature region is considered as a measure of the Brønsted acid site concentration (Pál-Borbély, 2007). Details regarding calculation of acid sites concentration are provided in Appendix C.

During the TPD test on the samples prepared in this work, three peaks at region of 150–250 ºC, 250–350 ºC and 350–450 ºC were observed which corresponded to weak, medium and strong acid sites, respectively (Kamalakar et al., 2000). The same method was used by Guo et al. (2002) for the study of naphthalene alkylation using long chain olefins over HY and Hβ zeolite modified by alkaline earth metals. To quantify weak, medium and strong acid sites, they recorded the desorption signals during heating the sample from 150 to 600 ºC at 15 ºC/min ramp rate following by fitting the TPD desorption profile into three peaks using a Gaussian and Lorentzian curve-fitting method.

The amounts of desorbed t-Butylamine for acid sites on the parent and modified HY catalysts with different strengths are listed in Table 4.3. It should be noted that the signal detected at high temperatures (e.g. 350-450 ºC) could be due to the decomposition of t-BA to ammonia and isobutylene over strong Brønsted acid sites, however, as the TCD signal area is proportion to the thermal conductivity of decomposed products (isobutylene and ammonia) and the thermal conductivity of decomposed products is very close to thermal conductivity of t-BA, it is possible to use same calibration curve for conversion of signal area to amount of desorbed t-

BA (thermal conductivity of t-BA and isobutylene are 0.021 and 0.022 W/m.K, respectively at same TCD conditions). Total acidity of HY zeolite measured by this method is in good agreement with total acidity measured using NH_3-TPD technique of same commercial HY zeolite (CBV-720) in literature of around 0.40 mmol/g (Boréave et al., 1997) or 0.47 mmol/g (Salzinger et al., 2011).

Table 4.3. Acidity of HY and modified zeolite measured by TPD of t-Butylamine.

Catalyst name	Amount of desorbed t-Butylamine (mmol/g catalyst)			
	Weak(A*)	Medium(B)	Strong(C)	Total acidity
HY	0.14 (34%)	0.14 (33%)	0.14 (33%)	0.43
Fe-HY	0.13 (32%)	0.18 (43%)	0.10 (25%)	0.41
Co-HY	0.22 (37%)	0.18 (29%)	0.21 (35%)	0.61
Ni-HY	0.16 (38%)	0.10 (25%)	0.15 (37%)	0.41
Cu-HY	0.14 (27%)	0.19 (37%)	0.17 (35%)	0.49

*Desorption temperature region: A = 150–250 °C, B = 250–350 °C, C = 350–450 °C

It can be seen that modification by transition metals not only changes the distribution of acidic centres but also can change the total acidity of the zeolite. For example, for the zeolite modified by Fe(III), strong acidic centres were decreased to 25% compared to the parent HY zeolite (33%), while the medium acidic centres were increased to 43% (from 33% for HY zeolite). For zeolite modified by Co(II), a decrease in medium type acidic centres was observed, although, the total acidity was increased to 0.61 (mmol/g catalyst). Higher conversion of naphthalene over Ni–HY and Cu–HY can be attributed to higher amount of strong acid sites for these samples.

4.3.2 XRD analysis

The XRD patterns of parent and modified HY zeolites are shown in Figure 4.33. All samples exhibit the typical diffraction peaks of the Faujasite (FAU) structure (Treacy and Higgins, 2007).
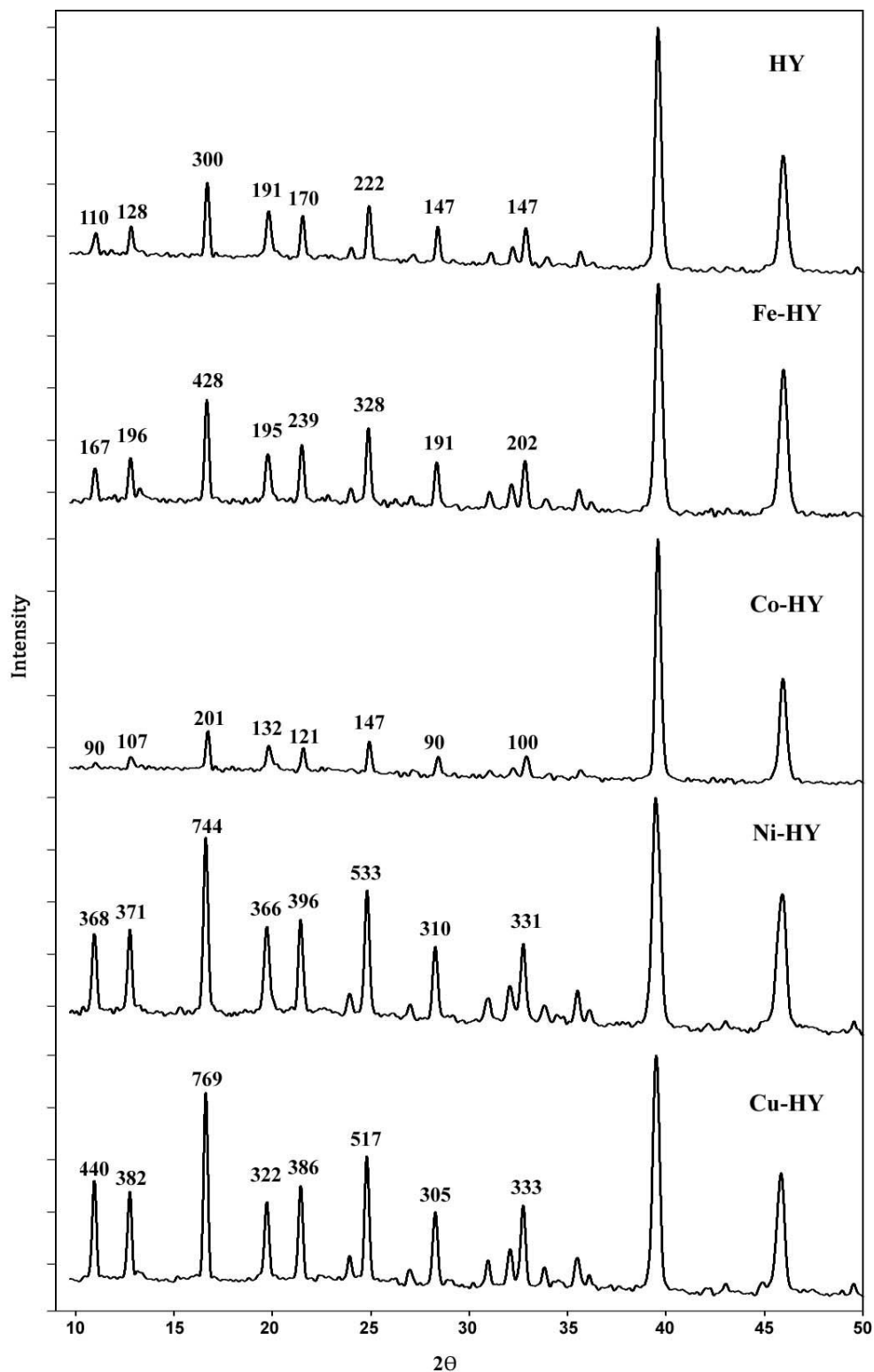
Figure 4.33. XRD pattern of parent HY and modified zeolite.

There are no amorphous phases detected in the pore structure and also metal ion modification

has not destroyed the crystalline structure of the zeolite catalysts. Furthermore, no crystalline

phases of metal ions were detected in modified samples. This implies that metal ions are finely dispersed at the cation sites of the zeolite making them undetectable by XRD (Xavier et al., 2004). The average crystallite size of samples were calculated by applying the Scherrer equation on (300), (191), (170) and (222) XRD reflections (Scherrer, 1918). The method for calculation of crystallite size using the Scherrer equation for HY zeolite is presented in Appendix E.

Considering HY zeolite as a reference standard, the relative crystallinity of modified zeolites was determined according to the ASTM D3906-2003 method (Appendix E) and is shown in Table 4.4. It can be seen that the relative crystallinity of Fe–HY, Ni–HY and Co–HY is higher than the parent HY zeolite, which means that the impregnation of metals can increase the crystallinity of zeolite (Kadarwati et al., 2010). Although, modification of HY zeolite by transition metal increased the relative crystallinity, deactivation of catalyst was indeed observed.

4.3.3   N$_2$ adsorption–desorption isotherms

Nitrogen adsorption–desorption at 77 K was used to determine the porosity, specific surface area and physisorption isotherms. All samples exhibit a typical reversible type IV adsorption isotherm as defined by IUPAC (Gregg and Sing, 1982). The hysteresis loop is very similar to the H3 type adsorption isotherm with hysteresis characterisation. Three different stages are observed in the isotherms. At low relative pressure (P/P$_0$ < 0.4), adsorption occurs only as monolayer on the pore walls. As the relative pressure increases (P/P$_0$ > 0.4), a hysteresis loop is observed which is a characteristic of capillary condensation of nitrogen in mesopores. At higher relative pressure (P/P$_0$ > 0.95), again another linear region is observed. This part is attributed to the multilayer adsorption on the external surface of the materials. There is no limiting uptake observed over high range of P/P$_0$, which is characteristic of aggregates with

plate-like particles (Sing et al., 1985). The specific surface areas were calculated using the BET model. More details and example plot are provided in Appendix D.
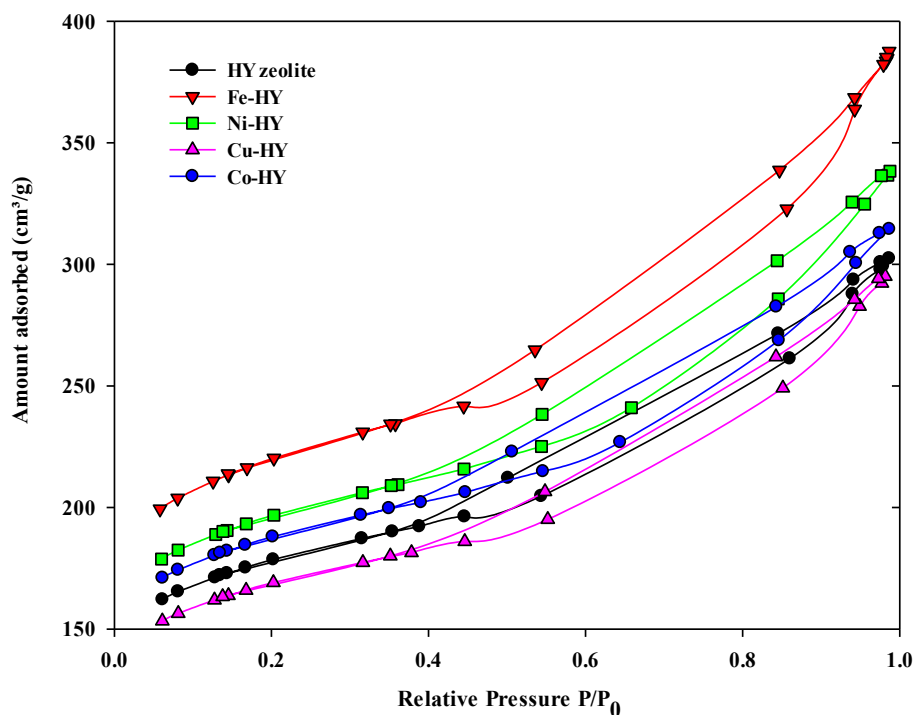
Figure 4.34. Nitrogen absorption-desorption isotherms at 77 K of HY and modified HY zeolite.

Table 4.4 summarises the properties of catalysts. The results show that Fe–HY has higher pore volume, while modification by Cu reduces the pore volume by blocking the pore opening. Mingjin et al. (2003) reported similar observations for the modification of mordenite zeolite with copper. Due to the smaller ionic radius of Fe (0.64 Å) and Ni (0.69 Å), impregnated metal ions can easily substitute into the zeolite lattice, while ions with larger ionic radii, e.g. Co (0.72Å) and Cu (0.72Å), resulted in lower pore volume (Shannon, 1976). It can be seen in Table 4.4 that BET surface area, pore volume and micropore area decrease in the order: Fe–HY > Ni–HY > Co–HY > HY > Cu–HY while the pore size does not change significantly for the different catalysts.

Table 4.4. Properties of zeolite catalysts.

Catalyst name	Amount of metal in zeolite (wt.%)	BET surface area (m²/g)	Crystal size (nm)	Relative Crystallinity (%)	Pore size (Å)	Pore volume (cm³/g)	Micropore area (m²/g)
HY	---	609	25.7	100	30.4	0.172	370
Fe-HY	2.3	762	29.3	139	31.7	0.212	457
Co-HY	1.6	641	33.0	59	30.7	0.182	393
Ni-HY	1.4	670	27.1	232	30.7	0.191	412
Cu-HY	1.5	584	30.8	228	31.5	0.161	348

Figure 4.35 shows the SEM image of HY zeolite before and after modification. The effect of impregnation of nickel on the HY zeolite structure can also be confirmed from the SEM image. It shows that the morphology and particle size of Ni-HY catalyst did not change compared to parent HY zeolite. This indicates that no crystalline transformations occurred during the impregnation of nickel onto HY zeolite.
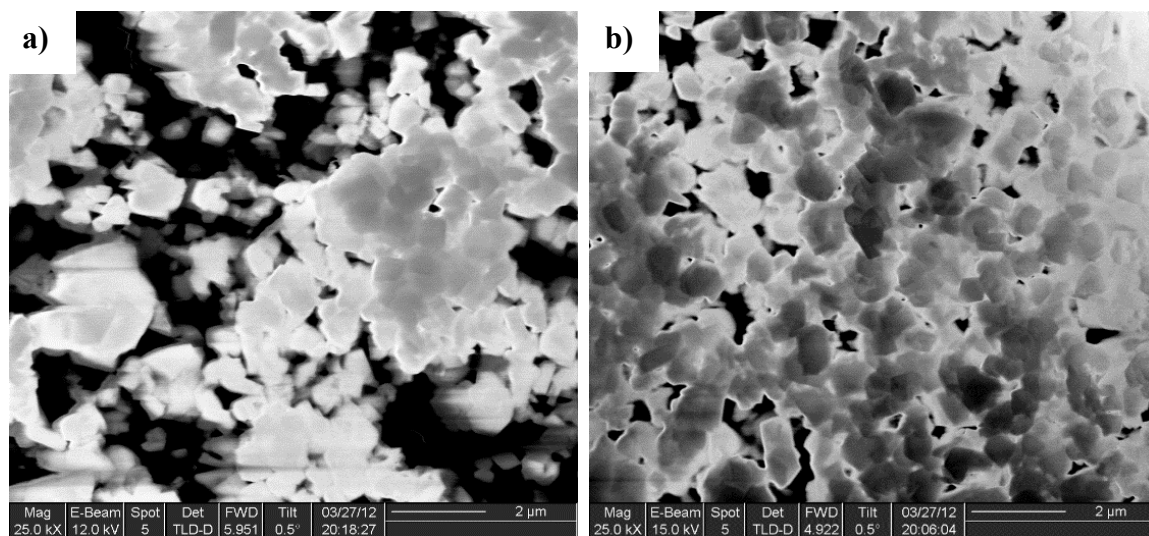
Figure 4.35. SEM image of fresh HY zeolite (a) and fresh Ni-HY zeolite (b).

4.4 Coke characterisation

The amount of coke deposited on the catalysts was measured by thermo-gravimetric analysis (TGA). Figure 4.36 illustrates the TGA curve of coked zeolite catalysts after 6 h. Each curve consists of three steps: the mass loss during the first step (150 ºC) is due to the removal of moisture from the samples. The second step refers to the removal of soft coke at temperature 150–800 ºC under nitrogen flow. The third step corresponds to removal of hard coke at high temperature (800 ºC) and under air flow.

The highest amount of coke was deposited on Co–HY (9.2%) and Cu–HY (8.7%) catalysts. This could be due to the higher total acidity of Co–HY (0.61 mmol/g cat.) and Cu–HY (0.49 mmol/g cat.) zeolite compared to the parent HY zeolite (0.43 mmol/g cat.). On the other hand, a higher amount of PIPN was produced on zeolite modified by Co and Cu. This confirms that PIPN molecules are possible coke precursors and therefore led to larger amount of coking on Co–HY and Cu–HY catalysts.
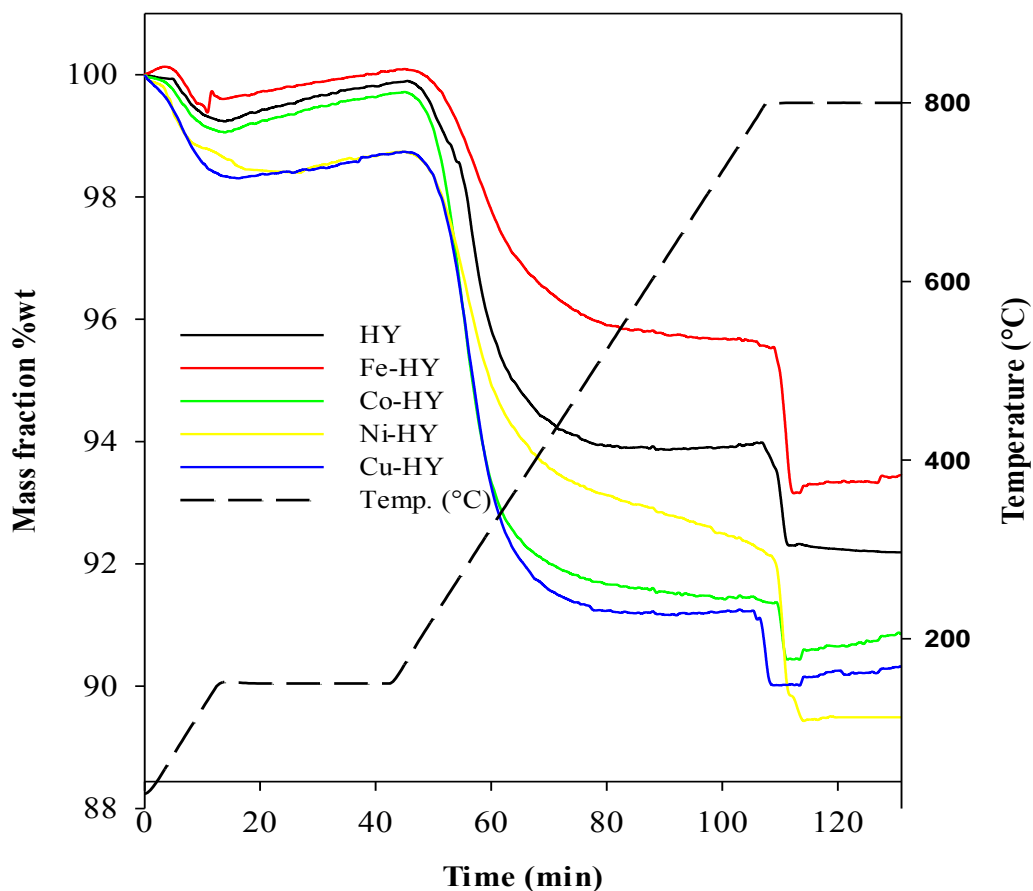
Figure 4.36. TGA profile of coked zeolite catalysts after 6 hours.

A higher amount of coke was observed on zeolite modified by Co and Cu while less coke material was found on zeolite modified by Fe and Ni compared to parent HY zeolite (Table 4.5). The higher amount of coke can be related to higher total acidity after modification.

Table 4.5. Coke deposition of used parent and modified HY zeolites.

Catalyst name	Soft Coke (wt%)	Hard Coke (wt%)	Total Coke (wt%)
HY	5.9	1.8	7.7
Fe-HY	4.5	2.4	6.8
Co-HY	8.3	0.9	9.2
Ni-HY	3.8	2.9	6.7
Cu-HY	7.5	1.2	8.7

4.5   Conclusion

The effect of reaction conditions (e.g. temperature, pressure, space velocity and reactant composition) on the catalyst's activity and selectivity of zeolite in dialkylation of naphthalene by isopropanol was studied. Maximum selectivity to DIPNs (desired products) was achieved at 220 ºC and 1 bar. An optimum WHSV of 18.8 h^{-1} and an isopropanol/naphthalene molar ratio of 4 was found as the most suitable values.

By changing the temperature and pressure of the reaction, the effect of phase change (e.g. sub critical and supercritical) upon the catalyst life time was investigated. The results of reaction at higher pressure proposed that PIPNs (which are coke precursors) are decreased in the supercritical region due to the higher diffusivity and solubility of the supercritical medium and thus prolong the catalyst life time.

HY zeolite was modified by transition metals (e.g. Fe, Co, Ni and Cu) to improve the catalyst selectivity to the desired product by changing the pore size or zeolite acid sites. It was found that modifying the zeolite significantly changed, not only the total acidity of the parent zeolite, but also the distribution of weak, medium and strong acid centres. Moreover, changes to the pore volume and BET surface area of modified samples are related to the ionic radius of the transition metal. It was observed that modification of zeolite by Co and Cu increased the total acidity of the zeolite, and therefore, less improvement of selectivity was observed on these catalysts. On the other hand, modification by Fe and Ni decreased the total acidity, and therefore better selectivity was observed on these catalysts. Among the catalysts tested for this reaction, Fe–HY was found to be the best catalyst for a selective dialkylation of naphthalene with optimum strength acidic centres and larger pore volume.

Chapter 5 DEHYDRATION OF METHANOL TO LIGHT OLEFINS OVER ZSM-5 CATALYST

5.1 Dehydration of methanol to light olefins

Methanol is a key ingredient in the synthesis of many organic molecules. It can be economically converted to ethene and propene, two largest volume petrochemical feedstocks. Zeolite as a catalyst for conversion of methanol to olefins has been studied widely with the main focus being to improve the process selectivity to light olefins (Mei et al., 2008, Stocker, 1999, Keil, 1999). Different types of zeolites such as ZSM-5, ZSM-22, ZSM-11, SAPO-18, SAPO-34, SAPO-44 have been reported to exhibit good selectivity to ethene and propene (Wilson and Barger, 1999, Chen et al., 1994a, Sano et al., 1992).

In this research, firstly, the effect of reaction conditions on the dehydration of methanol to other hydrocarbons over ZSM-5 zeolite with no support was studied and the effects of a number of reaction parameters upon methanol conversion and product selectivity were investigated. Fresh and selected used catalysts were characterised using Temperature Programmed Desorption (TPD) and Thermo-gravimetric Analysis (TGA). Secondly, the effect of using different ratios of alumina as a support to zeolite was studied. The conversion to propene over these catalysts was studied with respect to their characteristics such as acidity, pore volume and BET surface area. Subsequently, product distribution over ZSM-5 zeolites modified by iron, calcium, caesium, and phosphoric acid were studied in order to investigate the best promoter. The results are reported in terms of concentrations of ethene ($C_2^=$), propene ($C_3^=$) and butene ($C_4^=$), propane/propene ratio ($C_3/C_3^=$), light alkanes consisting of methane to butane (C_1-C_4), and

heavier hydrocarbons (C_5^+) including aromatic and aliphatic compounds. Due to a low amount of aromatics in this reaction (less than 5%), the aromatic components were lumped as C_5^+. A GC chromatogram of product analysis and calibration tables is shown in Appendix F. This chapter is based on the paper: Saeed Hajimirzaee, Mohammed Ainte, Behdad Soltani, Reza Mosayyebi Behbahani, Gary A. Leeke, Joseph Wood, Dehydration of methanol to light olefins upon zeolite/alumina catalysts: Effect of reaction conditions, catalyst support and zeolite modification, 2015, Chemical Engineering Research and Design, 2015. 93(0): p. 541-553 (Hajimirzaee et al., 2015).

5.1.1 Effect of Time on Stream

The effect of Time on Stream (TOS) on the methanol conversion and olefins distribution over ZSM-5(100) up to 21 h time on stream are shown in Figure 5.1.a. Over the observed reaction time, the conversion of methanol decreased gradually from 96% to 78%. Similarly, the selectivity to propene and butene decreased from 38% to 32% and 13% to 8%, respectively, whilst the selectivity to ethene increased over the same time, from 23% to 32%. The $C_3/C_3^=$ ratio was used in presenting the results as an indicator for hydride transfer reaction which facilitates the production of paraffins and aromatics. After 21 h, the $C_3/C_3^=$ ratio decreased from 0.18 to 0.13 which implies the suppression of hydride transfer reaction during the reaction time on stream due to faster deactivation of strong acid sites compared to medium or weak acid sites (Liu et al., 2009).

Figure 5.1.b shows the distribution of paraffinic products (C_1 to C_4) and C_5^+ (containing olefinic, paraffinic and aromatics compounds with more than five carbons) over 21 h time on stream. The selectivity to methane increased from 2% to 7%, whilst simultaneously, C_5^+ compounds increased from 6% to 12%. Ethane selectivity is almost constant and less than 1%. Propane decreased from 7 to 14% while butane increased slightly from to 11% to 13% after

12h and then decreased gradually. The decrease in the propene to ethene ratio and increase in the selectivity to C_5^+ products can be related to the deactivation of the acid sites via coke formation. Ivanova et al. (2009) relate this observation to the formation of coke which limit the transformation of methanol to DME and favour the formation of higher olefins.
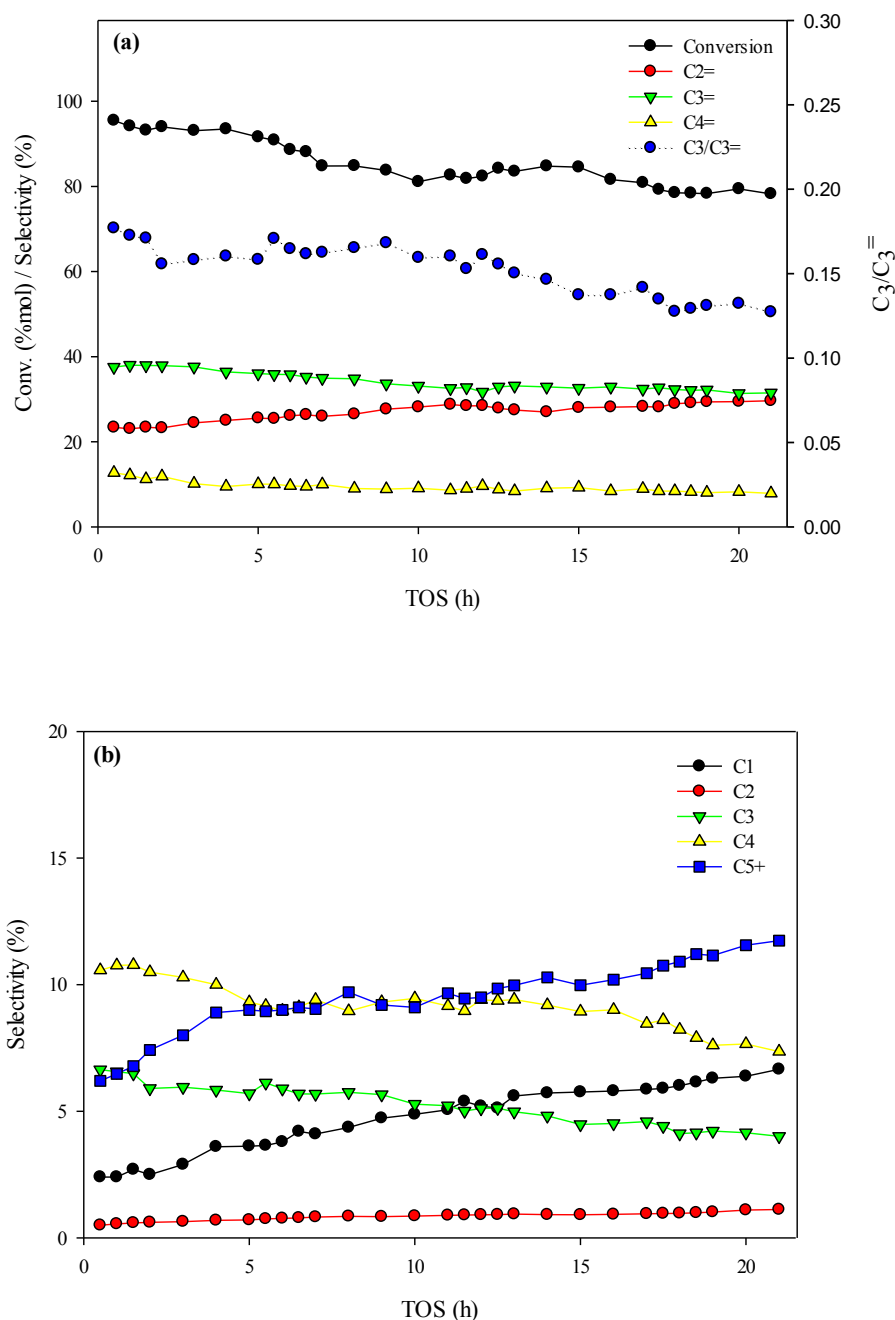
Figure 5.1. Effect of time on stream on (a) methanol conversion and olefins distribution (b) paraffins distribution over ZSM-5(100) catalyst under typical reaction conditions: temperature: 400 ºC, pressure: 1 bar, WHSV:34 h^{-1} methanol/water ratio: 1 w/w, TOS: 21 h.

An observed increase in the formation of methane is thought to be another result of coke formation. Chen et al. (1986) found that the yield of methane is related to the extent of coking. They conclude that the coke deposition on the acid sites of the catalyst enhances the secondary cracking reactions through non-ionic mechanism, which can lead to an increase in methane and the C_5^+ fraction.

Deactivation of ZSM-5 zeolite in the conversion of methanol to hydrocarbons, firstly occurs on the outside surface of the catalyst and then in the pore structure. Firstly, poly alkylation and the formation of cyclic compounds occur on the acidic centres located on the outer surface of the catalyst and these deposits block the access to the inner channels leading to slower coke formation in the second stage inside the zeolite channels (Guisnet and Magnoux, 1989, de Lucas et al., 1997a). This effect was confirmed as occurring in this study by the analysis of acid sites distribution of ZSM-5 zeolite before and after reaction. Table 5.1 shows the TPD results for both fresh and used catalyst after 4 h and 21 h time on stream, respectively. The results show that during the first few hours of the reaction (e.g. 4 h), all acid sites become deactivated evenly and the catalyst still has a uniform acid site distribution, but after longer reaction times, most of the medium acid sites become deactivated, suggesting that this type of acid site is more involved in the formation of coke precursors. Due to the stability of the catalyst during the first 4 h of reaction with negligible fluctuation in product composition at that time, the TOS of 4 h was chosen for further analysis of reaction conditions effect on catalyst activity and selectivity.

Table 5.1. TPD results of fresh and used catalyst (TOS=4 and 21 h).

Catalyst name	TOS (h)	Acidity(mmol t-BA/g) / distribution			
		Weak (150-300 ºC)	Medium (300-400 ºC)	Strong (400-500 ºC)	Total
Fresh ZSM-5(100)	0	0.52(77%)	0.13(19%)	0.03(4%)	0.68
Used ZSM-5(100)	4	0.45(76%)	0.12(20%)	0.02(4%)	0.59
Used ZSM-5(100)	21	0.25(86%)	0.03(10%)	0.01(4%)	0.29

5.1.2   Effect of Temperature

The effect of temperature on the conversion of methanol to hydrocarbons over ZSM-5(100) catalyst was investigated over the range 340 ºC to 460 ºC. Figure 5.2.a shows the methanol conversion and selectivity to olefins at the different temperatures. Methanol conversion increased from 80% to 94% by increasing the temperature from 340 ºC to 400 ºC. However, at higher temperatures, the conversion then decreased from 94% to 75%. This suggests faster deactivation of catalyst after 4 hours at such temperatures. The selectivity to propene increased from 23% to 36% by increasing the temperature from 340 ºC to 420 ºC, however it decreased to 19% once the temperature had been raised further to 460 ºC. Similarly, the selectivity to butene jumped from 3% to 10% by increasing the temperature from 340 ºC to 360 ºC, and then remained almost constant at this value in the range of 340 ºC to 420 ºC, but when the temperature was raised to 460 ºC, it decreased to 5%. The selectivity to ethene significantly decreased from 48% to 26% once the temperature had changed from 340 ºC to 360 ºC but it remained almost constant up until a temperature of 440 ºC. When the temperature was further increased to 460 ºC it decreased to 16%. Dehertog et al. (1991) observed that the yield of ethene decreases with increasing temperature, in contrast to the yields of propene and butene. They also observed strong temperature dependency of the olefin yield and distribution at high temperatures. They indicate that whereas the ethene is most abundant at low temperature, butene and especially propene become more important at higher temperature. It is believed that high temperature favours alkene formation at the expense of the aromatisation reactions and as a result, the yield of ethene decreases with increasing temperature, in contrast to the yields of propene and butene (Chang et al., 1984, Dehertog and Froment, 1991). However, a greater increase in the temperature leads to decomposition of methanol and produces other basic components, such as methane, H_2, and CO (Chen and Reagan, 1979, Al-Jarallah et al., 1997).

Increasing CO_x (not shown) from 0.1% at 420 ºC to 0.4% at 460 ºC could be evidence for this claim. The $C_3/C_3^=$ ratio increased from 0.15 to 0.17 by increasing the temperature from 340 to 380ºC indicates increasing temperature in this region promotes the hydride transfer reaction to produce more paraffins or aromatics as undesired products, however by further increasing the temperature to 420 ºC, this ratio dropped significantly to 0.10.
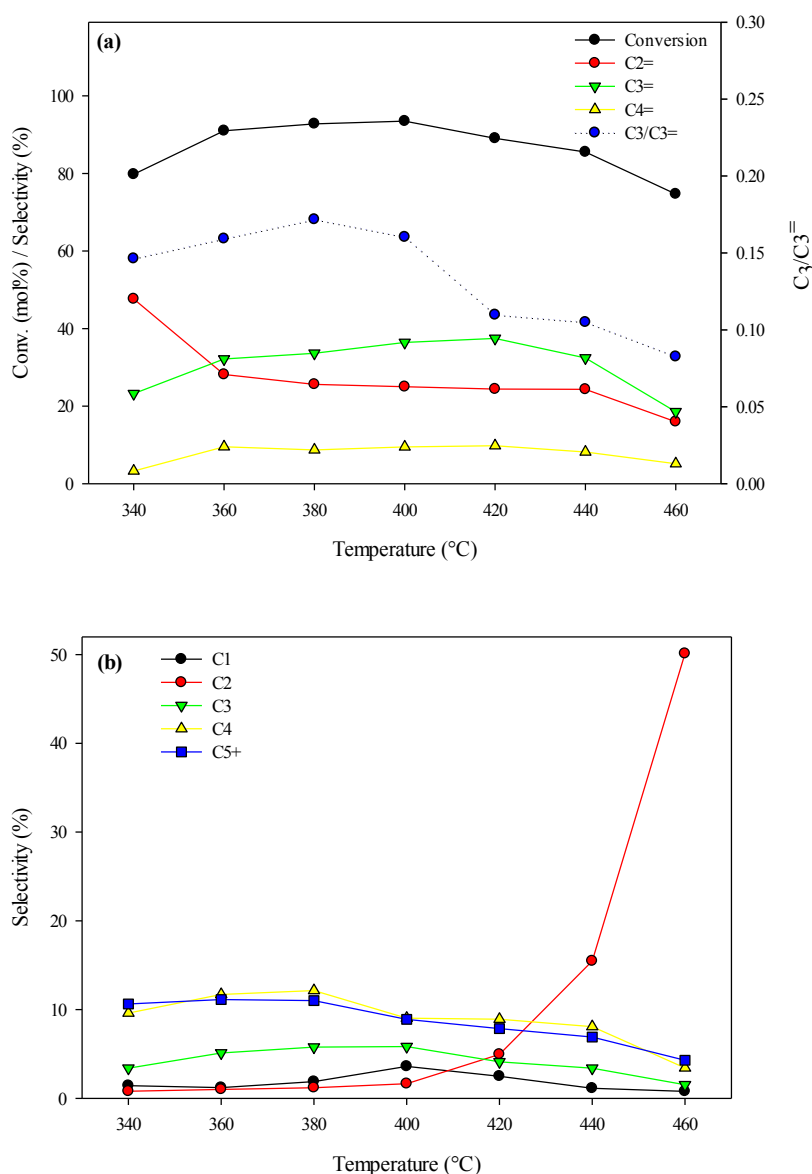
Figure 5.2. Effect of temperature on (a) methanol conversion and olefins distribution (b) paraffins and C_5^+ distribution over ZSM-5(100). Reaction conditions; pressure: 1 bar, WHSV:34 h^{-1}, methanol/ water ratio: 1 w/w, TOS: 4 h.

Figure 5.2.b shows the selectivity to light alkanes and C_5^+ compounds at different temperatures. By increasing the temperature from 340ºC to 400ºC, the methane content in the gas product increased slightly from 1% to 4%. Simultaneously, increasing temperature up to 380ºC, increased ethane and propane production by providing the required activation energy at elevated temperatures, however increasing temperature to more than 380 ºC, led to decreases in butane and propane content. The rapid increase in ethane is due to increasing secondary reaction rates favoured at high temperatures. Anthony and Singh (1980) studied the kinetics of the methanol conversion to olefins over ZSM-5 zeolite. They concluded that propylene, methane, and propane are produced by primary reactions and do not participate in any secondary reactions, whereas dimethylether, carbon monoxide, and ethane are produced through secondary reactions.

Lastly, regarding the selectivity towards C_5^+, only a negligible change was observed over 340ºC to 380ºC, the composition with respect to this product being around 11% over that temperature range. Once the temperature was increased from 380ºC to 460ºC, the selectivity to C_5^+ molecules decreased to 4%. At elevated reaction temperatures cracking of heavier hydrocarbons are induced over HZSM-5 (Mores et al., 2011, Bibby et al., 1992, Bibby et al., 1986). Hence, a low number of acidic centres and sufficiently high temperature provide appropriate conditions for obtaining optimum olefin selectivity whilst hindering the formation of heavy hydrocarbons. Based on these results, 400ºC was determined to be the optimum temperature for propene production.

5.1.3   Effect of Pressure

Since the optimum reaction temperature for the highest conversion and selectivity of propene was found at 400ºC, the effect of pressure was studied in the range 1–20 bar at this temperature.

As shown in Figure 5.3.a and 5.3.b, by increasing the pressure from 1 bar to 10 bar conversion of methanol was increased from 93% to 98% and declined slightly to 96% at 20 bar after 4h TOS.
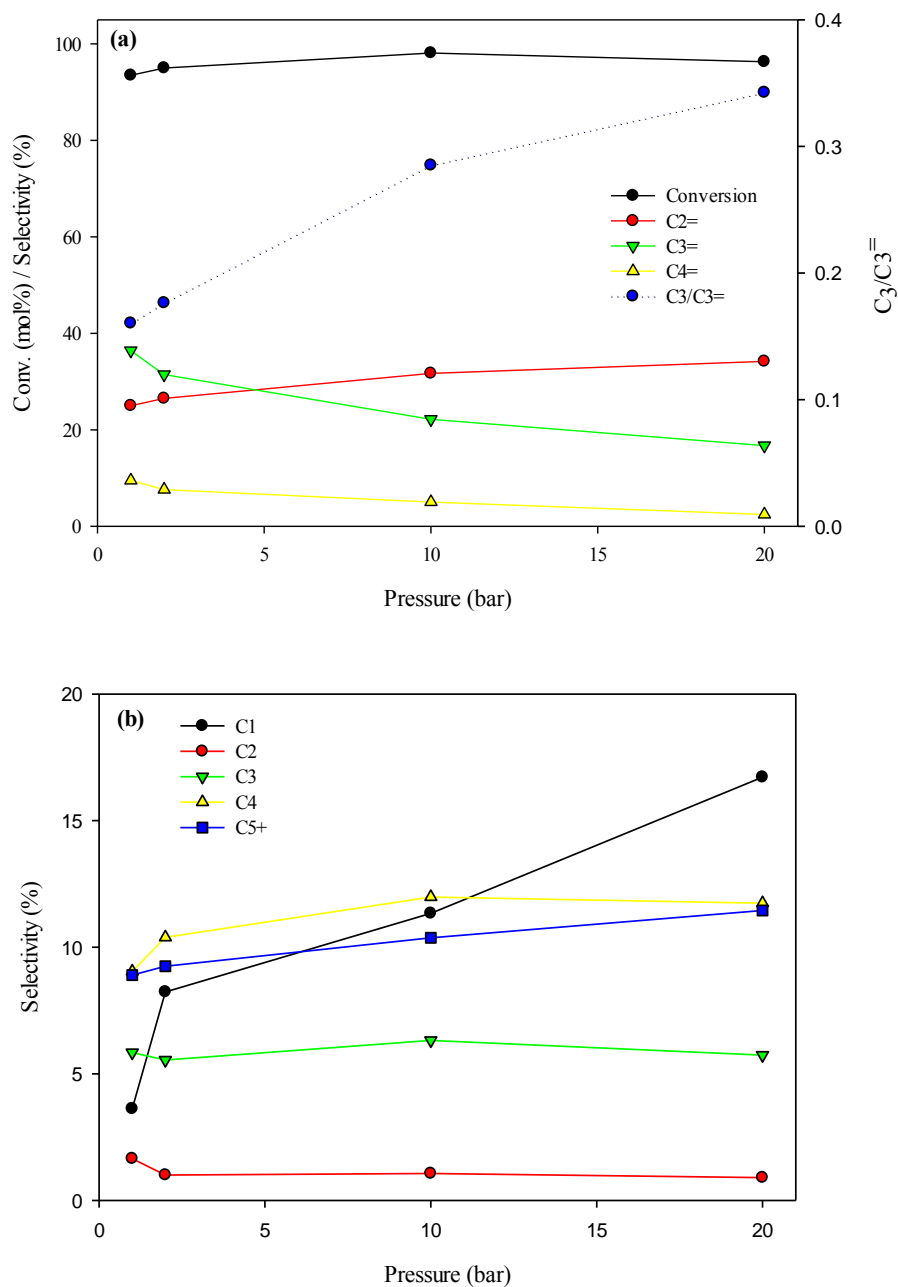
Figure 5.3. Effect of Pressure on (a) methanol conversion and olefins distribution, (b) paraffins and C_5^+ distribution over ZSM-5(100). Reaction conditions; temperature: 400 ºC, WHSV: 34 h^{-1}, methanol/ water ratio: 1 w/w, TOS: 4 h.

The selectivity to propene decreased significantly from 36% to half of this value, whereas the selectivity to ethene increased from 24% to 37%. Also, butene selectivity decreased from 10 to 3%. Increasing selectivity to ethene while decreasing selectivity to propene occurred with higher pressure, which can be concluded as a result of faster catalyst coking over the time due to increasing influence of the hydrogen transfer reaction (Gubisch and Bandermann, 1989). However, the $C_3/C_3^=$ ratio doubled from 0.16 to 0.34 in this range of pressure which confirms strong influence of pressure to enhance the hydride transfer reaction. At higher pressure sharp increase in methane formation is indicative of catalyst deactivation. In this case, reaction between coke and methanol is carried out through methylation and dehydrogenation (Schulz, 2010). An increase in C_5^+ compounds is another explanation for faster deactivation of catalyst at higher pressures. A similar result was observed by Chang et al. (1979) on methanol conversion over ZSM-5 at 370 ºC in the range of 0.04 to 50 bar. To provide further evidence to confirm this claim, the TGA result of used catalyst is reported in Table 5.2. As it can be seen, higher pressure favours faster coking.

Table 5.2. TGA result of used ZSM-5(100) catalyst at different pressures.

Pressure	Coke (wt%)
1	3.4
2	3.8
10	4.5
20	6.8

As highest selectivity of propene was obtained at 1 bar, this pressure was chosen as the optimum pressure. The choice of a low operating pressure also offers advantages for industrial operation in terms of lower cost of equipment and pumping, compared with high pressure processes.

5.1.4   **Effect of Feed composition**

The effects of different compositions of water/methanol mixtures upon conversion and product distribution were investigated by changing the methanol content in the feed from 25 to 75 wt.%. The results are shown in Figure 5.4.a and 5.4.b. By decreasing the amount of methanol in feed the conversion was increased from 87% to 97%. The lower conversion at higher concentration of methanol in the feed could be due to the faster coking of zeolite after 4 hours and/or dealumination by steam (Gayubo et al., 2004). This is confirmed by the TGA result of used catalyst which is shown in Table 5.3.

Table 5.3. TGA result of catalyst after reaction with different feed composition.

Methanol in Feed (wt.%)	Coke (wt.%)
75	4.4
50	3.4
25	2.1

The amount of coke on the used catalysts after 4h TOS is higher when the feed contains more methanol. Decreasing the concentration of methanol in the feed from 75 to 25% increased the selectivity to light olefins, and at the same time production of light alkanes and heavy hydrocarbons diminished. Ethene and propene increased from 22 and 31% to 27 and 40%, respectively. Water molecules seem to weaken the acid sites responsible for the hydrogen-transfer reactions and as a result, decreasing the conversion of olefins to paraffins (Froment et al., 1992). A noticeable increase in $C_3/C_3^=$ ratio and methane production at 75%wt. methanol in water, implies that faster coking occurs at more concentrated feed after 4 h TOS. As discussed by Schulz (2010), one of the issues on dehydration of methanol to olefins over HZSM-5 zeolite in fixed bed reactors is undesirable reactions that may proceed in the front- and tail-zone of the catalytic bed. Olefins can be converted to paraffins and aromatics in the entrance of the reactor (front zone) and by reaction of methanol with coke at the end of the reactor (tail-zone), further

coke and methane will be formed. These problems are more pronounced at higher feed concentrations. Gayubo et al. (2004) investigated the role of water on the acidity deterioration and coking of ZSM-5 zeolite in the MTO process. They found that at 400 ºC there is less coking (65%) on the ZSM-5 when 50% wt. methanol in water was used in comparison to pure methanol whereas no acidity deterioration was observed even after reaction regeneration cycles. They also report severe dealumination of zeolite at higher temperature (500 ºC) by the water produced during the reaction. The loss of strong acid sites is more pronounced with pure methanol than methanol diluted with water.
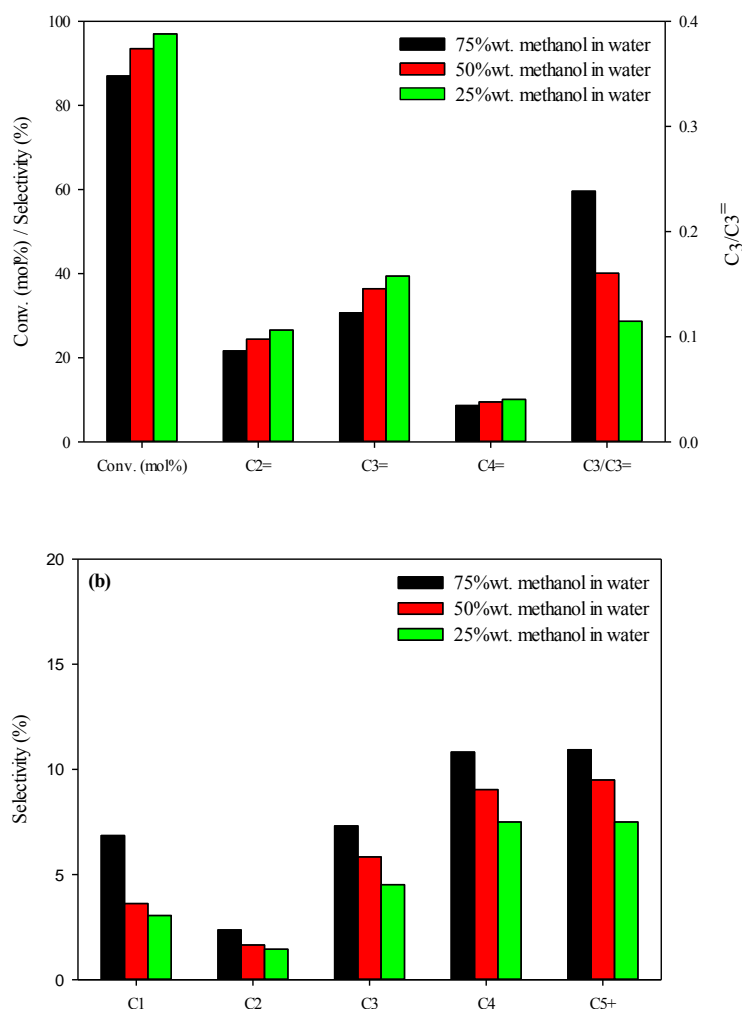
Figure 5.4. Effect of feed composition on (a) methanol conversion and olefins distribution (b) paraffins and C_5^+ distribution over ZSM-5(100). Reaction conditions; temperature: 400 ºC, pressure: 1 bar, WHSV: 34 h^{-1}, TOS: 4 h.

To better understand the effect of adding water to the feed on the weakening of the medium or strong acid centres of the zeolite, the TPD results of catalysts after reaction with different feed composition are summarised in Table 5.4. In a very diluted feed (25 wt.%), the number of medium and strong sites were not changed significantly after reaction but the number of weak acidic sites were decreased slightly, while, using feed with higher amount of methanol (75wt.%) led to a noticeable decrease in all acid sites.

Table 5.4. TPD result of catalyst after reaction with different feed composition.

	Methanol in Feed (wt.%)	Acidity distribution (mmol t-BA/g)			
		Weak (150-300 ºC)	Medium (300-400 ºC)	Strong (400-500 ºC)	Total
Fresh zeolite	--	0.52	0.13	0.03	0.68
Used zeolite	25	0.47	0.13	0.02	0.62
Used zeolite	50	0.45	0.12	0.02	0.59
Used zeolite	75	0.35	0.05	0.01	0.41

The addition of water to the reaction system is necessary to remove the reaction heat and to enhance light olefin selectivity and for this purpose, diluted methanol (55–65% wt. water) as feed is recommended (Liu et al., 2000). However, the problem of irreversible deactivation arises as the reaction temperature is increased, which is due to dealumination of the HZSM-5 zeolite at elevated temperatures (Aguayo et al., 2002, de Lucas et al., 1997b). To overcome this problem, use of an inert gas was proposed by Schulz and Bandermann (1994). They reported that high water concentrations in the ethanol feed has the same effect on product distribution as dilution by inert gas. In both cases lower methanol partial pressures lead to higher yields of light olefins in the product stream.

5.1.5   Effect of WHSV

The effect of varying the Weight Hourly Space Velocity (WHSV) from 7 h^{-1} to 53 h^{-1} on product distribution and conversion was investigated. To make sure that there is no internal diffusion resistance, samples with four different pellet sizes (e.g. 5, 3, 1 and 0.5 mm) were loaded in the reactor and tested under the same reaction conditions. No significant change in the methanol conversion was observed. Therefore, under the test conditions used, the internal mass transfer resistance was negligible. As shown in Figure 5.5.a, methanol conversion was decreased from 99% to 86% by increasing the WHSV from 7 h^{-1} to 53 h^{-1}. The selectivity to propene increased from 28% to 36% by increasing the WHSV from 7 h^{-1} to 53 h^{-1}. The selectivity to ethene decreased slightly from 27 to 25% in this range. The selectivity to butene increased from 6% to 11% by increasing the WHSV from 7 h^{-1} to 27 h^{-1}. This figure then decreased slightly to 10%. The remarkable decline of $C_3/C_3^=$ ratio from 0.45 to 0.1 suggests that olefins are the dominant products at higher WHSV (with correspondingly less contact time). As shown in Figure 5.5.b, by increasing the WHSV from 7 h^{-1} to 53 h^{-1} methane and ethane increased from 4 and 0.6% to 8 and 3%, respectively. In contrast, propane and butane decreased from 12 and 19% to 4 and 7%. Such an observation suggests that increasing WHSV only increases the formation of light paraffins (e.g. C_1 and C_2) while heavier paraffins undergo a different reaction pathway. With respect to the C_5^+ product distribution, the selectivity increased from 3% to 9% by increasing the WHSV from 7 h^{-1} to 27 h^{-1}. By further increasing WHSV up to 53 h^{-1}, the selectivity decreased slightly to 8%. At low WHSV (high contact time), formation of saturated paraffins are more favoured while by increasing WHSV, light olefins are more favoured. In other words, at high WHSV (low residence time), there is not enough time for ethene, propene or other low molecular weight olefin compounds to form paraffins and aromatics in a consecutive reaction and as a result the reaction sequence is hence shortened, with production stopping at the

intermediate species, resulting in product mixtures containing a higher proportions of olefins.

These consecutive reactions have been reported as follow (Stocker, 1999):

$$CH_3OH \leftrightarrow CH_3OCH_3 \rightarrow \text{light olefins} \rightarrow \text{paraffins} + \text{higher olefins} + \text{aromatics} + \text{naphthenes}$$
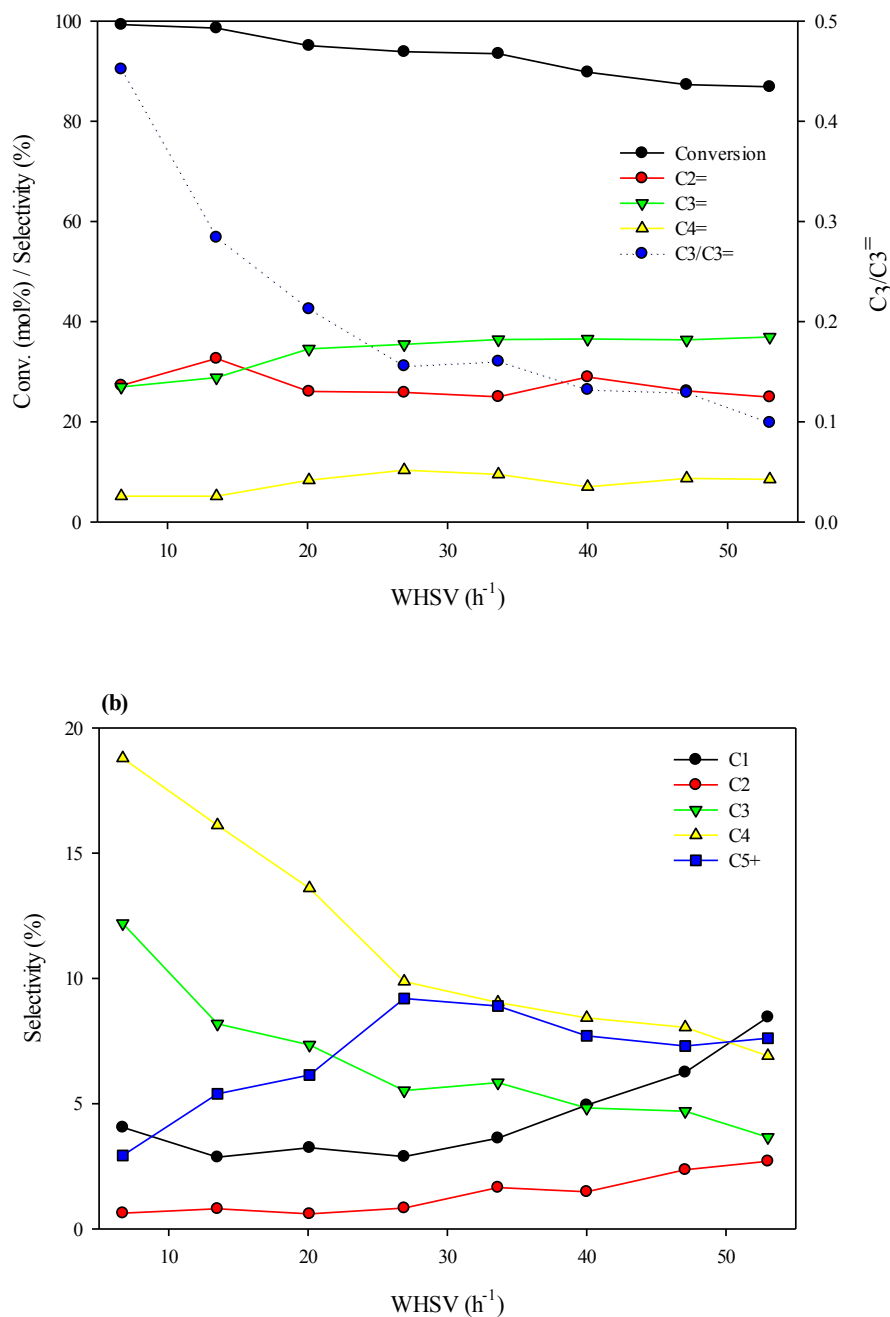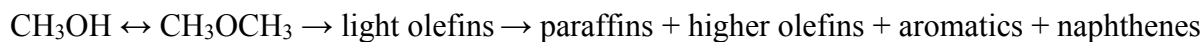
Figure 5.5. Effect of WHSV on (a) methanol conversion olefin distribution and (b) paraffins and C_5^+ distribution over ZSM-5(100). Reaction conditions; temperature: 400 °C, pressure: 1 bar, methanol/water ratio: 1 w/w, TOS: 4 h.

It has been shown that increasing WHSV leads to formation of coke due to growing influence of non-shape selective hydrogen transfer reactions (Chang and Silvestri, 1977, Al-Jarallah et al., 1997). Based on these results, 34 h^{-1} was therefore chosen, as the point at which optimum propene selectivity was obtained.

5.1.6   Effect of catalyst to support ratio

Figure 5.6.a and 5.6.b show the methanol conversion and product selectivity over catalyst with different amounts of ZSM-5 to γ-alumina support ratio. It can be seen that the conversion was not influenced significantly by this ratio, however by increasing the amount of zeolite in the catalyst from 25% to 85%, selectivity to propene decreased from 42% to 33%. Increasing the $C_3/C_3^=$ ratio from 0.09 to 0.21 suggests that higher amount of zeolite in the catalyst matrix can promote the hydride transfer reaction to some extent. In other words, although selectivity to saturated paraffins increased due to higher amount of zeolite in the catalyst, however selectivity to heavy hydrocarbons (C_5^+) decreased. Use of zeolite on alumina led to a decrease in micropore area and BET surface area, compared to the pure ZSM-5 (Table 5.6). It has been shown that using alumina as a binder with ZSM-5 zeolite can improve the production of DME from methanol (Kim et al., 2006). DME is the most important intermediate compound to produce light olefins through three steps: (a) dehydration of methanol to DME, (b) dehydration of DME to olefins, and (c) transformation of olefins to aromatics and alkanes. It should be noted that the initial dehydration step is rapid and reversible with close approach to equilibrium (Chang et al., 1979, Liu et al., 2000, Jiang et al., 2004). Though Al_2O_3 has high activity for production of DME, it tends to adsorb water on its surface and thereby loses its activity in the presence of

water because of its hydrophilic nature. Water blocks the active sites for methanol consumption

through competitive adsorption with methanol on the catalyst surface (Jun et al., 2003).
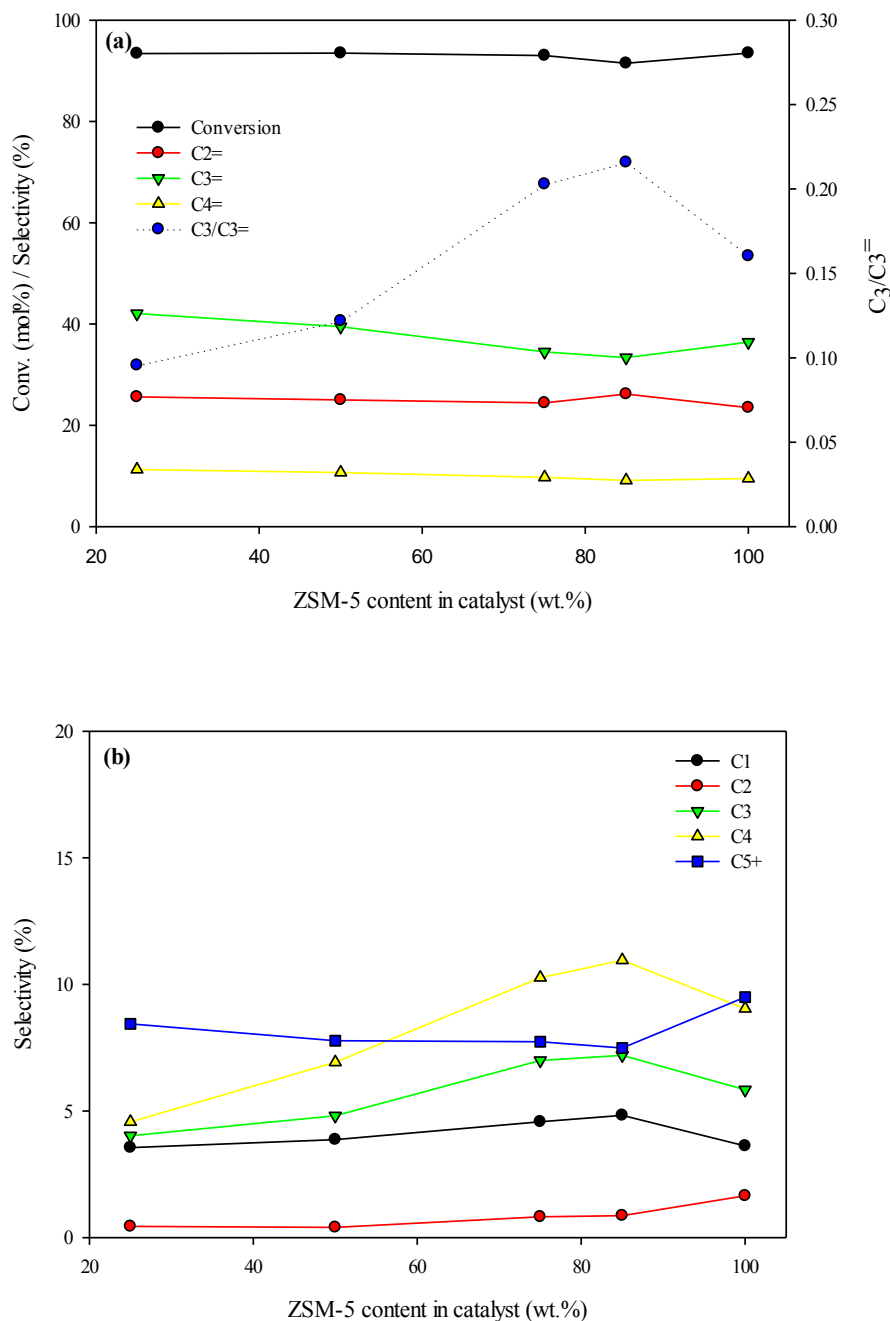
Figure 5.6. Effect of ZSM-5 content in catalyst on (a) methanol conversion and olefins distribution (b) paraffins and C_5^+ distribution; reaction conditions: temperature: 400 ºC, WHSV: 34 h^{-1}, pressure: 1 bar, methanol/ water ratio: 1 w/w, TOS: 4h.

Kim et al. (2006) investigated the effect of using γ-alumina as a binder with ZSM-5 zeolite on the production of DME. They reported that zeolite modified by sodium and containing 70% wt. alumina has a high stability against coke formation and water for 15 days at 270 ºC, with ca. 80% of DME yield. Although, ZSM-5 with the medium pore size showed a superior selectivity towards propene, at the same time boehmite gave a high strength and proper shape to the catalyst. Comparing the result of catalyst with no binder (ZSM-5 (100)) and catalyst with 25% zeolite on alumina (ZSM-5 (25)), it can be concluded that the catalyst with binder can improve the selectivity to light olefins (e.g. ethene or propene) while less by-products (e.g. paraffins or heavy hydrocarbons) were produced.

5.2   Zeolite modification

The ZSM-5(100) zeolite was ion exchanged using phosphorous, caesium, calcium and iron. Figure 5.7.a and 5.7.b illustrate the effect of modification on product distribution and conversion. Modification of zeolite with phosphoric acid (P-ZSM-5) improved the propene selectivity from 36% to 45%, whilst the selectivity to ethene was decreased slightly from 24% to 18% compared to the parent zeolite. The conversion of 96% was the highest amongst all the catalysts implying high activity and prolonged catalyst lifetime. However, the highest selectivity to C_5^+ molecules of 11% was also obtained. The addition of phosphoric acid therefore added to the total acidity of the catalyst by increasing the number of weak acid sites possibly on the outer surface of the zeolite and increased it from 0.52 to 0.72 mmol t-BA/g (Table 5.5). A decrease in the $C_3/C_3^=$ ratio from 0.16 to 0.05 from one side and decrease in selectivity to paraffins from other side imply the suppression of hydride transfer reaction to form more saturated hydrocarbons, however a slight increase on C_5^+ is still observed.
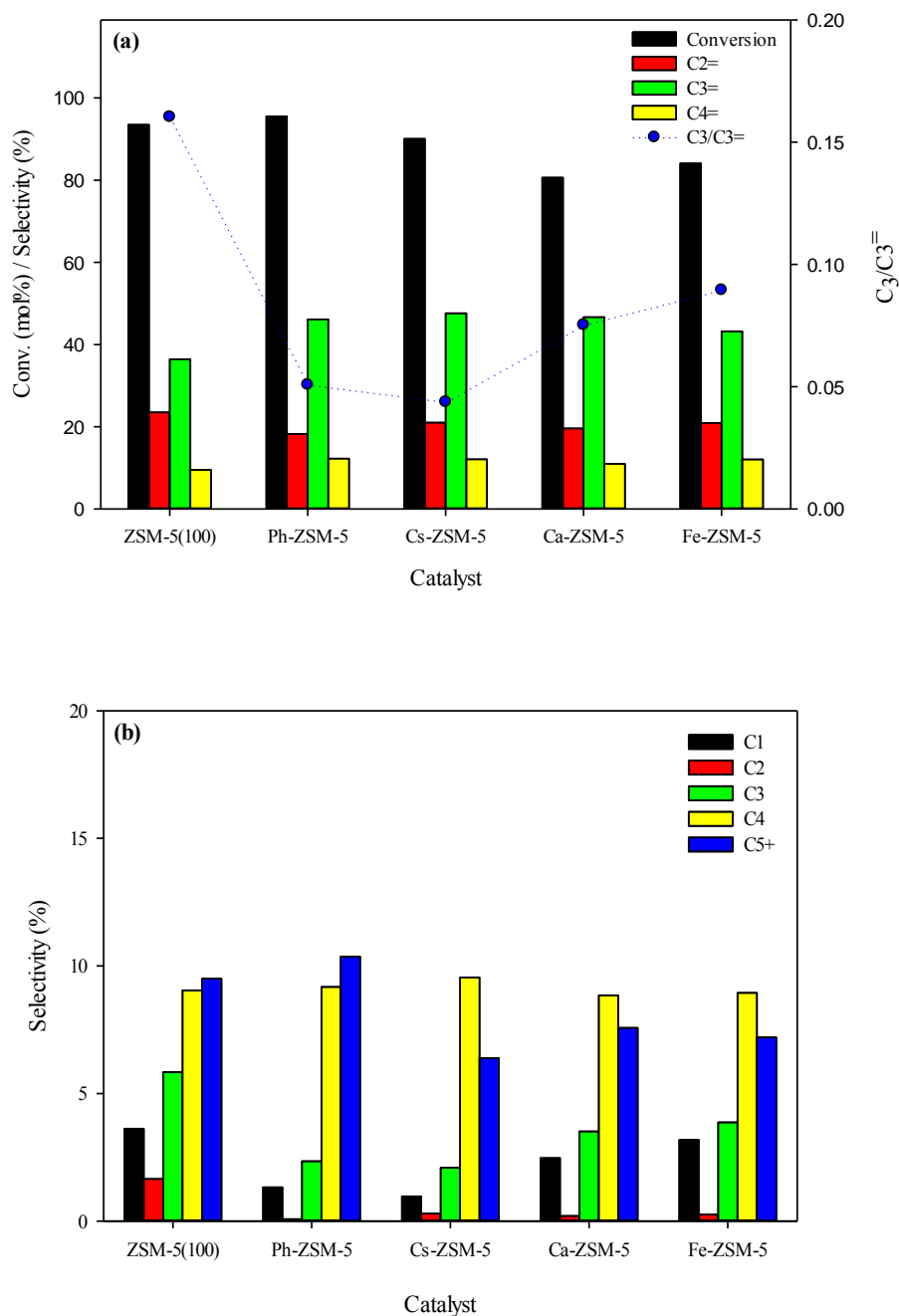
Figure 5.7. Effect of modification of ZSM-5 on (a) methanol conversion and olefins distribution (b) paraffins and C_5^+ distribution; reaction conditions: temperature: 400 ºC, WHSV: 34 h^{-1}, pressure: 1 bar, methanol/ water ratio: 1 w/w, TOS: 4h.

Van vu et al. (2010) treated ZSM-5 zeolite with H_3PO_4 solutions of various concentrations. They observed that the selectivity to olefins was significantly improved. They reported that higher phosphorus content in P-HZSM-5 significantly decreased the selectivity to ethene and

aromatics due to lower acidity of the H-ZSM-5's strong acid sites caused by dealumination. Dehertog and Froment (1991) modified zeolite by trimethylphosphite to make P-HZSM-5. They reported that this modification resulted in a significant decrease in activity but the yield of light olefins increased.

The conversion of 90% was obtained for the zeolite modified by caesium (Cs-ZSM-5). Propene selectivity of 48% was highest among the all samples. The selectivity to ethene was 21% and that of the butene selectivity was 12%. Similar to the P-ZSM-5 catalyst, selectivity to paraffins decreased after modification by Cs. In this case, selectivity to C_5^+ dropped to 6%. Caesium is an alkali metal and therefore it can reduce the acid sites zeolite after ion-exchanging. It is very important to use proper amount of alkali metals during the modification of zeolite as using high concentration of caesium cause the deactivation of medium and strong acid sites. From Table 5.5 it can be seen that the addition of caesium increased the total acidity of the catalyst, although the number of medium and strong sites is diminished.

The lowest conversion of 81% amongst all the catalysts was obtained on the catalyst ion exchanged by calcium (Ca-ZSM-5). After modification, the selectivity to ethene was decreased from 24% to 20% but propene selectivity increased from 37% to 47%. The C_3/C_3^+ ratio was reduced from 0.16 to 0.07. Similarly, the selectivity to C_5^+ slightly decreased from 10 to 8%. As mentioned before, the weak acid sites are responsible for the production of light olefins. Addition of an alkali metals such as calcium reduces the acidity of the catalyst by forming an acid-base centre (Blaszkowski and van Santen, 1996) leading to better selectivity to light olefins. The total acidity of Ca-ZSM-5 sample remains constant to 0.68 mmol t-BA/g after modification but more strong acid sites are generated.

The iron modified catalyst (Fe-ZSM-5) gave methanol conversion of 84%. The propene selectivity increased to 43%, whilst the ethene selectivity was decreased slightly to 21%. The

selectivity to butene was increased to 12%. The C_3/C_3^+ ratio decreased from 0.16 to 0.09 and selectivity to C_5^+ components was decreased to 7%. ZSM-5 zeolite containing Fe can inhibit the formation of aromatics and suppress the olefins hydrogenation by reduction of Fe_2O_3 to Fe_3O_4, resulting in a higher olefins/alkanes ratio (Lücke et al., 1999, Inaba et al., 2007).

5.3   Characterisation of the catalyst

In this section, the characterisation of catalysts is presented in terms of crystal analysis by XRD, acidity strength and distribution measurement by TPD, and pore size, pore volume and BET surface area measurement by nitrogen adsorption–desorption technique.

5.3.1   Acidity measurement by TPD

Temperature-programmed desorption (TPD) of tert-Butylamine (t-BA) was carried out in the temperature range of 50–500 ℃ to compare the acid properties of the catalysts. Use of t-BA for measuring the acid strength of microporous catalysts is recommended as its high vapour pressure and its molecular structure does not have diffusional limitation in the microporous zeolites (Aguayo et al., 1994). During the desorption of t-BA, three peaks were observed in the range of 150-300 ℃, 300-400 ℃ and 400-500 ℃ which correspond to weak, medium and strong type acid sites, respectively. Bibby et al. (1992) stated that the intensity of the peak in the range of 150-400 ℃ corresponds to the total Brønsted acid site population calculated from the aluminium content of the zeolite, while the next peak at higher temperature (400-500 ℃) was attributed to ammonia desorption from very strong Brønsted or Lewis sites. The results of TPD for ZSM-5 zeolite with no support, catalyst samples with different ZSM-5 zeolite to support ratios, alumina as support and metal doped zeolite are listed in Table 5.5. Details of TPD calculations and calibration curves are presented in Appendix C. As described in Section 4.3.1,

it is possible that t-BA becomes decomposed over strong Brønsted acid sites at high temperatures, however, as it has been shown by Gayubo et al., (1996), the difference between total acidity measured by NH_3-TPD method and measured decomposed t-Butylamine using online GC is negligible. For example, the values of total acidity for H-ZSM-5 (Si/Al=86) is 0.58 (mmol NH_3 g^{-1}) or 0.54 (mmol tert-Butylamine g^{-1}).

Table 5.5. TPD results of various catalyst samples.

Catalyst name	Acidity(mmol t-BA/g) / distribution			
	Weak (150-300 ºC)	Medium (300-400 ºC)	Strong (400-500 ºC)	Total
ZSM-5(100)	0.52(77%)	0.13(19%)	0.03(4%)	0.68
ZSM-5(85)	0.30(65%)	0.12(27%)	0.04(8%)	0.46
ZSM-5(75)	0.35(68%)	0.12(24%)	0.04(8%)	0.51
ZSM-5(50)	0.43(67%)	0.15(24%)	0.06(9%)	0.64
ZSM-5(25)	0.47(60%)	0.22(28%)	0.09(11%)	0.78
γ -alumina	0.44(58%)	0.21(28%)	0.11(15%)	0.76
Fe-ZSM-5	0.52(76%)	0.13(19%)	0.04(5%)	0.69
Ca-ZSM-5	0.53(78%)	0.11(16%)	0.04(6%)	0.68
Cs-ZSM-5	0.59(84%)	0.10(14%)	0.01(1%)	0.70
P-ZSM-5	0.72(85%)	0.11(13%)	0.02(3%)	0.85

The ZSM-5 zeolite contains mainly weak acid sites (77%) and very few strong acidic centres (4%), while the support (γ-alumina) contains more strong acid sites (15%). It is possible to change the acid distribution either by changing the Si/Al ratio of catalysts or by changing the zeolite to support ratio. For instance, by decreasing the amount of zeolite in the catalyst, the Si/Al is decreased and as a result weak acid sites are decreased, but strong acidic centres as well as total acidity is increased. Studies on the effect of Si/Al ratio on the acidity of ZSM-5 zeolite show that as Si/Al ratio decreases, the Brønsted/Lewis sites ratio (weak/strong acid sites ratio) is decreased, while total acidity as well as acidic site density is increased (Benito et al., 1996, Gayubo et al., 1996). It is well known that the presence of strong acid sites promotes the polymerisation of olefins and increases the rate of coke formation (Bibby et al., 1992, Xu et al.,

1997). As observed from the TPD measurements in Table 5.5, modification of ZSM-5 zeolite by iron and calcium seems to have no noticeable effect on catalyst acidity. Machado et al (2006) have studied production of hydrocarbons from ethanol over iron incorporated ZSM-5 zeolite. They observed that the total acidity of the samples with different amount of iron does not change significantly. Lersch and Bandermann (1991) impregnated the ZSM-5 zeolite with alkaline earth metals such as Ca, Mg and Ba. They observed that the peak corresponding to weak acidic sites in the TPD spectra is almost the same for all the catalysts, but a new third peak at higher temperature in which represents strong Lewis acid sites appeared in the case of impregnation with Mg and Ca.

Modification of zeolite with Cs and phosphoric acid increased the weak acidic and decreased the strong acidic centres. Haag (1994) reported that caesium can selectively poison the strongest acid sites of ZSM-5 zeolite first. He demonstrated that modification of zeolite with Cs-ions leads to a dramatic decrease of catalyst activity. Lercher and Rumplmayr (1986) reported that modification of ZSM-5 zeolite with H_3PO_4 could convert the strong Brønsted acid sites to weak Brønsted acid sites without changing the overall acidic properties of the sample.

5.3.2   XRD analysis

Figure 5.8 shows the XRD patterns of catalysts with different amounts of ZSM-5 zeolite on the support. All samples exhibit the typical pattern of calcined ZSM-5 zeolite. By increasing the amount of support, a new peak appears at 39 2Ө which confirms the presence of gamma alumina in the catalyst structure. All peaks are sharp within the range of 10-40 2Ө which indicates that the zeolite sample possesses a high degree of crystallinity, however by increasing the amount of alumina support peak broadening occurs at 46 2Ө. Peak broadening in XRD patterns of

zeolites can occur for a variety of reasons such as small crystal size (below 0.2μm), disorder, absorption, and inconsistent sample packing density (ASTM, 2004).
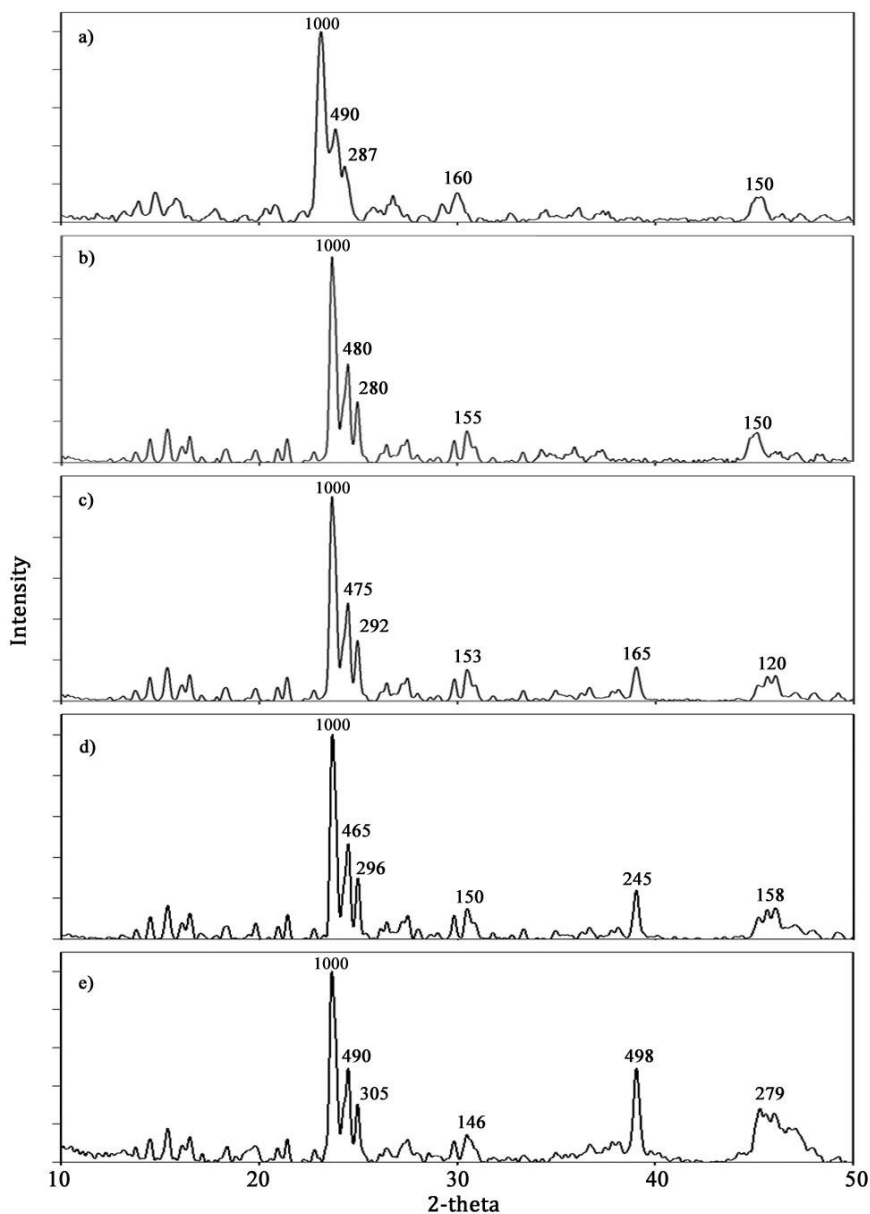
Figure 5.8. XRD patterns for the different amount of ZSM-5 on support: a) ZSM-5(100), b) ZSM-5(85), c) ZSM-5(75), d) ZSM-5(50), e) ZSM-5(25).

The XRD patterns of zeolite modified by metals are not shown in this figure as similar patterns to pure ZSM-5 were observed in all cases. The similar patterns confirm that modification has not destroyed the crystalline structure of the zeolite. Moreover, an undetectable crystalline

phase of metal ions implies that they are finely dispersed at the cation sites of the zeolite. The average crystallite size of samples were calculated by applying Scherrer equation on (1000), (490) and (287) XRD reflections. The relative crystallinity of the sample was determined according to the ASTM D5758 measuring the intensity of the reflection peak at 24.3 2Ө and comparing the intensities with that of the reference sample. The results confirm that all the samples had a high degree of crystallinity. Crystal size and relative crystallinity are listed in Table 5.6.

5.3.3   N$_2$ adsorption–desorption isotherms

Nitrogen adsorption–desorption at 77 K was used to determine the BET surface area, pore volume and micropore area. Figure 5.9 illustrates the nitrogen adsorption-desorption isotherms of samples with different amounts of zeolite on the support.
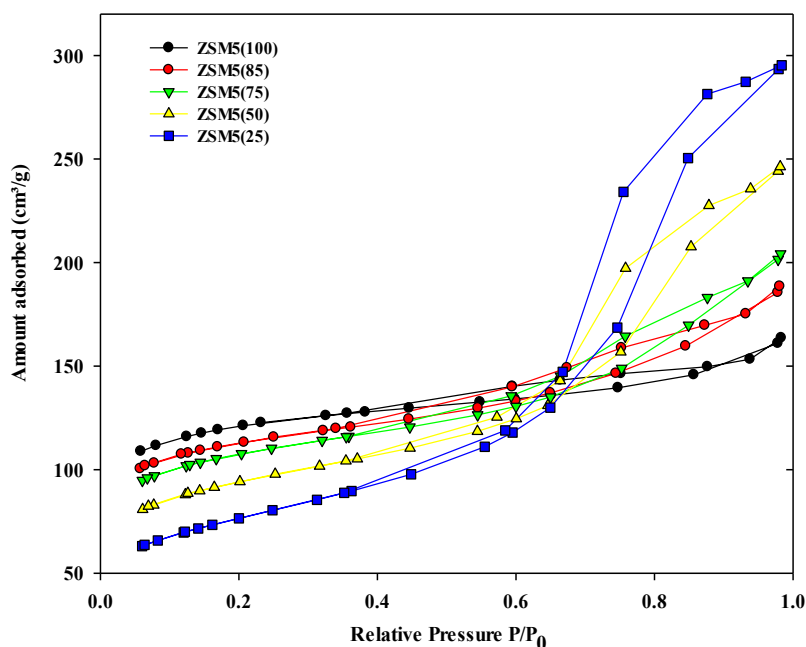
Figure 5.9. Nitrogen adsorption-desorption isotherms of samples with different amounts of zeolite.

All the isotherms are typical reversible Type IV adsorption isotherms as defined by IUPAC (Sing et al., 1985). The hysteresis loops are due to capillary condensation of nitrogen in mesopores. The hysteresis loop for pure ZSM-5 zeolite and samples with 85% or 75% ZSM-5 is very similar to the H4 type adsorption isotherm which is associated with narrow slit-like pores. In samples with lower amounts of zeolite (e.g. ZSM-5(50%) or ZSM-5(25%)) the loop is similar to H1 type which is associated with porous materials consisting of agglomerates in a fairly regular array, and therefore narrow distributions of pore size. The isotherms for zeolite modified by metals are shown in Figure 5.10 All the isotherms exhibit the general pattern of ZSM-5(100) sample. Modification in all cases except Fe has decreased the liquid nitrogen uptake due to blockage of pore channels by metal ions. It is well known that during the wet impregnation of ZSM-5 zeolite, metallic compounds can penetrate into the pores of ZSM-5 and block them, thereby greatly reducing the surface area (Berndt et al., 1996, Qian and Yan, 2001).
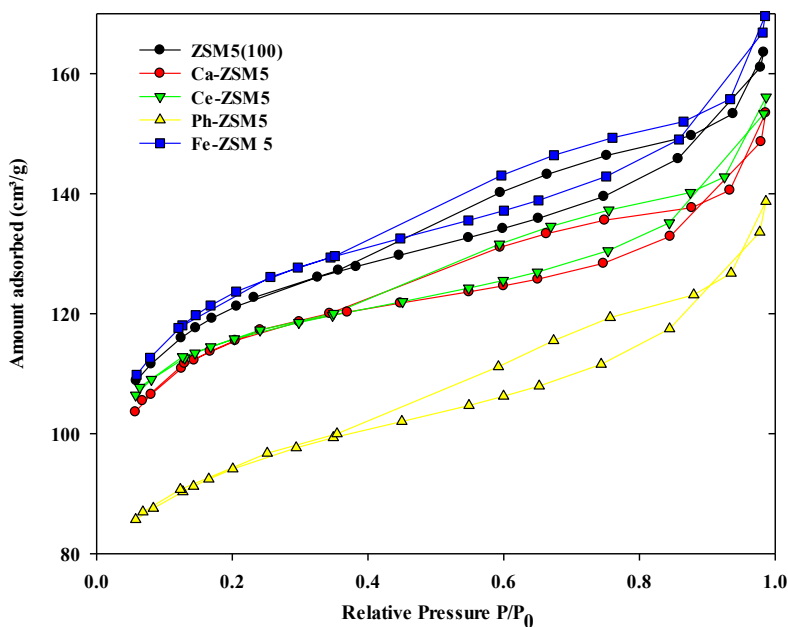
Figure 5.10. Nitrogen adsorption-desorption isotherms of modified zeolite.

Table 5.6 lists the physical properties of the parent ZSM-5 zeolite, samples with different zeolite to support ratio and zeolite ion exchanged by metals and phosphorous. In case of catalyst

samples with different amount of zeolite on support, by increasing the amount of γ-alumina in the sample, both BET surface area and micropore area are decreased, while the average pore volume are increased. Figure 5.11 shows the SEM image of P-ZSM-5 zeolite. The phosphorous particles cover the surface of ZSM-5 zeolite

Table 5.6. Properties of various catalyst samples.

Catalyst name	Zeolite/ Metal in the sample (wt.%)	BET surface area (m²/g)	Crystal size (nm)	Relative Crystallinity (%)	Micropore volume (cm³/g)	Micropore area (m²/g)
ZSM-5(100)	100	413	16	100	0.10	245
ZSM-5(85)	85	386	16	98	0.18	240
ZSM-5(75)	75	370	18	102	0.21	185
ZSM-5(50)	50	328	19	103	0.30	150
ZSM-5(25)	25	270	22	106	0.43	70
γ-alumina	--	218	28	100	0.50	14
Fe-ZSM-5	1.1	423	15	100	0.12	268
Ca-ZSM-5	1.4	395	14	101	0.11	236
Cs-ZSM-5	1.7	394	15	99	0.13	296
P-ZSM-5	1.2	322	15	101	0.10	212

.
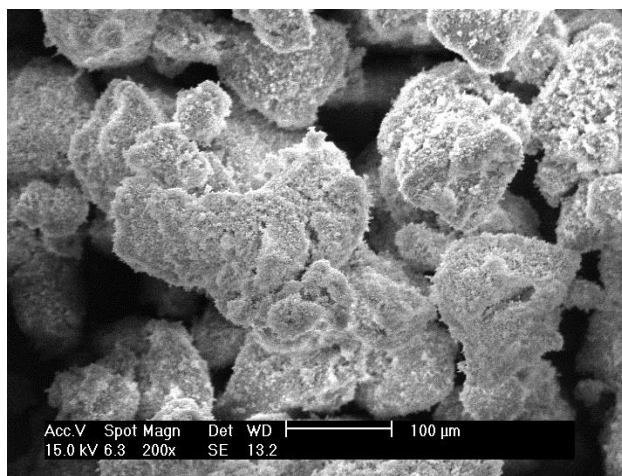
Figure 5.11. SEM image of P-ZSM-5 zeolite.

5.4 Coke characterisation

The amount of coke deposited on the catalysts was measured by TGA. Table 5.7 shows the TGA result of used catalyst under typical reaction conditions (temperature: 400 ºC, WHSV: 34 h^{-1}, pressure: 1 bar, methanol/ water ratio: 1 w/w, TOS: 4h). Figure 5.12.a and 5.12.b show the TGA curve of coked zeolite catalysts after 4 h for both zeolite with different amount of alumina in the matrix and modified zeolite.

The mass loss of the catalyst samples under air flow at temperature 120-700 ºC was taken as being due to coke deposits upon the catalyst samples. In case of zeolite bound with different amounts of γ-alumina, a higher amount of alumina led to an increase in coke weight from 2.2 to 2.9 wt.% possibly due to increase in strong acid sites (Table 5.5).

ZSM-5 zeolite samples with relatively high aluminium content (SiO_2/Al_2O_3 ratio < 70) display a remarkably high activity in the steps of olefin aromatisation (Luk'yanov, 1992, Mores et al., 2011). The trend of changing coke amount on catalyst samples is very similar to changing in C_5^+ components including aromatics. Modification by Ca and Cs decreased the amount of coke by reducing the strong and medium acid centres, while zeolite treatment by P led to faster coking due to higher amount of total acidity. The amount of coke on Fe-ZSM-5 zeolite samples is very similar to the parent ZSM-5. It was expected as both samples exhibit similar acid site distribution.

Table 5.7. TGA results of different catalyst samples under typical reaction conditions (temperature: 400 ºC, WHSV: 34 h^{-1}, pressure: 1 bar, methanol/ water ratio: 1 w/w, TOS: 4h).

Catalyst name	ZSM-5(100)	ZSM-5(85)	ZSM-5(75)	ZSM-5(50)	ZSM-5(25)	P-ZSM-5	Cs-ZSM-5	Ca-ZSM-5	Fe-ZSM-5
Coke (wt.%)	3.4	2.2	2.5	2.8	2.9	4.1	2.1	2.2	3.2
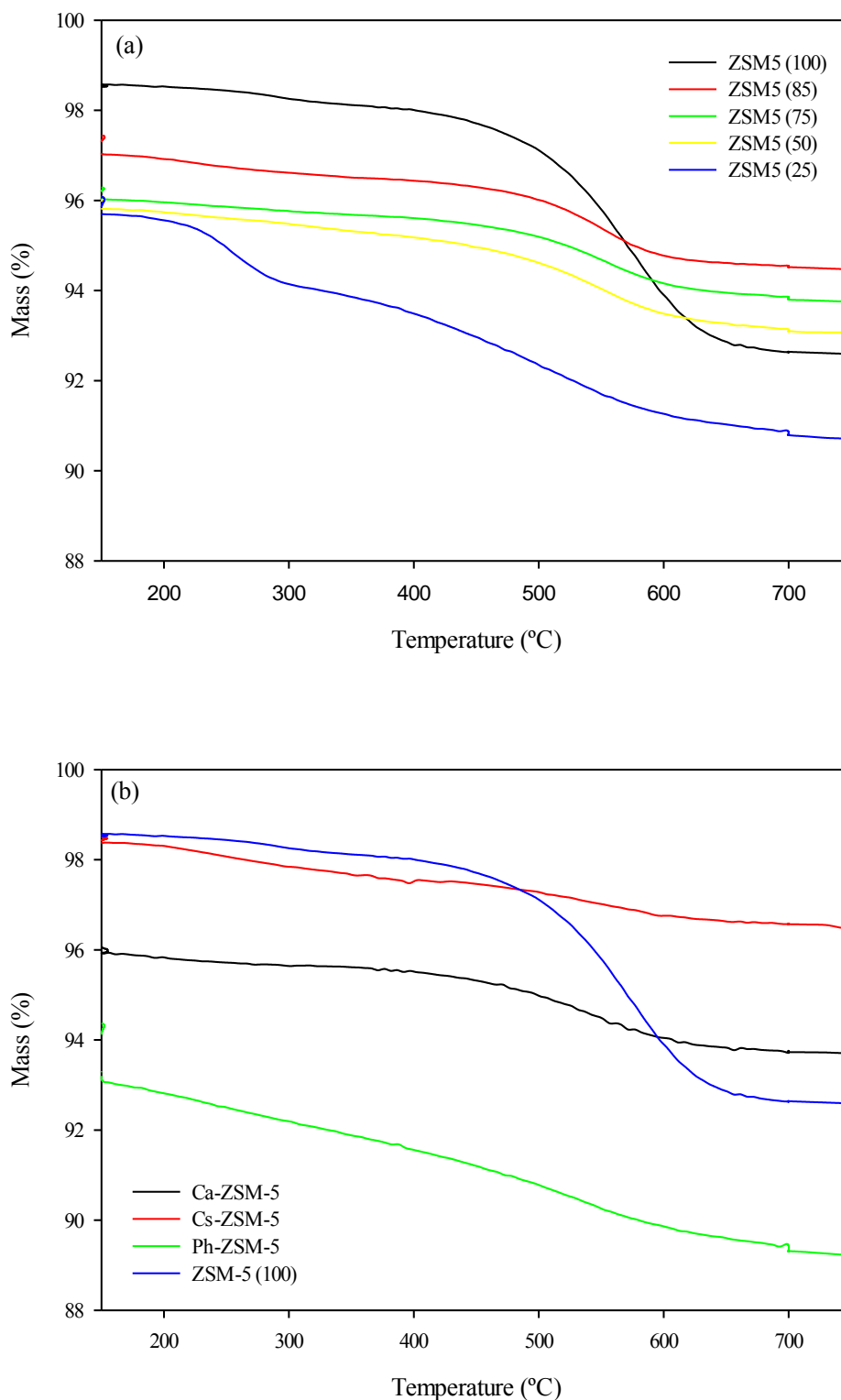
Figure 5.12. TGA profile of coked zeolite catalysts after 4 hours (a) samples with different amount of alumina in catalyst matrix (b) modified zeolite.

5.5 Conclusion

Firstly, the effect of reaction conditions (e.g. temperature, pressure, space velocity and feed composition) on the dehydration of methanol to light olefins over ZSM-5 zeolite with no support was studied. High temperature (e.g. 400 °C) is essential to produce light olefins more selectively, however elevated temperatures led to faster deactivation, more selectivity to alkanes and lower selectivity to light olefins. Pressure higher than 1 bar led to production of heavier hydrocarbons (C_5^+) and lower selectivity to light olefins. It was shown that high water concentrations in the feed led to higher yields of light olefins. High space velocity is required to produce more light olefins, although methanol conversion is decreased; however at WHSV higher than 34 h^{-1}, faster deactivation with no improvement in selectivity to propene or other light olefins was observed.

Secondly, the effect of using different ratios of alumina as a support to zeolite was studied. Use of γ-alumina as support improved the catalyst selectivity to propene and light olefins. Zeolite catalyst with 25 wt.% ZSM-5 in the catalyst sample led to highest selectivity to propene and light olefins, but faster deactivation was observed on this catalyst.

Thirdly, ZSM-5 zeolite was modified with P, Cs, Ca and Fe. Modification in all cases increased the shape-selectivity to propene. ZSM-5 zeolite ion exchanged by Cs led to highest selectivity to propene by changing the acid site distribution. The lowest selectivity to C_5^+ compounds and least amount of coking was observed on this catalyst.

Chapter 6 HYDROGENATION OF NAPHTHALENE OVER Ni/Co ZEOLITE BASED CATALYST

6.1 Hydrogenation of naphthalene

Hydrogenation of naphthalene is an important process in the chemical and petrochemical industries for manufacturing tetralin, a high boiling point solvent, or cis-decalin. Cis-decalin can be used for hydrogen storage in proton-exchange membranes (PEM) and fuel cells (Hiyoshi et al., 2006). It can also be used for production of sebacic acid to manufacture Nylon 6, 10, plasticisers and softeners (Weissermel and Arpe, 2003). Trans-decalin has higher thermal stability than cis-decalin, making it a desirable component in jet aircraft fuels where the fuel is exposed to high temperatures (Schmitz et al., 1996). Thus, designing a catalyst to be selective to each product has its own merits for certain applications.

Several researchers have studied liquid and gas phase hydrogenation of naphthalene over supported metal catalysts (Rautanen et al., 2002, Kirumakki et al., 2006, Pawelec et al., 2002). Transition metal based catalysts are more favoured for this reaction compared to noble metals due to their lower price, however these catalysts usually show low selectivity to tetralin (Ito et al., 2002). Designing a transition metal based catalyst with high selectivity to tetralin is still challenging. It has been shown that using zeolite as support can significantly improve the selectivity to cis-decalin in hydrogenation of naphthalene over Pd or Pt (Schmitz et al., 1996). However, the main drawback of the zeolite support is its micro-porosity, which could potentially result in diffusion limitation (He et al., 2013). Until now, only zeolites with large

micropores such as Y type, and β type have been used as support for hydrogenation of heavy aromatics. On the other hand, zeolite acidity increases undesirable cracking activity, which accelerates the rate of coke deposition on the catalyst (Albertazzi et al., 2004).

In this research, hydrogenation of naphthalene over two zeolite based catalyst Co/ZSM-5, Ni/HY were studied. Results were compared with a synthesised Co/Silica catalyst and a commercial NiMo/Alumina catalyst. Characterisation of catalyst samples was used as a tool to relate the catalyst activity and selectivity to their properties.

6.1.1 **Naphthalene conversion**

Figure 6.1 shows naphthalene conversion over four different catalyst samples at optimum reaction conditions. The optimal reaction conditions (temperature 300 ºC, pressure 60 bar) were determined by one the previous research group member (Hassan, 2011).

Both Co/Silica and NiMo/Alumina catalyst showed high activity with ~90 % naphthalene conversion during the first hour of the reaction; however after 2 hours, naphthalene conversion declined significantly over Co/Silica catalyst to around 20% and remained constant at this value while for NiMo/Alumina catalyst, conversion decreased to 60% after 6 h time on stream reaction. Ni/HY catalyst showed more stability in conversion of naphthalene. Conversion started from 69% and decreased slightly to 59% after 6 h TOS.

Comparing two zeolite based catalyst (Ni/HY and Co/ZSM-5), lower conversion can be observed over Co/ZSM-5 sample with almost 20% of naphthalene conversion over 6 h TOS. Such low activity can be related to mass transfer limitation due to small pore size of ZSM-5 zeolite, while higher naphthalene conversion for HY zeolite may be due to its larger pore size (7.4 Å) compared to ZSM-5 zeolite (5.4 Å). A larger pore size may lead to improved diffusion of coke precursors from the catalyst and thus a lower degree of deactivation. Fast deactivation

of Co/Silica at high temperatures and pressures due to hydrothermal degradation of the catalyst to form silicates is a common problem of this catalyst and has been reported widely in the literature (Bartholomew, 2001, Spivey et al., 2001, Tsakoumis et al., 2010).
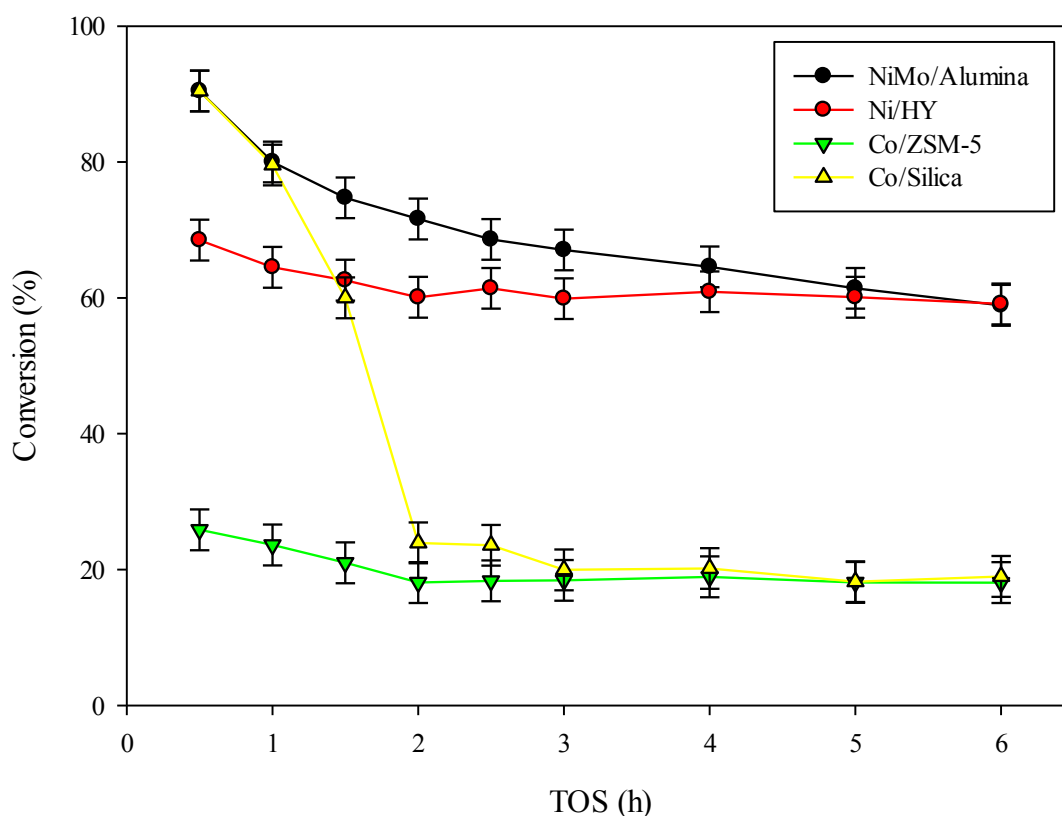
Figure 6.1. Conversion of naphthalene over different catalysts; Temperature: 300ºC, pressure: 60 bar, WHSV: 14 h^{-1}, feed: naphthalene in cyclohexane (50/50 wt./wt.), H$_2$/naphthalene: 0.136 mol.mol^{-1}.

6.1.2 **Tetralin yield**

Figure 6.2 illustrates tetralin yield over four different catalyst samples. The trends in tetralin yield are very similar to that of naphthalene conversion as this compound is the first product of naphthalene hydrogenation. NiMo/Alumina and Ni/HY showed better yield over 6 h TOS compared to Co/ZSM-5. During this time, tetralin yield decreased from 76% to 48% over NiMo/alumina catalyst while for Ni/HY catalyst sample, it slightly decreased from 60% to 55%.

Co/Silica exhibited high selectivity to tetralin during the first 2 h of the reaction; however, it declined significantly from 74% to 20% after 2 h TOS and then gradually decreased to 16%. Co/ZSM-5 exhibited lowest tetralin yield started from 23% and then decreased to 15% over 6h reaction time. Such low yield can be related to the small pores of ZSM-5 zeolite for hydrogenation of bulky naphthalene molecules. As it was discussed in Chapter 2 (Section 2.2.2) that HY zeolite is categorised as large pore zeolites with a three-dimensional 12-member rings channel (0.74 nm) and large internal cavities (1.3 nm). ZSM-5 zeolite with 10-member rings (0.53 × 0.56 nm) falls into the medium pore size group.

Schmitz et al., (1996) studied shape-selectivity of two types of zeolite (HM and HY) as support, impregnated by Pt for hydrogenation of naphthalene. They observed that Pt/HY catalyst exhibits higher selectivity to tetralin compare to Pt/HM with smaller pore size.
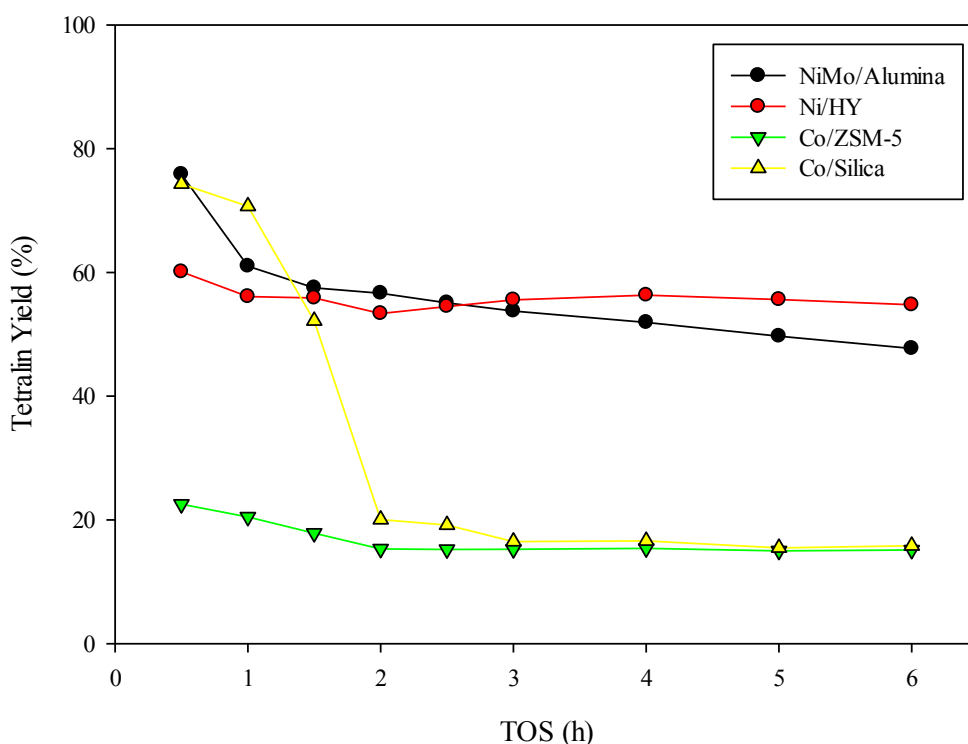
Figure 6.2. Yield of tetralin for different catalyst samples; Temperature: 300ºC, pressure: 60 bar, WHSV: 14 h^{-1}, feed: naphthalene in cyclohexane (50/50 wt./wt.), H$_2$/naphthalene: 0.136 mol.mol^{-1}.

6.1.3 **Trans- and cis-decalin yield**

Figure 6.3 shows the yield to trans- and cis-decalin for different catalyst samples under typical reaction conditions.
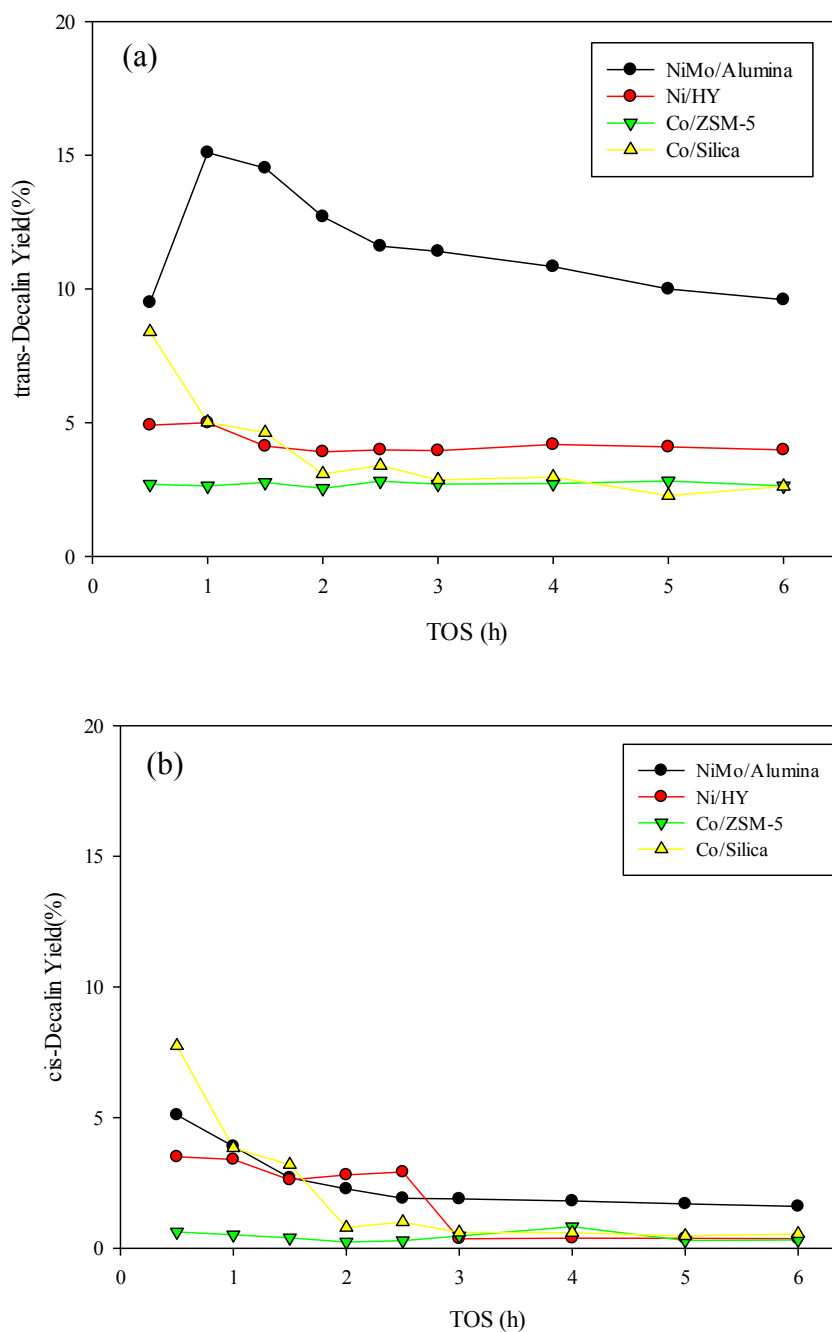
Figure 6.3. Yield of (a) trans-decalin and (b) cis-decalin for different catalysts; Temperature: 300ºC, pressure: 60 bar, WHSV: 14 h^{-1}, feed: naphthalene in cyclohexane (50/50 wt./wt.), H_2/naphthalene: 0.136 mol.mol^{-1}.

Generally, yield to trans-decalin is higher than cis-decalin for all catalysts. NiMo/Alumina catalyst exhibited higher yield to trans-decalin compared to other samples which starts from 15% on 1 h TOS and decreased to 10% after 6 h TOS. At the same time more stability in cis-decalin yield was observed for this catalyst which started from 5% and gradually decreased to 2%. Ni/HY exhibited ca. 5% yield to trans-decalin while yield of cis-decalin was about 4% during the first 2.5 h TOS and it decreased to less than 1% after this time. Co/ZSM-5 had the lowest yield ca. 3% to trans-decalin and less than 1% to cis-decalin during 6 h TOS.

At the beginning of the reaction, Co/Silica showed highest yield to cis-decalin (8%), but it decreased to less than 1% after 2 h and remained almost constant. Yield to trans-decalin started from 8% and decreased to 3% after 6 h TOS. Figure 6.4 illustrates the mechanism for hydrogenation of naphthalene to decalin and tetralin isomers proposed by Huang and Kang (1995). They reported k values and activation energy at different temperature and pressures. Table 6.1 lists the calculated values for hydrogenation of naphthalene over Pt/Al$_2$O$_3$ at 240 °C and 52 bar, based on proposed mechanism. These results suggest that the hydrogenation of tetralin to cis-decalin is faster than hydrogenation of tetralin to trans-decalin. From the other side, isomerisation of cis- to trans-decalin is carried out at lower rate.

Table 6.1. k values and activation energies for hydrogenation of tetralin to cis-/trans-decalin over Pt/Al$_2$O$_3$ catalyst at 240 °C and 52 bar.

k_2 (h^{-1})	k_3 (h^{-1})	k_4 (h^{-1})	$E_{a,2}$ (kcal/mol)	$E_{a,3}$ (kcal/mol)	$E_{a,4}$ (kcal/mol)
11.08	3.13	1.60	9.88	7.25	14.75

Although, cis-decalin is produced with higher reaction rate (kinetically favoured product), the trans-decalin is energetically more stable due to fewer steric interactions (thermodynamically favoured product).
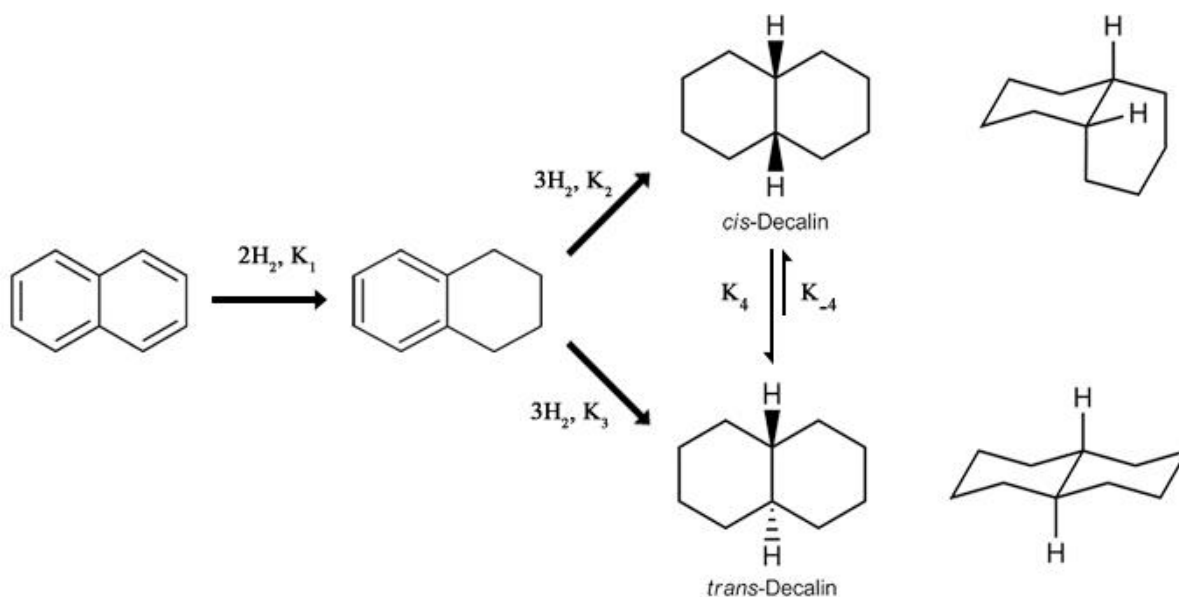
Figure 6.4. Reaction mechanism for hydrogenation of naphthalene and decalin (Huang and Kang, 1995).

According to Rocha et al., (2008), in hydrogenation of tetralin to decalin, the selectivity for the hydrogenation of double-bonds is to cis isomer, because at first, the hydrogen attack to the double-bond must occur from the same side of the molecule, i.e., the side that is facing the catalyst surface. Weitkamp (1968) explains that the formation of the trans-decalin in hydrogenation of tetralin requires the formation of a Δ1,9-octalin olefinic intermediate, which is formed during tetralin hydrogenation or cis-decalin dehydrogenation with the hydrogen in position 10 pointing down to the surface. Therefore, for formation of trans-decalin, it is necessary that this intermediate desorbs and re-adsorbs from the surface of the catalyst, so that the hydrogen in position 10 becomes oriented in a direction away from the surface.

Schmitz et al., (1996) showed that zeolite acid character can significantly influences the trans- or cis- selectivity as well as cis-isomerisation. They found that catalysts based on HM with small pores give the highest trans-decalin selectivity while HY zeolite based catalyst with bigger pore size shows better selectivity to cis-decalin isomer.

Corma et al., (2001) indicate that the pore size of zeolites influences the isomer product distribution, while the acidity and temperature do not affect the selectivity of isomerisation. Comparing four different catalyst samples, it can be concluded that Ni/HY sample showed better cis-/trans- selectivity during the first 2.5 h of the reaction, however this selectivity dropped significantly after this time, probably due the blockage of pore channels. It suggests that by modifying the acid sites or the metal loading, it is possible to prolong the catalyst lifetime so it can be used for selective hydrogenation of tetralin to cis-decalin. Although, NiMo/Alumina showed better yield to both isomers, the cis-/trans- ratio is small. This catalyst can be used when selectivity to trans isomer is desirable. Low yield to both cis and trans isomers observed over Co/ZSM-5. Thus this catalyst with small pore channels is not recommended for selective production of tran- or cis-decalin.

Co/Silica exhibited good yield to both isomers with high cis-/trans- ratio in the beginning of the reaction, however it dropped noticeably during the reaction probably due the rapid coking of cobalt metal crystals and/or hydrothermal degradation of the catalyst to form silicates.

6.2   Catalyst characterisation

6.2.1   TPR

The TPR profile of Ni/HY catalyst sample is shown in Figure 6.5. Three distinct peaks related to reduction of nickel can be observed at temperatures of 200, 300 and 365 ºC, respectively. Peaks at 200 and 365 ºC are attributed to the reduction of Ni^{2+} species located in the sodalite and hexagonal cavities respectively, while the peak with T_{max} at 300 ºC can be attributed to the reduction of NiO particles having no interaction with the support (Xu and Wang, 2005). Interaction of NiO with the support decreases its reducibility (Kirumakki et al., 2006) thus the peak at 365 ºC implies the presence of NiO species having strong interaction with HY zeolite.
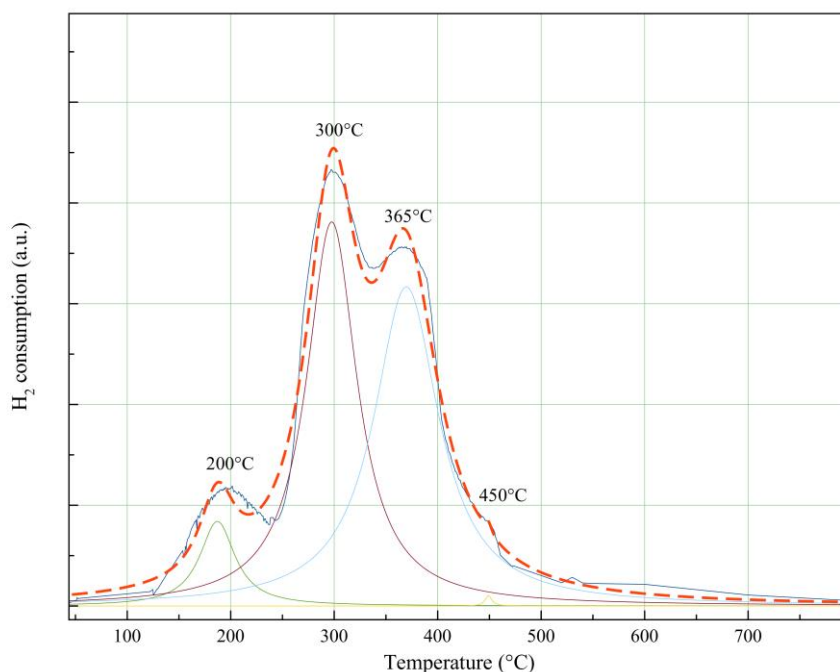
Figure 6.5 TPR profile of Ni/HY sample.

Figure 6.6 shows the TPR pattern of Co/Silica catalyst. Three peaks for cobalt reduction can be observed at temperatures of 180 ºC, 410 ºC and 490 °C, respectively.

It is known that bulk Co_3O_4 is completely reduced in two steps, the first one in the range of 200-300ºC for reduction of Co^{3+} to Co^{2+} and second one in the range of 300-450 ºC for reduction

of CoO to metallic cobalt (Wang et al., 2004, Li et al., 2012, Jong and Cheng, 1995). However, the TPR profile of Co_3O_4 supported on mesoporous silica typically shows three peaks. The first peak at lower temperature is due to the reduction of Co^{3+} to Co^{2+}, the second peak at higher temperature (less than 500 ºC) is ascribed to the reduction of Co^{2+} to Co^0 and an additional third peak at above 600 °C which is attributed to the reduction of cobalt species with strong metal–support interactions (Oliveira et al., 2012). Maia et al. (2010) also showed that reduction temperature for transition metals which are located inside the zeolite channel is higher than that located on external surface of the zeolite.
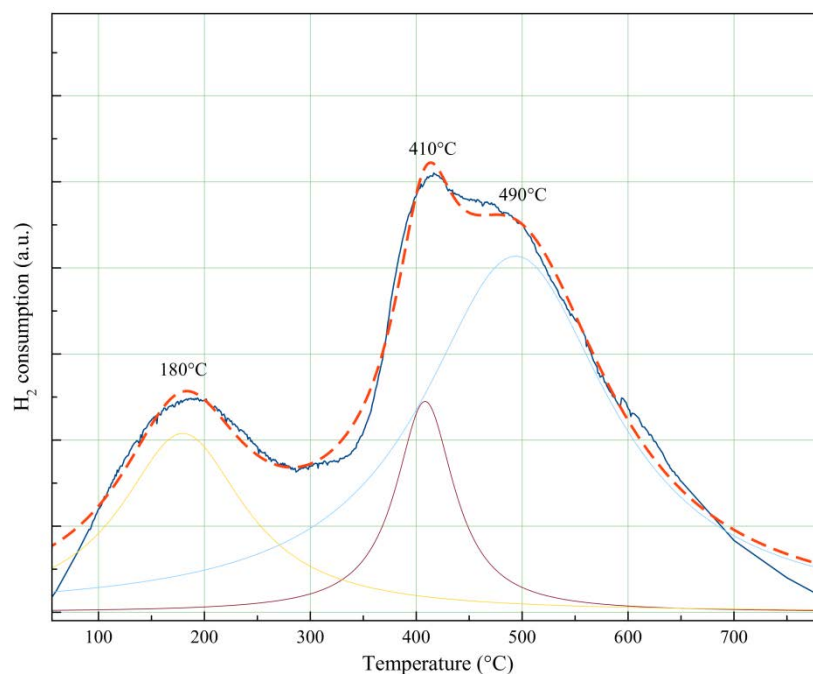
Figure 6.6. TPR profile of Co/Silica sample.

Wang and Chen (1991) observed that as the cobalt loading in a Co/Silica supported catalyst is increased, a peak starts to appear at around 550 ºC and shifts to 450 ºC. Moreover, the area of the related peak is increased by increasing the cobalt loading. They conclude that the peak location and the area related to that is proportional to the crystal size, location of the metal and the amount of metal loaded on the support. Therefore, the peak at 180 ºC in TPR profile of Co/Silica sample can be related to the reduction of free Co_3O_4 on the extra-framework of the

zeolite and the peak at 410 ºC can be assigned to the reduction of CoO inside the pores to metallic cobalt. Finally, the peak at 490 ºC can be assigned to the reduction of stronger Co-Si bonds.
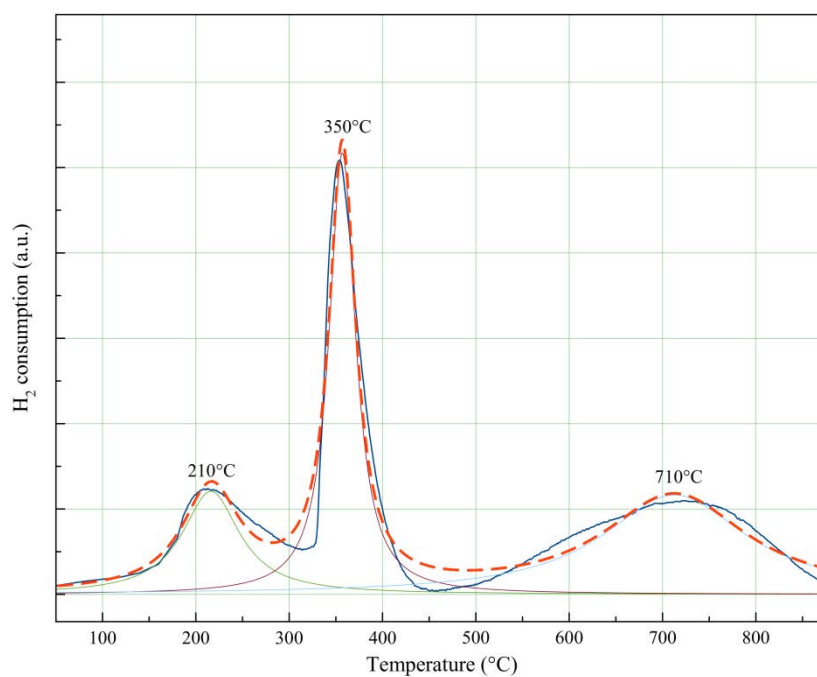
Figure 6.7. TPR profile of Co/ZSM-5 sample.

The TPR spectrum of Co/ZSM-5 catalyst sample is shown in Figure 6.7. Similar to Co/Silica samples, three peaks are observed during reduction of the sample. The first peak at 210 ºC is related to transition of Co_3O_4 to CoO and the second peak at 350 ºC is assigned to subsequent transition of CoO to metallic cobalt on the ZSM-5 zeolite and the third peak at 710 ºC is due to the reduction of strong cobalt-silicate species. Jong and Cheng (1995) studied the reduction behaviours and catalytic properties of cobalt containing ZSM-5 zeolites prepared by precipitating cobalt oxide onto ZSM-5 in alkaline solution. They observed three peaks in the TPR profile of catalyst. Two small peaks at 230 ºC, and 830 ºC and one sharp peak at 700 ºC. They explain that the peak at 230 ºC is due to the reduction of extra-framework cobalt oxide while the two peaks at 700 and 830 ºC correspond to two types of cobalt silicates, which were formed by cobalt ions reacting with the ZSM-5 framework in the precipitation impregnation

process. They conclude that any cobalt silicates that were formed during the precipitation-impregnation process require temperatures higher than 700 ºC for reduction.
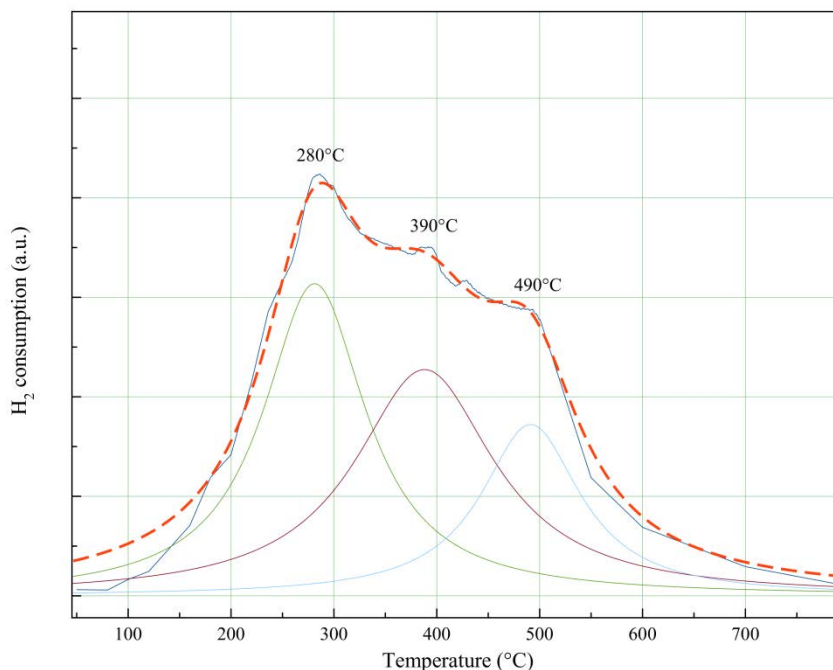
Figure 6.8. TPR profile of NiMo/Alumina sample.

Figure 6.8 shows the TPR profile of commercial NiMo/Alumina catalyst. Three peaks at temperature of 280 ºC, 390 ºC and 490 ºC can be observed. The first peak at 280 ºC can be ascribed to the partial reduction ($Mo^{6+} \rightarrow Mo^{4+}$) of amorphous, multi-layered Mo oxides or hetero-poly-molybdates octahedral Mo species (Qu et al., 2003). The peak at 390 ºC corresponds to reduction of Ni and the peak at 490 ºC comprises the reduction of all Mo species, including highly dispersed tetrahedral Mo species. It has been reported that the presence of nickel in the catalyst can promote the reduction of the Mo species, without changing the nature of MoO_3 (Brito and Laine, 1986). Qu et al. (2003) have shown that addition of Ni to Mo/Alumina catalyst can promote the reducibility of Mo and the peaks related to the reduction of Mo are shifted by 50 ºC to lower temperatures. A possible role of Ni in enhancing the Mo reducibility is due to facilitated hydrogen activation (i.e. decomposition of H_2 to atomic

hydrogen and migration to poly-molybdates). Table 6.2 lists the composition of catalyst samples measured by XRF.

Table 6.2. Elemental analysis of catalyst samples

Catalyst Name / Element	NiMo/ Alumina	Ni/HY	Co/ZSM-5	Co/Silica
Si	3.7	17.2	20	38.3
Al	20.3	19.2	21.5	0.1
Co	-	-	8.5	8.9
Ni	7.7	13.3	-	-
Mo	27	-	-	-
Na	0.7	1.3	0.7	1
S	0.7	2.9	1	1.3
O	39	45	47	49
Other elements[*]	0.9	1.1	1.3	1.4

[*] Other elements include Ca, K, P, Ce,V, Ti, Cl, Mg, La, Ba

6.2.2 XRD analysis

The XRD pattern of different catalyst samples are shown in Figure 6.9. These results are compared based on the type of active metal (e.g. Co/Silica and Co/ZSM-5). For the Co/Silica catalyst, a wide peak at $2\theta = 22°$ corresponds to SiO_2 crystals while for the Co/ZSM-5 catalyst, peaks corresponding to $2\theta = 24, 30$ and $47°$ are the typical ZSM-5 zeolite peaks (Figure 5.8 in Chapter 5). Peaks corresponding to the cobalt and cobalt oxide species, as well as peaks related to interaction between support and cobalt appear at the $2\theta = 31, 37, 45, 60$ and $66°$ (Rojanapipatkul and Jongsomjit, 2008, Li et al., 2010b). In this case, peaks at 2θ around 30 and 45 for Co/ZSM-5 catalyst sample may overlap.

Li et al., (2010b) have shown that depending on the cobalt precursor, some of these peaks may disappear due to the small size of cobalt oxide crystals which make them undetectable in XRD. For instance, using cobalt (II) nitrate as precursor may lead to a catalyst with large Co_3O_4 particles while using cobalt (II) acetate or cobalt(II) acetylacetonate leads to a catalyst with finely dispersed metals on the support.
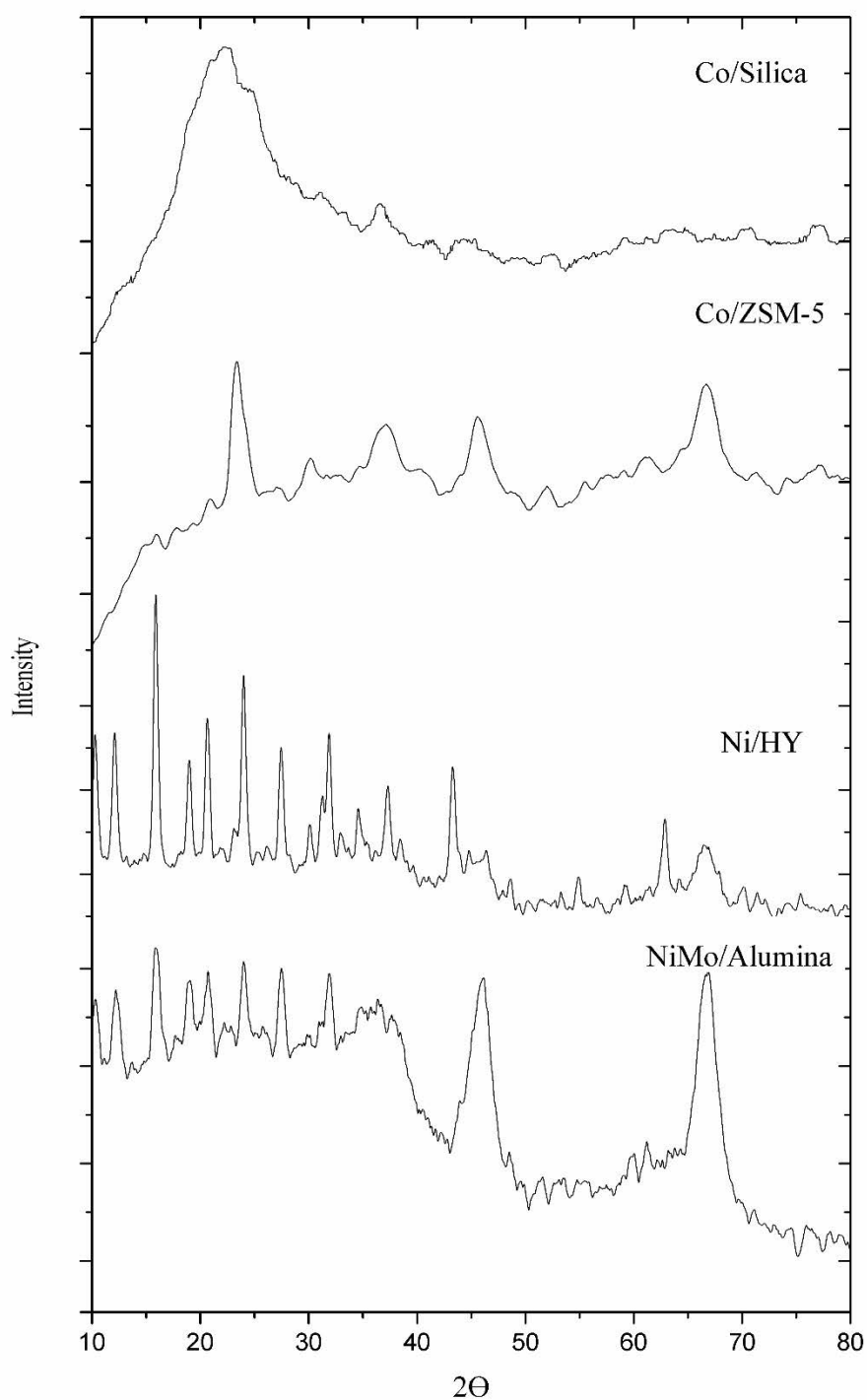
Figure 6.9. XRD spectra of different catalyst samples.

Thus, to calculate the average crystal size, the Scherrer equation is applied to the peaks at 2θ of 37 and 66. The calculated average crystal size is listed in Table 6.3. Small particle size of metals for Co/ZSM-5 sample is probably due to its small pores which can control to metal particle size during impregnation.

In the XRD pattern of Ni supported zeolite, NiO crystalline phases can be observed at $2\theta = 37$, 43, and 63° (Jeong et al., 2006, Li et al., 2010a). Thus, the average crystallite size was calculated by applying the Scherrer equation to these reflections.

Two distinct peaks related to alumina support are observed in the XRD spectra of NiMo/Alumina catalyst at $2\theta = 46$ and 67°. Very small peaks related to NiO crystalline phases can be observed at $2\theta = 37$, 43, and 63°, their small size being probably due to fine dispersion and lower amount of this metal on the support. Peaks at $2\theta = 24$, 28 and 32° are related to MoO_x species in the catalyst (Clark and Oyama, 2003) thus, these three peaks were used to measure the crystal size. Comparing catalyst conversion activity with the same metal and different particle sizes, there seem not to be any correlation between metal crystallite size and selectivity to decalin isomer. As a result, the overall reaction should be independent of metal particle size. This is in agreement with the observation of Schmitz et al., (1996).

6.2.3 N_2 adsorption-desorption isotherms

Nitrogen adsorption–desorption at 77 K was used to measure the BET surface area, micropore volume and micropore area. Figure 6.10 illustrates the nitrogen adsorption-desorption isotherms of different catalyst samples. All the samples show the characteristic of the typical reversible Type IV adsorption isotherms (defined by IUPAC). The hysteresis loop is associated with the capillary condensation of nitrogen in mesopores, and the limiting uptake over a range of high p/p_0 (Sing et al., 1985). This wider hysteresis loop for Co/Silica sample indicated its larger pores (172 Å).
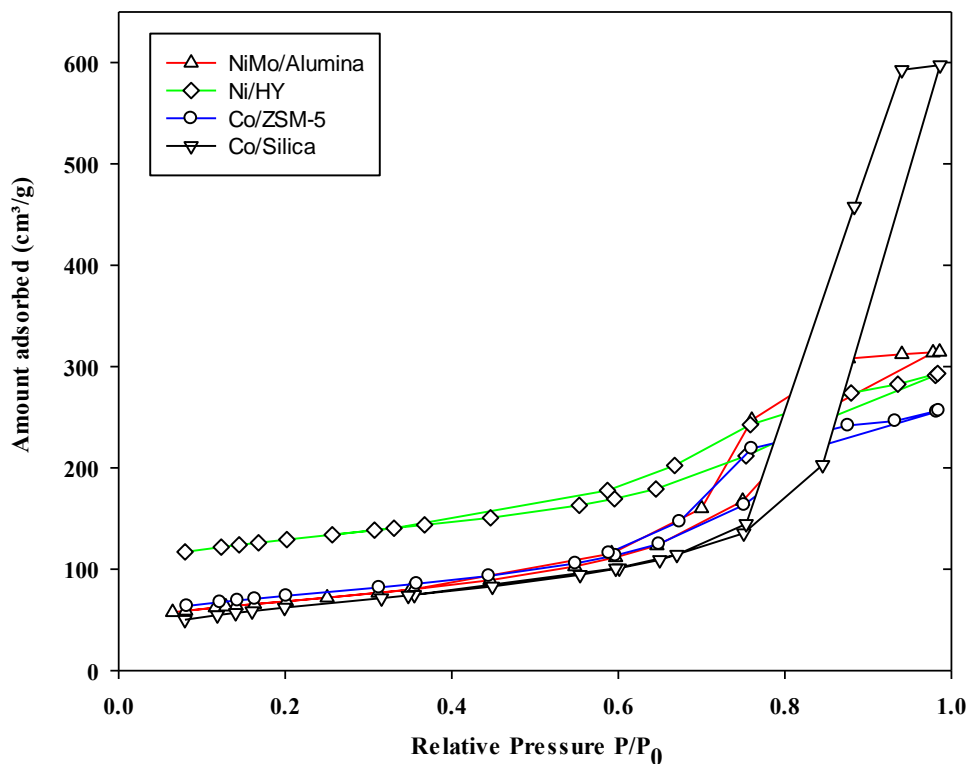
Figure 6.10. Nitrogen adsorption-desorption at 77 K for different catalyst samples.

Table 6.3 lists the physical properties of different catalyst samples. Ni/HY sample has the highest BET surface area, micropore volume and micropore area among the catalysts while the surface area of other samples is in the range of 230-278 $m^2.g^{-1}$. Co/Silica sample has the largest pore diameter and least micropore area and micropore volume compare to other samples.

Table 6.3. Physical properties of catalyst samples.

Catalyst name	BET surface area (m^2/g)	Metal crystal size (nm)	Pore diameter* (Å)	Micropore volume (cm^3/g)	Micropore area (m^2/g)
NiMo/Alumina	230	20.4	81	0.032	71
Ni/HY	445	34.0	40	0.105	228
Co/ZSM-5	260	8.4	61	0.034	75
Co/Silica	278	24.3	172	0.006	20

*Adsorption average pore diameter calculated from BET (4V/A)

The largest metal crystal size (34.0 nm) was observed over Ni/HY samples while the metal crystal size for the Co/ZSM-5 sample was the smallest (8.4 nm). The small crystal size of metals in Co/ZSM-5 catalyst or large metal crystal size for Ni/HY can be related to the size of zeolite pores which control the amount of metal incorporation during the catalyst impregnation (Moliner, 2012). As it was mentioned in section 6.2, it seems that larger pore size of silica as support can improve conversion by providing more space for bulky molecules to diffuse and react; however, rapid decrease in naphthalene conversion for this catalyst could be due to fast deactivation after 2 h either by covering the active metal sites and/or by pore blocking. Comparing two zeolite based catalyst, Ni/HY and Co/ZSM-5, it can be concluded that the small channels of ZSM-5 zeolite have been blocked during impregnation by metal crystallites.
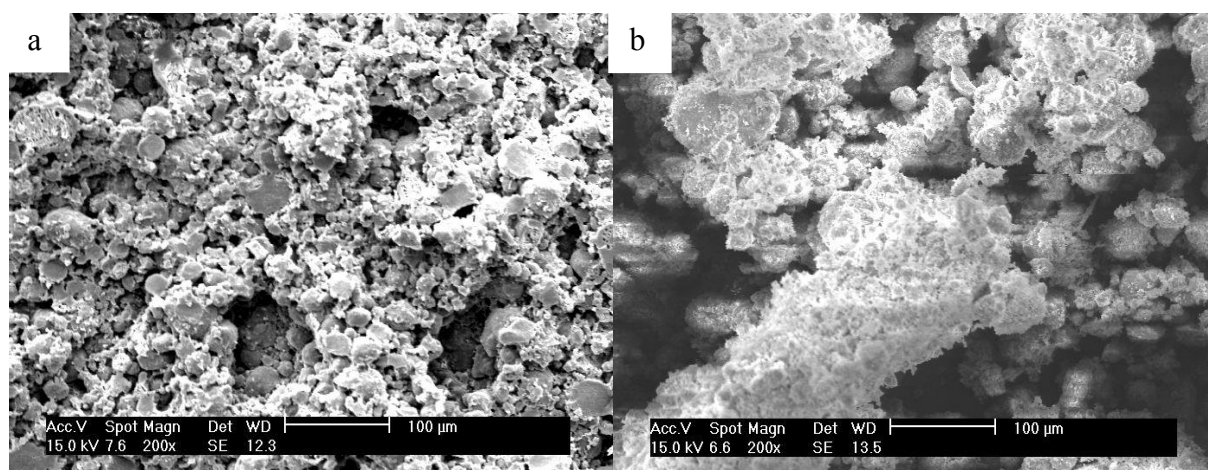
Figure 6.11. SEM image of a) Ni/HY and b) Co/ZSM-5 samples.

Figure 6.11 shows the SEM image of zeolite based catalyst samples (Ni/HY and Co/ZSM-5). No amorphous phase is observed on the SEM images for both zeolite based catalyst samples. For both samples small crystals as well as large crystals are observed. The big particles of alumina (Boehmite) are clearer on the SEM image of Co/ZSM-5 sample.

6.3   Coke characterisation

Coke deposition on the different catalyst samples was measured by TGA. Figure 6.12 shows the TGA curve of used catalysts after 6 h reaction. As it was mentioned in Chapter 3 (Section 3.4.6), the temperature ramp profile for TGA consists of four steps: 1) increasing the temperature from room temperature to 150 ℃ under air flow, 2) hold the sample at this temperature for 30 minutes to make sure all the physisorbed moisture is removed, 3) recording the mass change during increasing the temperature from 150 ℃ to 700 ℃ and 4) holding at this temperature for 15 min. This change was taken to account for the amount of deposited coke on the catalyst.

To better identify the temperature at which the deposited coke material are removed, the 1st derivative TGA curve (DTG) of used catalyst were plotted (Figure 6.13). The total amount of deposited coke on each sample, the DTG peak temperature and total acidity of each catalyst sample have been listed in Table 6.4. The highest amount of coke (5.4 wt.%) was observed over the Ni/HY catalyst with a maximum change at 560 ℃ although its total acidity is less than other samples (Table 6.4). Ardakani et al., (2007) studied hydrogenation of naphthalene over $Mo_2C/$ HY zeolite. They observed that using HY zeolite can improve the naphthalene conversion, but the conversion decreased very rapidly. They explained that the fast deactivation of the catalyst is due to coke formation which is a consequence of acid catalysed polymerisation reactions. They concluded that a moderate acidity is required to adjust the level of deactivation for this reaction.
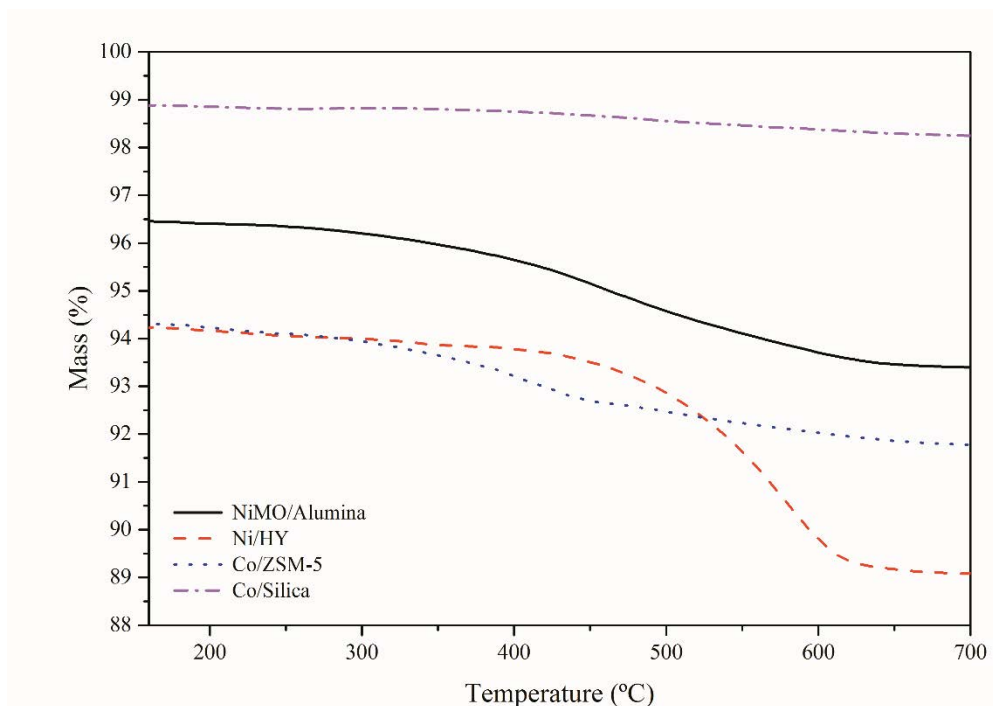
Figure 6.12. TGA profile of used catalyst after 6 h reaction.
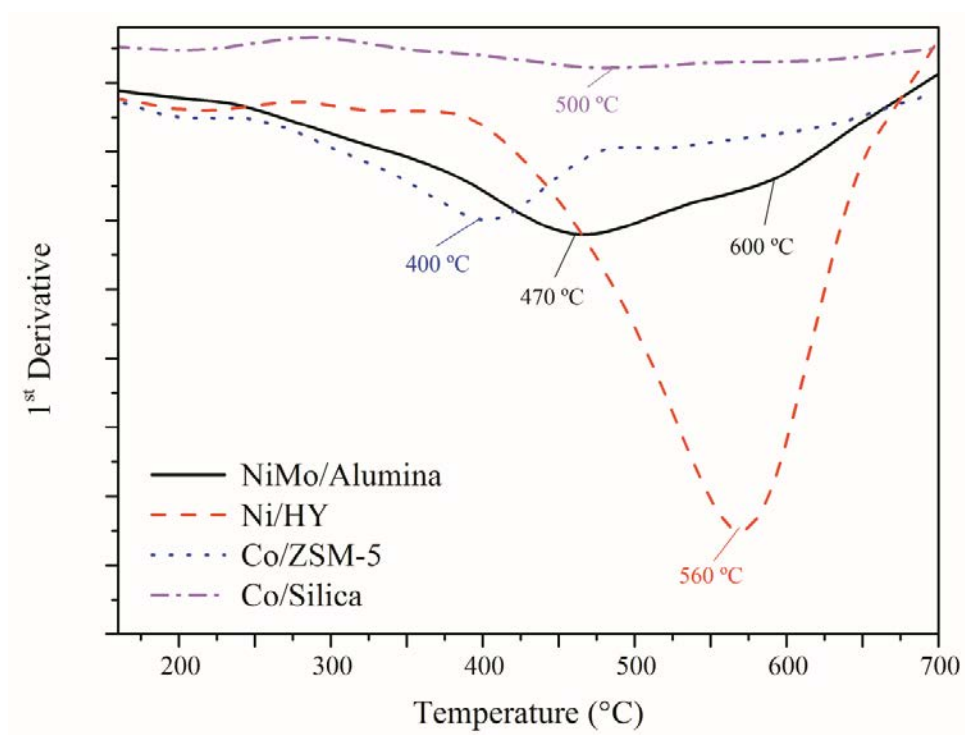
Figure 6.13. DTG profile of used catalyst after 6 h reaction

Venezia et al., (2004) studied the effect of acidity on the catalyst activity of amorphous silica-alumina during hydrogenation of naphthalene. They found that the coke formation is not in the order of total acidity strength and sometime catalyst with low acidity have high amount of coke on it. They interestingly observed that the catalyst with the highest activity (in spite of its large acidity) showed the lowest coke formation. They explained such observation by the fact that H-spillover in the hydrogenation of naphthalene not only enhances reaction rate but also decreases coke formation. Thus the amount of coke over Ni/HY sample can be due to its higher activity rather than its total acidity.

Table 6.4. TGA analysis of different catalyst samples after 6 h reaction

Catalyst name	NiMo/Alumina	Ni/HY	Co/ZSM-5	Co/Silica
Coke (wt.%)	3.2	5.4	3.2	0.8
1st Derivative peak(s) temperature (^{o}C)	470, 600	560	400	500
Total acidity (mmol t-BA/ g catalyst)	0.96	0.48	0.71	1.42

The overall amount of deposited coke over NiMo/Alumina and Co/ZSM-5 samples are same (3.2 wt.%), however, different peak temperature is an indication of different type of coke material over these two samples. The 1st derivative peak for Co/ZSM-5 is at 400 ^{o}C, while for NiMo/Alumina sample, two peaks at 470 ^{o}C and 600 ^{o}C imply on the two different coke materials with different chemical nature.

Co/Silica has the lowest amount of coking during 6 h TOS (0.8 wt.%) with DTG peak temperature at 500 ^{o}C. A lower amount of coke over this sample can be related to lower conversion activity of this catalyst during the reaction probably due to very small pore opening hindering the diffusion of bulky molecules to the pore channels.

6.4   Conclusion

Hydrogenation of naphthalene over two zeolite based catalyst Co/ZSM-5, Ni/HY were studied and results were compared with Co/Silica and NiMo/alumina catalyst. Ni/HY catalyst exhibited higher naphthalene conversion, longer life time and better selectivity to tetralin compared to Co/ZSM-5. After 6 h TOS, the activity of Ni/HY was still stable while the commercial NiMo/alumina catalyst showed some deactivation. Although Co/Silica catalyst showed high conversion during the first hour of the reaction, it decreased significantly after that time as a result of coke deposition on the surface of active metal particles which was facilitated by high catalyst acidity.

Ni/HY showed good selectivity to cis-decalin during the first 3 hours of the reaction; however this selectivity diminished after that time. The commercial NiMo/alumina performed better than the other catalysts studied with regard to selectivity to both cis- and tetra-decalin.

Finally, TGA/DTG analysis of used catalyst samples revealed a larger coke deposit on Ni/HY catalyst (in spite of its lower acidity) after 6 h TOS reaction compared to other catalysts. This confirms that the total amount of coke was not related to the total acidity of the catalyst but to the activity of catalyst in conversion of naphthalene.

Chapter 7 CONCLUSION AND FUTURE WORK RECOMMENDATION

7.1 Conclusion

The potential of using zeolite-based catalysts with environmentally benign nature, shape selectivity characteristic, well-defined microporous structure with pore sizes in the range of molecular dimensions and a flexible chemical composition for refinery, petrochemical and speciality chemical applications is rapidly expanding. In light of this, use of zeolite based catalyst for three important petrochemical processes such as alkylation of heavy aromatics, methanol to olefins and hydrogenation of heavy aromatics were studied.

In Chapter 4, the selective dialkylation of naphthalene to selectively produce 2,6-DIPN over modified zeolites was studied. Modified HY zeolites were found to be promising catalysts for this application. The effects of reaction conditions on the catalyst's activity and selectivity were studied and optimum conditions were reported. Maximum selectivity to DIPNs was achieved at 220 ºC and 1 bar. The results of reaction at higher pressure suggested that PIPNs as coke precursors are decreased in the supercritical region due to the higher diffusivity and solubility of the supercritical medium. An optimum WHSV of 18.8 h^{-1} and an isopropanol/naphthalene molar ratio of 4 was found as the most suitable value. HY zeolite was modified by transition metals (Fe, Co, Ni and Cu). It was found that modifying the zeolite significantly can change the total acidity of the parent zeolite as well as distribution of weak, medium and strong acid sites. Moreover, changes to the pore volume and BET surface area after zeolite modification can be related to the ionic radius of the transition metal. It was observed that modification of zeolite by Co and Cu increased the total acidity of the zeolite, and therefore, less improvement of

selectivity was observed on these catalysts. On the other hand, modification by Fe and Ni decreased the total acidity, and therefore enhanced selectivity was observed on these catalysts. Among the catalysts tested for this reaction, Fe-HY was found to be the best catalyst for a selective dialkylation of naphthalene with optimum strength acidic centres and larger pore volume.

In Chapter 5, effect of reaction temperature, pressure, space velocity and feed composition on the conversion of methanol to propene and light olefins was studied. Optimum temperature of 400 ℃ was found to yield more propene and light olefins. Higher temperatures led to faster deactivation and more selectivity to undesired sutured hydrocarbons (e.g. alkanes). Pressure higher than 1 bar led to production of heavier hydrocarbons (C_5^+) and lower selectivity to light olefins. It was shown that high water concentrations in the feed led to higher yields of light olefins. High space velocity is required to produce more light olefins, however, WHSV higher than 34 h^{-1} led to faster deactivation with no improvement in selectivity to light olefins. Use of γ-alumina as support improved the catalyst selectivity to light olefins. Zeolite catalyst with 25% wt. ZSM-5 in the catalyst sample led to highest selectivity to propene and light olefins, but faster deactivation was observed on this catalyst. ZSM-5 zeolite was modified with P, Cs, Ca and Fe. Modification in all cases increased the shape-selectivity to propene. ZSM-5 zeolite ion exchanged by Cs led to highest selectivity to propene by changing the acid site distribution. The lowest selectivity to heavy products (e.g. C_5^+ compounds) as well as lower amount of coking was observed on this catalyst.

In Chapter 6, hydrogenation of naphthalene was studied over two zeolite based catalyst (Co/ZSM-5, Ni/HY), one non-zeolite based catalyst (Co/Silica) and one commercial catalyst (NiMo/alumina). Among the samples, Ni/HY exhibited more stable and higher conversion activity.

Selectivity to tetralin and cis-decalin was better for this catalyst compared to Co/ZSM-5 catalyst sample. Co/Silica catalyst showed high naphthalene conversion during the first hour of the reaction, however, its activity decreased rapidly due to coke deposition on the surface of active metal particles. The commercial NiMo/alumina performed better than the other catalysts studied with regard to selectivity to both cis- and tetra-decalin.

The largest coke deposit was observed over Ni/HY catalyst, possibly due to its higher activity, although TPD analysis of this sample showed lower acidity strength. This confirms that the total amount of coke was not related to the total acidity of the catalyst but to the activity of catalyst in conversion of naphthalene.

7.2 Further investigation

The following are suggestions which would further extend the work presented in this thesis:

- Modification of zeolite by transition metal was studied in this work and it was shown that these metals can change the acid site distribution as well as pore size to increase the catalyst life time and improve selectivity to desired product. Modification using alkali metals and alkaline earth metals to tune the acid site distribution and weaken the strong acid sites is recommended as these metals can significantly change the acid site strength.

- Effect of metal loading over catalyst activity and selectivity can be studied and one can correlate the relation between metal loading, acid sites and selectivity.

- Metal loading on zeolite using wet impregnation method is a function of different mixing parameters. For example type of salt, temperature and duration of mixing, type of mixer (e.g. magnetic stirrer or ultrasonic bath), pH and salt concentration can influence the amount of metal loading as well as type of bond between metals and zeolite as support. Investigation on effect of these parameters on the metal loading and

its effect on the catalyst conversion activity, acidity and BET surface area is recommended. Using FT-IR to study the type of bond between metal oxide and the support is also informative.

- Using zeolite in powder form for industrial application is not useful or in some cases may be impossible; therefore, pelletising using a binder is required. Effect of using different microporous or mesoporous binders (e.g. alumina, silica, kaoline, etc.) to the catalyst activity is an interesting subject.

- Investigating the effect of metal particle size on the catalyst activity, selectivity and coking rate for these reactions is recommended. In this case, using different characterisation techniques (e.g. TEM, XRD and EXAFS) and comparing them can provide more accurate result.

References

Addiego, W. P., Brundage, K. R. and Glose, C. R. (2005) *Method of producing Alumina-Silica catalyst supports* Patent no. US 7,244,689 B2. [Online].

Aguayo, A. T., Gayubo, A. G., Ereña, J., Olazar, M., Arandes, J. M. and Bilbao, J. (1994) 'Isotherms of chemical adsorption of bases on solid catalysts for acidity measurement', *Journal of Chemical Technology & Biotechnology,* 60(2), pp. 141-146.

Aguayo, A. T., Gayubo, A. G., Tarrío, A. M., Atutxa, A. and Bilbao, J. (2002) 'Study of operating variables in the transformation of aqueous ethanol into hydrocarbons on an HZSM-5 zeolite', *Journal of Chemical Technology & Biotechnology,* 77(2), pp. 211-216.

Al-Jarallah, A. M., El-Nafaty, U. A. and Abdillahi, M. M. (1997) 'Effects of metal impregnation on the activity, selectivity and deactivation of a high silica MFI zeolite when converting methanol to light alkenes', *Applied Catalysis A: General,* 154(1-2), pp. 117-127.

Albertazzi, S., Rodríguez-Castellón, E., Livi, M., Jiménez-López, A. and Vaccari, A. (2004) 'Hydrogenation and hydrogenolysis/ring-opening of naphthalene on Pd/Pt supported on zirconium-doped mesoporous silica catalysts', *Journal of Catalysis,* 228(1), pp. 218-224.

Anand, R., Maheswari, R., Gore, K. U., Khaire, S. S. and Chumbhale, V. R. (2003) 'Isopropylation of naphthalene over modified faujasites: effect of steaming temperature on activity and selectivity', *Applied Catalysis A: General,* 249(2), pp. 265-272.

Anastas, P. and Eghbali, N. (2010) 'Green Chemistry: Principles and Practice', *Chemical Society Reviews,* 39(1), pp. 301-312.

Andersen, J. M. (2004) *Natural gas upgrading*.

Anthony, R. G. and Singh, B. B. (1980) 'KINETIC-ANALYSIS OF COMPLEX-REACTION SYSTEMS-METHANOL CONVERSION TO LOW-MOLECULAR WEIGHT OLEFINS', *Chemical Engineering Communications,* 6(4-5), pp. 215-224.

Ardakani, S. J., Liu, X. and Smith, K. J. (2007) 'Hydrogenation and ring opening of naphthalene on bulk and supported Mo2C catalysts', *Applied Catalysis A: General,* 324(0), pp. 9-19.

Arena, F., Dario, R. and Parmaliana, A. (1998) 'A characterization study of the surface acidity of solid catalysts by temperature programmed methods', *Applied Catalysis A: General,* 170(1), pp. 127-137.

Armengol, E., Corma, A., García, H. and Primo, J. (1997) 'Acid zeolites as catalysts in organic reactions. tert-Butylation of anthracene, naphthalene and thianthrene', *Applied Catalysis A: General,* 149(2), pp. 411-423.

Arunajatesan, V., Wilson, K. A. and Subramaniam, B. (2003) 'Pressure-Tuning the Effective Diffusivity of Near-critical Reaction Mixtures in Mesoporous Catalysts', *Industrial & Engineering Chemistry Research,* 42(12), pp. 2639-2643.

Author (2004)*: Test Methods for Rating Motor, Diesel, and Aviation Fuels; Catalysts; Manufactured Carbon and Graphite Products*. PA 19428-2959, United States.

Auerbach, S. M., Carrado, K. A. and Dutta, P. K. (2003) *Handbook of Zeolite Science and Technology.* Taylor & Francis.

Baerlocher, C., McCusker, L. B., Olson, D. A., Meier, W. M. and International Zeolite Association. Structure, C. (2007) *Atlas of zeolite framework types : Christian Baerlocher and Lynne B. McCusker, David H. Olson.* 6th rev. ed. edn. Amsterdam ;

London: Elsevier.

Bai, X., Sun, K., Wu, W., Yan, P. and Yang, J. (2009) 'Methylation of naphthalene to prepare 2,6-dimethylnaphthalene over acid-dealuminated HZSM-12 zeolites', *Journal of Molecular Catalysis A: Chemical,* 314(1-2), pp. 81-87.

Baiker, A. (1999) 'Supercritical Fluids in Heterogeneous Catalysis', *Chem Rev,* 99(2), pp. 453-474.

Bandiera, J. and Naccache, C. (1991) 'Kinetics of methanol dehydration on dealuminated H-mordenite: Model with acid and basic active centres', *Applied Catalysis,* 69(1), pp. 139-148.

Barrio, V. L., Arias, P. L., Cambra, J. F., Güemez, M. B., Pawelec, B. and Fierro, J. L. G. (2003) 'Aromatics hydrogenation on silica–alumina supported palladium–nickel catalysts', *Applied Catalysis A: General,* 242(1), pp. 17-30.

Bartholomew, C. H. (2001) 'Mechanisms of catalyst deactivation', *Applied Catalysis a-General,* 212(1-2), pp. 17-60.

Barthomeuf, D. (1987) 'Zeolite acidity dependence on structure and chemical environment. Correlations with catalysis', *Materials Chemistry and Physics,* 17(1-2), pp. 49-71.

Benito, P. L., Gayubo, A. G., Aguayo, A. T., Olazar, M. and Bilbao, J. (1996) 'Effect of Si/Al ratio and of acidity of H-ZSM5 zeolites on the primary products of methanol to gasoline conversion', *Journal of Chemical Technology & Biotechnology,* 66(2), pp. 183-191.

Berndt, H., Lietz, G., Lücke, B. and Völter, J. (1996) 'Zinc promoted H-ZSM-5 catalysts for conversion of propane to aromatics I. Acidity and activity', *Applied Catalysis A: General,* 146(2), pp. 351-363.

Berteau, P., Delmon, B., Dallons, J. L. and Van Gysel, A. (1991) 'Acid-base properties of silica-aluminas: use of 1-butanol dehydration as a test reaction', *Applied Catalysis,* 70(1), pp. 307-323.

Bibby, D. M., Howe, R. F. and McLellan, G. D. (1992) 'Coke formation in high-silica zeolites', *Applied Catalysis A: General,* 93(1), pp. 1-34.

Bibby, D. M., Milestone, N. B., Patterson, J. E. and Aldridge, L. P. (1986) 'Coke formation in zeolite ZSM-5', *Journal of Catalysis,* 97(2), pp. 493-502.

Blaszkowski, S. R. and van Santen, R. A. (1996) 'The Mechanism of Dimethyl Ether Formation from Methanol Catalyzed by Zeolitic Protons', *Journal of the American Chemical Society,* 118(21), pp. 5152-5153.

Bleken, F., Skistad, W., Barbera, K., Kustova, M., Bordiga, S., Beato, P., Lillerud, K. P., Svelle, S. and Olsbye, U. (2011) 'Conversion of methanol over 10-ring zeolites with differing volumes at channel intersections: comparison of TNU-9, IM-5, ZSM-11 and ZSM-5', *Physical Chemistry Chemical Physics,* 13(7), pp. 2539-2549.

Boréave, A., Auroux, A. and Guimon, C. (1997) 'Nature and strength of acid sites in HY zeolites: a multitechnical approach', *Microporous Materials,* 11(5–6), pp. 275-291.

Bouvier, C., Buijs, W., Gascon, J., Kapteijn, F., Gagea, B. C., Jacobs, P. A. and Martens, J. A. (2010) 'Shape-selective diisopropylation of naphthalene in H-Mordenite: Myth or reality?', *Journal of Catalysis,* 270(1), pp. 60-66.

Brito, J. and Laine, J. (1986) 'Characterization of supported MoO3 by temperature-programmed reduction', *Polyhedron,* 5(1–2), pp. 179-182.

Brzozowski, R. (2004) 'Shape-selectivity in diisopropylnaphthalene synthesis or analytical errors?', *Applied Catalysis A: General,* 272(1-2), pp. 215-218.

Brzozowski, R., Dobrowolski, J. C., Jamróz, M. H. and Skupinski, W. (2001) 'Studies on diisopropylnaphthalene substitutional isomerism', *Journal of Molecular Catalysis A: Chemical,* 170(1-2), pp. 95-99.

Brzozowski, R. and Vinu, A. (2009) 'Alkylation of Naphthalene Over Mesoporous Ga-SBA-1 Catalysts', *Topics in Catalysis,* 52(8), pp. 1001-1004.

Brzozowski, R., Vinu, A. and Gil, B. (2010) 'Comparison of the catalytic performance of the metal substituted cage type mesoporous silica catalysts in the alkylation of naphthalene', *Applied Catalysis A: General,* 377(1-2), pp. 76-82.

Caesar, P. D. and Morrison, R. A. (1978) *Process for manufacturing ethylene.* [Online].

Campanati, M., Fornasari, G. and Vaccari, A. (2003) 'Fundamentals in the preparation of heterogeneous catalysts', *Catalysis Today,* 77(4), pp. 299-314.

Carey, F. A. and Sundberg, R. J. (2007) *Advanced Organic Chemistry: Part A: Structure and Mechanisms.* Springer.

Čejka, J., Corma, A. and Zones, S. (2010) *Zeolites and Catalysis: Synthesis, Reactions and Applications.* John Wiley & Sons.

Chang, C. D., Chu, C. T. W. and Socha, R. F. (1984) 'Methanol conversion to olefins over ZSM-5: I. Effect of temperature and zeolite SiO2Al2O3', *Journal of Catalysis,* 86(2), pp. 289-296.

Chang, C. D., Lang, W. H. and Smith, R. L. (1979) 'The conversion of methanol and other O-compounds to hydrocarbons over zeolite catalysts: II. Pressure effects', *Journal of Catalysis,* 56(2), pp. 169-173.

Chang, C. D. and Silvestri, A. J. (1977) 'The conversion of methanol and other O-compounds to hydrocarbons over zeolite catalysts', *Journal of Catalysis,* 47(2), pp. 249-259.

Chen, C.-Y. and Zones, S. I. (2010) 'Post-Synthetic Treatment and Modification of Zeolites', *Zeolites and Catalysis*: Wiley-VCH Verlag GmbH & Co. KGaA, pp. 155-170.

Chen, G., Liang, J., Wang, Q., Cai, G., Zhao, S. and Ying, M. (1986) *New Developments in Zeolite Science and Technology. Studies in Surface Science and Catalysis*: Elsevier.

Chen, J., Wright, P. A., Natarajan, S. and Thomas, J. M. (1994a) 'Understanding The Brønsted Acidity of Sapo-5, Sapo-17, Sapo-18 and SAPO-34 and Their Catalytic Performance for Methanol Conversion to Hydrocarbons', in J. Weitkamp, H.G.K.H.P. & Hölderich, W. (eds.) *Studies in Surface Science and Catalysis*: Elsevier, pp. 1731-1738.

Chen, N. Y., Degnan, T. F. and Smith, C. M. (1994b) *Molecular Transport and Reaction in Zeolites: Design and Application of Shape Selective Catalysis.* John Wiley & Sons.

Chen, N. Y., Garwood, W. E. and Dwyer, F. G. (1989) *Shape selective catalysis in industrial applications.* M. Dekker.

Chen, N. Y. and Reagan, W. J. (1979) 'Evidence of autocatalysis in methanol to hydrocarbon reactions over zeolite catalysts', *Journal of Catalysis,* 59(1), pp. 123-129.

Cheng, Y., Fan, H., Wu, S., Wang, Q., Guo, J., Gao, L., Zong, B. and Han, B. (2009) 'Enhancing the selectivity of the hydrogenation of naphthalene to tetralin by high temperature water', *Green Chemistry,* 11(7), pp. 1061-1065.

Chu, S.-J. and Chen, Y.-W. (1995) 'Shape-selective alkylation of naphthalene with isopropanol over large pore zeolites', *Applied Catalysis A: General,* 123(1), pp. 51-58.

Clark, P. A. and Oyama, S. T. (2003) 'Alumina-supported molybdenum phosphide hydroprocessing catalysts', *Journal of Catalysis,* 218(1), pp. 78-87.

CMAI (2002) *World light olefins analysis*.

Collin, G. H., H. 1991. Naphthalene and Hydronaphthalenes. *Ullmann's Encyclopedia of Industrial Chemistry.* Verlag Chemie: Weinheim, Germany.

Colón, G., Ferino, I., Rombi, E., Selli, E., Forni, L., Magnoux, P. and Guisnet, M. (1998) 'Liquid-phase alkylation of naphthalene by isopropanol over zeolites. Part 1: HY zeolites', *Applied Catalysis A: General,* 168(1), pp. 81-92.

Corma, A. (2003) 'State of the art and future challenges of zeolites as catalysts', *Journal of Catalysis,* 216(1-2), pp. 298-312.

Corma, A., González-Alfaro, V. and Orchillés, A. V. (2001) 'Decalin and Tetralin as Probe Molecules for Cracking and Hydrotreating the Light Cycle Oil', *Journal of Catalysis,* 200(1), pp. 34-44.

Corma, A., Martinez, A. and MartinezSoria, V. (1997) 'Hydrogenation of aromatics in diesel fuels on Pt/MCM-41 catalysts', *Journal of Catalysis,* 169(2), pp. 480-489.

Csicsery, S. M. (1986) 'CATALYSIS BY SHAPE SELECTIVE ZEOLITES - SCIENCE AND TECHNOLOGY', *Pure and Applied Chemistry,* 58(6), pp. 841-856.

Dahl, I. and Kolboe, S. (1993) 'On the reaction mechanism for propene formation in the MTO reaction over SAPO-34', *Catalysis Letters,* 20(3-4), pp. 329-336.

Davis, M. E. E. and Davis, R. J. J. (2003) *Fundamentals of Chemical Reaction Engineering.* McGraw-Hill.

Davis, S. and Inoguchi, Y. (2009) *CEH Marketing Research Report: Zeolites*.

de Lucas, A., Canizares, P., Durán, A. and Carrero, A. (1997a) 'Coke formation, location, nature and regeneration on dealuminated HZSM-5 type zeolites', *Applied Catalysis A: General,* 156(2), pp. 299-317.

de Lucas, A., Canizares, P., Durán, A. and Carrero, A. (1997b) 'Dealumination of HZSM-5 zeolites: Effect of steaming on acidity and aromatization activity', *Applied Catalysis A: General,* 154(1–2), pp. 221-240.

Dehertog, W. J. H. and Froment, G. F. (1991) 'Production of light alkenes from methanol on ZSM-5 catalysts', *Applied Catalysis,* 71(1), pp. 153-165.

Derouane, E. G., Dejaifve, P., Gabelica, Z. and Vedrine, J. C. (1981) 'Molecular shape selectivity of ZSM-5, modified ZSM-5 and ZSM-11 type zeolites', *Faraday Discussions of the Chemical Society,* 72(0), pp. 331-344.

Deutschmann, O., Knözinger, H., Kochloefl, K. and Turek, T. (2000) 'Heterogeneous Catalysis and Solid Catalysts', *Ullmann's Encyclopedia of Industrial Chemistry*: Wiley-VCH Verlag GmbH & Co. KGaA.

Dogu, T. and Varisli, D. (2007) 'Alcohols as alternatives to petroleum for environmentally clean fuels and petrochemicals', *Turkish Journal of Chemistry,* 31(5), pp. 551-567.

Dondur, V., Rakic, V., Damjanovic, L. and Auroux, A. (2005) 'Comparative study of the active sites in zeolites by different probe molecules', *Journal of the Serbian Chemical Society*.

Dorta, R. L., Suárez, E. and Betancor, C. (1994) 'Triphenylbismuth dibromide-iodine: An efficient reagent for the dehydration of alcohols', *Tetrahedron Letters,* 35(28), pp. 5035-5038.

Du, M. X., Qin, Z. F., Ge, H., Li, X. K., Lu, Z. J. and Wang, J. G. (2010) 'Enhancement of Pd-Pt/Al2O3 catalyst performance in naphthalene hydrogenation by mixing different molecular sieves in the support', *Fuel Processing Technology,* 91(11), pp. 1655-1661.

Dubois, D. R., Obrzut, D. L., Liu, J., Thundimadathil, J., Adekkanattu, P. M., Guin, J. A., Punnoose, A. and Seehra, M. S. (2003) 'Conversion of methanol to olefins over cobalt-, manganese- and nickel-incorporated SAPO-34 molecular sieves', *Fuel Processing Technology,* 83(1-3), pp. 203-218.

Ertl, G., Knözinger, H., Schüth, F. and Weitkamp, J. (2008) *Handbook of Heterogeneous Catalysis, 8 Volumes*. Wiley.

Espinoza, R. L. (1986) 'Catalytic conversion of methanol to hydrocarbons: Autocatalysis reconsidered', *Applied Catalysis,* 26(0), pp. 203-209.

Farneth, W. E. and Gorte, R. J. (1995) 'Methods for Characterizing Zeolite Acidity', *Chemical Reviews,* 95(3), pp. 615-635.

Fernandes Machado, N. R. C., Calsavara, V., Astrath, N. G. C., Neto, A. M. and Baesso, M. L. (2006) 'Hydrocarbons from ethanol using [Fe,Al]ZSM-5 zeolites obtained by direct synthesis', *Applied Catalysis A: General,* 311(0), pp. 193-198.

Figueras, F., Nohl, A., de Mourgues, L. and Trambouze, Y. (1971) 'Dehydration of methanol and tert-butyl alcohol on silica-alumina', *Transactions of the Faraday Society,* 67(0), pp. 1155-1163.

Flanigen, E. (1984) 'Molecular Sieve Zeolite Technology: The First Twenty-Five Years', in Ribeiro, F.R., Rodrigues, A., Rollmann, L.D. & Naccache, C. (eds.) *Zeolites: Science and Technology NATO ASI Series*: Springer Netherlands, pp. 3-34.

Flanigen, E. M. (1980) 'MOLECULAR-SIEVE ZEOLITE TECHNOLOGY - THE 1ST 25 YEARS', *Pure and Applied Chemistry,* 52(9), pp. 2191-2211.

Forester, T. R. and Howe, R. F. (1987) 'In situ FTIR studies of methanol and dimethyl ether in ZSM-5', *Journal of the American Chemical Society,* 109(17), pp. 5076-5082.

Friedman, H. M. and Nelson, A. L. (1969) 'Alkylation of naphthalene with alkenes', *The Journal of Organic Chemistry,* 34(10), pp. 3211-3213.

Froment, G. F., Dehertog, W. J. H. and Marchi, A. J. (1992) 'Zeolite catalysis in the conversion of methanol into olefins', in Spivey, J.J. (ed.) *Catalysis: Volume 9*: The Royal Society of Chemistry, pp. 1-64.

Gayubo, A. G., Aguayo, A. T., Atutxa, A., Prieto, R. and Bilbao, J. (2004) 'Role of Reaction-Medium Water on the Acidity Deterioration of a HZSM-5 Zeolite', *Industrial & Engineering Chemistry Research,* 43(17), pp. 5042-5048.

Gayubo, A. G., Benito, P. L., Aguayo, A. T., Olazar, M. and Bilbao, J. (1996) 'Relationship between surface acidity and activity of catalysts in the transformation of methanol into hydrocarbons', *Journal of Chemical Technology & Biotechnology,* 65(2), pp. 186-192.

Gläser, R. and Weitkamp, J. (2003) 'Supercritical Carbon Dioxide as a Reaction Medium for the Zeolite-Catalyzed Alkylation of Naphthalene', *Industrial & Engineering Chemistry Research,* 42(25), pp. 6294-6302.

Gorte, R. J. (1999) 'What do we know about the acidity of solid acids?', *Catalysis Letters,* 62(1), pp. 1-13.

Goto, D., Harada, Y., Furumoto, Y., Takahashi, A., Fujitani, T., Oumi, Y., Sadakane, M. and Sano, T. (2010) 'Conversion of ethanol to propylene over HZSM-5 type zeolites containing alkaline earth metals', *Applied Catalysis A: General,* 383(1–2), pp. 89-95.

Gregg, S. J. and Sing, K. S. W. (1982) *Adsorption, Surface Area and Porosity.* 2nd edn.: Academic Press, p. 303.

Gubisch, D. and Bandermann, F. (1989) 'Conversion of methanol to light olefins over zeolite H-T', *Chemical Engineering & Technology,* 12(1), pp. 155-161.

Guenard, R. L., Fernández-Torres, L. C., Kim, B.-I., Perry, S. S., Frantz, P. and Didziulis, S. V. (2002) 'Selective surface reactions of single crystal metal carbides: alkene production from short chain alcohols on titanium carbide and vanadium carbide', *Surface Science,* 515(1), pp. 103-116.

Guisnet, M. and Magnoux, P. (1989) 'Coking and deactivation of zeolites: Influence of the Pore Structure', *Applied Catalysis,* 54(1), pp. 1-27.

Guo, H., Liang, Y., Qiao, W., Wang, G. and Li, Z. (2002) 'A study on alkylation of naphthalene with long chain olefins over zeolite catalyst', in R. Aiello, G.G. & Testa, F. (eds.) *Studies in Surface Science and Catalysis*: Elsevier, pp. 999-1006.

Guthrie, G. D. (1997) 'Mineral properties and their contributions to particle toxicity', *Environmental Health Perspectives,* 105, pp. 1003-1011.

Haag, W. O. (1994) 'Catalysis by Zeolites – Science and Technology', in J. Weitkamp, H.G.K.H.P. & Hölderich, W. (eds.) *Studies in Surface Science and Catalysis*: Elsevier, pp. 1375-1394.

Hagen, J. (2006) *Industrial Catalysis: A Practical Approach.* John Wiley & Sons.

Hajimirzaee, S., Ainte, M., Soltani, B., Behbahani, R. M., Leeke, G. A. and Wood, J. (2015) 'Dehydration of methanol to light olefins upon zeolite/alumina catalysts: Effect of reaction conditions, catalyst support and zeolite modification', *Chemical Engineering Research and Design,* 93(0), pp. 541-553.

Hajimirzaee, S., Leeke, G. A. and Wood, J. (2012) 'Modified zeolite catalyst for selective dialkylation of naphthalene', *Chemical Engineering Journal,* 207–208(0), pp. 329-341.

Hardacre, C., Katdare, P. S., Rooney, D. W. and Thompson, M. (2004) *Process utilising zeolites as catalysts/catalyst precursors*. The Queen's University of Belfast Patent no. EP1432511 A1. [Online].

Hassan, F. (2011) *Heterogeneous catalysis in supercritical fluids: the enhancement of catalytic stability to coking.* Ph.D., University of Birmingham [Online] Available at: http://etheses.bham.ac.uk/3166/ (Accessed.

Hattori, H. (1995) 'HETEROGENEOUS BASIC CATALYSIS', *Chemical Reviews,* 95(3), pp. 537-558.

Haw, J. F., Song, W. G., Marcus, D. M. and Nicholas, J. B. (2003) 'The mechanism of methanol to hydrocarbon catalysis', *Accounts of Chemical Research,* 36(5), pp. 317-326.

He, T., Wang, Y., Miao, P., Li, J., Wu, J. and Fang, Y. (2013) 'Hydrogenation of naphthalene over noble metal supported on mesoporous zeolite in the absence and presence of sulfur', *Fuel,* 106(0), pp. 365-371.

Hendriksen, E. D., Janssen, G. J. M. and Lattne, R. J. (2001) *Alkylation process using zeolite beta* Patent no. EP0929502 B1. [Online].

Hiyoshi, N., Inoue, T., Rode, C., Sato, O. and Shirai, M. (2006) 'Tuning cis-decalin selectivity in naphthalene hydrogenation over carbon-supported rhodium catalyst under supercritical carbon dioxide', *Catalysis Letters,* 106(3-4), pp. 133-138.

Horsley, J. A., Fellmann, J. D., Derouane, E. G. and Freeman, C. M. (1994) 'Computer-Assisted Screening of Zeolite Catalysts for the Selective Isopropylation of Naphthalene', *Journal of Catalysis,* 147(1), pp. 231-240.

Hsu, Y. S., Wang, Y. L. and Ko, A. N. (2009) 'Effect of Sulfation of Zirconia on Catalytic Performance in the Dehydration of Aliphatic Alcohols', *Journal of the Chinese Chemical Society,* 56(2), pp. 314-322.

Huang, T.-C. and Kang, B.-C. (1995) 'Kinetic Study of Naphthalene Hydrogenation over Pt/Al2O3 Catalyst', *Industrial & Engineering Chemistry Research,* 34(4), pp. 1140-1148.

Hunger, M. (2010) 'Catalytically Active Sites: Generation and Characterization', *Zeolites and Catalysis*: Wiley-VCH Verlag GmbH & Co. KGaA, pp. 493-546.

Inaba, M., Murata, K., Saito, M. and Takahara, I. (2007) 'Production of olefins from ethanol by Fe-supported zeolite catalysts', *Green Chemistry,* 9(6), pp. 638-646.

Inui, T. and Kang, M. (1997) 'Reliable procedure for the synthesis of Ni-SAPO-34 as a highly selective catalyst for methanol to ethylene conversion', *Applied Catalysis A: General,* 164(1–2), pp. 211-223.

irocks.com, R. L. (2008) *Mordenite*: Mindat.org. Available at: http://www.mindat.org/photo-157193.html 2010).

Ito, K., Kogasaka, Y., Kurokawa, H., Ohshima, M.-a., Sugiyama, K. and Miura, H. (2002) 'Preliminary study on mechanism of naphthalene hydrogenation to form decalins via tetralin over Pt/TiO2', *Fuel Processing Technology,* 79(1), pp. 77-80.

Ivanova, S., Lebrun, C., Vanhaecke, E., Pham-Huu, C. and Louis, B. (2009) 'Influence of the zeolite synthesis route on its catalytic properties in the methanol to olefin reaction', *Journal of Catalysis,* 265(1), pp. 1-7.

IZA (2001) *Clinoptilolite*: International Zeolite Association (IZA). Available at: http://www.iza-online.org/natural/Datasheets/Clinoptilolite/clinoptilolite.html.

Jeong, H., Kim, K. I., Kim, D. and Song, I. K. (2006) 'Effect of promoters in the methane reforming with carbon dioxide to synthesis gas over Ni/HY catalysts', *Journal of Molecular Catalysis A: Chemical,* 246(1–2), pp. 43-48.

Jiang, S., Hwang, J., Jin, T., Cai, T., Cho, W., Baek, Y. and Parkd, S. (2004) 'Dehydration of Methanol to Dimethyl Ether over ZSM-5 Zeolite', *Bulletin of the Korean Chemical Society,* 25(2), pp. 185-189.

Johnson-Matthey *Catalytic Reaction Guide to Hydrogenation of Aromatic Ring Compounds*: Johnson-Matthey Catalysis and Chiral Technologies. Available at: http://jmcct.com/catalytic-reaction-guide/aromatic-ring-compounds_s2.html.

Johnson-Matthey (2009) 'Handbook of pharmaceutical catalysis', pp. 108, Available: J&M Catalysts.

Jong, S.-J. and Cheng, S. (1995) 'Reduction behavior and catalytic properties of cobalt containing ZSM-5 zeolites', *Applied Catalysis A: General,* 126(1), pp. 51-66.

Jun, K. W., Lee, H. S., Roh, H. S. and Park, S. E. (2003) 'Highly water-enhanced H-ZSM-5 catalysts for dehydration of methanol to dimethyl ether', *Bulletin of the Korean Chemical Society,* 24(1), pp. 106-108.

Kadarwati, S., Wahyuni, S., Trisunaryanti, W. and Triyono, T. (2010) *PREPARATION, CHARACTERIZATION, AND CATALYTIC ACTIVITY TEST OF Ni-Mo/NATURAL ZEOLITE ON PYRIDINE HYDRODENITROGENATION. 2010*.

Kamalakar, G., Kulkarni, S. J., Raghavan, K. V., Unnikrishnan, S. and Halgeri, A. B. (1999) 'Isopropylation of naphthalene over modified HMCM-41, HY and SAPO-5 catalysts', *Journal of Molecular Catalysis A: Chemical,* 149(1-2), pp. 283-288.

Kamalakar, G., Prasad, M. R., Kulkarni, S. J. and Raghavan, K. V. (2002) 'Vapour phase tert-butylation of naphthalene over molecular sieve catalysts', *Microporous and Mesoporous Materials,* 52(3), pp. 151-158.

Kamalakar, G., Ramakrishna Prasad, M., Kulkarni, S. J., Narayanan, S. and Raghavan, K. V. (2000) 'Vapor phase ethylation of naphthalene with ethanol over molecular sieve catalysts', *Microporous and Mesoporous Materials,* 38(2-3), pp. 135-142.

Karge, H. G. (1997) 'Post-synthesis modification of microporous materials by solid-state reactions', in Chon, H., Ihm, S.K. & Uh, Y.S. (eds.) *Progress in Zeolite and Microporous Materials, Pts a-C Studies in Surface Science and Catalysis*. Amsterdam: Elsevier Science Bv, pp. 1901-1948.

Karge, H. G., Dondur, V. and Weitkamp, J. (1991) 'Investigation of the distribution of acidity strength in zeolites by temperature-programmed desorption of probe molecules. 2. Dealuminated Y-type zeolites', *The Journal of Physical Chemistry,* 95(1), pp. 283-288.

Katayama, A., Toba, M., Takeuchi, G., Mizukami, F., Niwa, S.-i. and Mitamura, S. (1991) 'Shape-selective synthesis of 2,6-diisopropylnaphthalene over H-mordenite catalyst', *Journal of the Chemical Society, Chemical Communications,* (1), pp. 39-40.

Keane, M. A. and Patterson, P. M. (1999) 'The Role of Hydrogen Partial Pressure in the Gas-Phase Hydrogenation of Aromatics over Supported Nickel', *Industrial & Engineering Chemistry Research,* 38(4), pp. 1295-1305.

Keil, F. J. (1999) 'Methanol-to-hydrocarbons: process technology', *Microporous and Mesoporous Materials,* 29(1-2), pp. 49-66.

Kim, J. H., Sugi, Y., Matsuzaki, T., Hanaoka, T., Kubota, Y., Tu, X. and Matsumoto, M. (1995) 'Effect of SiO2/Al2O3 ratio of H-mordenite on the propylation of naphthalene with propylene', *Microporous Materials,* 5(3), pp. 113-121.

Kim, S. D., Baek, S. C., Lee, Y. J., Jun, K. W., Kim, M. J. and Yoo, I. S. (2006) 'Effect of gamma-alumina content on catalytic performance of modified ZSM-5 for dehydration of crude methanol to dimethyl ether', *Applied Catalysis a-General,* 309(1), pp. 139-143.

Kirk, R. E. and Othmer, D. F. (1981) *Encyclopaedia of Chemical Technology.* New York: Wiley, p. 698.

Kirumakki, S. R., Shpeizer, B. G., Sagar, G. V., Chary, K. V. R. and Clearfield, A. (2006) 'Hydrogenation of Naphthalene over NiO/SiO2–Al2O3 catalysts: Structure–activity correlation', *Journal of Catalysis,* 242(2), pp. 319-331.

Kozo Tanabe, M. M. Y. O. and Hideshi, H. (1989) 'Acid and Base Centers: Structure and Acid-Base Property', *Studies in Surface Science and Catalysis*: Elsevier, pp. 27-213.

Kresnawahjuesa, O., Gorte, R. J., de Oliveira, D. and Lau, L. Y. (2002) 'A Simple, Inexpensive, and Reliable Method for Measuring Brønsted-Acid Site Densities in Solid Acids', *Catalysis Letters,* 82(3-4), pp. 155-160.

Krithiga, T., Vinu, A., Ariga, K., Arabindoo, B., Palanichamy, M. and Murugesan, V. (2005) 'Selective formation 2,6-diisopropyl naphthalene over mesoporous Al-MCM-48 catalysts', *Journal of Molecular Catalysis A: Chemical,* 237(1-2), pp. 238-245.

Kulprathipanja, S. (2010) *Zeolites in Industrial Separation and Catalysis.* Wiley.

Lancaster, M. (2002) *Green Chemistry: An Introductory Text.* Royal Society of Chemistry.

Lee, J. H., Hamrin Jr, C. E. and Davis, B. H. (1992) 'Catalytic conversion of alcohols and amines using metal nitride catalysts', *Catalysis Today,* 15(2), pp. 223-241.

Lercher, J. A. and Rumplmayr, G. (1986) 'Controlled decrease of acid strength by orthophosphoric acid on ZSM5', *Applied Catalysis,* 25(1–2), pp. 215-222.

Lersch, P. and Bandermann, F. (1991) 'Conversion of chloromethane over metal-exchanged ZSM-5 to higher hydrocarbons', *Applied Catalysis,* 75(1), pp. 133-152.

Li, J., Lu, G., Wu, G., Mao, D., Wang, Y. and Guo, Y. (2012) 'Promotional role of ceria on cobaltosic oxide catalyst for low-temperature CO oxidation', *Catalysis Science & Technology,* 2(9), pp. 1865-1871.

Li, J., Tian, W.-p. and Shi, L. (2010a) 'Hydrogenation of Maleic Anhydride to Succinic Anhydride over Ni/HY-Al2O3', *Industrial & Engineering Chemistry Research,* 49(22), pp. 11837-11840.

Li, N., Wang, X., Derrouiche, S., Haller, G. L. and Pfefferle, L. D. (2010b) 'Role of Surface Cobalt Silicate in Single-Walled Carbon Nanotube Synthesis from Silica-Supported Cobalt Catalysts', *ACS Nano,* 4(3), pp. 1759-1767.

Liang, J., Li, H. Y., Zhao, S., Guo, W. G., Wang, R. H. and Ying, M. L. (1990) 'CHARACTERISTICS AND PERFORMANCE OF SAPO-34 CATALYST FOR METHANOL-TO-OLEFIN CONVERSION', *Applied Catalysis,* 64(1-2), pp. 31-40.

Liu, J., Zhang, C. X., Shen, Z. H., Hua, W. M., Tang, Y., Shen, W., Yue, Y. H. and Xu, H. L. (2009) 'Methanol to propylene: Effect of phosphorus on a high silica HZSM-5 catalyst', *Catalysis Communications,* 10(11), pp. 1506-1509.

Liu, Z., Moreau, P. and Fajula, F. (1997) 'Liquid phase selective alkylation of naphthalene with t-butanol over large pore zeolites', *Applied Catalysis A: General,* 159(1-2), pp. 305-316.

Liu, Z. M., Sun, C. L., Wang, G. W., Wang, Q. X. and Cai, G. Y. (2000) 'New progress in R&D of lower olefin synthesis', *Fuel Processing Technology,* 62(2-3), pp. 161-172.

Lücke, B., Martin, A., Günschel, H. and Nowak, S. (1999) 'CMHC: coupled methanol hydrocarbon cracking: Formation of lower olefins from methanol and hydrocarbons over modified zeolites', *Microporous and Mesoporous Materials,* 29(1–2), pp. 145-157.

Luk'yanov, D. B. (1992) 'Effect of SiO2Al2O3 ratio on the activity of HZSM-5 zeolites in the different steps of methanol conversion to hydrocarbons', *Zeolites,* 12(3), pp. 287-291.

Lylykangas, M. S., Rautanen, P. A. and Krause, A. O. I. (2002) 'Liquid-phase hydrogenation kinetics of multicomponent axomatic mixtures on Ni/Al2O3', *Industrial & Engineering Chemistry Research,* 41(23), pp. 5632-5639.

Maheswari, R., Shanthi, K., Sivakumar, T. and Narayanan, S. (2003) 'Mesoporous molecular sieves: Part 1. Isopropylation of naphthalene over AlMCM-41', *Applied Catalysis A: General,* 245(2), pp. 221-230.

Maia, A. J., Louis, B., Lam, Y. L. and Pereira, M. M. (2010) 'Ni-ZSM-5 catalysts: Detailed characterization of metal sites for proper catalyst design', *Journal of Catalysis,* 269(1), pp. 103-109.

Marathe, R. P., Mayadevi, S., Pardhy, S. A., Sabne, S. M. and Sivasanker, S. (2002) 'Alkylation of naphthalene with t-butanol: use of carbon dioxide as solvent', *Journal of Molecular Catalysis A: Chemical,* 181(1-2), pp. 201-206.

Marchi, A. J. and Froment, G. F. (1991) 'Catalytic conversion of methanol to light alkenes on SAPO molecular sieves', *Applied Catalysis,* 71(1), pp. 139-152.

Marchi, A. J. and Froment, G. F. (1993) 'Catalytic conversion of methanol into light alkenes on mordenite-like zeolites', *Applied Catalysis A: General,* 94(1), pp. 91-106.

Marczewski, M., Bodibo, J. P., Perot, G. and Guisnet, M. (1989) 'Alkylation of aromatics: Part I. Reaction network of the alkylation of phenol by methanol on ushy zeolite', *Journal of Molecular Catalysis,* 50(2), pp. 211-218.

Martinez, C. and Corma, A. (2011) 'Inorganic molecular sieves: Preparation, modification and industrial application in catalytic processes', *Coordination Chemistry Reviews,* 255(13-14), pp. 1558-1580.

McKinney, M. L., Schoch, R. M. and Yonavjak, L. (2007) *Environmental Science: Systems And Solutions.* Jones & Bartlett Learning.

McMurry, J. (2011) *Fundamentals of Organic Chemistry.* Cengage Learning, p. 672.

Mehrotra, R. C. (2007) *Organometallic Chemistry.* New Age International (P) Limited.

Mei, C., Wen, P., Liu, Z., Liu, H., Wang, Y., Yang, W., Xie, Z., Hua, W. and Gao, Z. (2008) 'Selective production of propylene from methanol: Mesoporosity development in high silica HZSM-5', *Journal of Catalysis,* 258(1), pp. 243-249.

Meyers, R. (2004) *Handbook of Petrochemicals Production Processes.* McGraw-Hill Education.

Micromeritics (2003) 'Characterization of Acid Sites Using Temperature-Programmed Desorption (Application Note 134)', [Application Notes and Technical Tips].

Micromeritics (2008) 'Acid Site Characterization of HY (SiO2/Al2O3:30/1):A Pulse Chemisorption and TPD Application for the AutoChem (Application Note 145)', [Application Notes and Technical Tips].

Mingjin, Z., Anmin, Z., Feng, D., Yong, Y. and Chaohui, Y. (2003) 'Surface chemical modification of zeolites and their catalytic performance for naphthalene alkylation', *Science in China Series B: Chemistry,* 46(2), pp. 216-223.

Moliner, M. (2012) 'Direct Synthesis of Functional Zeolitic Materials', *ISRN Materials Science,* 2012, pp. 24.

Moreau, P., Finiels, A., Geneste, P., Moreau, F. and Solofo, J. 1992a. Shape-selective synthesis of 2,6-dicyclohexylnaphthalene over HY zeolites. *The Journal of Organic Chemistry.* American Chemical Society.

Moreau, P., Finiels, A., Geneste, P., Moreau, F. and Solofo, J. (1993) 'Comparative study of isopropoylation and cyclohexylation of naphthalene over zeolites: shape selective synthesis of a 2,6-dialkylnaphthalene', in M. Guisnet, J.B.J.B.C.B.D.D.G.P. & Montassier, C. (eds.) *Studies in Surface Science and Catalysis*: Elsevier, pp. 575-580.

Moreau, P., Finiels, A., Geneste, P. and Solofo, J. (1992b) 'Selective isopropylation of naphthalene over zeolites', *Journal of Catalysis,* 136(2), pp. 487-492.

Moreau, P., Liu, Z., Fajula, F. and Joffre, J. (2000) 'Selectivity of large pore zeolites in the alkylation of naphthalene with tert-butyl alcohol: analysis of experimental results by computational modelling', *Catalysis Today,* 60(3-4), pp. 235-242.

Mores, D., Kornatowski , J., Olsbye, U. and Weckhuysen, B. M. (2011) 'Coke Formation during the Methanol-to-Olefin Conversion: In Situ Microspectroscopy on Individual H-ZSM-5 Crystals with Different Brønsted Acidity', *Chemistry – A European Journal,* 17(10), pp. 2874-2884.

Nitta, M., Sakoh, H. and Aomura, K. (1984) 'The conversion of methanol into hydrocarbons over modified zirconia', *Applied Catalysis,* 10(2), pp. 215-217.

Oliveira, H. A., Franceschini, D. F. and Passos, F. B. (2012) 'Support effect on carbon nanotube growth by methane chemical vapor deposition on cobalt catalysts', *Journal of the Brazilian Chemical Society,* 23, pp. 868-879.

Ono, Y. and Mori, T. (1981) 'Mechanism of methanol conversion into hydrocarbons over ZSM-5 zeolite', *Journal of the Chemical Society, Faraday Transactions 1: Physical Chemistry in Condensed Phases,* 77(9), pp. 2209-2221.

Pál-Borbély, G. (2007) 'Thermal Analysis of Zeolites', in Karge, H. & Weitkamp, J. (eds.) *Characterization II Molecular Sieves*: Springer Berlin Heidelberg, pp. 67-101.

Papageorgiou, G. Z. and Karayannidis, G. P. (2001) 'Crystallization and melting behaviour of poly(butylene naphthalene-2,6-dicarboxylate)', *Polymer,* 42(6), pp. 2637-2645.

Park, J. W. and Seo, G. (2009) 'IR study on methanol-to-olefin reaction over zeolites with different pore structures and acidities', *Applied Catalysis A: General,* 356(2), pp. 180-188.

Parrillo, D. J., Adamo, A. T., Kokotailo, G. T. and Gorte, R. J. (1990) 'Amine adsorption in H-ZSM-5', *Applied Catalysis,* 67(1), pp. 107-118.

Pawelec, B., Mariscal, R., Navarro, R. M., van Bokhorst, S., Rojas, S. and Fierro, J. L. G. (2002) 'Hydrogenation of aromatics over supported Pt-Pd catalysts', *Applied Catalysis A: General,* 225(1–2), pp. 223-237.

Pena, J. A., Herguido, J., Guimon, C., Monzon, A. and Santamaria, J. (1996) 'Hydrogenation of acetylene over Ni/NiAl2O4 catalyst: Characterization, coking, and reaction studies', *Journal of Catalysis,* 159(2), pp. 313-322.

Pidko, E. A. (2008) *Chemical Reactivity of Cation-Exchanged zeolites.* PhD, Eindhoven University of Technology, The Netherlands.

Pramatha, P. and Prabir, D. (2003) 'Zeolites', *Handbook of Zeolite Science and Technology*: CRC Press.

Qian, L. and Yan, Z. F. (2001) 'Micropore modification of zeolites with transition-metal oxides', *Colloids and Surfaces A: Physicochemical and Engineering Aspects,* 180(3), pp. 311-316.

Qu, L., Zhang, W., Kooyman, P. J. and Prins, R. (2003) 'MAS NMR, TPR, and TEM studies of the interaction of NiMo with alumina and silica–alumina supports', *Journal of Catalysis,* 215(1), pp. 7-13.

Rautanen, P. A., Lylykangas, M. S., Aittamaa, J. R. and Krause, A. O. I. (2002) 'Liquid-phase hydrogenation of naphthalene and tetralin on Ni/Al2O3: Kinetic modeling', *Industrial & Engineering Chemistry Research,* 41(24), pp. 5966-5975.

Reddy, K. S. N., Rao, B. S. and Shiralkar, V. P. (1993) 'Alkylation of benzene with isopropanol over zeolite beta', *Applied Catalysis A: General,* 95(1), pp. 53-63.

Rewitzer, C. (2009) *Clinoptilolite-Na*: Mindat.org. Available at: http://www.mindat.org/photo-269082.html 2010).

Richardson, J. T. (1989) *Principles of Catalyst Development.* Springer.

Rocha, A. S., Moreno, E. L., da Silva, G. P. M., Zotin, J. L. and Faro Jr, A. C. (2008) 'Tetralin hydrogenation on dealuminated Y zeolite-supported bimetallic Pd-Ir catalysts', *Catalysis Today,* 133–135(0), pp. 394-399.

Roesky, P. W. and Cui, D. (2010) *Molecular Catalysis of Rare-Earth Elements.* Springer.

Rojanapipatkul, S. and Jongsomjit, B. (2008) 'Synthesis of cobalt on cobalt-aluminate via solvothermal method and its catalytic properties for carbon monoxide hydrogenation', *Catalysis Communications,* 10(2), pp. 232-236.

Rothenberg, G. (2008) *Catalysis : concepts and green applications.* Weinheim :: Wiley-VCH.

Rueping, M. and Nachtsheim, B. J. (2010) *A review of new developments in the Friedel-Crafts alkylation - From green chemistry to asymmetric catalysis.*

Sachtler, W. M. H. and Stakheev, A. Y. (1992) 'Electron-deficient palladium clusters and bifunctional sites in zeolites', *Catalysis Today,* 12(2–3), pp. 283-295.

Salzinger, M., Fichtl, M. B. and Lercher, J. A. (2011) 'On the influence of pore geometry and acidity on the activity of parent and modified zeolites in the synthesis of methylenedianiline', *Applied Catalysis A: General,* 393(1–2), pp. 189-194.

Sano, T., Kiyozumi, Y. and Shin, S. (1992) 'Synthesis of Light Olefins from Methanol Using ZSM-5 Type Zeolite Catalysts', *Journal of the Japan Petroleum Institute,* 35(6), pp. 429-440.

Santen, R. A. v. (1991) 'Concepts in Catalysis', *Theoretical Heterogeneous Catalysis*: World Scientific.

Scherrer, P. (1918) 'Determining the size and internal structure of colloidal particles by means of X-rays ', *Nachrichten Göttingen*, pp. 98-100.

Schmitz, A. D., Bowers, G. and Song, C. S. (1996) 'Shape-selective hydrogenation of naphthalene over zeolite-supported Pt and Pd catalysts', *Catalysis Today,* 31(1-2), pp. 45-56.

Schulz, H. (2010) 'Coking of zeolites during methanol conversion: Basic reactions of the MTO-, MTP- and MTG processes', *Catalysis Today,* 154(3–4), pp. 183-194.

Schulz, J. and Bandermann, F. (1994) 'Conversion of ethanol over zeolite H-ZSM-5', *Chemical Engineering & Technology,* 17(3), pp. 179-186.

Scott, R. B. (1970) 'Cancer chemotherapy - The first twenty-five years', *British Medical Journal,* 4(5730), pp. 259-265.

Shannon, R. (1976) 'Revised effective ionic radii and systematic studies of interatomic distances in halides and chalcogenides', *Acta Crystallographica Section A,* 32(5), pp. 751-767.

Sherrington, D. C., Kybett, A. P. and Chemistry, R. S. o. (2001) *Supported Catalysts and Their Applications.* Royal Society of Chemistry.

Sing, K. S. W., Everett, D. H., Haul, R. A. W. and Moscou, L. (1985) *Reporting physisorption data for gas/solid systems with special reference to the determination of surface area and porosity.*

Smith, K. and Roberts, S. D. (2000) 'Regioselective dialkylation of naphthalene', *Catalysis Today,* 60(3-4), pp. 227-233.

Smith, M. B. (2013) *March's Advanced Organic Chemistry: Reactions, Mechanisms, and Structure.* Wiley.

Song, C. and Kirby, S. (1994) 'Shape-selective alkylation of naphthalene with isopropanol over mordenite catalysts', *Microporous Materials,* 2(5), pp. 467-476.

Song, C., Ma, X., Schmitz, A. D. and Schobert, H. H. (1999) 'Shape-selective isopropylation of naphthalene over mordenite catalysts: Computational analysis using MOPAC', *Applied Catalysis A: General,* 182(1), pp. 175-181.

Song, C. S. and Schmitz, A. D. (1997) 'Zeolite-supported Pd and Pt catalysts for low-temperature hydrogenation of naphthalene in the absence and presence of benzothiophene', *Energy & Fuels,* 11(3), pp. 656-661.

Spivey, J. J., Roberts, G. W. and Davis, B. H. (2001) *Catalyst Deactivation 2001: Proceedings of the 9th International Symposium, Lexington, KY, USA, October 2001.* Elsevier Science.

Stocker, M. (1999) 'Methanol-to-hydrocarbons: catalytic materials and their behavior', *Microporous and Mesoporous Materials,* 29(1-2), pp. 3-48.

Suarez-Fernandez, G. P., Vega, J. M. G., Fuertes, A. B., Garcia, A. B. and Martínez-Tarazona, M. R. (2001) 'Analysis of major, minor and trace elements in coal by radioisotope X-ray fluorescence spectrometry', *Fuel,* 80(2), pp. 255-261.

Süd-Chemie (2014) *Süd Chemie India Catalysts.* Available at: http://www.sud-chemie-india.com/prod.htm 2014).

Sugi, Y. (2010) 'Shape-Selective Alkylation of Naphthalene over Zeolites: Steric Interaction of Reagents with Zeolites', *Journal of the Chinese Chemical Society,* 57(1), pp. 1-13.

Sugi, Y., Maekawa, H., Hasegawa, Y., Naiki, H., Komura, K. and Kubota, Y. (2008) 'The alkylation of naphthalene over three-dimensional large pore zeolites: The influence of zeolite structure and alkylating agent on the selectivity for dialkylnaphthalenes', *Catalysis Today,* 132(1-4), pp. 27-37.

Szostak, R. (2001) 'Chapter 6 Secondary synthesis methods', in H. van Bekkum, E.M.F.P.A.J. & Jansen, J.C. (eds.) *Studies in Surface Science and Catalysis*: Elsevier, pp. 261-297.

Travalloni, L., Gomes, A. C. L., Gaspar, A. B. and da Silva, M. A. P. (2008) 'Methanol conversion over acid solid catalysts', *Catalysis Today,* 133–135(0), pp. 406-412.

Treacy, M. M. J. and Higgins, J. B. (2007) 'FAU - Faujasite', *Collection of Simulated XRD Powder Patterns for Zeolites (fifth)*. Amsterdam: Elsevier Science B.V., pp. 166-167.

Tsakoumis, N. E., Ronning, M., Borg, O., Rytter, E. and Holmen, A. (2010) 'Deactivation of cobalt based Fischer-Tropsch catalysts: A review', *Catalysis Today,* 154(3-4), pp. 162-182.

UCIL (1984) *Statement of Union Carbide Corporation Regarding the Bhopal Tragedy*. Bhopal. Available at: http://www.bhopal.com/union-carbide-statements.

UOP (2011) *Expanding routes for olefins production: UOP olefins value chain*. Available at: www.uop.com/olefins-chain/.

Venezia, A. M., Parola, V. L., Pawelec, B. and Fierro, J. L. G. (2004) 'Hydrogenation of aromatics over Au-Pd/SiO2-Al2O3 catalysts; support acidity effect', *Applied Catalysis A: General,* 264(1), pp. 43-51.

Vollhardt, K. P. C. and Schore, N. E. (2007) *Organic Chemistry: Structure and Function.* W. H. Freeman.

Vu, D. V., Hirota, Y., Nishiyama, N., Egashira, Y. and Ueyama, K. (2010) 'High Propylene Selectivity in Methanol-to-olefin Reaction over H-ZSM-5 Catalyst Treated with Phosphoric Acid', *Journal of the Japan Petroleum Institute,* 53(4), pp. 232-238.

Wang, B. and Manos, G. (2007) 'A novel thermogravimetric method for coke precursor characterisation', *Journal of Catalysis,* 250(1), pp. 121-127.

Wang, C.-B., Lin, H.-K. and Tang, C.-W. (2004) 'Thermal Characterization and Microstructure Change of Cobalt Oxides', *Catalysis Letters,* 94(1-2), pp. 69-74.

Wang, J., Park, J.-N., Park, Y.-K. and Lee, C. W. (2003) 'Isopropylation of naphthalene by isopropyl alcohol over USY catalyst: an investigation in the high-pressure fixed-bed flow reactor', *Journal of Catalysis,* 220(2), pp. 265-272.

Wang, W., Jiang, Y. J. and Hunger, M. (2006) 'Mechanistic investigations of the methanol-to-olefin (MTO) process on acidic zeolite catalysts by in situ solid-state NMR spectroscopy', *Catalysis Today,* 113(1-2), pp. 102-114.

Wang, W. J. and Chen, Y. W. (1991) 'INFLUENCE OF METAL LOADING ON THE REDUCIBILITY AND HYDROGENATION ACTIVITY OF COBALT ALUMINA CATALYSTS', *Applied Catalysis,* 77(2), pp. 223-233.

Wang, Y., Xu, L., Yu, Z., Zhang, X. and Liu, Z. (2008) 'Selective alkylation of naphthalene with tert-butyl alcohol over HY zeolites modified with acid and alkali', *Catalysis Communications,* 9(10), pp. 1982-1986.

Weissermel, K. and Arpe, H. J. (2003) *Industrial Organic Chemistry.* Wiley-VCH.

Weitkamp, A. W. (1968) 'Stereochemistry and Mechanism of Hydrogenation of Naphthalenes on Transition Metal Catalysts and Conformational Analysis of the Products', in D.D. Eley, H.P. & Paul, B.W. (eds.) *Advances in Catalysis*: Academic Press, pp. 1-110.

Weitkamp, J. and Puppe, L. (1999) *Catalysis and Zeolites: Fundamentals and Applications.* Springer.

Wilson, S. and Barger, P. (1999) 'The characteristics of SAPO-34 which influence the conversion of methanol to light olefins', *Microporous and Mesoporous Materials,* 29(1-2), pp. 117-126.

Wu, W., Guo, W., Xiao, W. and Luo, M. (2013) 'Methanol conversion to olefins (MTO) over H-ZSM-5: Evidence of product distribution governed by methanol conversion', *Fuel Processing Technology,* 108(0), pp. 19-24.

Xavier, K. O., Chacko, J. and Mohammed Yusuff, K. K. (2004) 'Zeolite-encapsulated Co(II), Ni(II) and Cu(II) complexes as catalysts for partial oxidation of benzyl alcohol and ethylbenzene', *Applied Catalysis A: General,* 258(2), pp. 251-259.

Xu, M., Lunsford, J. H., Goodman, D. W. and Bhattacharyya, A. (1997) 'Synthesis of dimethyl ether (DME) from methanol over solid-acid catalysts', *Applied Catalysis A: General,* 149(2), pp. 289-301.

Xu, S. and Wang, X. (2005) 'Highly active and coking resistant Ni/CeO2–ZrO2 catalyst for partial oxidation of methane', *Fuel,* 84(5), pp. 563-567.

Yadav, G. D. and Salgaonkar, S. S. (2005) 'Alkylation of naphthalene with isopropanol over a novel catalyst UDCaT-4: Insight into selectivity to 2,6-diisopropylnaphthalene and its kinetics', *Applied Catalysis A: General,* 296(2), pp. 251-256.

Zhang, S., Zhang, B., Gao, Z. and Han, Y. (2010) 'Ca modified ZSM-5 for high propylene selectivity from methanol', *Reaction Kinetics, Mechanisms and Catalysis,* 99(2), pp. 447-453.

Zhao, T.-S., Takemoto, T. and Tsubaki, N. (2006) 'Direct synthesis of propylene and light olefins from dimethyl ether catalyzed by modified H-ZSM-5', *Catalysis Communications,* 7(9), pp. 647-650.

Appendices

Appendix A: Composition of calibration gas

Components	Quantity	Unit	Relative Accuracy (%)
HYDROGEN	1	%	0.5
METHANE	1	%	0.5
ETHANE	1	%	0.5
ETHYLENE	1	%	0.5
PROPANE	1	%	0.5
PROPYLENE	1	%	0.5
ISOBUTANE	1	%	0.5
N-BUTANE	1	%	0.5
1-BUTENE	1	%	0.5
TRANS-2-BUTENE	1	%	0.5
CIS-2-BUTENE	1	%	0.5
N-PENTANE	1	%	0.5
ISOPENTANE	1	%	0.5
CARBON DIOXIDE	3	%	0.5
CARBON MONOXIDE	4	%	0.5
NITROGEN	80	%	0.5

Appendix B: GC analysis of naphthalene alkylated products

The peaks for isopropylnaphthalene (IPN(in this figure show some overlap and therefore the IPNs were integrated as a group and the IPNs are reported as overall fraction of the product. The 2,6 and 2,7 DIPNs show a slight overlap of the peaks detected.
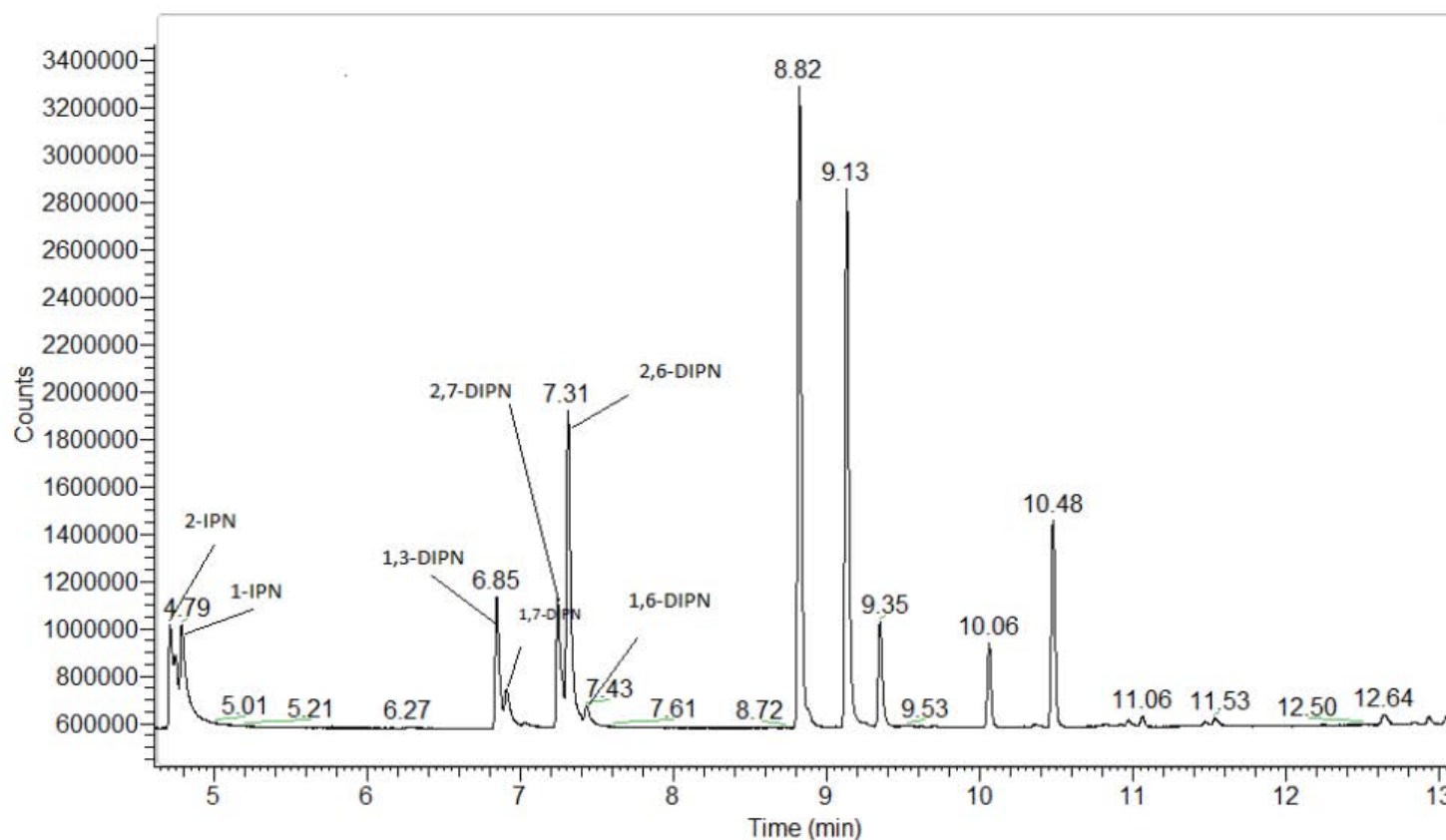
Figure A. 1. Gas chromatography trace showing peak separation of DIPN and other isomers as labelled. Sample conditions T=220 °C, P=50 bar, Catalyst= HY zeolite, TOS= 6 h,WHSV=18.8 h^{-1}, isopropanol/naphthalene= 4 (molar ratio).

Time	Compound
9.93	Naphthalene
16.85	1-Isopropylnaphthalene
16.95	2-Isopropylnaphthalene
21.81	1,3-Siisopropylnaphthalene
21.98	1,7-Diisopropylnaphthalene
22.85	2,6-Diisopropylnaphthalene
23.06	2,7-Diisopropylnaphthalene
23.09	1,5-Diisopropylnaphthalene
26.17-27.46	Triisopropylnaphthalene
28.82-31.9	Tetraisopropylnaphthalene
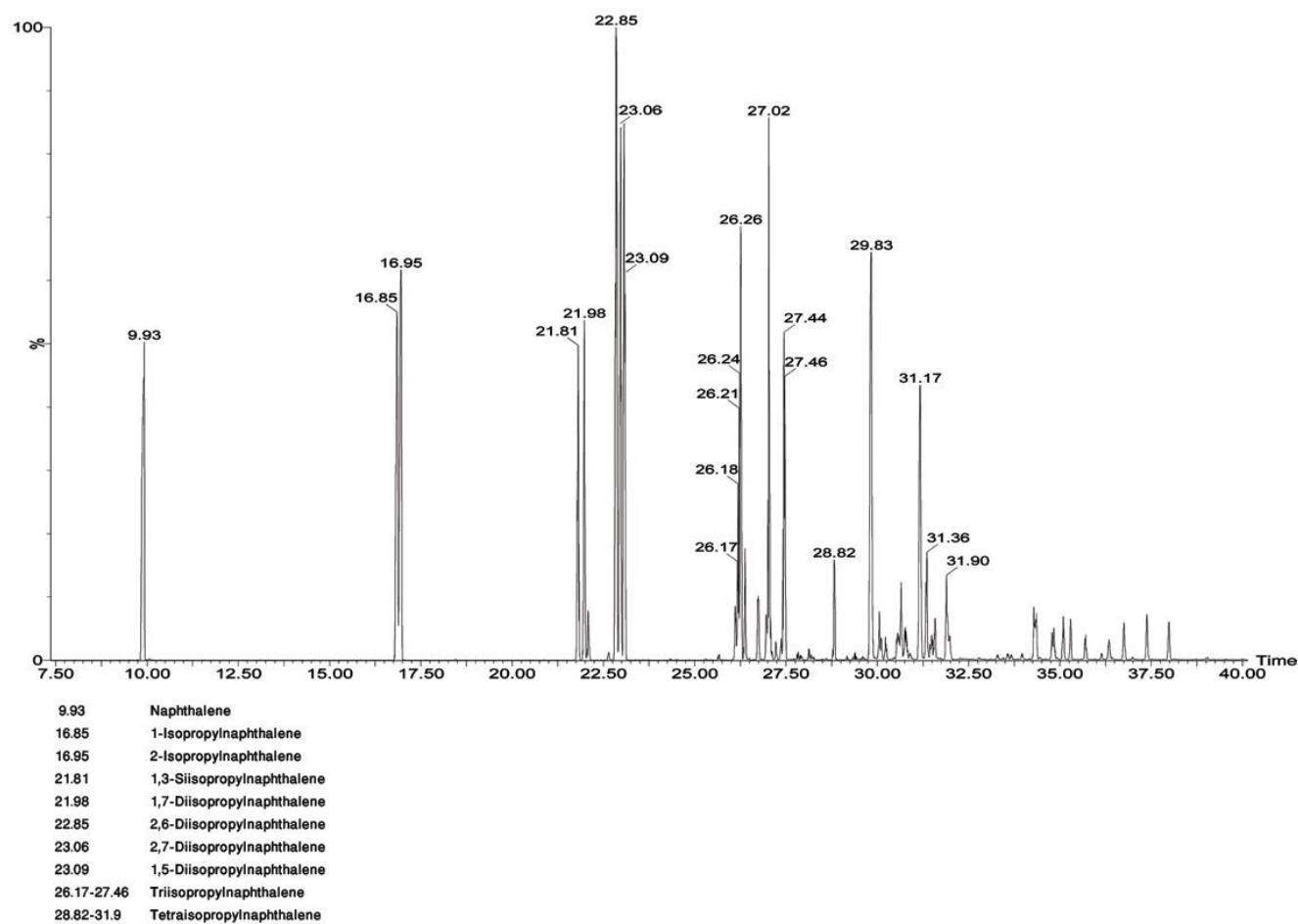
Figure A. 2. Gas chromatography-mass spectroscopy (GC-MS) trace showing peak separation of DIPN and other isomers as labelled. Sample conditions T=220 °C, P=50 bar, Catalyst= HY zeolite, TOS= 6 h, WHSV= 18.8 h^{-1}, isopropanol/naphthalene= 4 (molar ratio). Time axis (minutes).

Appendix C: TPD calculations

The calculations below were used to determine the number of moles of adsorbed tert-Butylamine on acid sites of the catalyst from the detected peak area.

<u>**Vapour Calibration**</u>

A separate calibration of the Thermal Conductivity Detector TCD must be made when vapour is to be used during analysis. The Vapour Calibration experiment is used to calibrate the TCD so that peak area data can be converted to volume data. During a Vapour Calibration, a series of injection at specified temperatures is flowed through the analyser and the resultant signal readings are recorded. The analyser can then use this data to calculate the unknown concentrations of vapours flowing past it during subsequent analyses.

The partial pressure of the vapour is estimated using the Antoine equation:

$$Ln\ p_v = A - \frac{B}{T + C}$$

p_v= Partial pressure of vapour at reflux temperature (bar)
A, B, C=Antoine coefficients
T=Reflux temperature (K)=313 K (40 ºC)

<p align="center">Antoine coefficients for t-Butylamine</p>

A	B	C	T_{min} (K)	T_{max} (K)
3.90694	992.719	-62.727	292.47	348.36

Assuming t-Butylamine in loop as an ideal gas:

Number of moles of t-Butylamine in loop: $n = \frac{P.V}{R.T}$

P= loop pressure= 1 bar
V= loop volume=0.5 ml
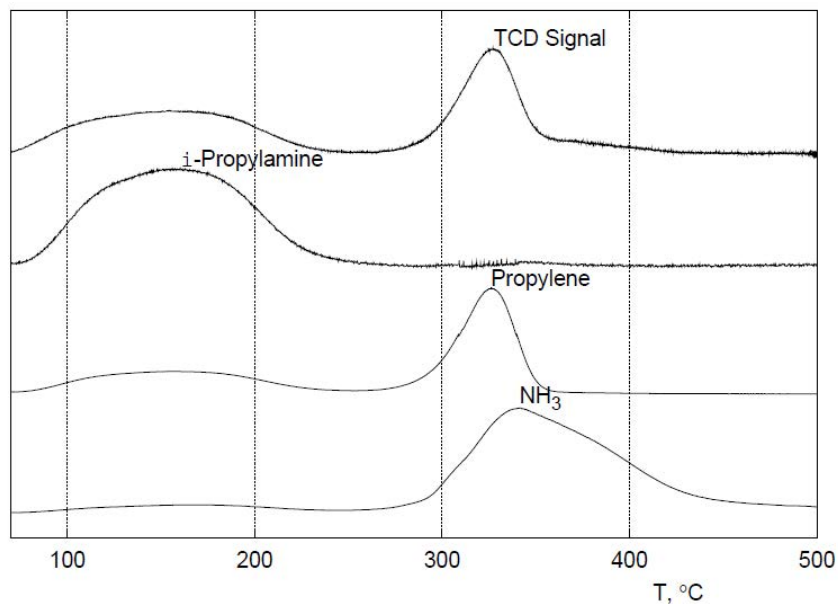T= loop temperature= 383 K (110 ºC)
R= 83.14 (ml bar K^{-1} mol^{-1})
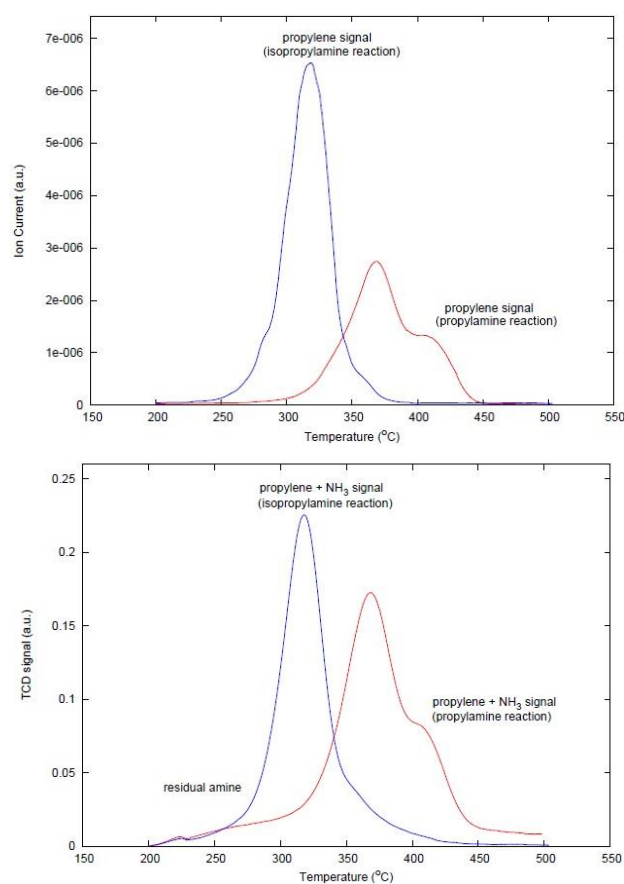n=0.0181 mmol t-BA
A=Average Area (from calibration curve) = 0.176 ➔ n/A=0.1028

TPD Calibration curve for t-Butylamine
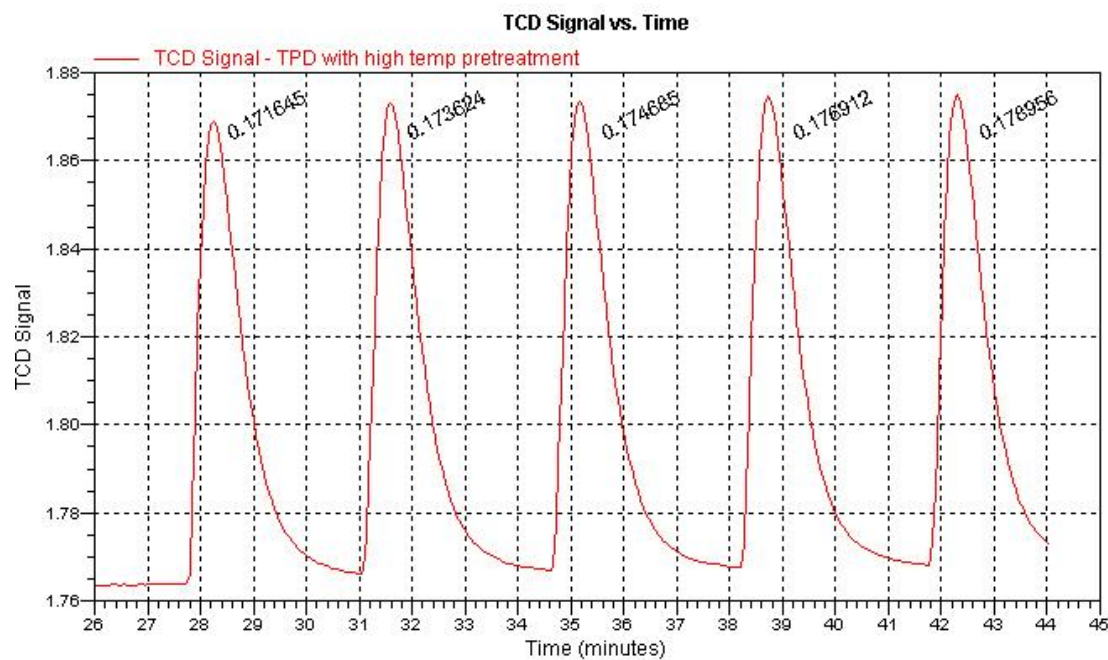
Figure A. 3. TPD Calibration curve for t-Butylamine

Acidity=Peak area*0.1028/ Catalyst weight

Figure A. 4 Temperature-programmed decomposition of i-propylamine over ZSM-5 zeolite (Micromeritics, 2003)

Figure A. 5 MS and TCD results of TPD analysis of HY zeolite (SiO$_2$/Al$_2$O$_3$=30) (Micromeritics, 2008)

Using the TCD method includes residual amine and ammonia from the chemisorption, whereas a mass spectrometer can isolate the propylene signal for more accurate calculation. However, it is possible to calculate acid site density with an acceptable margin of error by heating the sample with lower ramping rate (e.g. 5 °C/min) to isolate residual amine from decomposed products. Moreover, from Figure A. 4, it can be seen that ammonia desorption lags the propylene desorption which is led to overlapping the TCD signal of decomposed products. This is due to the readsorption of ammonia onto the ZSM-5 zeolite. Thus, the TCD signal area is proportion to the thermal conductivity of decomposed products (alkene and ammonia). As the thermal conductivity of decomposed products is very close to thermal conductivity of alkylamine, it is possible to use same calibration curve for conversion of signal area to amount of desorbed alkylamine.

Appendix D: BET surface area calculations

The specific surface area of a powder can be determined by physical adsorption of a gas (e.g. N_2, Ar or Kr) on the surface of the solid and by calculating the amount of adsorbate gas corresponding to a monomolecular layer on the surface. Physical adsorption results from relatively weak forces (van der Waals forces) between the adsorbate gas molecules and the adsorbent surface area of the test powder. The collected data are treated according to the Brunauer, Emmett and Teller (BET) adsorption isotherm equation:

$$\frac{1}{V_a(\frac{P_0}{P} - 1)} = \frac{C - 1}{V_m . C} . \frac{P}{P_0} + \frac{1}{V_m . C}$$

P = partial vapour pressure of adsorbate gas in equilibrium with the surface at 77 K (pa)

P_0 = saturated pressure of adsorbate gas (pa)

V_a = volume of gas adsorbed at standard temperature and pressure (STP), (ml)

V_m = volume of gas adsorbed at STP on the sample surface, (ml)

C = dimensionless constant

By plotting the left term versus P/P_0, it is possible to calculate V_m

BET surface area calculation for HY zeolite:

P/P_0	V_a (ml)	$1/[V_a(P_0/P-1)]$
0.061243334	162.1913	402.2335
0.081277954	165.3782	534.94652
0.128065364	171.1875	857.97713
0.16700868	175.2515	1144.0284
0.20234483	178.5846	1420.4728

The chart shows a linear plot with the equation $y = 7195.6x - 49.014$, plotting $1/[V_a(P_0/P-1)]$ versus Relative Pressure (P/P_0).
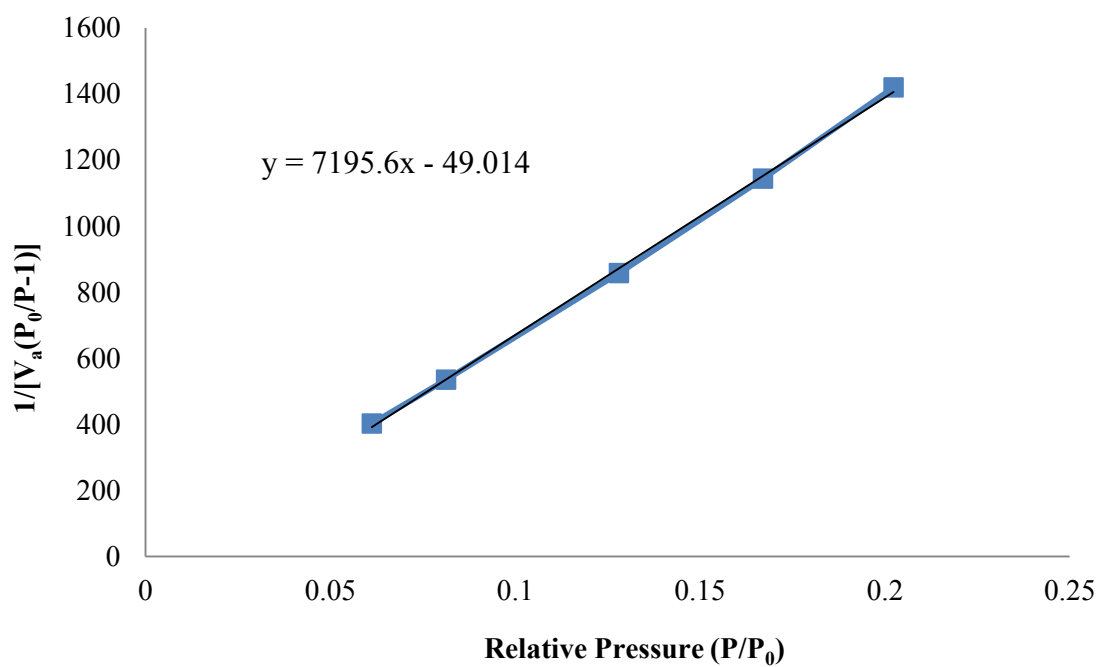
Gradient	Intercept	V_m	$n_m = V_m/V_N$	Area (m^2/g)
7195	-49	0.00014	0.006247	**609**

Weight of sample= 1 g

Effective cross-sectional area (σ^0) for N_2 = 0.162 (nm^2)
N_A= 6.02 * 10^{23}
V_m= 1/(Gradient+Intercept)
V_N= 0.0224
Area=n_m* σ^0 * N_A

Appendix E: XRD calculations

The average crystallite size of samples were calculated by applying Scherrer equation on (300), (191), (170) and (222) XRD reflections

$$d = \frac{K * \lambda}{B * \cos\theta_B}$$

d = thickness of crystallite

K = constant dependent on crystallite shape (0.9)

λ = X-ray wavelength (0.154056)

B = FWHM (full width at half max) or integral breadth

θ_B = Bragg Angle

HY zeolite

Peaks Intensity	306	193	172	222
2Θ	16.69	19.81	21.54	24.91
FWHM	0.3	0.35	0.3	0.31
B (=π.FWHM/180)	0.005233	0.006106	0.005233	0.005408
Cos (Θ)	0.989	0.985	0.982	0.976
Crystal size (nm)	26.78838	23.05471	26.97934	26.26954

I_{avg}=Average Peak Intensity= 893
Average crystal size= 25.77 nm
Crystallinity= 100% (as Ref.)

Fe-HY zeolite

Peaks	450	211	250	333
2Θ	16.67	19.77	21.5	24.88
FWHM (degree)	0.26	0.32	0.27	0.26
Beta (=π.FWHM/180)	0.0045356	0.005582	0.00471	0.004536
Cos (Θ)	0.989	0.985	0.982	0.976
Crystal size (nm)	30.909668	25.21609	29.97704	31.32137

I_{avg}=Average Peak Intensity= 1244
Average crystal size= 29.35 nm
Crystallinity= I_{avg} (Sample)/ I_{avg} (Ref.)=1244/893=139%

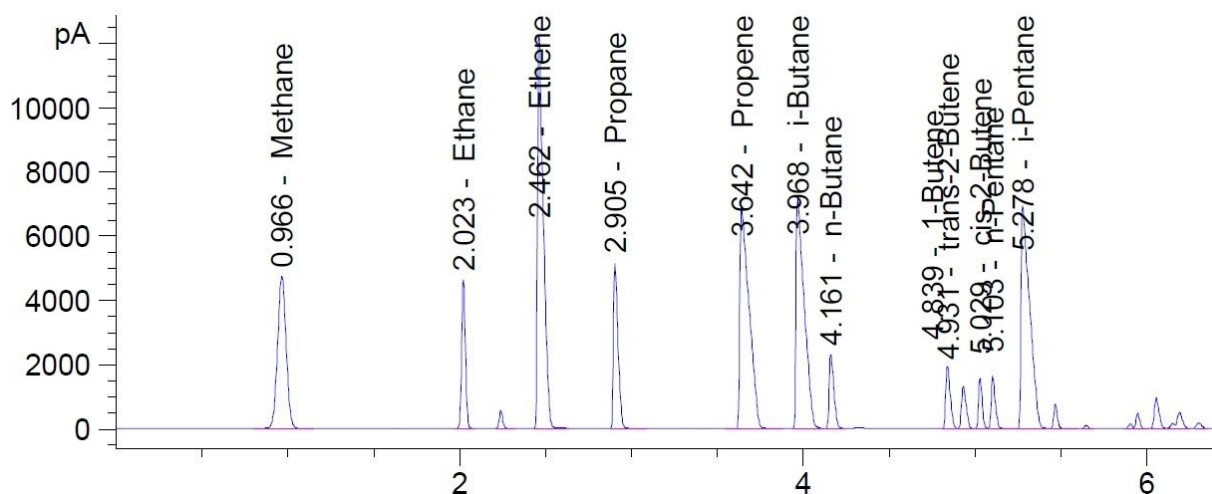**Appendix F: GC analysis of methanol dehydration products**

Figure A. 6. GC analysis of a sample product analysed by RGA (Agilent 7890A)

Signal 1: FID1 A, Front Signal

Peak #	RT (min)	Withs (min)	Area (pA*s)	Area (%)	Name
1	0.78	0	0	0	Inert
2	0.966	0.0538	1.66E+04	10.56542	Methane
3	2.023	0.0246	6880.34082	4.38268	Ethane
4	2.241	0.0234	801.52698	0.51056	?
5	2.462	0.0392	2.90E+04	18.44163	Ethene
6	2.905	0.0272	9464.35156	6.02865	Propane
7	3.642	0.0512	2.56E+04	16.32779	Propene
8	3.968	0.0433	2.38E+04	15.13683	i-Butane
9	4.161	0.0312	4335.60937	2.76172	n-Butane
10	4.839	0.0294	3568.17822	2.27288	1-Butene
11	4.931	0.0301	2475.04785	1.57657	trans-2-Butene
12	5.029	0.0232	2295.71484	1.46234	cis-2-Butene
13	5.103	0.0236	2625.27075	1.67226	n-Pentane
14	5.278	0.0472	2.39E+04	15.2505	i-Pentane
15	5.467	0.0212	1068.7251	0.68076	?
16	5.647	0.0218	132.75015	0.08456	?
17	5.946	0.0309	916.03717	0.5835	?
18	6.054	0.0314	1815.1261	1.15621	?
19	6.189	0.0426	1271.67639	0.81004	?
20	6.302	0.034	364.37851	0.2321	?
21	11.236	0.2522	98.8978	0.063	?

Composition of calibration gas

Components	Quantity (vol%)	Unit	Relative Accuracy (%)
Hydrogen	1	%	0.5
Methane	1	%	0.5
Ethane	1	%	0.5
Ethylene	1	%	0.5
Propane	1	%	0.5
Propylene	1	%	0.5
Isobutane	1	%	0.5
n-Butane	1	%	0.5
1-Butene	1	%	0.5
trans-2-Butene	1	%	0.5
cis-2-Butene	1	%	0.5
n-Pentane	1	%	0.5
Isopentane	1	%	0.5
Carbon dioxide	3	%	0.5
Carbon monoxide	4	%	0.5
Nitrogen	80	%	0.5

Analysis of calibration gas

Peak #	RT (min)	Withs (min)	Area (pA*s)	Area (%)	Name
1	0.739	0.1111	39.82581	0.41173	?
2	0.78	0	0	0	Inert
3	1.564	0.0204	218.75912	2.2616	Methane
4	1.734	0.0197	421.94278	4.36218	Ethane
5	1.946	0.0197	415.41248	4.29466	Ethene
6	2.321	0.0196	637.14197	6.58697	Propane
7	3.07	0.0189	628.87061	6.50146	Propene
8	3.376	0.0198	895.06921	9.25351	i-Butane
9	3.512	0.0195	930.24194	9.61713	n-Butane
10	4.194	0.0192	922.9339	9.54158	1-Butene
11	4.278	0.0197	925.74426	9.57063	trans-2-Butene
12	4.483	0.0198	939.17102	9.70944	cis-2-Butene
13	4.679	0.0209	1314.72302	13.59202	i-Pentane
14	4.797	0.0216	1382.92175	14.29708	n-Pentane
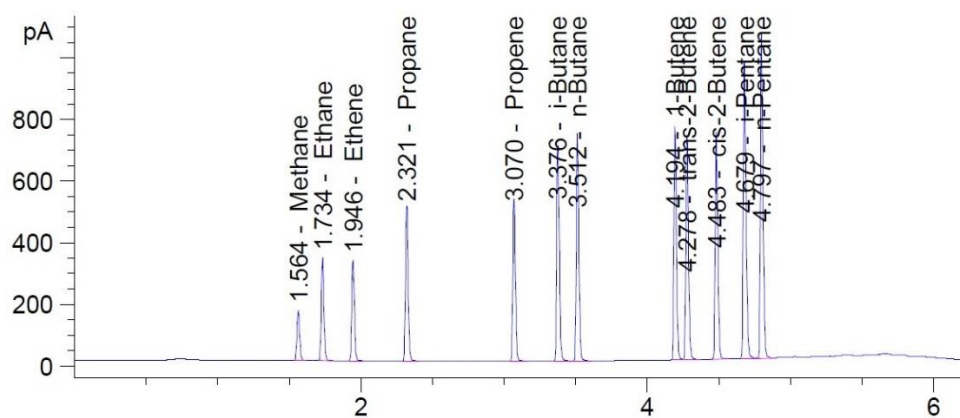
Appendix G: Published papers

- Saeed Hajimirzaee, Gary A. Leeke and Joseph Wood 2012. Modified zeolite catalyst for selective dialkylation of naphthalene. Chemical Engineering Journal, 207–208, 329-341

- Hajimirzaee, S., Ainte, M., Soltani, B., Behbahani, R. M., Leeke, G. A. and Wood, J. (2015) 'Dehydration of methanol to light olefins upon zeolite/alumina catalysts: Effect of reaction conditions, catalyst support and zeolite modification', Chemical Engineering Research and Design, 93(0), pp. 541-553.